OCS Study
MMS 2007-044

Characterization of Northern Gulf of Mexico Deepwater Hard-Bottom Communities with Emphasis on *Lophelia* Coral

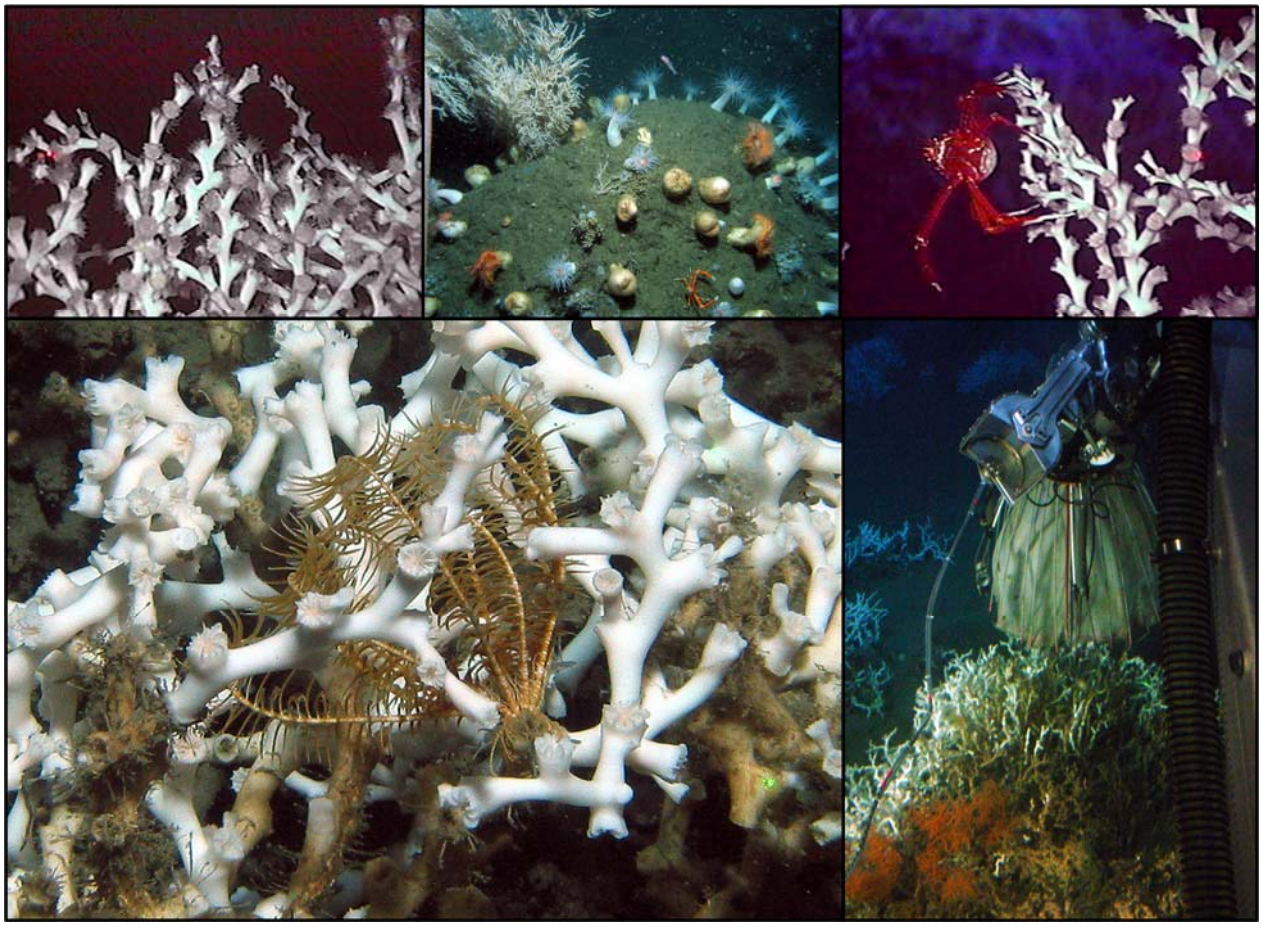

MMS U.S. Department of the Interior
Minerals Management Service
Gulf of Mexico OCS Region

OCS Study
MMS 2007-044

Characterization of Northern Gulf of Mexico Deepwater Hard-Bottom Communities with Emphasis on *Lophelia* Coral

Author

CSA International, Inc.

Prepared under MMS Contract
1435-01-03-CT-72323 (MC03PC00006)
by
CSA International, Inc.
759 Parkway Street
Jupiter, Florida 33477-9596

Published by

U.S. Department of the Interior
Minerals Management Service
Gulf of Mexico OCS Region

New Orleans
July 2007

Disclaimer

This report was prepared under contract between the Minerals Management Service (MMS) and CSA International, Inc. This report has been technically reviewed by the MMS, and it has been approved for publication. Approval does not signify that the contents necessarily reflect the views or policies of the MMS, nor does mention of trade names or commercial products constitute endorsement or recommendation for use. It is, however, exempt from review and compliance with MMS editorial standards.

Report Availability

Extra copies of this report may be obtained from the Public Information Office at the following address:

U.S. Department of the Interior
Minerals Management Service
Gulf of Mexico OCS Region
Public Information Office (MS 5034)
1201 Elmwood Park Boulevard
New Orleans, LA 70123-2394

Telephone: (504) 736-2519 or
1-800-200-GULF

Citation

Suggested citation:

CSA International, Inc. 2007. Characterization of northern Gulf of Mexico deepwater hard bottom communities with emphasis on *Lophelia* coral. U.S. Department of the Interior, Minerals Management Service, Gulf of Mexico OCS Region, New Orleans, LA. OCS Study MMS 2007-044. 169 pp. + app.

Acknowledgments

The program was conducted by a multidisciplinary team under the direction of CSA International, Inc. (CSA). Dr. Alan Hart was the Program Manager, and Stephen Viada was the Deputy Program Manager. Dr. Neal Phillips was the Scientific Editor for the Final Report. Principal Investigators are acknowledged at the head of each chapter.

We appreciate the assistance of MMS staff, including Gregory Boland (Contracting Officer's Technical Representative), Debra Bridge (Contracting Officer), and Dr. Thomas Ahlfeld.

We wish to acknowledge the ship and submersible crews of Harbor Branch Oceanographic Institution and the following individuals for their assistance during the fieId surveys:

- Erin Becker[1]
- Dr. Stephen Cairns[2]
- Sharmishtha Dattagupta[1]
- Benjamin Grupe[3]
- Mike Holmes[3]
- Katie Koval[3]
- Stephanie Lessard-Pilon[1]
- Kate Luley[1]
- Dr. Cheryl Morrison[4]
- Elizabeth Podowski[1]
- Tracey Smart[3]
- Guy Telesnicki[1]
- Maya Wolff[3]

We also wish to acknowledge Dr. Kenneth Sulak for his assistance in the deployment of sediment traps in 2004, Dr. Stephen Cairns (National Museum of Natural History) and Dr. Dennis Opresko (Oak Ridge National Laboratory) for their assistance in taxonomic identifications of collected specimens, Dr. Wayne Isphording (University of South Alabama) for conducting laboratory grain size analyses of collected sediment core samples, and Dr. Tom McDonald for conducting laboratory petroleum hydrocarbon analyses of collected water samples.

The CSA document production team included Karen Stokesbury (Document Production Coordinator and Word Processor), Melody Powell (Technical Editor), Suzanne Short (Graphics Illustrator), and Lynanne Rockhill and Virginia Frankfurth (Word Processors).

---

[1] Pennsylvania State University.

[2] National Museum of Natural History.

[3] Oregon Institute of Marine Biology.

[4] U.S. Geological Survey.

Table of Contents

Page

Contents
(continued)

Page

Contents
(continued)

Page

List of Figures

List of Figures
(continued)

List of Figures
(continued)

List of Figures
(continued)

List of Figures
(continued)

List of Figures
(continued)

List of Figures
(continued)

Figure **Page**

List of Figures
(continued)

List of Figures
(continued)

List of Tables

List of Tables
(continued)

List of Acronyms and Abbreviations

ACM	acoustic current meter
AFDW	ash-free dry weight
ANOVA	analysis of variance
CDT	Cañon Diablo troilite
COADS	Comprehensive Ocean-Atmosphere Data Set
CSA	CSA International, Inc.
CTD	conductivity, temperature, depth
DGPS	differential global positioning system
DIC	dissolved inorganic carbon
DW	dry weight
EA/IRMS	elemental analyzer/isotope ration mass spectrometer
FSI	Falmouth Scientific
GC	Green Canyon
GC/FID	gas chromatography/flame ionization detection
GIS	geographic information system
HAPC	Habitat Area of Particular Concern
HSD	Honestly Significant Difference
IPS	integrated positioning system
JSL	*Johnson-Sea-Link*
MC	Mississippi Canyon
MDS	multidimensional scaling
MMS	Minerals Management Service
NOAA-OE	National Oceanic and Atmospheric Administration, Office of Ocean Exploration
OCS	outer continental shelf
PSU	The Pennsylvania State University
PVC	polyvinyl chloride
QA/QC	quality assurance/quality control
ROV	remotely operated vehicle
SA	surface area
TPH	total petroleum hydrocarbons
UC	University of California
UTC	Coordinated Universal Time
VK	Viosca Knoll
VPDB	Vienna Peedee belemnite

Chapter 1
Introduction

Stephen T. Viada, Sandra D. Brooke, and Erik E. Cordes

This is the final report of a study of deepwater hard bottom communities on the northern Gulf of Mexico continental slope. The study was conducted for the Minerals Management Service (MMS) by a team of scientists under the management of CSA International, Inc. (CSA). Key participants are listed in the Acknowledgments, and authors/principal investigators are listed at the head of each chapter.

The MMS is responsible for managing exploration and development of mineral resources on submerged Federal outer continental shelf (OCS) lands. Through its Environmental Studies Program, the MMS collects information for leasing and management decisions. On the Gulf of Mexico continental slope, sensitive biological areas such as chemosynthetic communities have been studied extensively (Brooks et al. 1984; Kennicutt et al. 1988; MacDonald 2002) and are currently protected. Soft bottom areas of the continental slope have been investigated (Rowe and Kennicutt 2002). This study of non-chemosynthetic hard bottom areas of the continental slope represents another logical step for MMS deepwater investigations.

1.1 BACKGROUND ON DEEPWATER CORALS

Interest in deepwater corals has increased rapidly in the last decade as more coral systems are discovered and their importance in providing habitat for a diverse community, including commercially important fisheries species, is realized. With the increasing influence of human activity in deep waters, including deepwater fisheries and energy resource development, an understanding of the biology and distribution of these corals has become vital to their protection (for examples, see Rogers 1999; Koenig et al. 2000; Gage 2001; Koslow et al. 2001; Fossa et al. 2002; Hall-Spencer et al. 2002; Schroeder 2002). Efforts are currently underway to minimize anthropogenic disturbance on the *Lophelia* "Darwin Mounds" off the coast of Ireland, Norwegian *Lophelia* banks, Australian seamount corals, *Primnoa* (a deepwater octocoral) stands in the Gulf of Alaska, and *Primnoa* off the eastern coast of Canada. These corals often provide habitat for deepwater fisheries species, most notably rockfish, orange roughy, and grenadiers (Koslow et al. 2001; Andrews et al. 2002; Hall-Spencer et al. 2002). In addition to these commercially important species, these deepwater coral habitats may contain abundances of macrofauna orders of magnitude higher than the surrounding seafloor (Mortensen et al. 1995). Higher estimates of diversity are also obtained in samples from coral thickets as compared to the surrounding soft bottom (Jensen and Frederiksen 1992; Mortensen et al. 1995), emphasizing the importance of this habitat to the ecology of the deep benthos.

The most common and well-studied deepwater scleractinian is *Lophelia pertusa* (Linne 1758). This species belongs to the family Caryophyllidae (Gray 1846), is a pseudocolonial species, and like other deepwater scleractinians is ahermatypic and azooxanthellate. As with other corals there is a high level of flexibility in the skeletal morphology. *Lophelia* has a dendroid branching skeleton consisting of either dense short or long thin corallites. As the branches become denser they frequently anastomose (fuse together), creating a highly complex, large, and stable structure.

Colonies typically develop from irregular small bushes to hemispherical cauliflower-like colonies and eventually coalesce into the "thicket" stage, which is composed of an outer layer of live coral over a dead inner core.

1.1.1 Distribution

The distribution of *Lophelia* is not continuous over the seafloor; rather, it exhibits patterns both geographically and bathymetrically (Mortensen 2000). Most records of *L. pertusa* are from the Northeast Atlantic, probably reflecting the intensity of exploration and fishing activities in this area. Live *Lophelia* also has been recorded from a few locations in the South Atlantic Ocean (Rogers 1999), Mediterranean Sea (Reyss 1971), Indian Ocean (Zibrowius 1980), and Pacific Ocean (Cairns 1994). In the Northwest Atlantic, *Lophelia* structures (lithoherms and bioherms) are found on the continental slope off the Carolinas, Florida, and the Bahamas (Stetson et al. 1962; Neumann et al. 1977; Mullins et al. 1981). In the Northeast Atlantic, extensive structures occur from the Iberian Peninsula to Ireland (LeDanois 1948), Scotland (Wilson 1979a; Frederiksen et al. 1992), and in shelf and coastal Norwegian waters (Hovland et al. 1994). *Lophelia* has been recorded from depths of 3,600 m near the Mid-Atlantic Ridge (Bett 1997) to 50 m in the Fjords of Norway (Rogers 1999). Deepwater coral systems are continually being discovered on topographic features such as shelf edges, seamounts, canyons, and fjords of most of the world's oceans.

Although the global bathymetric distribution of *Lophelia* varies greatly, on a regional scale occurrence is more predictable, with coral predominantly on shelf breaks or topographic high points with the hard substrata necessary for larval recruitment. On the upper Louisiana slope of the Gulf of Mexico, topographic highs are often associated with authigenic carbonate produced as a by-product of coupled methane oxidation and sulfate reduction by microbial consortia (Aharon and Fu 2000; Boetius et al. 2000). Authigenic carbonate precipitation may therefore provide a link between *Lophelia* distribution and hydrocarbon seepage.

Below depths of 300 m in the Gulf of Mexico, the surficial sediment regime is dominated by fine-grained pelagic and hemipelagic material (Coleman et al. 1991). Notable exceptions are authigenic carbonate deposits precipitated in conjunction with biogeochemical activity associated with hydrocarbon and related fluid seepage (Schroeder 1992). This seepage is the result of the deformational effects of the Jurassic-age Louann salt unit first forming extensive hydrocarbon reservoirs and then developing networks of growth faults above these reservoirs that serve as conduits for fluid movement to the seafloor (Roberts and Aharon 1994). Research over the past decade and a half has clearly documented that this seafloor lithification is a regular component of hydrocarbon seep sites (Schroeder 1992; Roberts and Aharon 1994; Sager et al. 1999). Aharon et al. (1997) present radiocarbon and U-series radiometric ages for both abiotic carbonates and shells of the chemosynthetic mytilid *Bathymodiolus* sp. that indicate that seepage has occurred in the northern Gulf of Mexico from at least the late Pleistocene to the present. These indurated substrates provide suitable surfaces for the colonization and development of sessile megafauna assemblages (e.g., ahermatypic scleractinians, octocorals, antipatharians, and anemones). Little is known of the composition and distribution of these sessile assemblages because, to date, not a single study has been conducted that specifically examines this component of the deep Gulf of Mexico ecosystem. What we know is based on occasional information in publications

investigating hydrocarbon seepage and/or chemosynthethic activity (MacDonald et al. 1989, 1990, 1995) or in faunal distribution and range extension reports (Cairns 1979; Opresko and Cairns 1992; Cairns et al. 1994).

In 1955, Moore and Bullis (1960) collected *L. pertusa* (=*prolifera*) in 420 to 512 m of water from the northeastern continental slope approximately 74 km east of the Mississippi River delta. Since then, reports of living *Lophelia* in the Gulf of Mexico have been published by Cairns (1979), Viada and Cairns (1987), MacDonald et al. (1989), and Schroeder (2002), and Newton et al. (1987) have described Late Pleistocene age *L. pertusa* structures on the west Florida carbonate ramp slope at depths of 500 m. In addition, reliable scientific sources have confirmed, either through direct observations or video records, the presence of *Lophelia* or *Madrepora* colonies at a number of locations in the northern Gulf of Mexico.

1.1.2 Environmental Factors

Various regulating factors for *Lophelia* have been proposed by different authors, including availability of suitable substrate, hydrographic characteristics, organic input, and seepage of hydrocarbons. The importance of substrate has been alluded to in the preceding section.

The primary hydrographic characteristics believed to affect *Lophelia* distribution are water temperature and current speed. Different regional maximum depths of *Lophelia* occurrence generally reflect maximum depths of water masses with suitable temperatures (Frederiksen et al. 1992; Freiwald 1998). With the exception of some Scandanavian fjords and the Mid-Atlantic Ridge, *Lophelia* is most common at intermediate depths and at water temperatures between 4 °C and 12 °C. The question of temperature limitation on *Lophelia* distribution is addressed in this report.

Suspension feeders such as cnidarians require current speeds that are sufficient to deliver food and oxygen but not so fast that the feeding structures are inhibited or damaged. The branches of some deepwater corals are quite fragile and may be broken by excessive current. Frederiksen et al. (1992) suggested a threshold current speed of 1 m/s for *Lophelia pertusa*, which would generally restrict this species to depths below 100 m. Coral morphology can change in response to the environment (Freiwald et al. 1997); therefore, some of the observed differences in colony morphology in the Gulf of Mexico may be a function of water energy and/or other environmental factors.

Bathymetric limits to distribution also may also be influenced by organic input. Deepwater corals cannot depend on internal photosynthetic symbionts, so they presumably rely predominantly on zooplankton to meet their nutritional requirements. Zooplankton at intermediate depths may migrate into relatively shallow water to feed, but deep-sea populations are supported primarily by detritus falling from the euphotic zone or resuspended from the bottom by currents. Local primary production by chemosynthetic or methanotrophic microbes may provide an additional food source near areas of hydrocarbon seepage. In this way, hydrocarbon seepage may influence *Lophelia* distribution not only by increasing the availability of suitable substrate, but also by providing additional nutritional input to this aphotic habitat. This may allow the corals to thrive in deeper waters near localized sources of production. In this context, it should be noted that

monospecific stands of cnidarians are abundant at many Mid-Atlantic Ridge and Indian Ocean vent fields.

Whether the distribution of *L. pertusa* in the Gulf of Mexico is linked to local hydrocarbon seepage or present simply because hard substrate is produced and often available where seepage occurs is unknown and warrants further investigation. Hovland et al. (1997, 1998), working on the continental shelf off Norway, report that many of the large *L. pertusa* banks they investigated occurred at sites where there were relatively high levels of light hydrocarbons present in the near-surface sediments. Specifically, they suggest that the establishment and growth of coral banks in this region preferentially occurs at locations of hydrocarbon micro-seepage. The correlation between the presence of deepwater corals at sites where hydrocarbon seepage has or is occurring is a critical question to both their ecology and effective management.

1.1.3 Growth

Several authors have described the formation of growth bands in shallow water corals (Barnes and Lough 1989, 1993; Taylor et al. 1993; Le Tissier et al. 1994), but there is less information on growth and skeletal structure in azooxanthellate scleractinians (Freiwald et al. 1997; Nagelkerken et al. 1997). Growth rates of *Lophelia* (patterns and rate of corallite extension) have been studied using growth bands and/or stable oxygen isotope analysis (Wilson 1979b; Mikkelsen et al. 1982; Freiwald et al. 1997; Mortensen and Rapp 1998). Mean annual linear extension rate varies between 2 and 25 mm/yr (average 11 mm/yr) for *Lophelia* sampled from Atlantic coral structures (Wilson 1979b; Mikkelsen et al. 1982; Freiwald et al. 1997; Mortensen and Rapp 1998). A growth study on *Lophelia* maintained in aquaria (Mortensen 2000) showed a similar linear extension rate of 9.4 mm/yr using growth bands and direct measurement. Mortensen (2000) suggested that growth line formation in *Lophelia* is correlated with seasonal temperature variations but also noted that temperature may co-vary with other factors such as food supply. Aquarium studies of *Lophelia* in Norway and Scotland (Mortenson 2000; Roberts and Anderson 2002) indicated that increased food supply was followed by high extension rates. Therefore, seasonal changes in food supply, rather than temperature directly, may be controlling growth rates of *Lophelia* in the field. All of this work has focused on samples from the North Atlantic. Growth of *Lophelia* from the Gulf of Mexico has not been studied to date.

1.1.4 Reproduction

In all but a few species, coral colonies grow asexually via replication of polyps, which occurs by unequal intratentacular budding in *Lophelia* (Cairns 1979, 1995). Several less common modes of asexual reproduction (polyp bail-out, parthenogenesis, etc.) are known in shallow-water corals (Sammarco 1982; Krupp 1983; Stoddart 1983), but have not been reported for any deepwater coral species. In *Lophelia* and other deepwater scleractinians, pieces of established colonies frequently break off through mechanical stresses or disturbance and continue to grow, thereby establishing new colonies that are genetically identical to the parents (Wilson 1979b). Asexual reproduction, however, does not account for the establishment of new colonies when habitat becomes available, nor can it be invoked as a mechanism of genetic exchange between established coral systems. These processes, which are central to the question of coral distribution, depend on sexual reproduction by means of dispersive planktonic larvae.

Most stony corals that have been studied in shallow water are hermaphroditic, though about 25% of species have separate sexes. Fertilization may occur either internally or externally. In the former case, embryogenesis is completed within the polyps, and the larvae are released fully formed and often are competent to settle and begin a new colony. These species tend to have relatively short-distance dispersal. Larvae produced by external fertilization often disperse much greater distances, as the embryonic stages are carried passively with the currents. Dispersal may be enhanced by egg buoyancy, especially in species with lecithotrophic larvae. Analysis of dispersal potential, local reseeding and retention, constraints on dispersal imposed by near-bottom flows, and ability to colonize distant habitats all depend on a basic knowledge of reproductive mode and larval development.

The little information available on the reproductive biology of *Lophelia pertusa* comes from histological sections of samples collected from the North Atlantic (Waller and Tyler 2005; Brooke and Jarnegren unpublished). Colonies are separate sexes (gonochoristic), and although gametes were absent in many of the samples, large numbers (3,146 oocytes/polyp) of mature oocytes (140 µm in diameter) were found in colonies collected in January/February. This limited seasonal data implies non-continuous gametogenesis, but insufficient samples have been taken for complete analysis of the *Lophelia* reproductive cycle. It is not known if fertilization occurs internally or externally; however, developing embryos have never been observed in section, so external fertilization is more likely. Natural recruitment rates are also unknown, and recruitment estimates are logistically difficult in the deep sea. Genetic techniques can provide information on genetic exchange (larval dispersal) between habitats, and a study is currently being conducted by U.S. Geological Survey to investigate the population structure of *L. pertusa* in the Gulf of Mexico and South Atlantic Bight.

1.2 STUDY OBJECTIVES

The objectives of the study were threefold:

- To select study sites on the northern Gulf of Mexico continental slope consisting of hard bottom areas with non-chemosynthetic biological communities, particularly areas with dense assemblages of the coral *Lophelia pertusa*;

- To design and implement submersible survey and sampling techniques to characterize the biological communities on these deepwater hard bottom areas; and

- To investigate and describe environmental conditions that correlate with the observed distribution and development of these communities.

1.3 STUDY OVERVIEW

Ten sites on the northern Gulf of Mexico continental slope were visited during the study using a submersible, the *Johnson-Sea-Link* (*JSL*). Three of these were alpha (primary) sites, four were beta (secondary) sites, and three were National Oceanic and Atmospheric Administration's Office of Ocean Exploration (NOAA-OE) sites (see **Section 2.1**) (**Figure 1.1**). Water depths ranged from 310 to 686 m (1,018 to 2,250 ft). Details of sites, cruises, and types of sampling conducted are provided in *Chapter 2*.

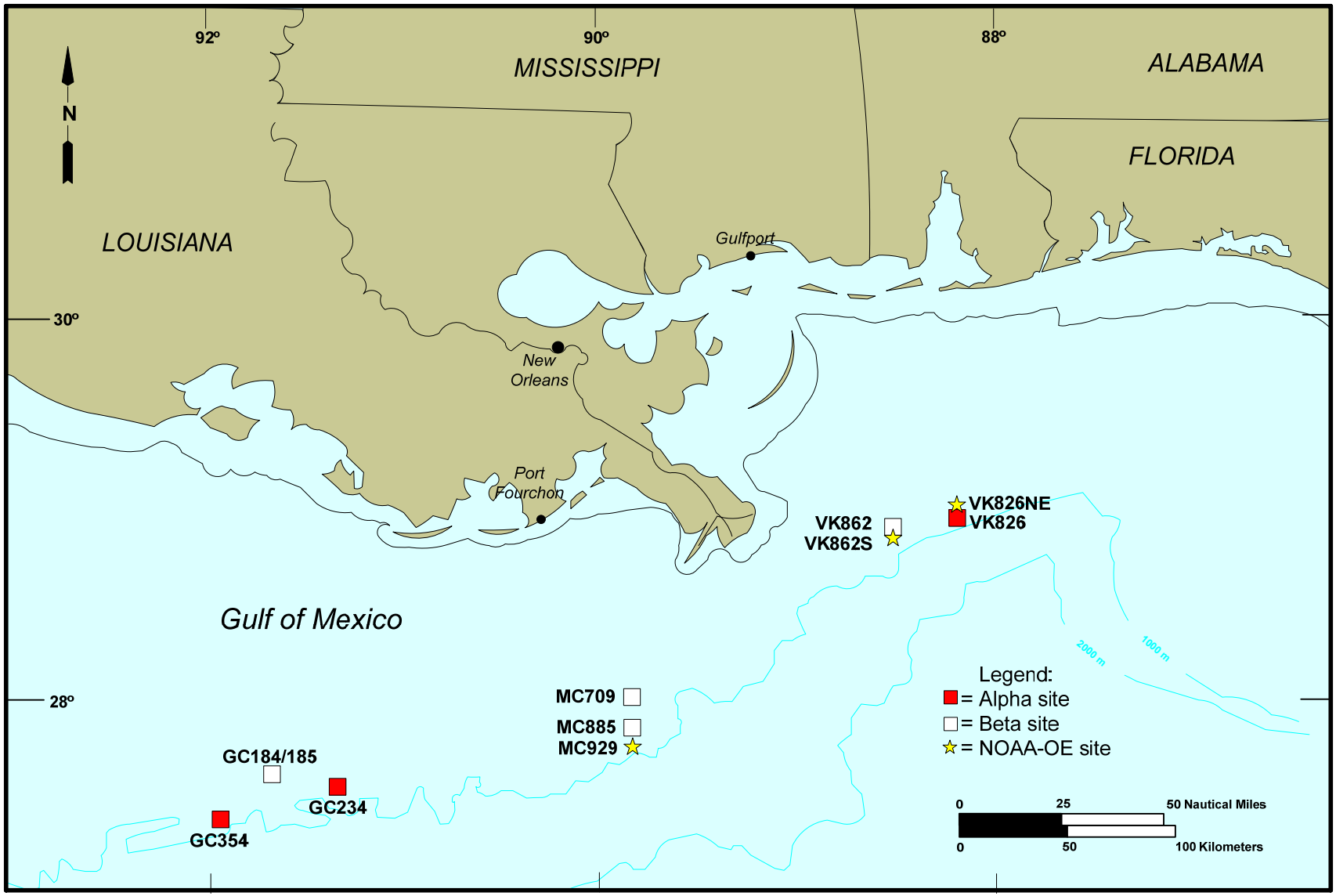

Figure 1.1. Study sites.

Study elements included the following:

- Physical oceanography (*Chapter 3*) – both short-term and long-term current meter arrays were deployed at two sites to yield information about the structure of the bottom boundary layer and examine the variability of the local currents above the boundary layer. Modeling was conducted to simulate the dispersal of coral larvae.
- Geological characterization (*Chapter 4*) – video and photographic observations were analyzed to develop a geological characterization of sites; sediment samples were collected and analyzed for grain size; and carbonate rock samples were collected and analyzed for carbon and oxygen isotopes.
- Biological characterization and studies, part I (*Chapter 5*) – video and photographic observations including video and still photo transects and photomosaics were analyzed to develop a biological characterization of sites; a Bushmaster sampling device was used to collect *Lophelia* and associated fauna; selected specimens were analyzed for carbon, oxygen, and sulfur isotopes to aid in understanding the food web; temperature probes were deployed within coral thickets at two sites; and near-bottom water samples were collected at selected sites and analyzed for total petroleum hydrocarbons (TPH).
- Biological characterization and studies, part II (*Chapter 6*) – sediment traps were deployed to estimate sediment flux; *Lophelia* transplantation and *in-situ* staining studies were conducted in the field; and laboratory studies were conducted to investigate *Lophelia* morphology and skeletal density, reproduction, temperature and sediment tolerance, and feeding.

In addition to characterizing sites, study elements were designed to test specific hypotheses about *Lophelia* distribution, growth, survival, dispersal, and relationship to environmental factors. These are discussed in individual chapters and in the Synthesis (*Chapter 7*).

1.4 REPORT ORGANIZATION

Study sites, sampling cruises, and general methodology are discussed in *Chapter 2*. Subsequent chapters include field and laboratory methods, results, and a discussion of the results for each discipline. *Chapter 7* (Synthesis) draws together findings from the various disciplines and presents key conclusions and recommendations. References are presented at the end of the report. Additional supporting data are presented in the *Appendices*.

Chapter 2
Sites and General Methods

Stephen T. Viada and William W. Schroeder

Table 2.1 lists the 10 sites on the northern Gulf of Mexico continental slope that were visited during the study. The sites are on the upper continental slope near the Mississippi River Delta (**Figure 2.1**). Each site was visited on one or both of two cruises (Cruise 1 in July 2004; Cruise 2 in September 2005).

Table 2.1. Study sites.

Study Site	Latitude	Longitude	Water Depth		Visited	
			m	ft	Cruise 1	Cruise 2
Alpha Sites						
GC234	27°44.81'N	91°13.44'W	501	1,643	X	X
GC354	27°35.89'N	91°49.60'W	525	1,722	X	X
VK826	29°09.50'N	88°01.07'W	472	1,549	X	X
Beta Sites						
MC885	28°03.97'N	89°43.04'W	634	2,079	X	X
VK862	29°06.37'N	88°23.09'W	310	1,018	X	X
MC709	28°03.78'N	89°42.62'W	686	2,250	X	--[a]
GC184/185	27°35.90'N	91°49.60'W	528	1,733	--	X[a]
NOAA-OE Sites						
MC929	28°01.47'N	89°43.63'W	650	2,132	--	X
VK826NE	29°10.21'N	88°00.72'W	457	1,500	--	X
VK862S[b]	29°05.80'N	88°23.09'W	335	1,100	--	X

GC = Green Canyon; MC = Mississippi Canyon; VK = Viosca Knoll; NOAA-OE = National Oceanic and Atmospheric Administration, Office of Ocean Exploration.

[a] On Cruise 2, the beta site MC709 was replaced by GC184/185.

[b] Part of this site is located in the adjacent block VK906.

2.1 SITE SELECTION

Sites were selected based on the known or suspected presence of high-density epibenthic communities on hard bottom features. Criteria included 1) confirmed presence of *Lophelia pertusa* and other significant hard bottom megafaunal assemblages from submersible or remotely operated vehicle (ROV) operations; 2) sites where unidentified corals or other hard-bottom non-chemosynthetic megafauna had been reported from direct observations or documented on video or still photography; 3) sites where corals or other megafauna had been collected using conventional sampling gear from surface ships (e.g., trawling or dredging); and 4) availability of geophysical data from MMS, industry, and academic databases. Additional information on candidate sites was obtained from MMS in-house geophysical resources (e.g., 3D-seismic surface amplitude anomaly data and bathymetry data) and during three research cruises to the upper Louisiana slope in the summer and fall of 2003 by several principal investigators on this study.

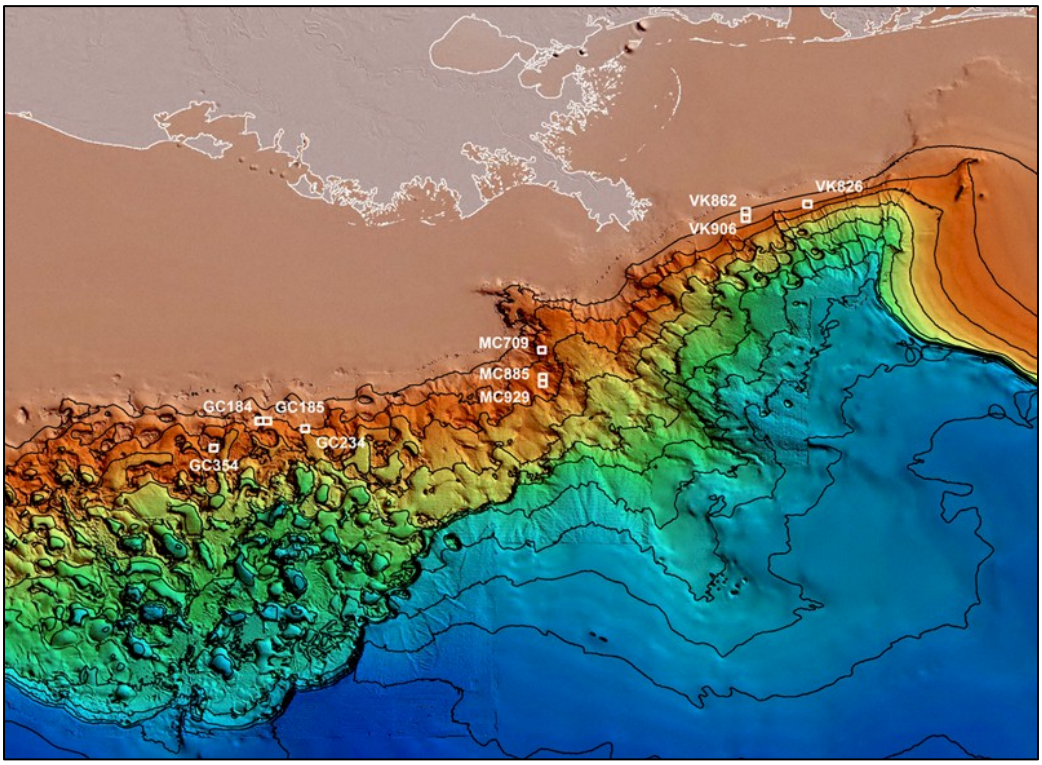

Figure 2.1. Site locations in relation to continental slope bathymetry.

Prior to Cruise 1, a preliminary list of candidate sites was assembled. In the Green Canyon (GC) lease area, these included GC81, GC184/185, GC204, GC238, GC272, and GC354. In the Mississippi Canyon (MC) lease area, MC118, MC709, and MC885 were candidate sites. In the Viosca Knoll (VK) lease area, potential sites considered were VK826 and VK862/906.

From this list of candidate sites, six were selected for study during Cruise 1. Three alpha (primary) sites were designated for intensive study (GC354, GC184/185, and VK826) and three beta (secondary) sites were selected for more limited characterization (MC709, MC885, and VK862). Just prior to Cruise 1, the list was altered by substituting GC234 for GC184/185 as an alpha site. The change was made because of reports of abundant *Lophelia* and other cnidarian communities at GC234 by Dr. Charles Fisher during an NSF-funded *JSL* submersible cruise.

Cruise 2 revisited all Cruise 1 sites, with one exception. One of the beta sites (MC709) was replaced by GC184/185, also known as Bush Hill. The substitution was made because only soft bottom substrates were seen during the Cruise 1 dive at MC709. Also on Cruise 2, a grant from the NOAA-OE program (Grant NA05OAR4601062) to the study's principal investigators provided funds for three additional ship days. Three sites (MC929, VK826NE, and VK862S) were selected to visit during this period to meet NOAA-OE's thematic priorities to explore, map, and characterize deep-sea coral habitats. Results from this additional work are presented in this report and in an unpublished report to NOAA-OE (Schroeder, 2006).

Narrative descriptions of each site are provided in *Chapter 4*.

2.2 CRUISES AND TASKS

Two cruises were conducted. Cruise 1 was conducted between 20 and 28 July 2004. The cruise was mobilized in Gulfport, Mississippi and demobilized in Port Fourchon, Louisiana. Cruise 2 was conducted between 5 and 15 September 2005, beginning and ending in Panama City, Florida.

Sites were visited with the *JSL* submersible (**Figure 2.2**), owned and operated by the Harbor Branch Oceanographic Institution. The *JSL* was deployed from the support vessel *R/V Seward Johnson II*. **Table 2.2** summarizes the tasks that were conducted during each cruise, including data and samples collected.

Figure 2.2. The *Johnson-Sea-Link* submersible.

At each site, the *JSL* collected video and still photographs and samples that were used to develop geological and biological characterizations. The submersible, where possible, maintained a constant distance above the substrate with an area of approximately 8 m^2 visible through the video camera. Integrated positioning system software showed the submersible's position relative to the ship and calculated the submersible's real time location using a differential global positioning system (DGPS) throughout each dive. The *JSL* was equipped with a manipulator arm (including a 20-cm clam-shell grab for sediment samples, jaw, and suction hose), 12 Plexiglas® buckets, and a conductivity, temperature, depth (CTD) data recorder (Seabird SBE 25 Sealogger) that continuously recorded time, temperature, conductivity, salinity, oxygen, and depth. Video footage was recorded continuously during each dive with an external pan and tilt videocamera (Sony DX2 3000A), with parallel lasers (25 cm apart) for scale reference. The video data overlay provided information on time, date, depth, salinity, and temperature.

Table 2.2. Types of sampling and data collection at each study site. Pairs of numbers refer to samples collected on Cruise 1 and Cruise 2, respectively, or where indicated, equipment deployed/retrieved. Bullets indicate sampling or collection was conducted but not quantified.

Task	Alpha Sites			Beta Sites				NOAA-OE Sites		
	GC234	GC354	VK826	MC709*	MC885	VK862	GC184/185	VK826NE	VK862S	MC929
Physical Oceanography										
Long-term current meters (deployed, retrieved)	1,1	--	1,1	--	--	--	--	--	--	--
Short-term current meters (deployed, retrieved)	1,1	--	1,1	--	--	--	--	--	--	--
Water Chemistry										
Water samples for hydrocarbon analysis	2,1	1,1	2,0	--	1,1	2,0	0,1	--	--	0,1
Geological Characterization										
Geological reconnaissance	•	•	•	•	•	•	•	•	•	•
Sediment samples for grain size analysis	5,0	6,0	5,0	--	0,3	3,0	0,3	--	--	--
Rock samples for isotope analysis	--	--	0,5	--	--	3,5	0,1	--	0,3	0,2
Biological Characterization and Studies										
Video transects	3,0	1,4	5,0	--	1,5	2,0	0,0	0,8	--	--
Photomosaics	3,0	2,1	2,0	--	1,1	1,1	0,2	0,2	--	--
Bushmaster collections	3,0	1,0	2,1	--	--	--	--	0,1	--	--
Organisms for stable isotope analyses	•	•	•	--	•	•	•	•	•	•
Lophelia live colony collections	•	•	•	--	•	•	•	•	•	•
Voucher specimen collections	•	•	•	--	•	•	•	•	•	•
Lophelia in situ staining	--	--	•	--	--	--	--	--	--	--
Lophelia transplants	--	--	•	--	--	--	--	--	--	--
Sediment traps (deployed, retrieved)	6,6	6,3	12,8	--	3,0	3,3	--	--	--	--
Temperature probes (deployed, retrieved)	--	1,1	--	--	--	1,1	--	--	--	--

* MC 709 was visited on Cruise 1, but only soft substrates were found, so no site was established or sampled. MC 709 was replaced by GC184/185 on Cruise 2.
GC = Green Canyon; MC = Mississippi Canyon; NOAA-OE = National Oceanic and Atmospheric Administration Ocean Exploration Program; VK = Viosca Knoll.

In addition to video and photographic observations, the following tasks were conducted at selected sites:

- Short-term and long-term current meter arrays were deployed at two alpha sites (GC234 and VK826) (see *Chapter 3*). Short-term arrays were deployed and retrieved on Cruise 1. Long-term arrays were deployed on Cruise 1 and retrieved on Cruise 2.
- Sediment cores were collected for grain size analysis (see *Chapter 4*).
- Carbonate rock samples were collected for isotope analysis (see *Chapter 4*).
- Samples of *Lophelia* and associated fauna were collected using a Bushmaster sampling device (see *Chapter 5*).
- Temperature probes were deployed within coral thickets at one alpha site (GC354) and one beta site (VK862) (see *Chapter 5*). The probes were deployed on Cruise 1 and retrieved on Cruise 2.
- Water samples were collected for analysis of total petroleum hydrocarbons concentrations (TPH) (see *Chapter 5*).
- Voucher specimens of invertebrate species (primarily cnidarians) were collected opportunistically using the submersible manipulators to verify taxonomy, since most benthic taxa (especially sponges and gorgonians) cannot be identified to the species level from videotapes or photographs (see *Chapters 5* and *6*).
- Sediment traps were deployed during Cruise 1 at all three alpha sites and two beta sites (MC885 and VK862) (see *Chapter 6*). Traps were deployed within and outside the coral complex to investigate the effect of the coral structure on particulate deposition. The traps were recovered on Cruise 2.
- *Lophelia* transplantation experiments were conducted at one alpha site, VK826, which has areas of dense coral cover and other areas of hard substrate with no coral (see *Chapter 6*). The objective of this experiment was to determine whether the uncolonized areas are unsuitable for adult coral survival.

In addition to the field sampling, several laboratory studies were conducted, focusing on *Lophelia* morphology and skeletal density, reproduction, temperature and sediment tolerance, and feeding (see *Chapter 6*).

Chapter 3
Physical Oceanography

Steven L. Morey

3.1 FIELD METHODS

3.1.1 Current Measurements

Physical Oceanography

- Studies focused on two alpha sites (GB234 and VK826).
- Short-term current meters deployments were conducted during Cruise 1.
- Long-term current meter deployments were conducted between Cruise 1 and Cruise 2.
- Simulation modeling of larval advection was conducted.

Four Falmouth Scientific (FSI) 2-D acoustic current meters (ACM) were used to measure currents at VK826 (29°09.5005'N, 88°01.066'W) and GC234 (27°44.812'N, 91°13.483'W). The FSI 2-D ACM is a solid-state 2-axis acoustic current meter with internal data logging. The 2-D ACM uses an electronic magnetoresistive compass and a 2-axis tilt sensor for computing velocity. Instrument specifications indicate a speed accuracy of 2% or 1 cm/s with a resolution of 0.01 cm/s, and directional accuracy of 2° with 0.01° resolution. The 2-D ACM also records temperature at 0.5 °C accuracy and resolution.

Two types of moorings were designed for this study. The first was a short-term mooring to collect high-frequency velocity data within the bottom boundary layer to estimate the bottom stress using a spectral approach. An ACM was affixed to an inverted plastic milk crate (measuring 33 cm x 33 cm x 27 cm high), which was turned upside-down and weighted (**Figure 3.1**). This placed the sensor height at 60 cm above the bottom. The ACM was programmed to internally record 15-second averaged velocities at 15-second intervals. One of these short-term moorings was manually deployed by the *JSL* at VK826 at a depth of 461 m. A location was chosen to be within an area populated by coral growth, but far enough away (approximately 150 m) from the nearest large obstacle to eliminate flow distortion. Sporadic obstacles approximately 30 cm in height were observed in the surrounding area. The VK826 current meter recorded useable data starting at 21:00 Coordinated Universal Time (UTC) on 21 July 2004 for 102 minutes. A second mooring was similarly placed at GC234 at a depth of 511 m. This current meter recorded 24 hours of velocity data beginning at 15:30 UTC on 27 July 2004. Both short-term current meter moorings were recovered, had their data archived, and were reprogrammed for deployment on long-term moorings.

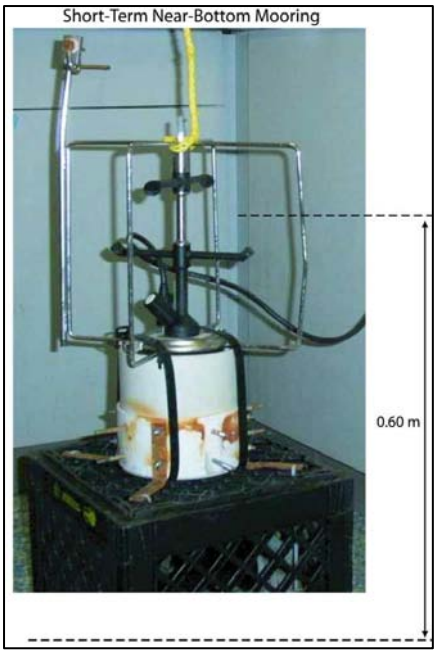

Figure 3.1. Photograph and dimensions of the FSI 2D acoustic current meter prepared for deployment as a short-term mooring. Note that the data cable was removed prior to deployment.

The second type of current meter mooring for this study was designed to collect data over several months to 1 year. Two of these long-term moorings with two current meters

each were constructed and deployed at VK826 and GC234. Each ACM was programmed to record horizontal currents averaged over 30-second intervals every 20 minutes. The VK826 mooring was deployed on 22 July 2004. The mooring was constructed of a mass of heavy chain for an anchor, a current meter secured 1.8 m above the anchor, a second current meter 22.1 m above the anchor, and floatation balls 2 m above the top current meter (**Figure 3.2**). The mooring was deployed over the side of the ship and later positioned manually by the *JSL* to be in the same location as the short-term mooring. Video from the *JSL* was used to estimate lift of the anchor chain above the bottom at 0.60 m.

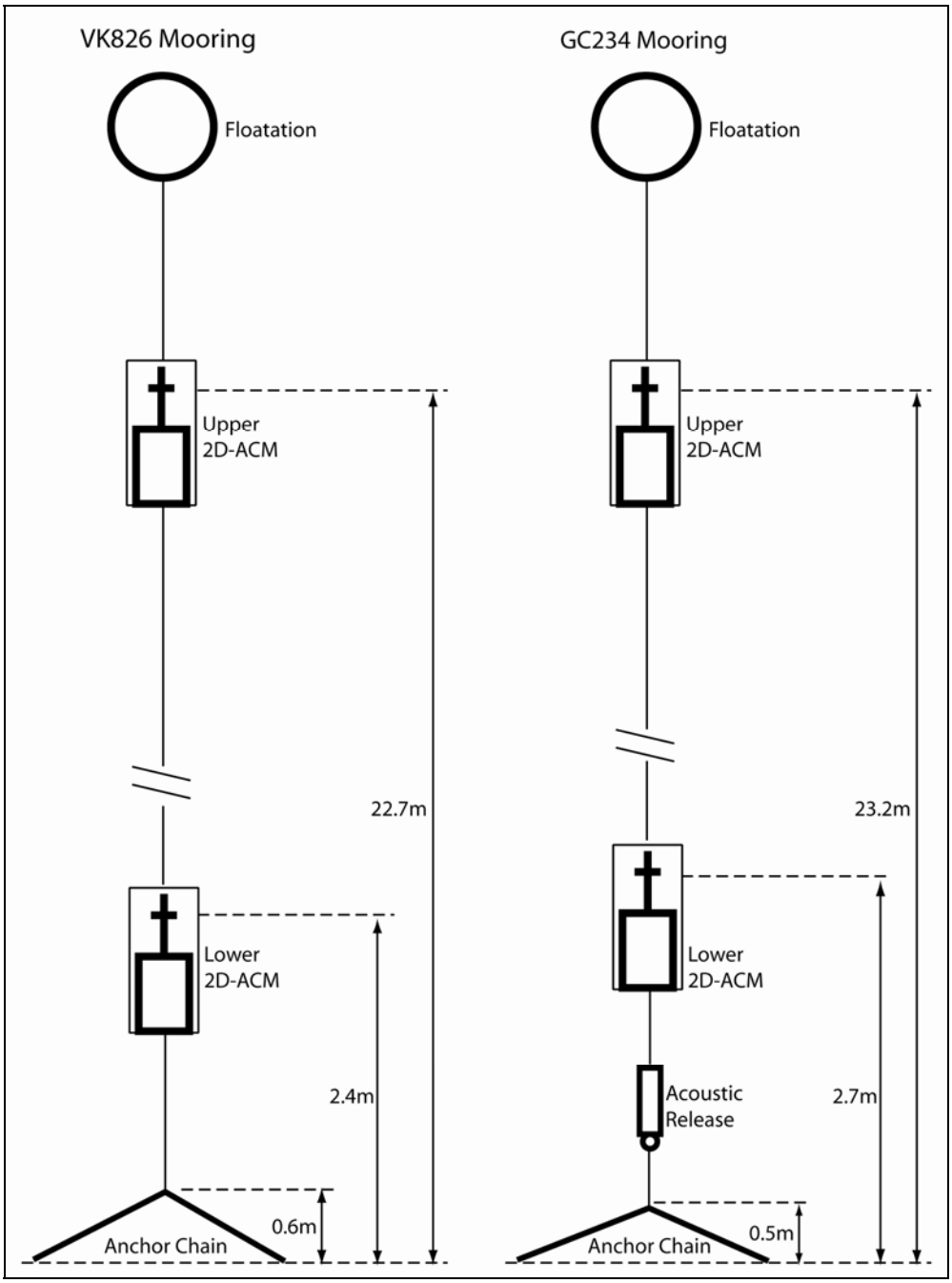

Figure 3.2. Schematics of long-term moorings deployed at VK826 and GC234.

The GC234 mooring was deployed on 28 July 2004. This mooring had an anchor of chain and lead weight attached to an acoustic release. Two current meters were placed along the mooring line, which had floatation at the top. The sensor height of the lower current meter was 2.1 m above the anchor, and the upper current meter had its sensor 22.7 m above the anchor. Additional height of the current meters off the bottom due to the anchor lift was estimated from *JSL* video to be 0.5 m (**Figure 3.2**). Due to mechanical failure of the *JSL*, this mooring could not be manually positioned to be in the same location as the short-term mooring. However, *JSL* video during recovery shows no obvious large obstacles nearby that could cause flow distortion affecting the velocity measurements. The mooring was at a depth of 503 m.

The two long-term moorings were recovered during the second cruise, and the data were retrieved from the ACMs. The lower current meter on the VK826 mooring recorded approximately 11 days (22 July to 2 August 2004) of data prior to instrument failure, and the upper current meter recorded no data. The lower current meter on the GC234 mooring operated as intended, recording approximately 9 months (28 July 2004 to 22 April 2005) of data prior to filling internal memory, but the upper current meter recorded only 45 days (28 July to 10 September 2004) of data prior to malfunctioning. An additional 7 days of data were recorded, but at a 30-second sampling interval when the instrument's programming became corrupted. Premature battery failure is the likely cause of all instrument malfunctions.

3.1.2 Analysis Methods

The two types of moorings were designed to yield information about the structure of the bottom boundary layer in areas with *Lophelia* populations and to examine the variability of the local currents above the boundary layer. The velocity time series permits two methods to be used to compute the bottom stress and boundary layer profiles. From the high-frequency short current meter records, the inertial dissipation method is used to calculate the friction velocity u_* from the spectra of the turbulent fluctuations within the bottom boundary layer. A second estimate is obtained by fitting the lower current meter velocity data from the long-term moorings to a logarithmic profile using an estimate of the bottom roughness height z_0.

The bottom stress is calculated from the friction velocity by

$$\tau = \rho \ u_*^{\,2} \tag{3.1}$$

when the coordinate is aligned so that the x axis is parallel to the stress vector. Here, ρ is the *in situ* seawater density. Using the high-frequency velocity records from the short-term moorings, u_* is estimated using the inertial dissipation method presented by Huntley (1988). If the velocity time series is measured within the constant stress part of the logarithmic layer, then the dissipation rate is

$$\varepsilon = u_*^3 \left(\kappa z\right)^{-1} \tag{3.2}$$

where $\kappa = 0.4$ is von Karman's constant and z is the height above the seafloor. By Buckingham Pi analysis (Stull 1988), the scalar wavenumber spectrum $E(k)$ is related to the dissipation rate by

$$E\left(k\right) = \alpha \varepsilon^{2/3} k^{-5/3} \tag{3.3}$$

where k is the wavenumber and α is the three-dimensional Kolmogorov constant. Taking $\phi(k)$ to be the along-mean flow wavenumber spectrum of the turbulent flow, then substitution of (3.3) into (3.2) yields

$$u_* = \left(\phi(k) k^{5/3} \alpha^{-1}\right)^{1/2} (\kappa z)^{1/3} \tag{3.4}$$

The procedure for estimating the friction velocity, and thus bottom stress, then is as follows: Calculate the mean flow direction and wavenumber spectrum in this direction, plot $\phi(k)$ versus k on a log/log plot and fit a -5/3 slope line to the data, then estimate u_* from a set of ($\phi(k)$, k) that lies along this line using (3.4).

For this method, it is assumed that the wavenumber spectra are known. However, for measurements at a single location, only the frequency spectra can be computed. Therefore, Taylor's frozen turbulence hypothesis is applied to convert between frequency spectra $\phi(f)$ and wavenumber spectra using

$$\phi(k) = \phi(f)(2\pi/\overline{u}) \tag{3.5}$$

where $\overline{u}$ is the mean speed. A form of (3.4) after application of Taylor's hypothesis can be found in Weatherly (1972).

The above-described inertial dissipation method is applied to the high-frequency short-term mooring velocity data at GC234 and VK826 taking $\alpha = 0.56$. The 24-hour long record at GC234 is divided into 23 overlapping 2-hour segments and the method applied to each segment. Six of these segments are thrown out where a reasonable -5/3 slope fit cannot be found on the wavenumber spectra plot. The average and standard deviation for the friction velocity estimates can then be computed. The VK826 record consisted of only 102 minutes of data, so only one estimate of the friction velocity was computed using the inertial dissipation method.

A second method of estimating the friction velocity, and thus bottom stress, is to fit the measurements to an assumed logarithmic boundary layer profile. If the flow at the roughness height z_0 is assumed to be zero, then the classical logarithmic profile for the speed is given by

$$u(z) = u_* \kappa^{-1} \ln z/z_0 \tag{3.6}$$

(Weatherly 1972). For this method, time averaging is applied to the speed records to filter out the effects of individual eddies in the turbulent flow. Analysis of the velocity records yields that a 2-hour averaging interval is sufficient to filter the eddies without causing the appearance of an unstable flow. When velocity measurements at various depths are taken within the boundary layer, the logarithmic function can be fit to the data to estimate the unknown parameters z_0 and u_*. Since only two current meters were available for each long-term mooring, and there was a desire to place one above the boundary layer, velocity at only one level is available for fitting this function. Thus, in order to estimate the friction velocity u_*, other methods must be used to estimate z_0, and this is described in *Section 3.4*.

3.2 LABORATORY METHODS

3.2.1 Modeling

A numerical model of the circulation of the Gulf of Mexico was used to examine the ocean circulation variability in the northern Gulf. The model was also used to simulate the dispersal of larvae (passively advected Lagrangian particles) by the ocean flow field at two specified release sites, VK826 and GC234. Results from previous modeling studies of potential relevance are discussed.

The numerical simulation used for this report is based on the Navy Coastal Ocean Model (Martin 2000) configured for the Gulf of Mexico and northwestern Caribbean (Morey et al. 2003a). This numerical simulation has a horizontal resolution of 1/20° in latitude and longitude and a total of 60 vertical grid points in the deep ocean. The upper 20 grid points are sigma coordinates in which the depths of the grid points are set fractions of the minimum of the total water column depth or 100 m. The lower 40 grid points are geopotential (z-level) surfaces, with grid spacing of 5 m just below 100 m and stretched spacing to the bottom at 4,000 m. The ocean bathymetry, primarily derived from the NOAA ETOP02 data set, has been interpolated to the model horizontal grid, smoothed with two applications of a 9-point box filter, and then rounded to the nearest model vertical level depth.

The simulation was initialized from rest with World Ocean Atlas 1994 monthly climatology temperature and salinity fields, and run for 13 years with monthly climatology forcing. This forcing consists of inflow in the Caribbean relaxed to a velocity profile consistent with climatology density profiles, yielding a mean Yucatan Strait transport of roughly 27 Sv (10^6 m/s). Surface momentum and heat fluxes are derived from the DaSilva et al. (1994) climatology (derived from the Comprehensive Ocean-Atmosphere Data Set, COADS). Additionally, fresh water is discharged into the domain at 30 point sources to simulate river inflow. There is no tidal forcing in this particular simulation.

Beginning in the sixth year of the simulation, data from the simulation have been extracted for the northern Gulf of Mexico at depths down to 1,000 m with an output frequency of once every 48 hours, yielding 8 years of temperature, salinity, and velocity data.

3.2.2 Simulations of Larval Advection

An algorithm has been implemented to advect simulated Lagrangian particles in the model horizontal flow field using a fourth-order Runge-Kutta scheme to solve the equation

$$\frac{\mathrm{d}\vec{x}}{\mathrm{d}t} = \vec{u}(x, y, t) \tag{3.7}$$

for $\vec{x} = (x, y)$, the two-dimensional position vector of each particle. $\vec{u}(x, y, t) = (u, v)$ is the two-dimensional horizontal velocity vector (with x and u oriented eastward, and y and v oriented northward). The algorithm outputs particle locations at 6-hour intervals.

An experiment was set up using this algorithm to estimate the typical dispersal patterns of particles released from a given location. Here, the particles are assumed to travel along a constant geopotential surface with the horizontal flow field. One hundred particles are released randomly distributed within 1/20° (about 5 km) of a specified location every 6 hours for 3 days, yielding a total of 1,200 particles. The advection routine is run for a total of 28 days (so the first group of particles released has been advected for 28 days and the last group of particles has been advected for 25 days at the end of the run). The positions of the particles are archived every 6 hours for later analysis. This procedure is repeated beginning the first day of each calendar month for each of the 8 years of model data.

Two sites were chosen for particle releases. The first site is VK826 (29.15°N, 88.02°W). Particles are advected in the horizontal flow field at a depth of 400 m. The second site is GC234 (27.75°N, 91.22°W), where the horizontal velocity field at 487 m is used for the advection calculation. Maps of particle density were created by summing the total number of particles existing in each 0.2° x 0.2° bin some given time after their release, and dividing by the total number of particles existing throughout the entire domain. A bin location was then colored by the percentage of total particles in the domain that existed within the bin. These particle densities were computed using particle positions 5, 10, 15, 20, and 25 days after their release. For each of the 8 years, the 12 monthly particle density maps were combined into annual mean analyses, and similar maps were created for the combined 96 months studied over the 8-year model integration period. Monthly average maps were created by combining the particle density data for all eight instances of each month.

3.3 RESULTS

3.3.1 Description of the Physical Oceanographic Environment

The study sites are located on the continental slope at such depths that the locations can be influenced by the offshore circulation in the Gulf of Mexico. The circulation offshore of the continental shelves in the Gulf is dominated by the Loop Current, which enters the Gulf through the Yucatan Channel and exits through the Straits of Florida. This current penetrates northward into the basin before turning clockwise to exit the Gulf to the east, thus forming the famous loop. The Loop Current's northward penetration varies. A mature Loop Current can sometimes extend northwestward to the outer continental shelf off of the southeastern Louisiana coast, and in its immature phase will immediately turn eastward once past Cuba. When the Loop Current penetrates far into the Gulf, it aperiodically constricts, forming a large anticyclonic (clockwise) eddy that separates and drifts generally westward. These energetic Loop Current eddies have current speeds of roughly 1 to 2 m/s, comparable to the Loop Current itself, and can exist for many months before decaying in the western Gulf. Associated with these Loop Current eddies and the Loop Current itself are a series of smaller frontal cyclonic eddies that travel around the periphery. Smaller cyclonic and anticyclonic features are ubiquitous in the Gulf.

Anticyclonic eddies are considered "warm-core" features, in that there is a depression of the thermocline within the center so that water at a given level is warmer within the center than outside the feature. Conversely, cyclonic eddies are cold-core features. The thermal and dynamic expressions of these features can be found several hundred to over 1,000 m deep. Due to potential vorticity conservation, these features remain offshore of the continental shelf.

However, the Loop Current and mesoscale eddies in the Gulf can influence the circulation over the continental slope and can be influenced by topographic features.

HOBO temperature data loggers were deployed at VK862 (29°6.37'N, 88°23.09'W) and GC354 (27°35.90'N, 91°49.60'W) at depths of 316 and 528 m, respectively, as described in *Chapter 5*. Inspection of the temperature time series (following application of a 40-hour low-pass filter) shows greater variability at the shallower VK862 site with a temperature range of approximately 9 °C to 13 °C compared to the deeper GC354 location, which shows temperatures ranging from approximately 6.8 °C to 8.8 °C (**Figure 3.3**).

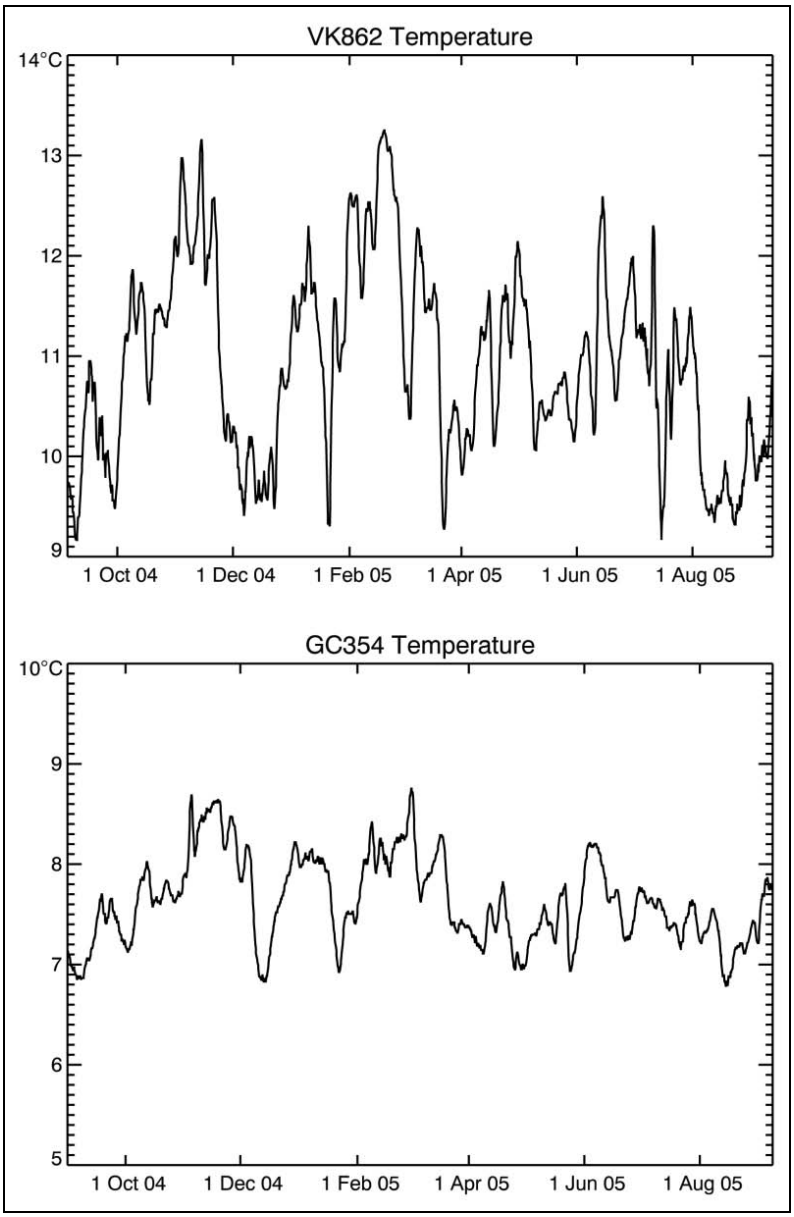

Figure 3.3. Temperature time series recorded from the HOBO temperature data loggers at VK862 and GC354 following application of a 40-hour low-pass filter.

The VK826 current meter mooring was placed at a depth of 461 m. The FSI 2D ACM records temperature with a coarse 0.5 °C resolution, and the temperature data from the 11-day record range from 7.5 °C to 9 °C with a mean of 8.3 °C. The salinity sensor on the *JSL* recorded a salinity of 35.0 during deployment. The GC234 mooring was placed at a depth of 511 m. During the approximately 9-month (267-day) record, the temperature data range from 7 °C to 9 °C with a mean of 8.1 °C. During recovery, the *JSL* salinity sensor also recorded a salinity of 35.0.

The velocity data from the long-term moorings were filtered with a 36-hour running average and their time series were plotted (**Figure 3.4**). The top current meter at VK826 failed entirely, and the bottom current meter recorded only 11 days of data. A persistent northward current existed at this location during this time period. The speed and direction of the mean vector is 5.8 cm/s directed toward a compass heading of 355.6°. Prior to filtering, the maximum speed in the data record is 18.3 cm/s (**Figure 3.5**).

At GC234, the bottom current meter recorded approximately 9 months of velocity data, and the top current meter recorded useable data for the first 45 days of this period. During the 45 days where both instruments were operating, the maximum speed recorded at 23.2 m above the bottom is 33.0 cm/s compared to 22.5 cm/s at 2.7 m. The mean vector speed and direction from the upper current meter is 10.1 cm/s at 281.0°. The mean vector speed and direction from the lower current meter over this time period is 5.2 cm/s at 286.6°. The anti-clockwise rotation of the current vectors with height is evident from the time series plots (**Figure 3.4**). Over the entire 9-month data record from the lower instrument, the maximum is 44 cm/s (the maximum 2-hour averaged speed is 36 cm/s). The mean vector speed is 6.7 cm/s directed at a compass heading of 275.7°.

Current fluctuations are dominantly east to west, oriented perpendicular to the large-scale topographic gradient (i.e., generally along-isobath). Only intermittent episodes of cross-slope currents are evident in the data record. Examples of instances of southward (downslope) current with southward velocity of 5 to 10 cm/s in magnitude occurred in September 2004. At this time a large Loop Current eddy had separated and a series of frontal cyclones along this eddy's periphery impacted the GC234 region (**Figure 3.6**). It is possible that the interaction of these cyclones with the topography result in the episodic downslope currents.

Diurnal tidal energy is not wholly removed by the 36-hour low-pass filter and is evident as directional fluctuations of a few degrees with nearly 1-day periods in the plotted vector time series. A harmonic analysis of the unfiltered velocity data from the bottom current meter at GC234 is used to find the dominant tidal constituents. Diurnal tides dominate in the western Gulf of Mexico, and the analysis show that the diurnal K1 signal dominates at this location (**Table 3.1**). The major tidal components contribute to current fluctuations oriented from northwest to southeast.

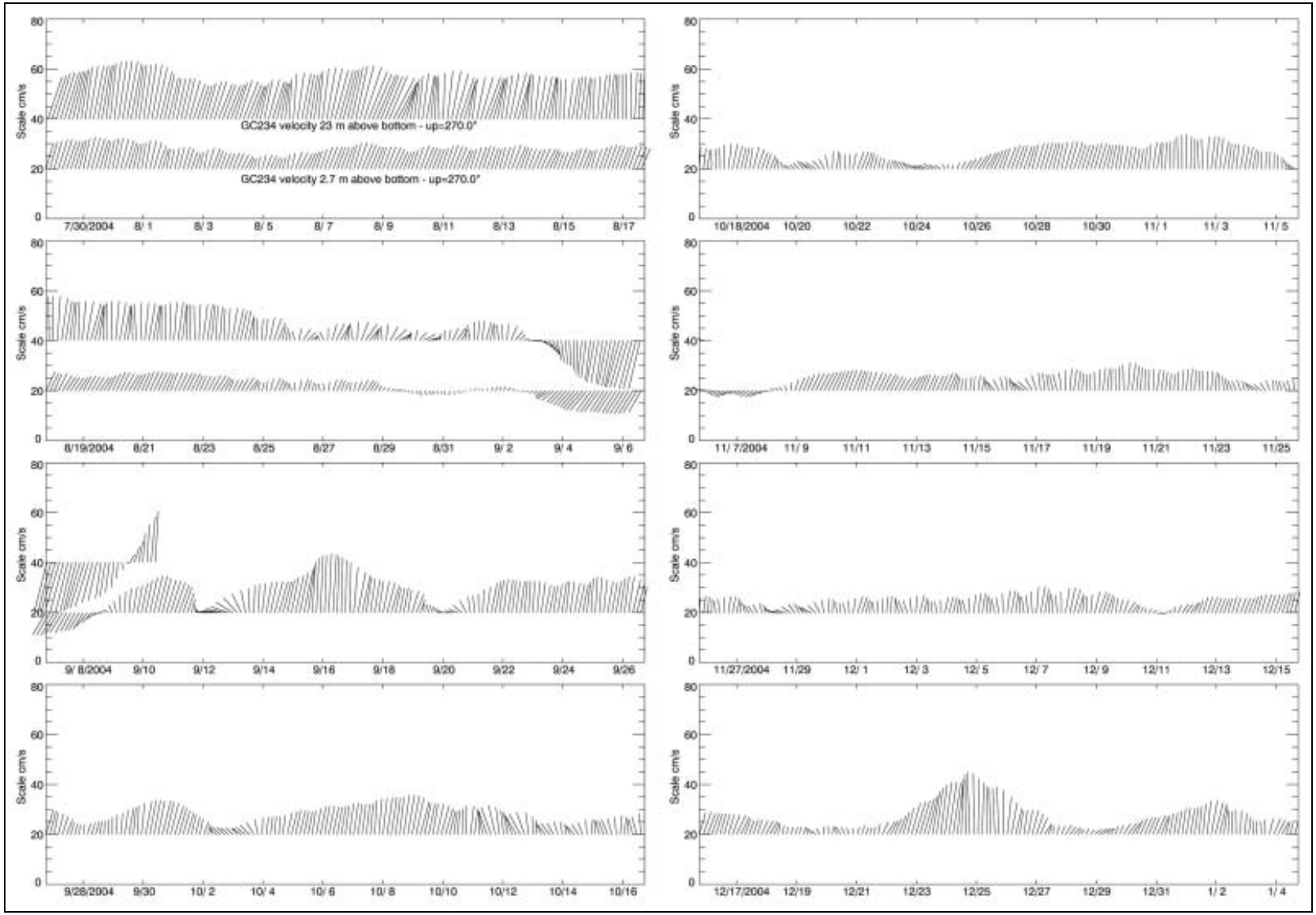

Figure 3.4. 36-hour low-pass filtered velocity vectors recorded by the upper and lower current meters at GC234 and VK826. The GC234 vectors have been rotated so west is oriented to the top of the figure. Note that no data were recorded by the VK826 upper current meter.

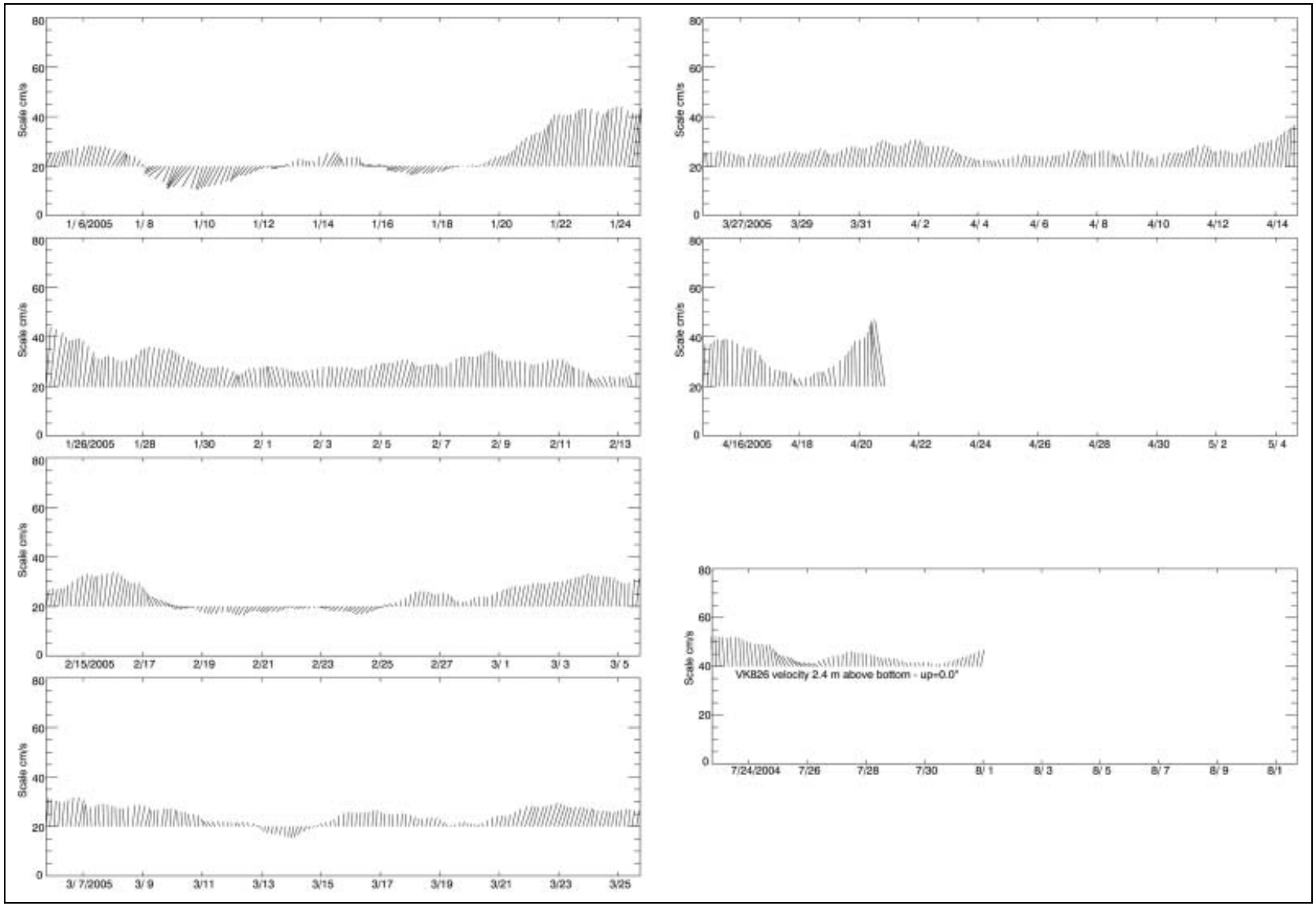

Figure 3.4. (continued).

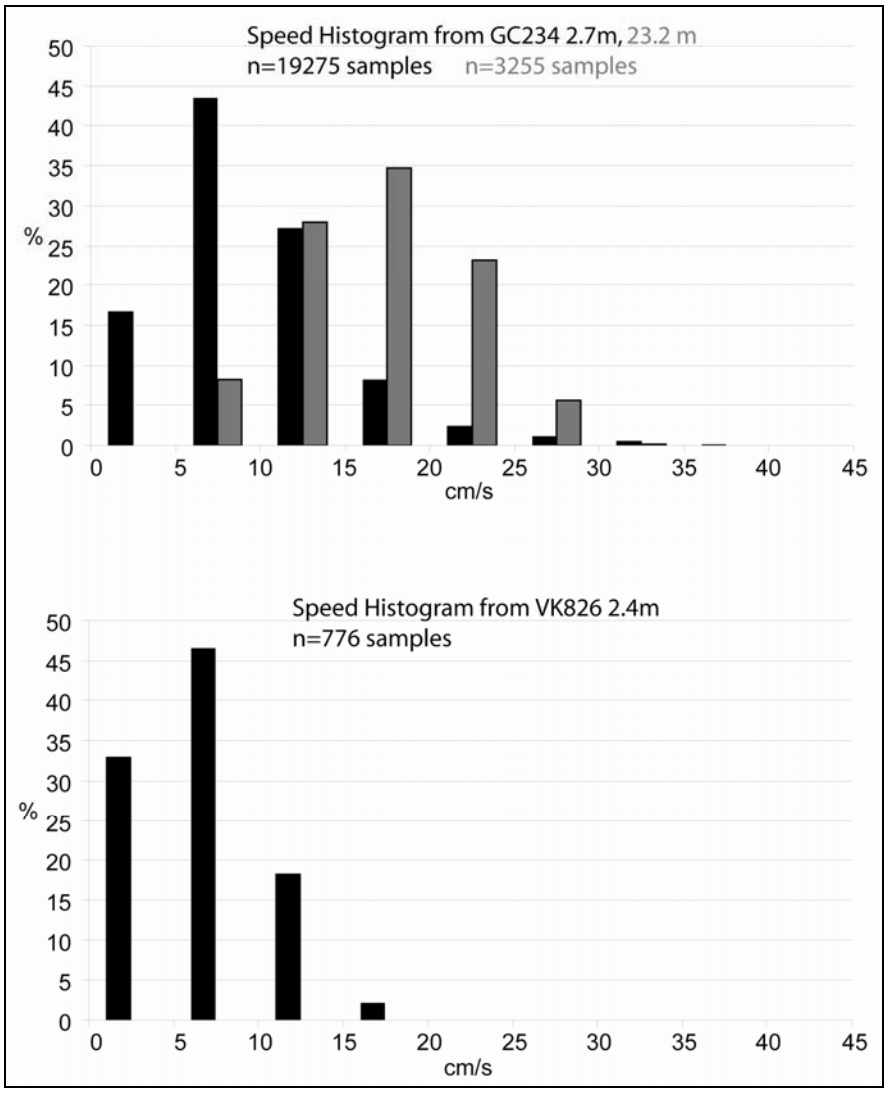

Figure 3.5. Histogram of the unfiltered current speeds recorded by the GC234 upper and lower current meters, and by the VK826 lower current meter.

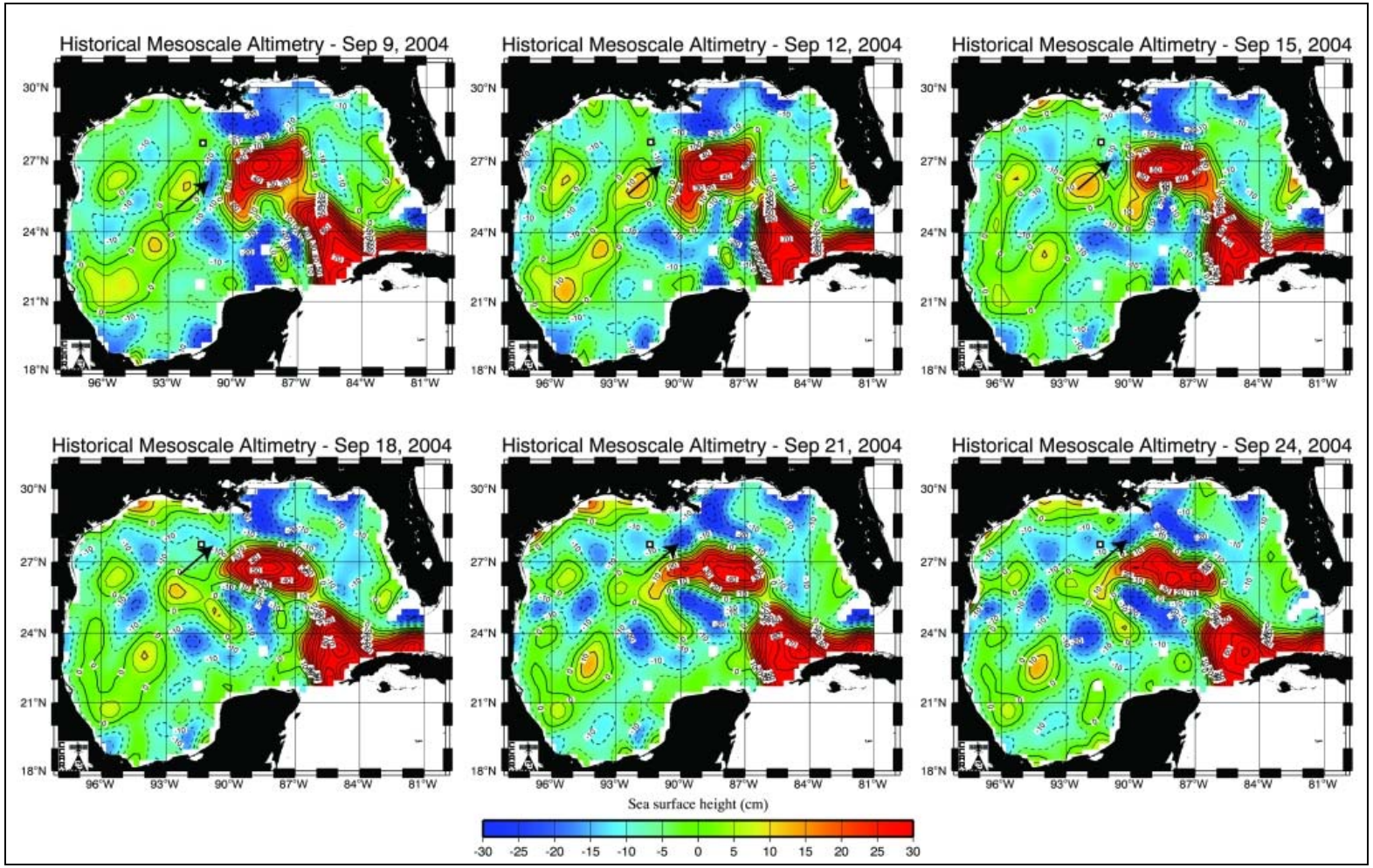

Figure 3.6. Maps of sea surface height produced by the Colorado Center for Astrodynamics Research using the Jason, TOPEX/POSEIDON, Geosat Follow-On, ERS-2, and Envisat satellite altimeter data (http://argo.colorado.edu/~realtime/gsfc_gom-real-time_ssh/). Maps are sea surface height anomalies plus a mean height produced from a numerical model. The small white boxes denote the location of the GC234 mooring, and the arrows point to the cyclonic eddy of interest traveling around the Loop Current eddy periphery.

Table 3.1. Dominant tidal constituents from a harmonic analysis of the GC234 bottom current meter of the long-term mooring. The magnitudes of the semi-major and semi-minor axes of the tidal ellipses are given in cm/s, and the inclination angle of the ellipse is a compass heading from north.

Tidal Constituent	Semi-major Axis (cm/s)	Semi-minor Axis (cm/s)	Inclination Angle
K1	2.5	0.7	129°
P1	1.4	0.6	107°
O1	1.1	0.6	164°
M2	1.4	0.4	134°

3.3.2 Bottom Boundary Layer Structure

The sites instrumented with current meters have a seafloor featuring sporadic carbonate outcroppings or boulders with large areas of sediment-covered bottom in between. Flow over the large obstacles will result in turbulent wakes on their lee sides. The objective of this research component is not to measure the flow around these carbonate features on which the coral attach, but rather to characterize the local bottom boundary layer structure at the sites not influenced by the exposed obstacles. Estimates of the bottom stresses from observations can yield information about how the hard substrate might be exposed for future colonization, and on the velocity profile impacting obstacles or organisms in the area.

Applying the inertial dissipation method to the high-frequency current meter record from the short-term mooring at GC234, the friction velocity is computed from 17 of the 23 2-hour overlapping record segments. The average of the u_* estimates is 0.21 cm/s with a standard deviation of 0.07 cm/s. High-frequency velocity measurements at the VK826 site are limited to a 104-minute record. The friction velocity estimated from this data record is $u_* = 0.36$ cm/s. The average speeds for the GC234 and VK826 short-term velocity records are 6.4 cm/s and 9.7 cm/s, respectively.

Fitting a classic logarithmic boundary layer profile to the bottom current meter velocity data of the long-term mooring requires an estimate of z_0 since velocity data are available at only one depth within the boundary layer. One method is to solve equation (3.6) for z_0 using velocity measurements and u_* values calculated with the inertial dissipation method from the short-term current meter moorings. However, with this method, uncertainties in the friction velocity estimates can lead to large errors in estimates of z_0. A second method of estimating z_0 requires knowledge of the characteristic size of the bottom roughness elements. These roughness elements can consist of waves in the bottom sediment, for example. The flow is considered hydrodynamically rough if the turbulent wakes from the bottom roughness elements erode the viscous sublayer, the laminar layer that can exist just above the surface in fluid flow. Empirically, the bottom is considered rough if the size of the bottom "roughness elements" $d > 90\nu / u_*$, in which case $z_0 \approx d/30$ (Weatherly 1972). The bottom is considered smooth if $d < 3\nu / u_*$, and empirically $z_0 \approx 0.1\nu / \rho$. Taking $\nu = 1.4 \times 10^{-6}$ m^2/s and $u_* = 0.3$ cm/s, the condition for rough bottom is $d > 4.2$ cm, and smooth if $d < 0.14$ cm. The minimum z_0 for a

rough bottom is thus 1.4 x 10^{-3} m, and the maximum z_0 for a smooth bottom is 1.4 x 10^{-10} m. Video from the *JSL* indicate that over the areas covered by sediment, a characteristic height for the waves in the sediment is roughly 2 cm, indicating that the bottom satisfies the criteria for neither smooth nor rough bottom, but is rather somewhere in between. Using the average u_* and speed from the GC234 short-term mooring, inverting equation (3.6) yields an estimate for z_0 of 4.5 x 10^{-6} m, but with a standard deviation on the order of 10^{-5} m. From the VK826 short-term mooring, z_0 is estimated at 1.5 x 10^{-5} m. These z_0 estimates are indeed between the minimum for a rough bottom and the maximum for a smooth bottom. The expressions for z_0 for a smooth to rough transitioning bottom are given in Weatherly (1972). For roughness elements of size d = 2 cm, the appropriate expression for z_0 is

$$z_0 \approx \frac{1}{1.21}\left(u_*\left(\frac{d}{30}\right)^5 \nu^{-1}\right)^{\frac{1}{4}}, \tag{3.8}$$

which gives a z_0 estimate of 3.4 x 10^{-5} m.

From these various estimates of z_0, it seems reasonable to take z_0 = 1.0 x 10^{-5} m for estimating the friction velocity from the bottom current meter records from the long-term moorings using equation (3.6). At GC234, applying the profile method to the 267-day record of 2-hour averaged velocity results in a mean of $\overline{u}_*$ = 0.31 cm/s with a standard deviation of 0.16 cm/s (n = 19,265 profiles). The maximum friction velocity over the data record is 1.16 cm/s. Applying this method to the 11-day record at VK826 yields a mean $\overline{u}_*$ = 0.22 cm/s with a standard deviation of 0.11 cm/s (n = 766). The histograms (**Figure 3.7**) show that the estimates are not normally distributed, as expected since u_* is never negative; however, a normal distribution gives a reasonable approximation away from the tails and the expected values nearly are equal to the mean. The friction velocity estimates from the high-frequency velocity record differ from $\overline{u}_*$ because the average speeds at VK826 and GC234 during the short-term mooring near the bottom are 9.7 and 6.4 cm/s, respectively, compared to long-term averages of 7.0 and 9.6 cm/s.

The friction velocity estimates are used to compute bottom stresses from equation (3.1) (**Figure 3.8**). Taking ρ = 1,030 kg/m^3, the maximum bottom stress estimated from the long-term mooring at GC234 is 0.14 N/m^2, occurring when the 2-hour averaged velocity at 2.5 m above the bottom was 36 cm/s. The expected value of the bottom stress magnitude is E(τ) = 0.0125 N/m^2. At VK826, the expected value of bottom stress magnitude over the 11-day velocity record is E(τ) = 0.0074 N/m^2.

Logarithmic speed profiles are computed for $\overline{u}_*$ and max(u_*) from the long-term bottom velocity data record at GC234 using equation (3.6) (**Figure 3.9**). Using these profiles, current speeds at different heights above the bottom can be estimated. For example, at a height of 10 cm above the bottom, the maximum 2-hour averaged speed during the data record is estimated at 27 cm/s, corresponding to a 2.7 m speed of 36 cm/s.

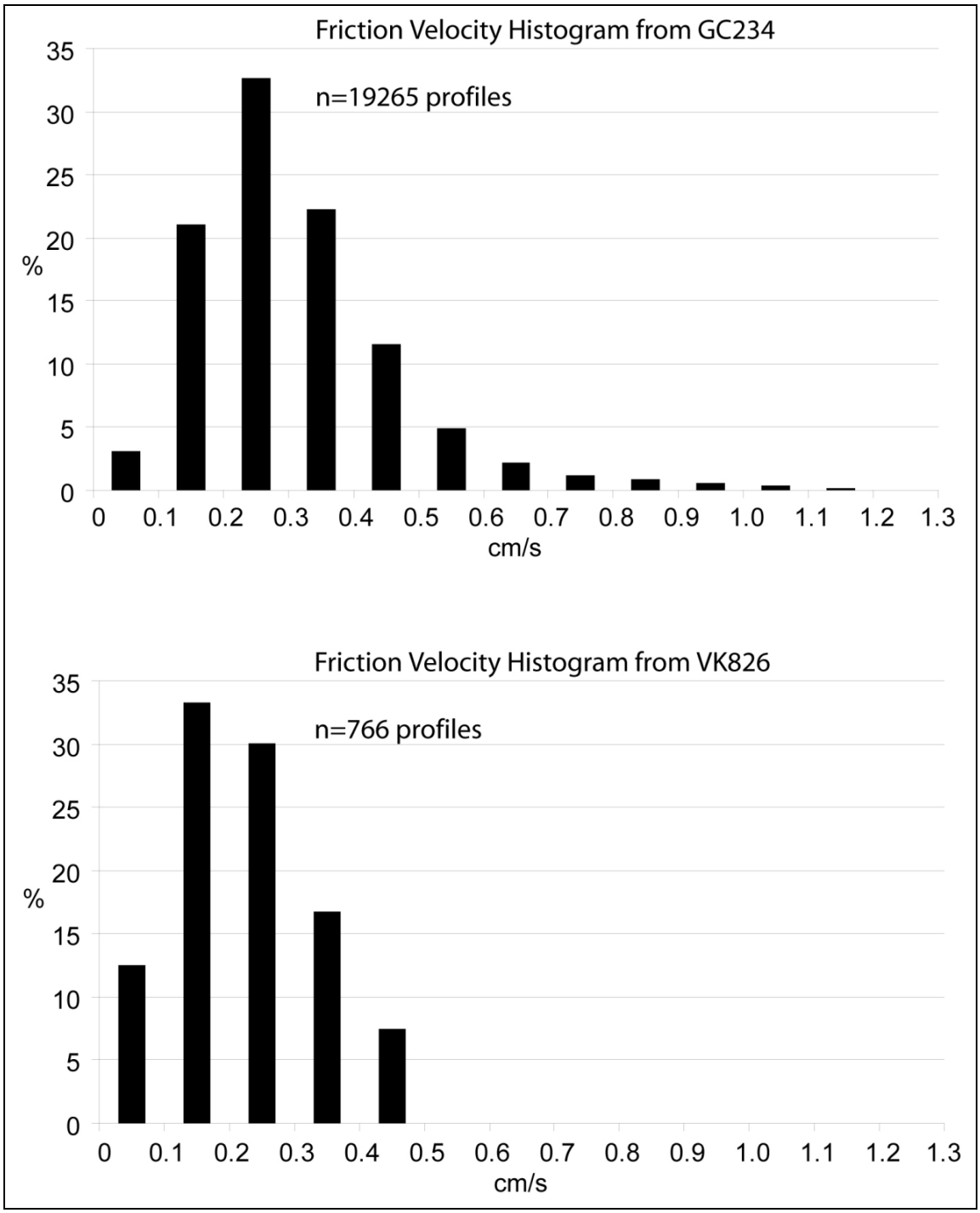

Figure 3.7. Histograms of the friction velocity u_* estimated from the profile method applied to the lower current meter data at GC234 and VK826.

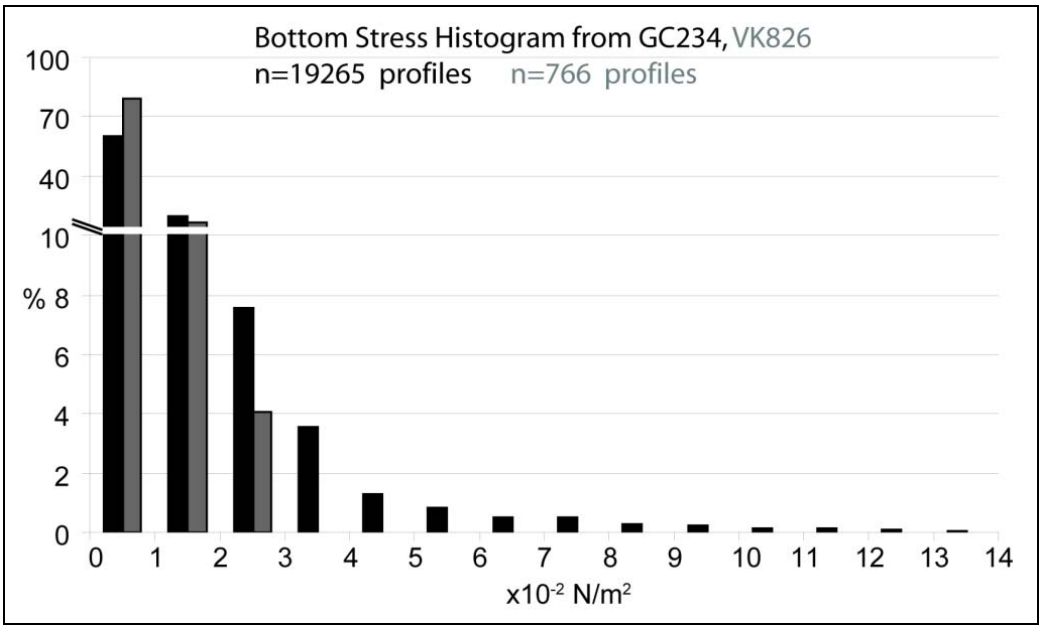

Figure 3.8. Histogram of bottom stress magnitude τ at GC234 (black) and VK826 (gray). Note that the ordinate is expanded from 0 to 10%.

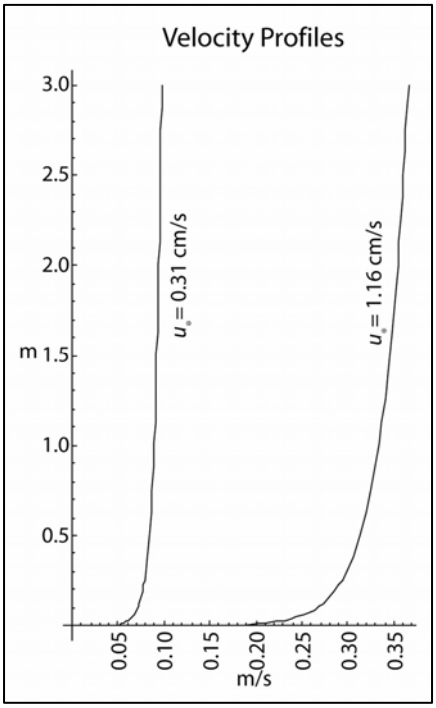

Figure 3.9. Velocity profiles estimated by a logarithmic boundary layer for $z_0 = 10^{-5}$ m. Profiles are drawn for the average and maximum friction velocities calculated from the GC234 current meter data.

3.3.3 Model Velocity and Upper Ocean Chlorophyll Climatology

Morey et al. (2003a,b) and Zavala-Hidalgo et al. (2003) describe the seasonal variability of the near surface circulation in the northern Gulf of Mexico, focusing particularly on the continental shelves. These works showed that the circulation on the shelves is primarily driven by the local winds, which have a strong seasonal signal. The wintertime circulation is typically downcoast (with the coast to the right of the current direction in the northern hemisphere), with rather stagnant conditions over the LATEX (Louisiana–Texas) Shelf and weak eastward flow to the east of the Mississippi River Delta during the late spring through summer. These papers also discuss the fact that the ocean circulation offshore of the continental shelf break is largely governed by the mesoscale eddy field. Thus, the seasonal cycle of local forcing dominates the variability on the shelves, and mesoscale eddy variability dominates offshore of the continental shelf.

Mean surface currents are dominated by the Loop Current and other anticyclonic features (**Figure 3.10**). One should not infer from the mean fields that these are persistent features, as the circulation in the Gulf is highly variable. The anticyclone to the northwest of the Loop Current appears in the mean field due to the slow propagation of Loop Current Eddies during their final stage before detachment from the Loop Current and their early stages subsequent to detachment. Another anticyclonic feature in the northwestern Gulf appears due to this being a preferred location for old Loop Current Eddies to spin down during the decaying phase of their life cycle. Westward currents over the inner LATEX Shelf appear in the mean due to the strong wintertime downcoast flow that is stronger than the weak and variable flow that exists over this shelf during the summer months. This seasonal cycle has been demonstrated using a similar numerical model (Zavala-Hidalgo et al. 2003) and in drifter observations (Nowlin et al. 2001).

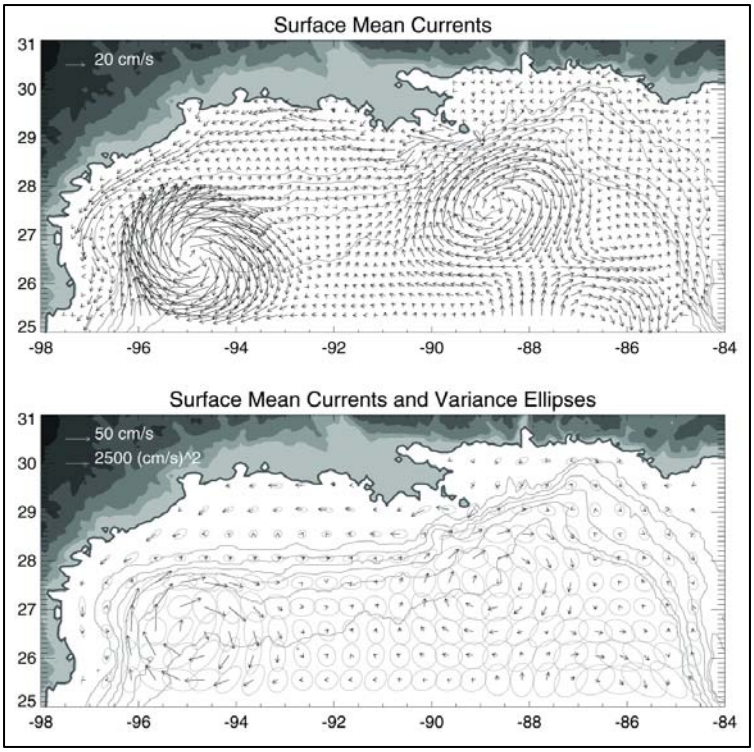

Figure 3.10. Mean surface currents and variance ellipses computed from 8 years of data from a climatologically forced Gulf of Mexico numerical simulation. Isobaths are contoured at 50, 100, 200, 500, 1,000, and 2,000 m in this and subsequent maps. Tails of the vectors are placed in the centers of the model grid cells, and every fourth vector in each direction is plotted. The vectors with anomalous directions near the Mississippi Delta in this and Figure 3.12 are due to velocities associated with the grid cell in which the river mass source is specified, and the effects are only localized about this surface grid cell.

The mean currents at 400 m (**Figure 3.11**) show a similar pattern to the surface currents away from the shelf, with an anticyclonic feature to the south of De Soto Canyon and another in the northwestern Gulf. One important difference is an eastward flow along the continental shelf slope south of the LATEX Shelf. This, together with the anticyclonic features and the Loop Current, forms an anticyclonic circulation around the northern Gulf of Mexico basin. This trait has been shown at the 500 m level from a different numerical model (Nowlin et al. 2001). Another characteristic of the 400 m velocity field is that the semimajor axes of the variance ellipses are strongly oriented in the along-isobath direction near the shelf slope, indicative of primarily along-isobath variability of the currents.

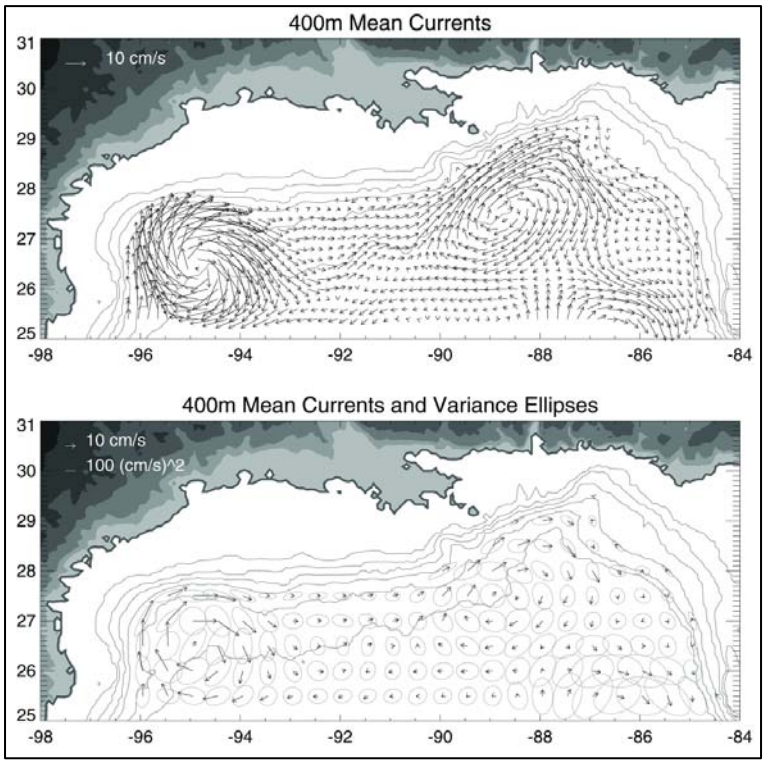

Figure 3.11. 400-m currents and variance ellipses computed from 8 years of data from a climatologically forced Gulf of Mexico numerical simulation.

Monthly climatology surface current maps for January and July appear similar to the maps of the long term averaged currents, with the exception of seasonal current reversals over the shelves (**Figure 3.12**). The wintertime coastally trapped westward flow over the LATEX Shelf disappears during the summer when an eastward flow over the outer shelf appears. Less evident, but of great importance to the redistribution of shelf water, is a seasonal reversal over the MAFLA (Mississippi–Alabama–Florida) Shelf to the east of Louisiana. The flow is weakly southward and westward toward the Mississippi Delta during the winter months and eastward toward De Soto Canyon in the summer months, due to seasonal wind reversals.

No seasonal variability of significance is evident in the January and July monthly climatology velocity maps at 400 m (**Figure 3.13**). This should be expected as the impacts of local wind-driven variability are primarily confined to the upper Ekman layer and not felt at this depth. The local surface forcing is the greatest contributor to seasonal variability in the Gulf of Mexico as the mesoscale eddy field, which dominates the circulation variability below the surface mixed layer, has no seasonal component.

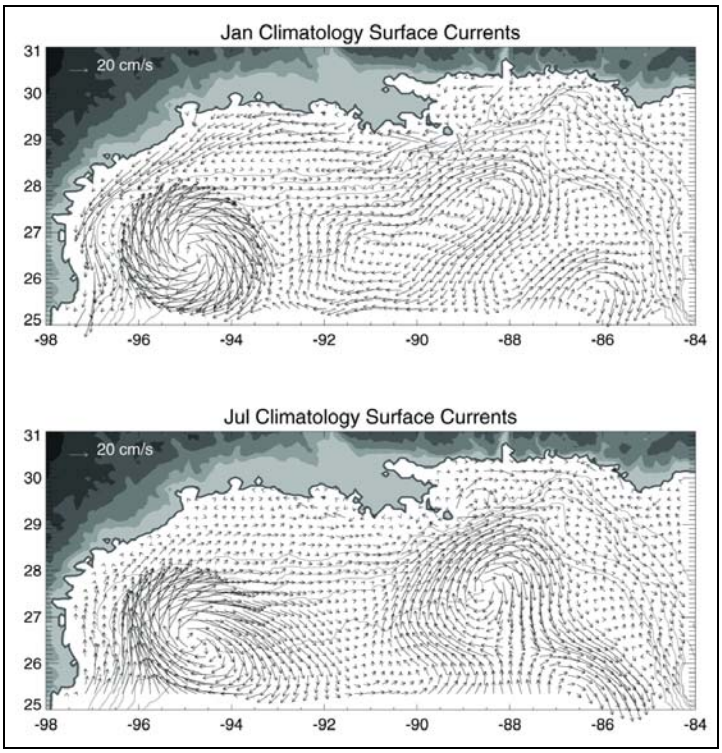

Figure 3.12. Monthly climatology surface currents for January and July computed from 8 years of model data.

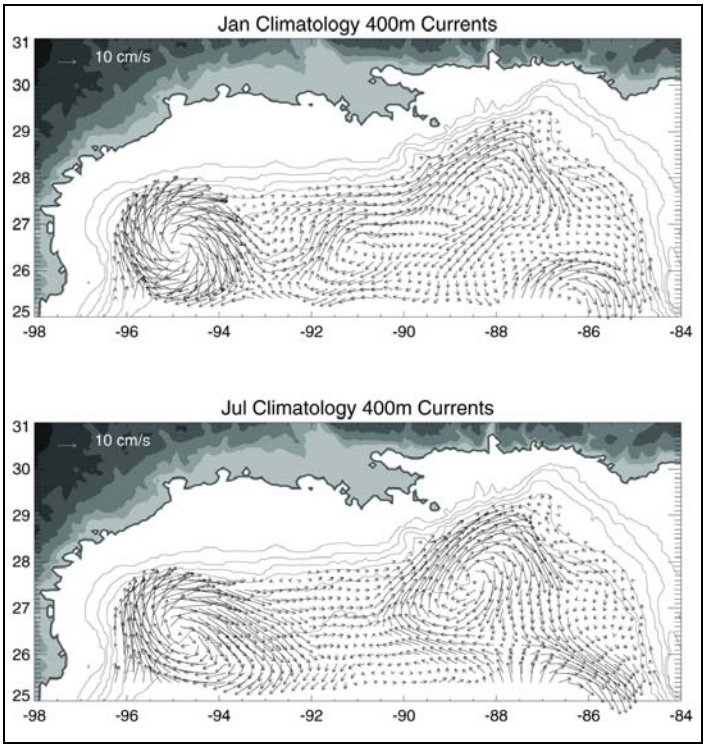

Figure 3.13. Monthly climatology currents at 400 m for January and July computed from 8 years of model data.

At the shelf break, there is significant interaction between the shelf water and the deep ocean due to the interaction of the wind-driven cross-shelf transport and the subsequent entrainment and transport throughout the deep ocean by the deep ocean eddies. Morey et al. (2003b) showed that the seasonal variability of the wind-driven circulation over the shelf in the region of large freshwater input largely dictated the salinity of the shelf water, most importantly near the shelf break. Therefore, the properties of the water transported offshore from the outer shelf edge by eddies also can have a large seasonal component. The most striking example of this occurs at the western De Soto Canyon near the MAFLA Shelf. The weak eastward wind-driven flow over the shelf during the spring and summer (shown in **Figure 3.12**) transports low salinity water from the Mississippi (and Atchafalaya) Rivers eastward over the shelf break at De Soto Canyon, where it can be entrained by the offshore eddy field and transported away from the shelf. This riverine influenced water is also biologically rich due to the enhanced nutrient concentrations of the river discharged fresh water. This means that the seasonal cycle of the redistribution of the riverine influenced water leads to a seasonal cycle of the upper ocean chlorophyll content in the northeastern Gulf of Mexico that can be observed from satellite ocean color data (Morey et al. 2003b). Extending eastward over De Soto Canyon and southeastward offshore of the West Florida Shelf, there is a high chlorophyll tongue-like pattern during the summer and low chlorophyll concentrations during the late fall and winter (**Figure 3.14**). This signal is stronger closer to the shelf, and weakens along the pathway (roughly following the eastern edge of the mean position of the Loop Current) by which this water is exported from the region. Elsewhere in the Gulf of Mexico, wintertime deepening of the surface mixed layer (entraining nutrient-rich water from below) can enhance the productivity in the upper ocean.

Monthly climatologies of chlorophyll *a* derived from the SeaWiFS ocean color satellite are averaged within 0.5° x 0.5° bins centered at the Viosca Knoll and Green Canyon locations (**Figure 3.15**). Viosca Knoll exists in the heart of the summertime high chlorophyll tongue discussed above. The influence of this seasonal pattern is evident in the monthly climatology time series from the Viosca Knoll location as a summertime maximum. The Green Canyon location lies outside of this high chlorophyll tongue. Here, there is a secondary maximum in the upper ocean chlorophyll content during the summer, possibly due to the spreading of the riverine influenced coastal water over the shelf by the slow broad eastward flow, or perhaps due to the late spring maximum of river discharge. The January chlorophyll maximum here could be a result of enhanced productivity in the upper ocean due to wintertime mixed-layer deepening.

3.3.4 Simulations of Larval Advection

Particle density maps produced by the numerical advection algorithm show typical distances and pathways that particles may travel at a constant depth in a given time from a specific location. This experiment has been carried out to provide some insight on how freely drifting particles at a particular depth released at a given location may be redistributed by ocean currents. The experiment is designed to yield information on how far larvae released from a specific site may typically travel during their lifespan, and to test hypotheses that larvae distributions may vary from season to season, or year to year.

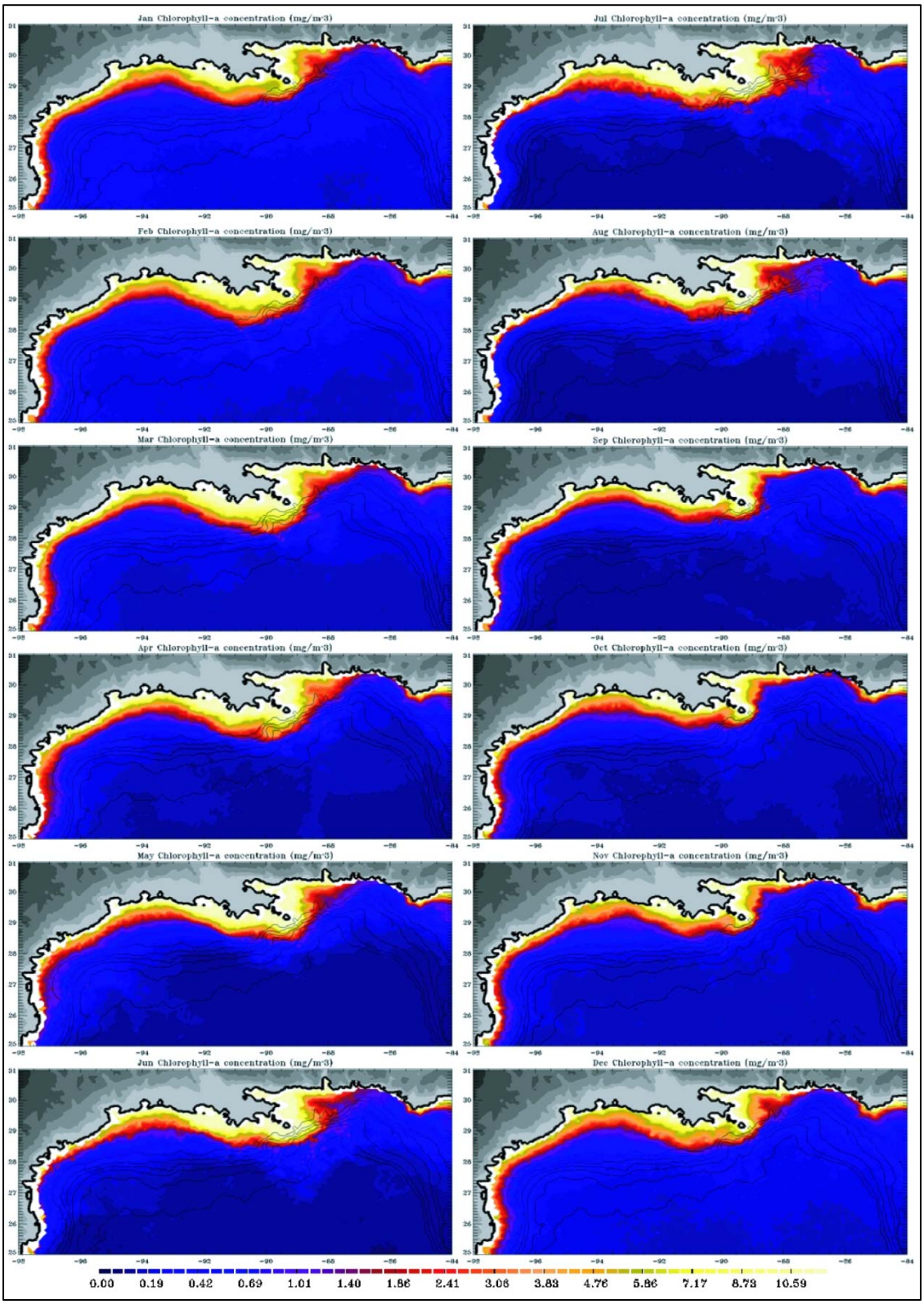

Figure 3.14. Monthly climatology chlorophyll *a* concentration (mg/m^3) from SeaWiFS ocean color data (1997-2004) mapped to a 9-km grid. Note the eastward spreading of a high-chlorophyll tongue over De Soto Canyon during the summer.

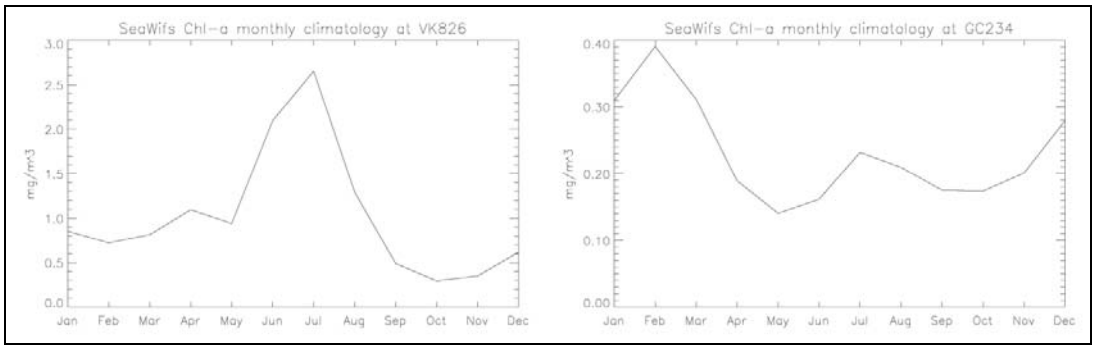

Figure 3.15. Monthly climatology chlorophyll *a* from SeaWiFS ocean color data (1997-2004) averaged over 0.5° x 0.5° bins centered at the locations of Viosca Knoll (29.15°N, 88.02°W) and Green Canyon (27.75°N, 91.22°W).

Particles released from the of VK826 location are distributed primarily along the continental shelf slope, and preferentially eastward (**Figure 3.16**). The eastward drifting particles travel around the De Soto Canyon and southward along the West Florida Shelf slope. Few particles find their way west of the Mississippi Canyon. Some particles are transported out into deeper water. Due to the configuration of the numerical model and the design of this Lagrangian particle experiment, it is not possible for the simulated particles to be advected into shallower water.

The particles released from the GC234 site initially spread nearly symmetrically east and west along isobaths (**Figure 3.17**). After the initial few days, dispersion of particles to the west slows and the eastward extent of the particle distribution expands past the Mississippi Canyon. With time, this eastward spreading continues primarily along the shelf slope around the De Soto Canyon and southward along the outer West Florida Shelf slope. This eastward limb of the particle concentration pattern is similar to the pattern of particle distribution from Viosca Knoll.

Inspection of monthly climatology maps shows little interseasonal variability in the distribution patterns. There is some evidence that particles released during the winter may be less widely dispersed than during the other seasons, but the lack of *obvious* interseasonal variability is consistent with the analysis of the model climatology at 400 m presented earlier in this chapter. Interannual variability in the distribution patterns might be expected due to the interannual variability of the deep ocean mesoscale eddy field. However, the particle distribution maps show only minor differences from year to year, with the characteristic along-isobath and eastward preference exhibited in all years.

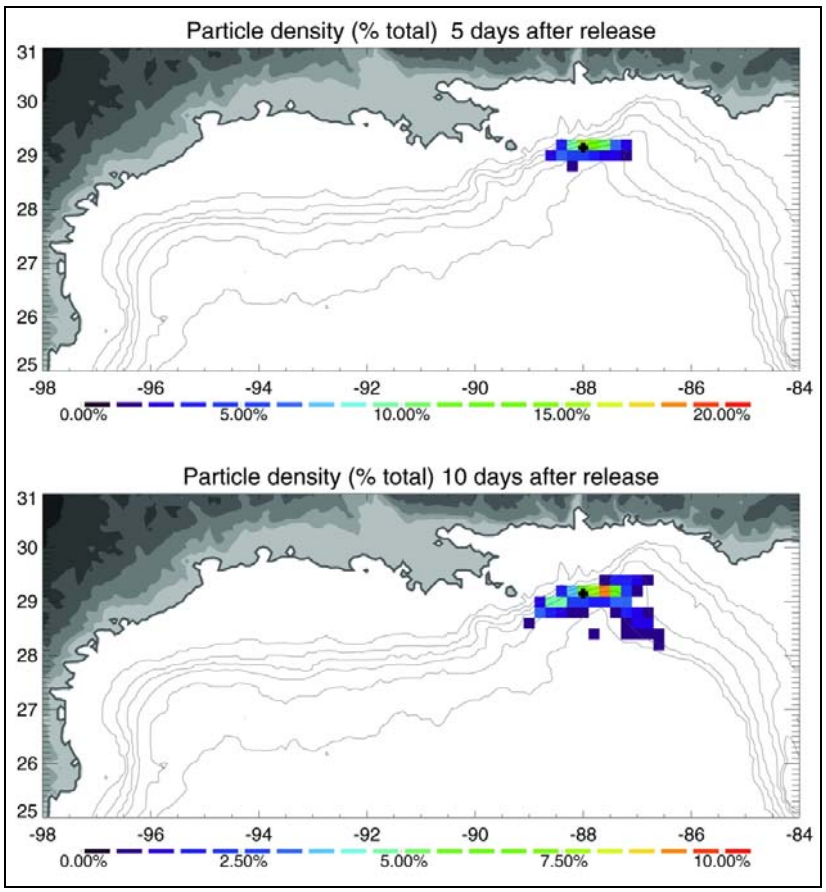

Figure 3.16. Mean particle distributions for particles released from VK826 at 5, 10, 15, 20, and 25 days after release. In this and the following figures, each 0.2 x 0.2° box is colored by the concentration of particles existing within it a given time after deployment in any month or year. The concentrations are measured in percentage of total particles (1,200 per month for 8 years, or 115,200 particles). These maps are essentially the mean particle concentrations for given particle lives over the entire 8-year model simulation. Note that the scale on the colorbar may change for each map. The release location is identified with a +. On these and subsequent maps, the 50, 100, 200, 500, 1,000, and 2,000 m isobaths are plotted.

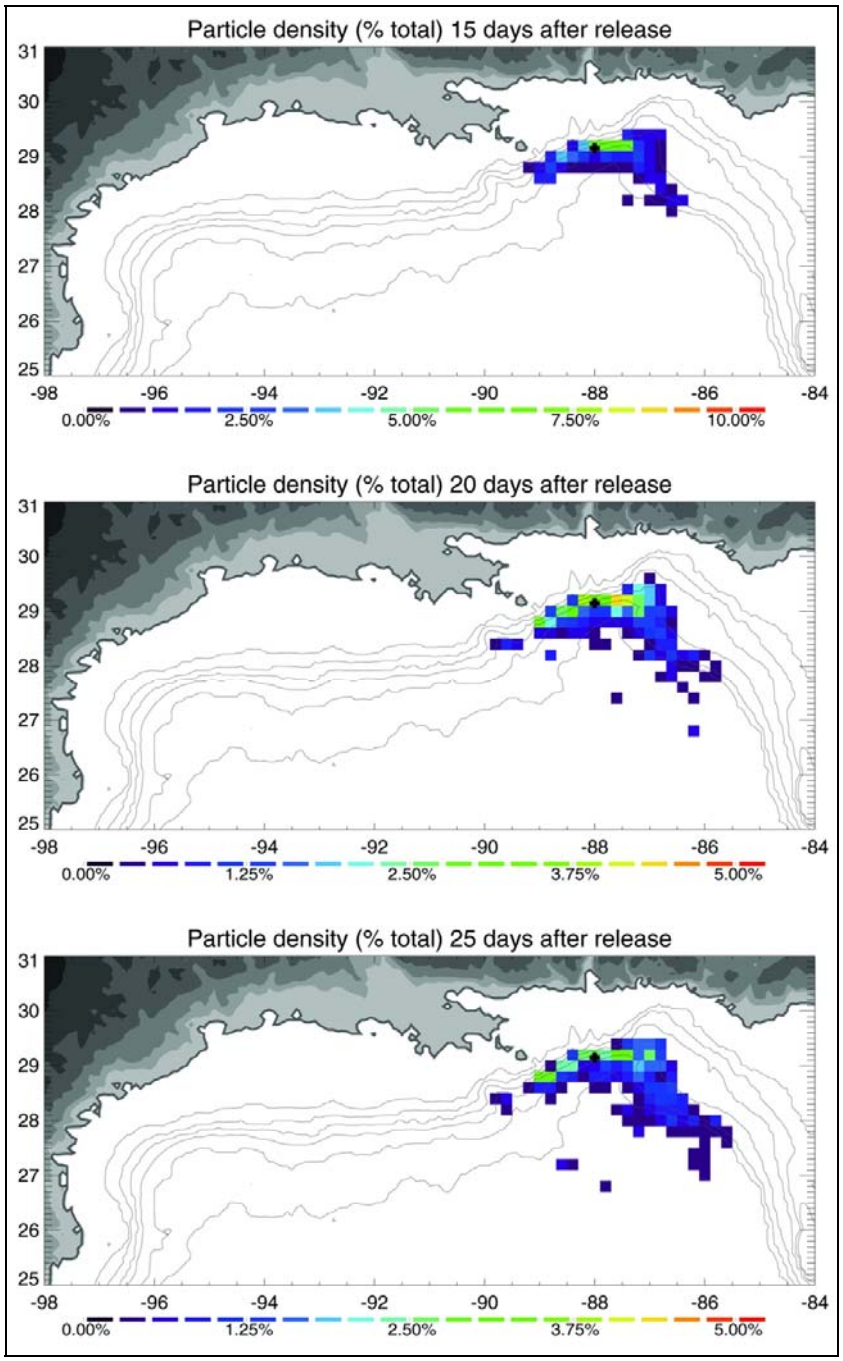

Figure 3.16. (Continued).

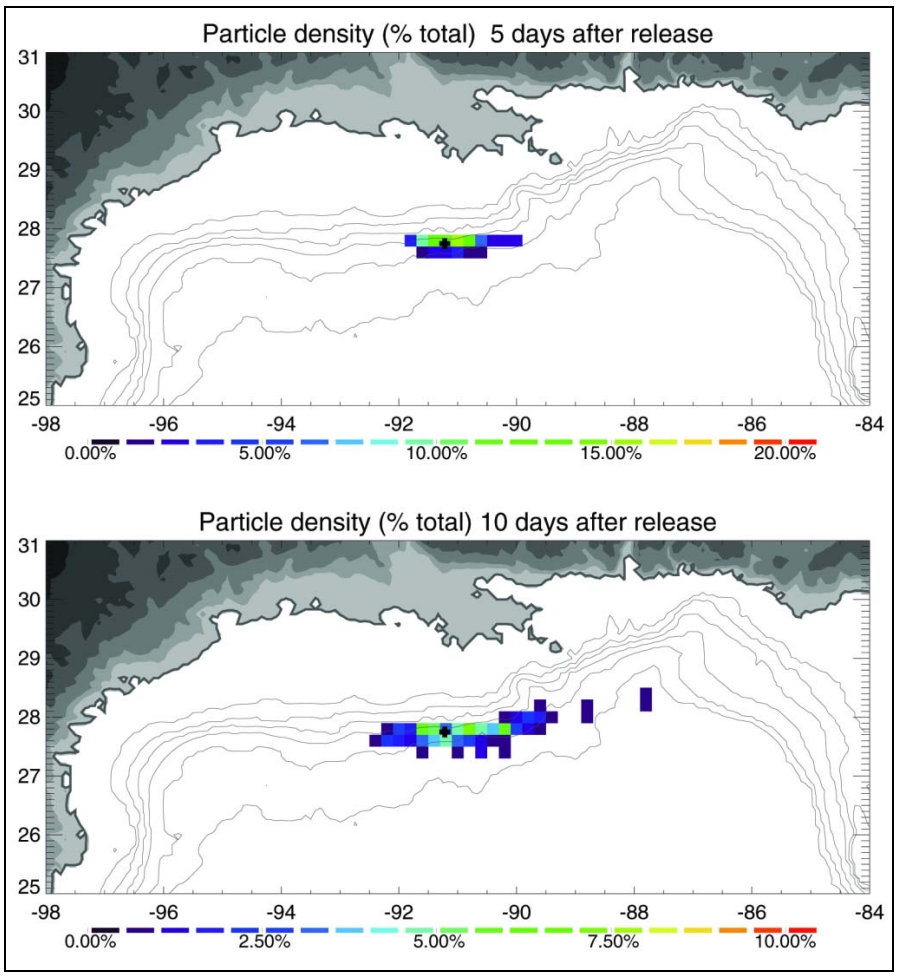

Figure 3.17. Mean particle distributions for particles released from GC234 at 5, 10, 15, 20, and 25 days after release, as in **Figure 3.16**.

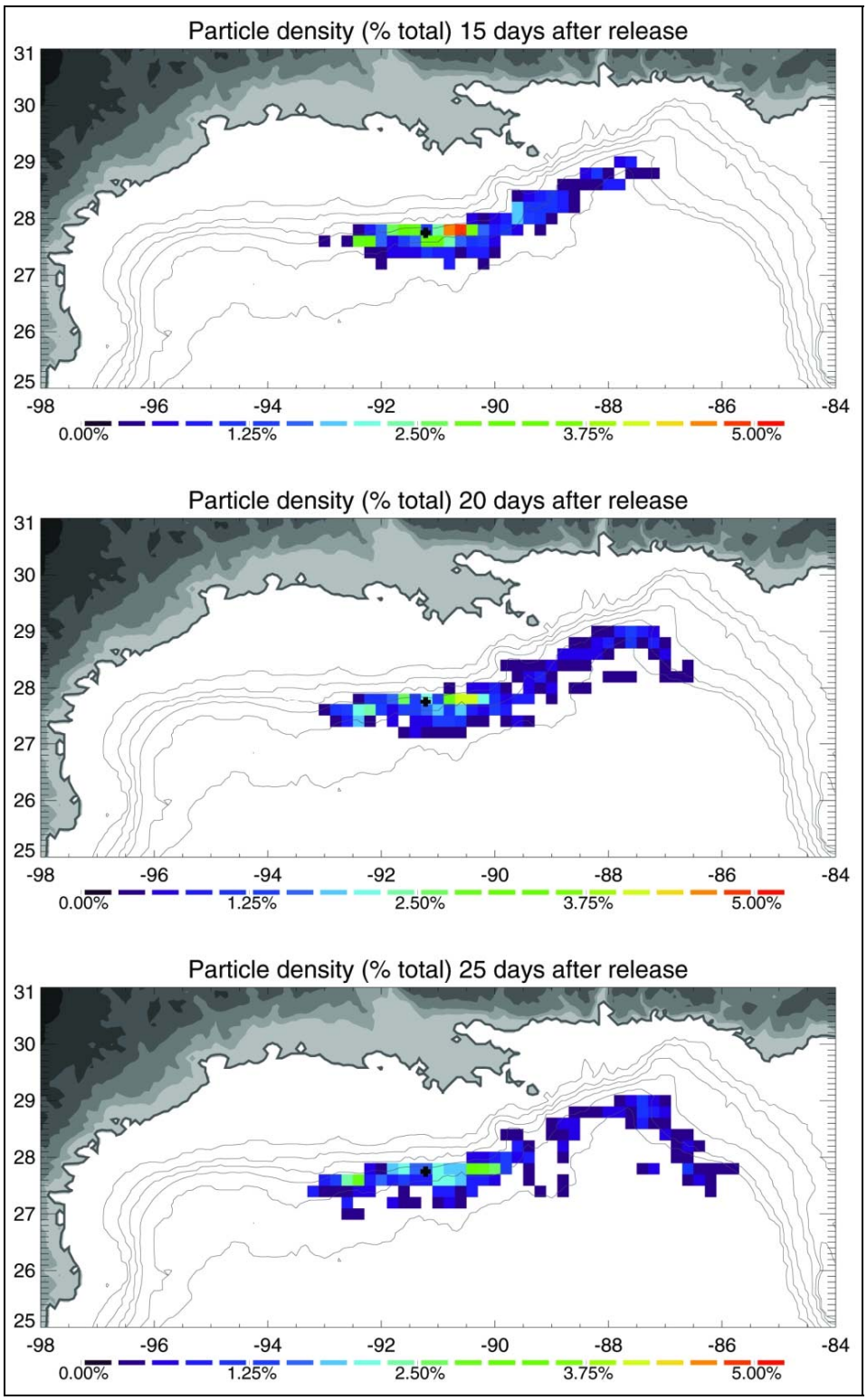

Figure 3.17. (Continued).

Chapter 4
Geological Characterization

William W. Schroeder

4.1 INTRODUCTION

The geological characterization of study sites included visual observations of each site, collection of sediment samples for grain size analysis, and collection of rock samples for carbon and oxygen isotope analysis. Prior to Cruise 1, bathymetric and local-landscape scale descriptions for each study site were prepared from published and unpublished reports, maps, and other data (e.g., archived submersible dive logs, photographic records, and geophysical data). These descriptions, along with logs from previous submersible dives, were then used to select target dive locations for each study site.

Geological Characterization

- The seabed was characterized at all sites based on video and photographic observations.
- Sediment grain size samples were collected at all alpha and beta sites (except MC709).
- Carbonate rock samples were collected at selected sites for isotope analysis.

4.2 METHODS

4.2.1 Seabed Characterization

Video and digital photography and visual observation records were collected during each submersible dive. These data serve as the principal sources of documentation used for characterization of the site-specific features and sampling-site micro-habitats at each study site. The quantity and quality of the documentation obtained during each dive varied significantly in that it was dependent on the planned dive-work tasks, the actual times required to successfully achieve those tasks, the area covered during the dive, and visibility.

Additional bathymetric data for each site were also collected during both the 2004 and 2005 cruises when the *R/V Seward Johnson II* was not conducting submersible operations. These surveys served to confirm target locations for scheduled dives and provide documentation of the bathymetry adjacent to each site.

Seabed characterizations of the surficial geology at and surrounding the study sites were developed at four spatial scales:

- Continental slope regions or major physiographic feature(s)
- Local-landscape
- Site-specific features
- Sampling-site micro-habitats

Continental slope regions or major physiographic features, at scales of 2,500 km^2 (50 x 50 km) to 10,000 km^2 (100 x 100 km), are modifications of classification systems found in Martin and Bouma (1978), Bryant et al. (1991) and Taylor et al. (2000). Local-landscape descriptions of the seabed surrounding each site, at scales of 4 km^2 (2 km x 2 km) to 25 km^2 (5 km x 5 km), are based on published literature (e.g., Reilly et al. 1996; Sager et al. 1999; Schroeder 2002; MacDonald et al. 2003), unpublished reports (e.g., Fugro-McClelland undated), maps (e.g.,

Taylor et al. 2000), and available archived geophysical data (e.g., multibeam bathymetry and side-scan sonograph records). Descriptions of site-specific features are principally based on photographic documentation (video and digital images) and *in situ* observations obtained during manned submersible and U.S. Navy submarine NR-1 operations and, when possible, supplemented with material from published (e.g., Roberts and Aharon 1994) and unpublished sources.

Accurate navigation data for determining the position of the *JSL* during some dives in both 2004 and 2005 were problematic. For example, water depths reported at positions for the *JSL* do not agree with the known bathymetry of the dive site. This most often occurred during dives that investigated large areas or required long transits between work sites. In other cases the recorded positions for the *JSL* plot out in a scattered manner not consistent with the known sequence of stops and moves made during the dive. For some dives, subjective/qualitative corrections could be applied to the questionable dive tracks to reduce the degree of position uncertainty. Unfortunately, the navigation during a few dives remains unreliable.

4.2.2 Sediment and Rock Samples

Sediment samples were collected at the study sites for laboratory analysis of sediment grain size. In addition, carbonate rock samples were collected at each study site for laboratory analysis of carbon and oxygen stable isotopes (^{13}C and ^{18}O). **Table 4.1** summarizes the numbers of samples collected at each site. Sediment grain size was analyzed by Dr. Wayne Isphording (University of South Alabama/Tierra Consulting). Standard sieve and hydrometer methodologies were used as specified in American Society for Testing and Materials (ASTM) D-422. Sediment textural descriptions were prepared based on Folk (1954). Analytical methodologies for the isotope analyses are described in *Chapter 5*.

Table 4.1. Geological tasks by cruise.

Site	Geological Reconnaissance		Sediment Grain Size Samples		Carbonate Rock Samples for Isotope Analysis	
	Cruise 1	Cruise 2	Cruise 1	Cruise 2	Cruise 1	Cruise 2
Alpha Sites						
GC234	X	X	5	--	5	--
GC354	X	--	6	--	2	--
VK826	X	X	5	--	--	5
Beta Sites						
MC885	X	X	--	3	--	--
VK862	X	--	3	--	2	5
MC709	X	--	--	--	--	--
GC184/185	--	X	--	3	--	1
NOAA-OE Sites						
MC929	--	X	--	--	--	2
VK826NE	--	X	--	--	--	--
VK862S	--	X	--	--	--	4

4.3 RESULTS AND DISCUSSION

The sites investigated during the 2004 and 2005 field seasons represent four continental slope regions (**Table 4.2**, **Figure 4.1**). These regions and categories are modified versions of the submarine topography classification schemes presented in Martin and Bouma (1978), Bryant et al. (1991) and Taylor et al. (2000). Sediment texture data are presented in **Table 4.3**, and isotope data for rock samples are summarized in **Table 4.4**.

Table 4.2. The study sites, grouped by the continental slope region or major physiographic feature category in which they are located (Modified from Martin and Bouma [1978], Bryant et al. [1991] and Taylor et al. [2000]).

Continental Slope Region	Study Sites
Upper Central Dome and Basin region – Texas-Louisiana Slope subprovince	GC354, GC184/185, GC234
Upper Henderson Ridge – Upper Mississippi Fan subprovince	MC929, MC885
Upper Mississippi Canyon – Upper Mississippi Fan subprovince	MC709
Upper DeSoto Slope subprovince	VK862 and 862S; VK826 and 826NE

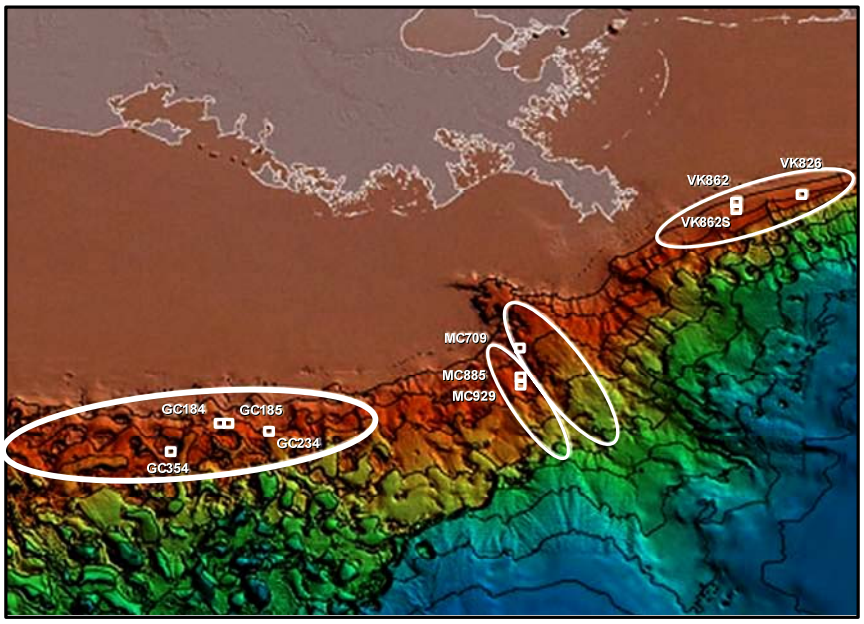

Figure 4.1. Continental slope regions or major physiographic feature categories in which study sites are located. From left to right: Upper Central Dome and Basin region – Texas-Louisiana Slope subprovince; Upper Henderson Ridge – Upper Mississippi Fan subprovince; Upper Mississippi Canyon – Upper Mississippi Fan subprovince; and Upper DeSoto Slope subprovince.

Table 4.3. Sediment textural descriptions (after Folk 1954).

Site	Sample No.	Textural Description
GC354	C1	Clay
	C2	Clay
	C3	Clay
	C4	Clay
	C5	Clay
	C6	Clay
GC184/185	C1	Clay
	C2	Mud
	C3	Clay
GC234	C1	Clay
	C2	Clay
	C3	Clay
	C4	Clay
	C5	Clay
MC929	No samples	--
MC885	C1	Clay
	C2	Clay
	C3	Clay
MC709	No samples	--
VK862	C1	Gravelly mud
	C2	Slightly gravelly sandy mud
	C3	Slightly gravelly muddy sand
VK862S	No samples	--
VK826	C1	Slightly gravelly mud
	C2	Slightly gravelly sandy mud
	C3	Slightly gravelly sandy mud
	C4	Slightly gravelly sandy mud
	C5	Gravelly mud
VK826NE	No samples	--

Table 4.4. Carbon and oxygen isotope data from rock samples. Samples are reported in standard delta notation relative to Vienna Peedee belemnite (VPDB).

Site	ID	$\delta^{13}C$	$\delta^{18}O$	Species
GC 354	4741-1	-42.45	–	Carbonate
	4741-2	-43.76	–	Carbonate
GC184/185	4862-100	-24.89	3.49	Carbonate
GC 234	4724-1	-3.37	–	Carbonate
	4724-2	-42.51	–	Carbonate
	4724-3	-37.22	–	Carbonate
	4724-4	-41.42	–	Carbonate
	4724-5	-45.88	–	Carbonate
MC929	4864-4	-40.61	3.71	Carbonate
	4864-100	-43.08	3.83	Carbonate
VK826	4867-1	-13.12	3.51	Carbonate
	4867-5	-14.02	3.36	Carbonate
	4867-32	-11.05	3.62	Carbonate
	4867-33	-11.14	3.17	Carbonate
	4867-34	-18.01	3.86	Carbonate
VK862	4734-100	-23.60	5.81	Carbonate
	4734-101	-9.05	5.89	Carbonate
	4734-102	-26.89	4.91	Carbonate
	4734-103	-21.39	–	Carbonate
	4734-104	-23.87	–	Carbonate
	4869-46	-12.06	5.48	Carbonate
	4869-48	-23.61	3.84	Carbonate
	4869-50	-22.18	3.67	Carbonate
	4869-100	-12.53	4.54	Carbonate
	4869-101	-21.00	4.25	Carbonate
VK862S	4870-1	-3.02	3.86	Carbonate
	4870-2	-3.00	4.34	Carbonate
	4870-100	-15.25	3.52	Carbonate

4.3.1 Upper Central Dome and Basin Region – Texas-Louisiana Slope Subprovince

Three study sites are located in this region: GC354, GC184/185, and GC234. A detailed view of the area encompassing these three sites is presented in **Figure 4.2** and illustrates the multifaceted nature of the seabed in this region. The complex dome and basin physiography is the result of the interplay between the accumulation of thick sediment deposits and compensating salt and shale tectonics (Bryant et al. 1991).

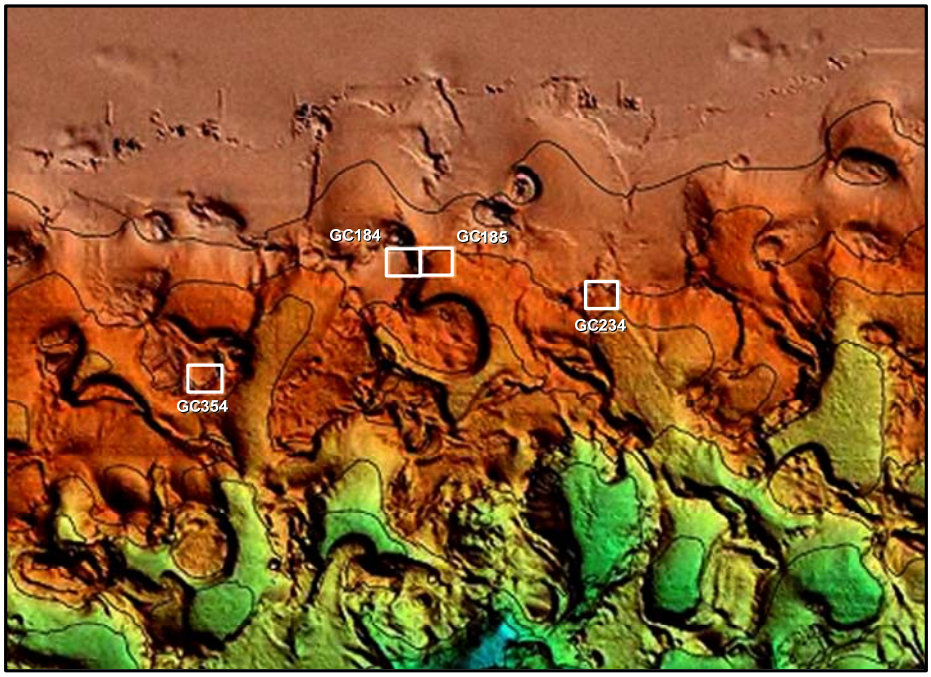

Figure 4.2. Detailed view of the locations of study sites GC354, GC184/185 and GC234 in the Upper Central Dome and Basin region on the Texas-Louisiana Slope subprovince.

Green Canyon 354

GC354 is the westernmost study site (**Figure 4.1**). It is located on the seaward edge of the rim of a plateau-like feature adjacent to a steep scarp (**Figure 4.2**). The explored portion of this site, centered at approximately 27°35.85'N, 91°49.50'W, lies on a slope descending from 520 to 560 m. Clay size sediment was collected in all six of the cores obtained from this site (**Table 4.3**). Based on the observed chemosynthetic activity in this area it is assumed that the indurated substrates present are authigenic in origin[1]. Scattered across the slope are low-relief buildups/outcrops (**Figure 4.3**), what appear to be mounds of sediment capped with medium to small clasts and nodules (**Figure 4.4**), and very low-relief buildups/outcrops with assorted boulder to debris size clasts (**Figure 4.5**). The buildups/outcrops tend to be moderately to highly eroded and therefore are generally irregular in shape (**Figures 4.3** and **4.6**) with very rugose surfaces (**Figure 4.7**). On the other hand, the mounds are most often conical in shape with generally smooth sloping sides (**Figure 4.4**). Many of these features are covered with

[1] In this report, authigenic carbonate refers to carbonate produced as a by-product of coupled methane oxidation and sulfate reduction by microbial consortia.

predominantly dead *L. pertusa* colonies (**Figures 4.3**, **4.4**, and **4.8**), while others are mostly uncolonized (**Figures 4.6** and **4.7**). Some of these features have large tubeworm aggregations at their bases (**Figure 4.9**). In addition, living and dead *Madrepora oculata* colonies have been observed on the lower-slope mounds.

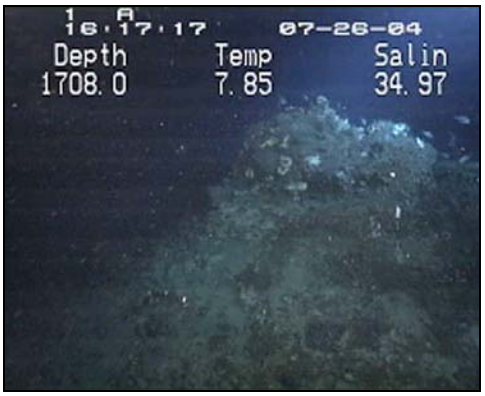

Figure 4.3. A 2.1-m tall buildup partially covered with mostly dead *L. pertusa* colonies (GC354).

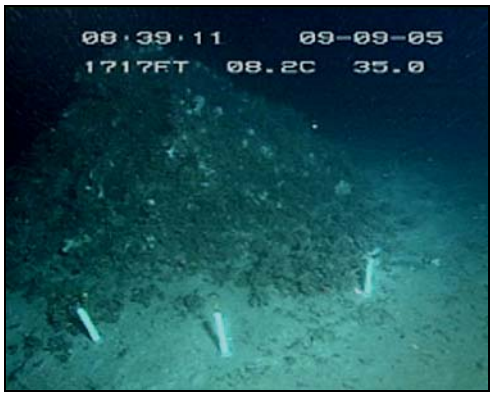

Figure 4.4. A 1.9-m tall carbonate capped mound partially covered with mostly dead *L. pertusa* colonies (GC354).

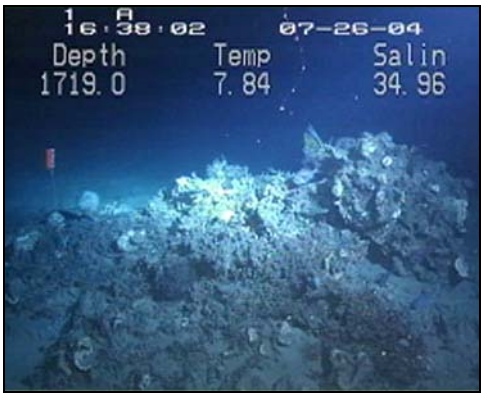

Figure 4.5. Low-relief buildups/outcrops with assorted boulder to debris size clasts (GC354).

Figure 4.6. Example of eroded irregular shaped buildup (GC354).

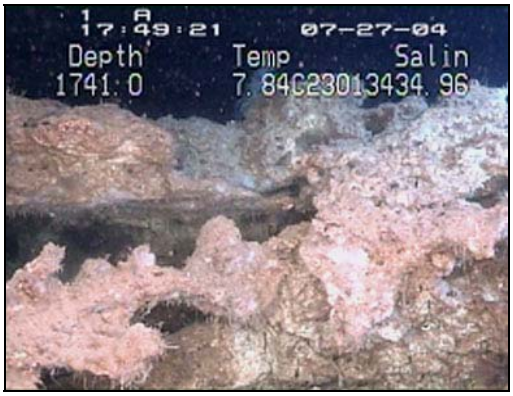

Figure 4.7. Close-up of a rugose, uncolonized surface on the buildup in **Figure 4.6** (GC354).

Figure 4.8. Close-up of mostly dead *L. pertusa* near the top of the mound in **Figure 4.4** (GC354).

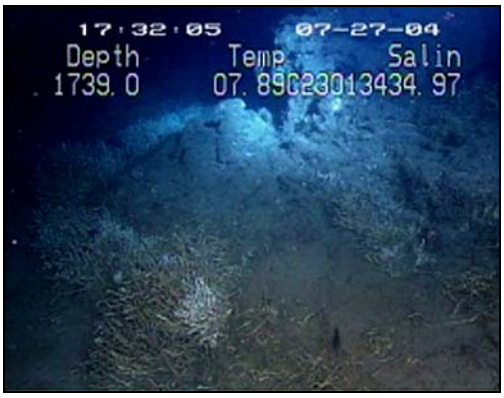

Figure 4.9. Uncolonized 1.9-m tall buildup with large tubeworm brushes around its base (GC354).

Green Canyon 184/185

Known as Bush Hill and located on the boundary of MMS lease blocks GC184 and GC185, this site is situated on the crest of a 40-m tall, authigenic carbonate capped hillock in about 540 m water depth (**Figure 4.2**). Although only one dive was made here during this project, previous investigations over the past two decades provide extensive documentation of this site (Brooks et al. 1984; Kennicutt et al. 1988; MacDonald et al. 1989; Roberts et al. 1989; Aharon et al. 1997; MacDonald 2002). *JSL* Dive 4862 conducted a northeast to southwest survey across the top of the hillock, generally along a low-relief ridge-like feature composed of a series of exposed buildups/outcrops of authigenic origin (**Table 4.4**; W. Schroeder unpublished data). The area surveyed was centered at approximately 27°46.9'N, 91°30.5'W. Water depths varied from 540 to 546 m. Cored sediments included mud to clay size particles (**Table 4.3**).

In most cases the buildups/outcrops are elongated, somewhat irregular shapes up to 2.5 m in height by 2 to 4 m wide by several meters in length with long-axes predominantly oriented northeast to southwest. Most of them have steep sides, some nearly vertical (**Figure 4.10**). Their

tops vary from nearly flat (**Figure 4.10**) to bumpy or eroded (**Figure 4.11**). Mound surfaces range from smooth (**Figure 4.11**) to eroded/rugose (**Figure 4.10**), often with overhangs on the sides (**Figure 4.12**) and/or undercut at the base (**Figure 4.11**). Most of the buildups/outcrops are covered by large individuals of the gorgonian *Callogorgia americana delta* (**Figures 4.10** and **4.11**) and occasionally by small colonies of *L. pertusa*. Boulder to smaller size clasts and nodules are often observed immediately adjacent to or at gaps between buildups (**Figure 4.13**).

Figure 4.10. A buildup with steep nearly vertical sides and a flat top covered with an assemblage of large *Callogorgia americana delta* colonies (GC184/185).

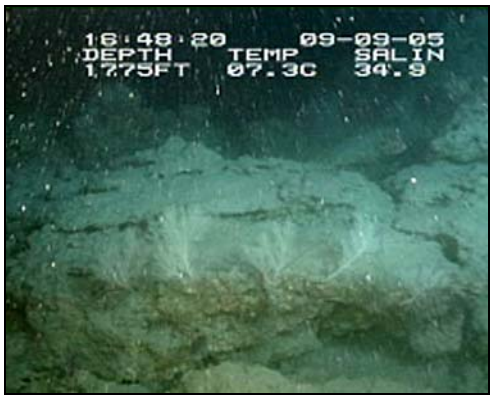

Figure 4.11. A buildup with a bumpy top and undercut at its base with large *Callogorgia americana delta* colonizing the sides (GC184/185).

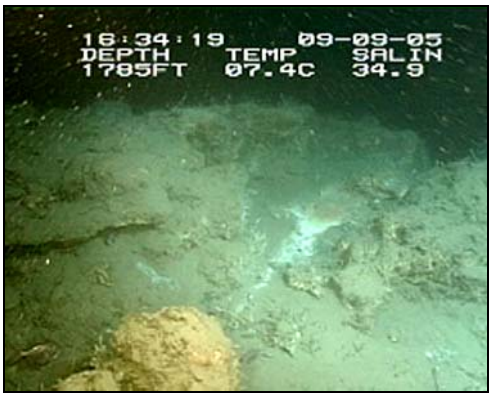

Figure 4.12. A buildup with a small overhang (left) on its side (GC184/185).

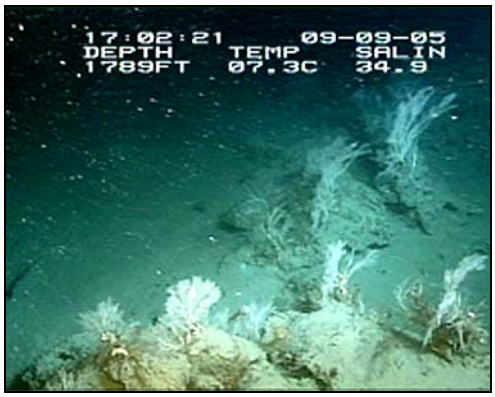

Figure 4.13. Boulders and smaller clasts and nodules in a gap between two buildups colonized by large *Callogorgia americana delta* (GC184/185).

Green Canyon 234

Also located in the upper central dome and basin subprovince on the Texas-Louisiana slope, GC234 is situated within a graben/half-graben complex in a shallow depression (Reilly et al. 1996) (**Figure 4.2**). The study area is centered at about 27°44.8'N, 91°13.4'W, in water depths of 500 to 530 m. The fault that formed the half-graben is aligned roughly north-south so that the vertical offset along the fault produces a west-facing slope. The indurated substrates present are authigenic in origin (**Table 4.4**; W. Schroeder unpublished data), and sediments are clay size (**Table 4.3**).

The primary study area is the set of low-relief, linear outcrops in a ridge-and-swale type setting (**Figures 4.14** and **4.15**) extending across the western rim of the half-graben. Outcrop dimensions are up to 4 to 5 m in width by 250 m in length by 1 m in height. The structure of the linear outcrops alternates between segments of low-relief ridge-like sections of highly rugose substrate (**Figure 4.16**) to partially exposed carbonate at the sediment line (**Figure 4.17**). Short gaps of bare sediment occasionally occur along all the outcrops. Many of the outcrops are covered by both individual and aggregated colonies of primarily dead *L. pertusa* and large colonies of *C. americana delta* (**Figures 4.15, 4.16,** and **4.17**). Down slope to the east, the longer low-relief linear outcrops are replaced by buildups and carbonate capped mounds, and assemblages of *C. americana delta* and tubeworm bushes replace *L. pertusa* as the dominate megafauna (**Figures 4.18** and **4.19**).

Figure 4.14. Low-relief, linear outcrop on the western rim of a half-graben (GC234).

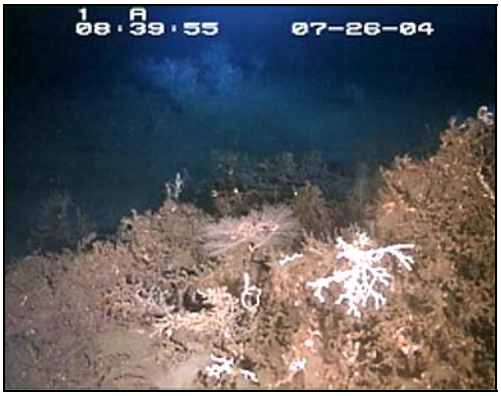

Figure 4.15. Mostly dead *L. pertusa* covering one of the linear outcrops with an adjacent outcrop visible in the background (GC234).

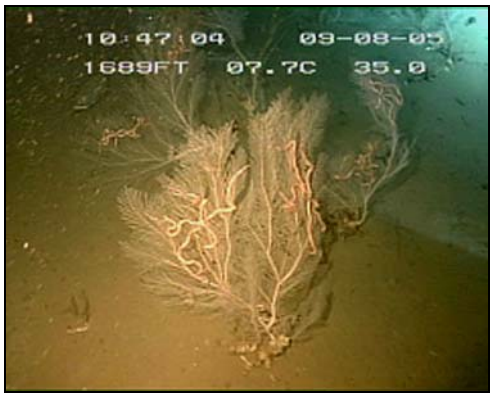

Figure 4.16. Partially exposed carbonate at the sediment line supporting large colonies of *Callogorgia americana delta* (GC234).

Figure 4.17. Low-relief ridge-like section of highly rugose substrate with large colonies of *Callogorgia americana delta* and both living and dead colonies of *L. pertusa* (GC234).

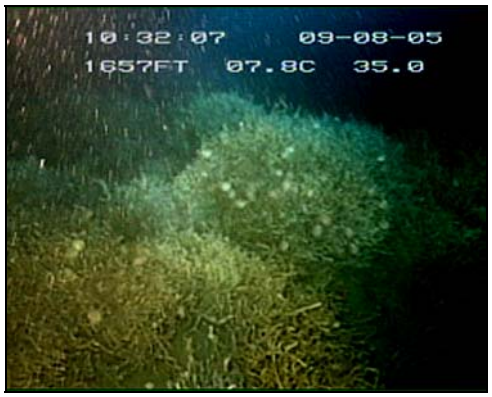

Figure 4.18. Large tubeworm bushes on a carbonate capped mound on the lower slope of the western rim (GC234).

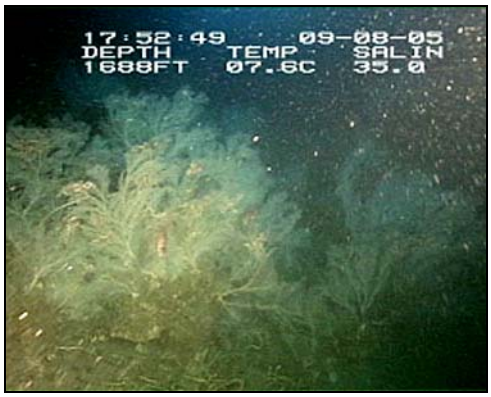

Figure 4.19. Large *Callogorgia* colonies on a carbonate capped mound on the lower slope of the western rim (GC234).

4.3.2 Upper Henderson Ridge – Upper Mississippi Fan Subprovince

The upper portion of Henderson Ridge runs northwest to southeast along the western flank of the Mississippi Canyon from the shelf-break down to 1,500 to 2,000 m (**Figure 4.1**). This region overlies a zone of ongoing salt deformation that is producing currently active sites of hydrocarbon and brine seepage. Two of the study sites, MC929 and MC885, are located on the ridge. A detailed view of the region is presented in **Figure 4.20**.

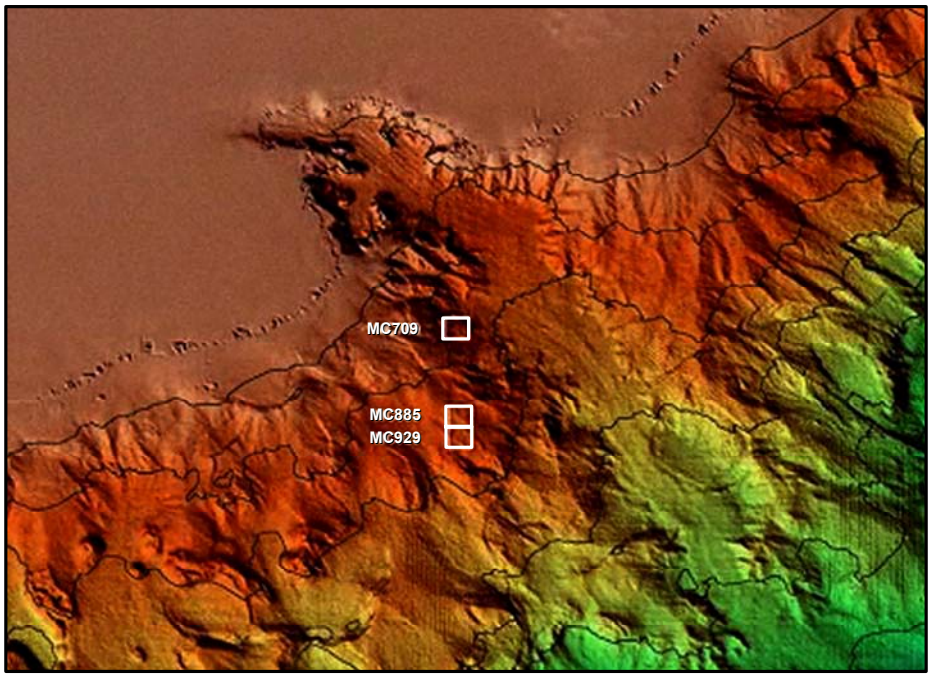

Figure 4.20. Detailed view of the locations of study sites MC929 and MC885 on the upper portion of Henderson Ridge. Also shown is MC709, on the western side of the Mississippi Canyon.

Mississippi Canyon 929

The MC929 study site is a low-relief mound centered at about 28°01.7'N, 89°43.6'W on the generally featureless, gently sloping western side of upper Henderson Ridge (**Figure 4.20**). The mound is approximately 900 m north to south, 400 m west to east, and 35 m tall. It is a geologically active area where Aharon et al. (2001) studied the extensive seepage of barium and radium-rich fluids that have produced radioactive barite chimneys. Similar to the GC184/185 study site, only one dive was undertaken to investigate MC929. *JSL* Dive 4864 carried out a south to north survey across the mound in water depths that ranged from 663 to 637 m. For the most part the seabed was flat unconsolidated fine sediment, often with disarticulated shells and shell fragments. The occasional seabed features that were encountered all appear to be authigenic carbonate in the form of either partially exposed hardgrounds (**Figure 4.21**), very low-relief outcrops (**Figure 4.22**), or small clasts and nodules. These substrates were often colonized with large *C. americana delta* and/or small *L. pertusa* colonies. Also observed were beds of both living and dead mussels (**Figure 4.23**) as well as small brine pools.

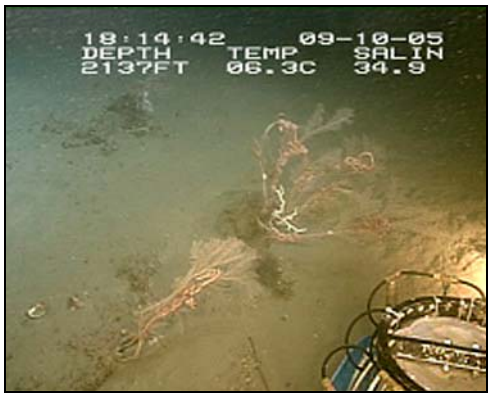

Figure 4.21. Partially exposed hardgrounds colonized with large *Callogorgia americana delta* and small *L. pertusa* colonies (MC929).

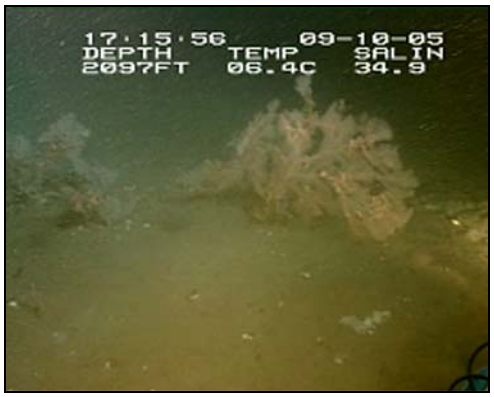

Figure 4.22. Low-relief outcrop colonized with large *Callogorgia americana delta* colonies (MC929).

Figure 4.23. Beds of both living and dead mussels (MC929).

Mississippi Canyon 885

The MC885 study site is located approximately 4.1 km north of the MC929 site (**Figure 4.20**). It is situated on a small, gently sloping low-relief mound covered with clay size sediment (**Table 4.3**) often with a mixture of shell debris. It is centered at about 28°03.96'N, 89°43.05'W in water depths of 626 to 643 m. Active brine seepage is occurring that supports scattered bacterial mats, mussel beds, and tubeworm aggregations. Also present are widely spaced clusters of indurated substrates (**Figure 4.24**) ranging from clasts and nodules of various sizes and shapes (**Figure 4.25**) to low-relief outcrops/buildups (**Figure 4.26**). Based on the observed chemosynthetic activity in this area, it is assumed that the indurated substrates present are authigenic in origin. Attached to some of these features are *L. pertusa* and *M. oculata* colonies. The largest coral colonies observed were *M. oculata*, which were seen up to 65 cm tall. Also present are large colonies of *C. americana delta* (**Figure 4.25**). It is estimated that up to 50% of the carbonate at this site is not colonized by megafauna.

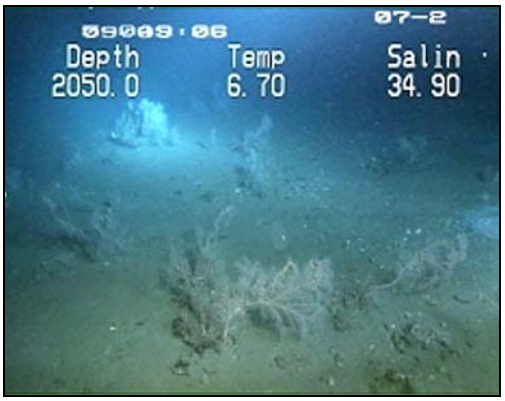

Figure 4.24. *Madrepora oculata* colony in an area of scattered, low-relief boulders and outcrops (MC885).

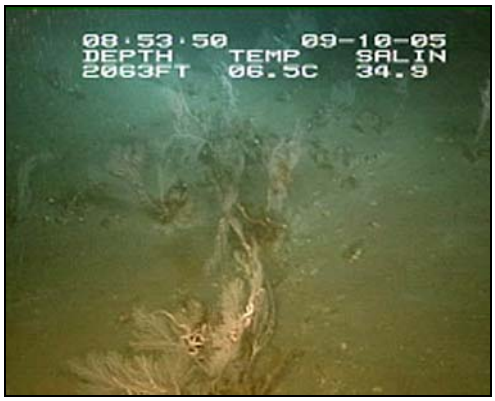

Figure 4.25. Small *L. pertusa* colony and *Callogorgia americana delta* on a low-relief outcrop (MC885).

Figure 4.26. Small *L. pertusa* colonies and *Callogorgia americana delta* on a low-relief boulder or outcrop (MC885).

4.3.3 Upper Mississippi Canyon – Upper Mississippi Fan Subprovince

Mississippi Canyon is a major reentrant feature incised into the continental margin south of the Mississippi River delta (**Figure 4.1**). It extends from a water depth of about 50 m on the shelf southeastward out onto the upper slope. It is generally accepted that it has formed as a result of large-scale slumping (Goodwin and Prior 1989; Bryant et al. 1991). One study site, MC709, is located on the western side of the upper canyon. A detailed view of the upper portion of the canyon and the adjacent region is presented in **Figure 4.20**.

Mississippi Canyon 709

MC709, the deepest site investigated, is located on what appears to be a low-relief, more or less circular expulsion feature approximately 100 m tall by 900 m in diameter with an irregular shaped caldera-like crest. Single-beam fathometer records suggest that sections of the rim-wall have collapsed, creating a knobby or hummocky morphology. The shallowest fathometer depth recorded, 668 m, was from a hillock that exhibited extensive gas venting. Only one dive, *JSL* Dive 4739, was conducted at this site. The dive surveyed over 2 km of the bottom, but it was

limited to just the southeastern quadrant of this feature (centered at 28°13.40′N, 89°42.2′W) across a depth range of 681 to 703 m. The observed seabed generally alternated between flat featureless expanses to hummocky terrain to bowl-like depressions tens of meters across predominantly covered with fine unconsolidated sediments. Exceptions were small areas of scattered low-relief outcrops, clasts, and nodules presumably composed of authigenic carbonate because of the chemosynthetic activity in the area (**Figures 4.27** and **4.28**). Many of these indurated substrates are colonized with large *C. americana delta* and/or small *L. pertusa* colonies (**Figure 4.28**). Also encountered were two small brine pools with mussels (**Figure 4.29**).

Figure 4.27. Small area of scattered low-relief outcrops, clasts, and nodules (MC709).

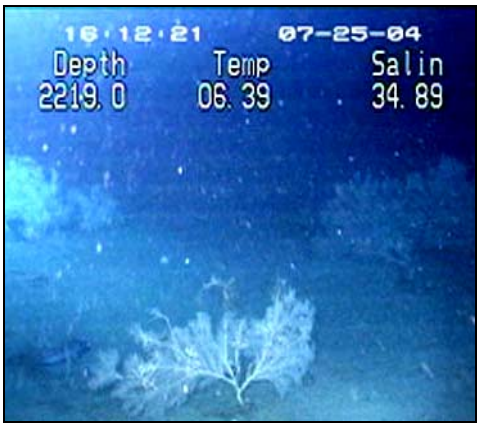

Figure 4.28. Area of scattered low-relief outcrops, clasts, and nodules colonized with large *Callogorgia americana delta* and small *L. pertusa* colonies (MC709).

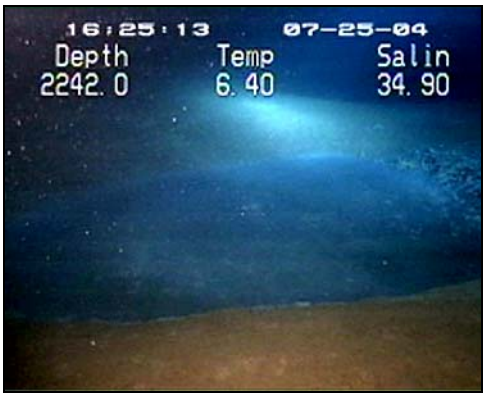

Figure 4.29. Small brine pools with mussels (MC709).

4.3.4 Upper DeSoto Slope Subprovince

The DeSoto Slope extends westward from the northern end of the West Florida Terrace and the DeSoto Canyon to the eastern side of the upper Mississippi Fan (Martin and Bouma 1978) (**Figure 4.1**). Two study sites, VK862 and VK826, are located on the upper slope, which has a relatively smooth surface only occasionally altered locally by low-relief hillocks and small submarine canyons (**Figure 4.30**). Adjacent to each site was an additional site that was visited as part of the NOAA-OE sampling effort. These were VK862S (part of which is actually in VK906) and VK826NE.

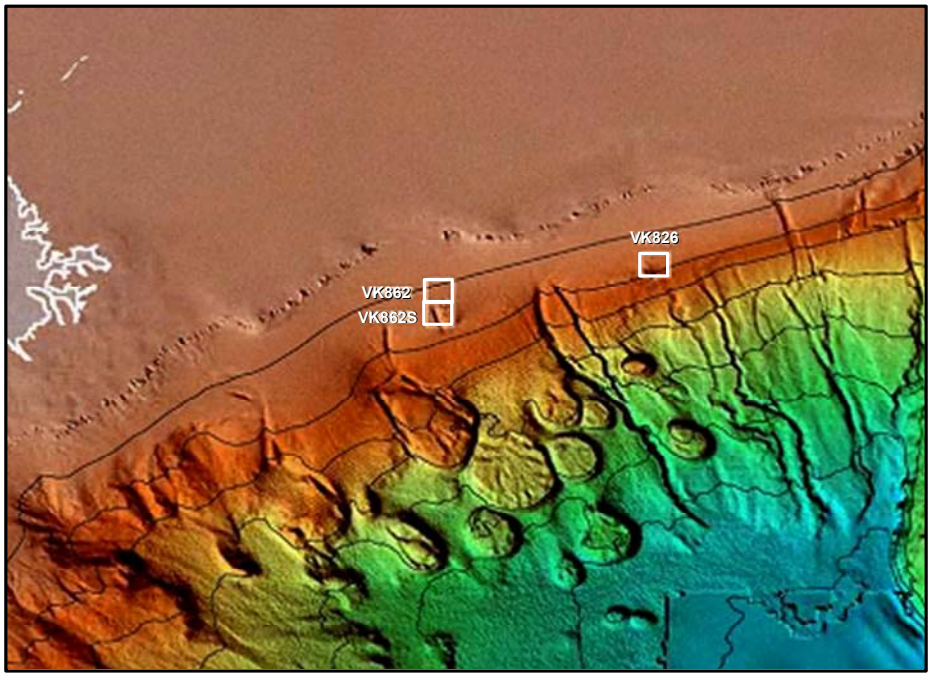

Figure 4.30. Detailed view of study sites VK862 and VK826 located on the upper portion of the DeSoto Slope in the northeastern Gulf of Mexico.

Viosca Knoll 862 and 862S

VK862 and VK862S, the shallowest areas investigated, are located in a low-relief mound and ridge complex adjacent to a small submarine canyon on the upper DeSoto Slope subprovince (**Figure 4.30**). The primary study site is a small, low-relief mound in the southeast corner of VK862. It is centered on 29°06.4′N, 88°23.0′W, approximately 2.3 km northeast of the eastern rim of the submarine canyon. Water depths at the study site range between 304 and 333 m. The upper half of the mound is predominantly formed from large, authigenic carbonate (see **Table 4.4**) blocks and boulders, some with vertical and/or horizontal dimensions on the order of 5 m (**Figures 4.31** and **4.32**). Gaps and deep-crevices between the blocks and boulders result in a very rugged, irregular, and often steep-sided topography (**Figures 4.33** and **4.34**). Conversely, the flanks of the mound are generally gently sloping and covered with combinations of smaller boulders and blocks (**Figure 4.35**) and pavements made from clasts and nodules of varying sizes and shapes (**Figures 4.36** and **4.37**). The bottom immediately surrounding the mound is flat and

composed of sediments ranging from gravelly muddy sand to gravelly mud (**Table 4.3**) or partially exposed hardgrounds (**Figure 4.38**).

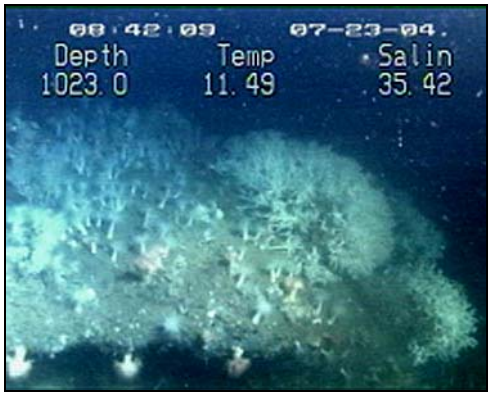

Figure 4.31. Large block near the top of the mound densely colonized by anemones and large colonies of *L. pertusa* (VK862).

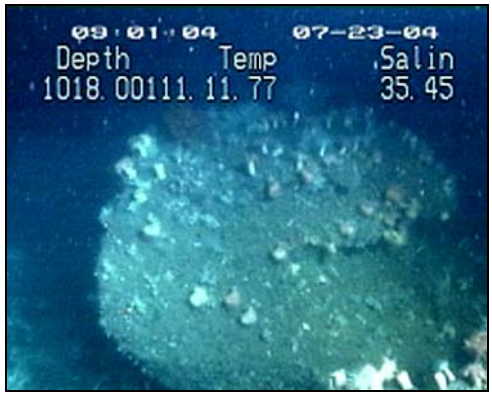

Figure 4.32. Large boulder near the top of the mound colonized mostly by anemones (VK862).

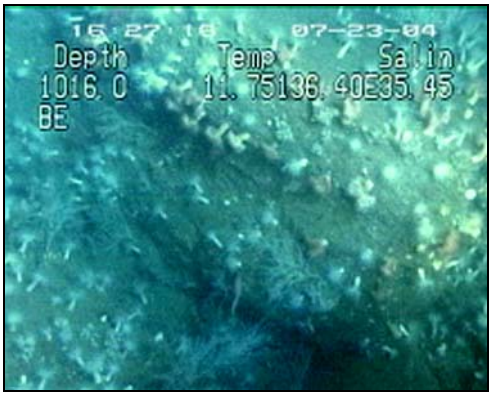

Figure 4.33. Wide gap between two boulders, densely colonized by anemones, near the top of the mound (VK862).

Figure 4.34. Deep-crevice between two blocks with generally uncolonized surfaces (VK862).

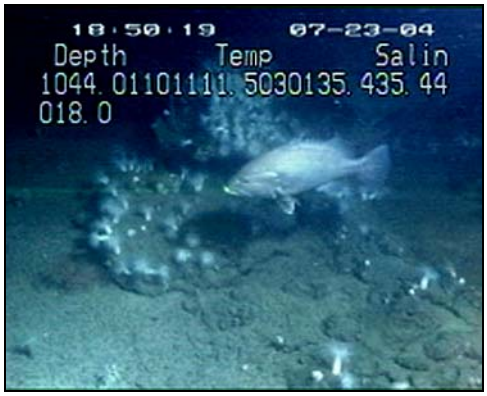

Figure 4.35. Small boulders covered with anemones on the gently sloping southeastern flank of the mound (VK862).

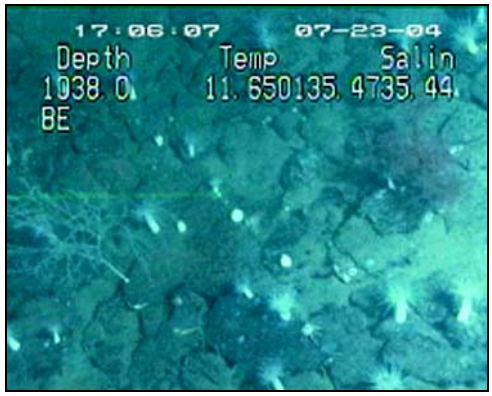

Figure 4.36. Northern flank of the mound covered with a pavement of small flat slabs of varying sizes and shapes (VK862).

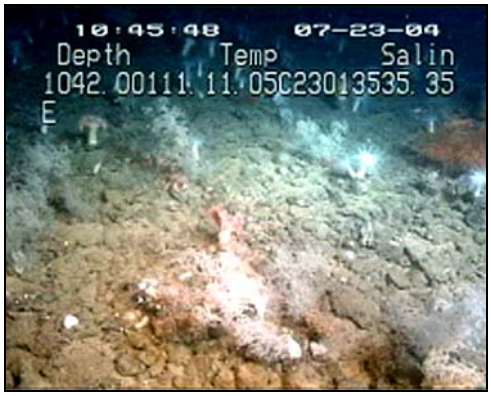

Figure 4.37. Western flank of the mound covered with a pavement of clasts and nodules of varying sizes and shapes (VK862).

Figure 4.38. Partially exposed flat hardground just to the south of the mound (VK862).

A secondary site (VK862S), located in the northeast corner of VK906 approximately 1,100 m to the southwest of the primary site, was also investigated. The area surveyed, centered on 29°05.9′N, 88°23.1′W, includes portions of two generally north-south oriented parallel ridges in water depths of 328 to 352 m. The crests and most of the sides of the ridges are covered with authigenic carbonate (see **Table 4.4**) pavements in the form of small-boulder to cobble size nodules and flat plates or slabs (**Figures 4.39** and **4.40**), while the deeper adjacent regions are all covered with fine unconsolidated sediment.

Figure 4.39. Small-boulder to cobble size nodules and flat plates or slabs covering the crest of the western ridge (VK862S).

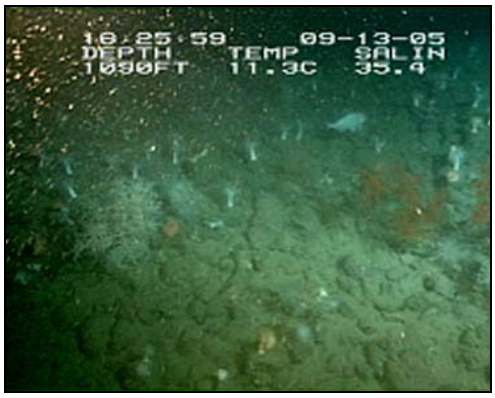

Figure 4.40. Small-boulder to cobble size nodules and flat plates or slabs covering the side of the western ridge (VK862S).

Viosca Knoll 826 and 826NE

VK826 is the easternmost study site (**Figure 4.1**). It was discovered in 1990 during an ROV survey conducted for Oryx Energy Company, Inc., Dallas, Texas, in conjunction with pre-exploratory drilling activity and later described by Schroeder (2002). This site has the most extensive *L. pertusa* development found in the Gulf of Mexico to date (Schroeder et al. 2005). It is located on a 90 m tall, isolated knoll on the seaward steepening upper De Soto Slope (**Figure 4.30**). The explored region is centered on 29°09.5′N, 88°01.0′W, in water depths of 430 to 534 m, and covers most of the crest, south, west, and north sides, and portions of the southern and western base/flank regions. Indurated substrates are authigenic in origin (**Table 4.4**; W. Schroeder unpublished data) and cored sediments ranged from slightly gravelly sandy mud to gravelly mud (**Table 4.3**). The presence of apparently very old living tubeworm aggregations (**Figure 4.41**) and numerous accumulations of disarticulated lucinid and vesicomyid shells (**Figure 4.42**) suggest this area is at a senescent phase of chemosynthetic community activity. A second site, the crest and upper portions of a small mound (VK826NE), lies approximately 1 km northeast of the top of the main knoll at 29°10.2′N, 88°00.7′W, in water depths of 458 to 481 m.

The crest of the knoll is generally flat and covered with a combination of broken hardgrounds, low-relief outcrops/buildups, shell pavements, and fine sediments (**Figure 4.43**). The adjacent, moderately sloping crest-rim consists of locally hummocky terrain made up of carbonate capped knolls and ridges, some with abrupt vertical relief (**Figure 4.44**), and relatively flat terraces built from carbonate substrate, shell pavement, and fine sediment (**Figure 4.45**). Individual colonies of *L. pertusa*, as large as 1.5 m in diameter, and colony aggregations up to 1.5 m wide by 1.5 m high by 4 m long occur in this region (**Figure 4.44**) along with carbonate surfaces that are practically uncolonized (**Figure 4.45**). The upper regions of the south and north sides of the knoll are a mixture of moderate to steep slopes and terrace-like features composed of carbonate outcrops/buildups, sediment veneered hardgrounds, and/or open flats of fine sediment (**Figures 4.46** and **4.47**). Extensive assemblages of *L. pertusa* have developed within these areas. Fields of individual colonies, up to 2 m in diameter, and clusters/aggregations of colonies, some as large as 2 m wide by 2 m high by 4 m long occur on both exposed hardground/buildups and sediment veneered hardgrounds (**Figures 4.46** and **4.47**).

The slope on the western side of the knoll is steep and consists of a series of ridges or hummocks and swales of fine unconsolidated sediment that are oriented along-isobath and have vertical

relief of 1 to 3 m from crest to trough. Carbonate outcrops occasionally occur on the crests of these features and provide substrate for individual and aggregations of *L. pertusa* colonies (**Figure 4.48**). To the immediate east and southeast, the bottom levels off into a relatively flat area consisting mostly of fine, unconsolidated sediment and patches of both exposed and sediment veneered carbonate, some with small *L. pertusa* colonies. The lower portion of the south-southwestern side of the knoll exhibits evidence of slumping. At the base of this zone, at depths of 510 to 540 m, the bottom flattens out into at least one terrace-like feature that is covered with broken hardground, large boulders and blocks (up to 3 to 4 m tall by 1 to 2 m wide), and smaller debris of various sizes and shapes. Most of the carbonate substrate is barren; however, large colonies of *C. americana delta* as well as smaller *L. pertusa* have occasional been observed (**Figure 4.49**).

L. pertusa development at the small mound to the northeast (VK862NE), named "Knobby Knoll" because of its hummocky crest, is extraordinary. It is so dense that hard substrate is visible in only a few locations and thicket production has either covered the numerous knob-like features or has reached a level of initial coppice development (**Figure 4.50**).

Figure 4.41. Large tubeworm bush on the southwestern flank of the knoll (VK826).

Figure 4.42. Deposit of disarticulated lucinid and vesicomyid shells and fine unconsolidated sediment on southwest side of the knoll (VK826).

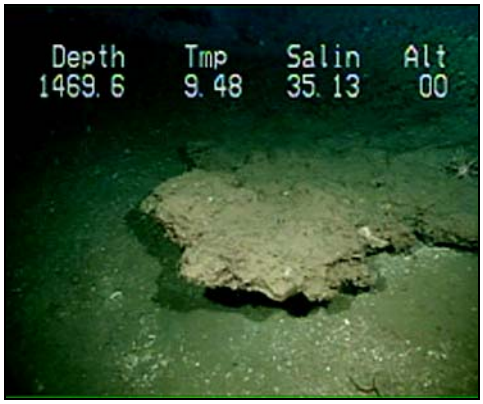

Figure 4.43. Mostly uncolonized hardground and a mixture of gravelly sandy mud near the crest of the knoll (VK826).

Figure 4.44. Individual and large aggregations of *L. pertusa* on carbonate capped knolls and ridges on the southwestern crest-rim of the knoll (VK826).

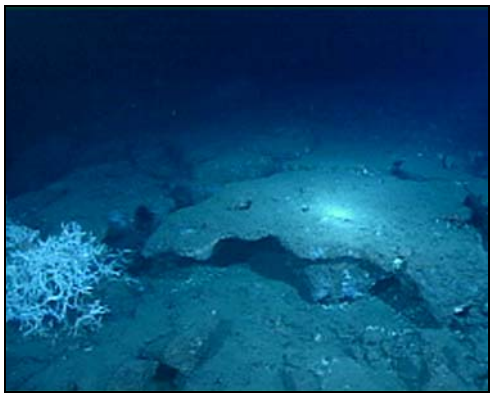

Figure 4.45. Mostly uncolonized hard substrate on the southeastern crest-rim of the knoll (VK826).

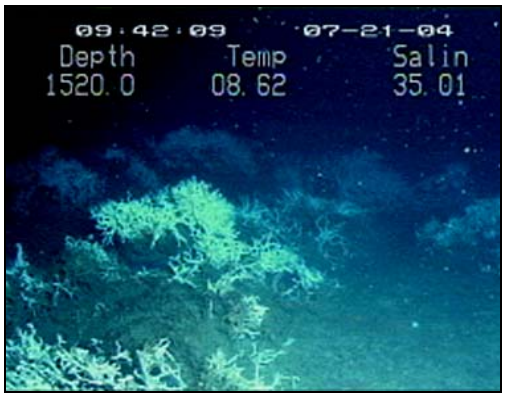

Figure 4.46. *L. pertusa* aggregations/thickets on sediment veneered hardground on the south side of the knoll (VK826).

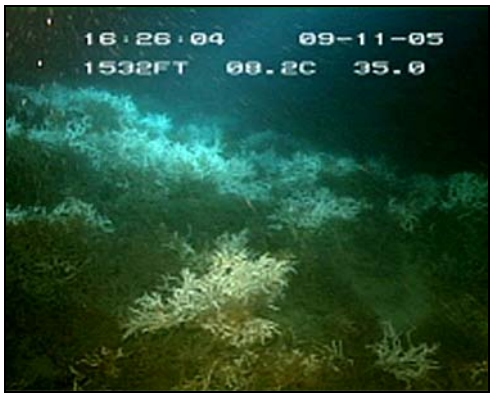

Figure 4.47. *L. pertusa* aggregations/thickets on exposed hardground/buildups on the north side of the knoll (VK826).

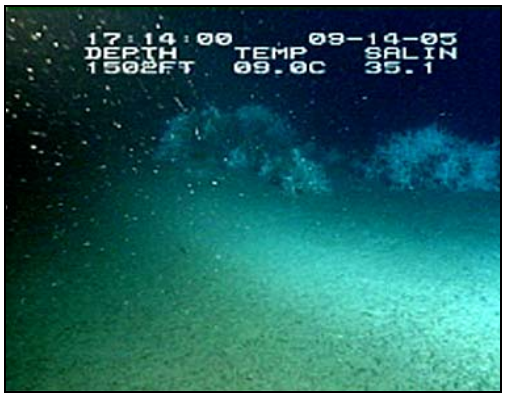

Figure 4.48. Carbonate capped ridge on the western side of the knoll colonized by large *Lophelia pertusa* colonies (VK826).

Figure 4.49. *Callogorgia americana delta* on a large block at the base of the south side of the knoll. Small *Lophelia* colonies are often found in this area (VK826).

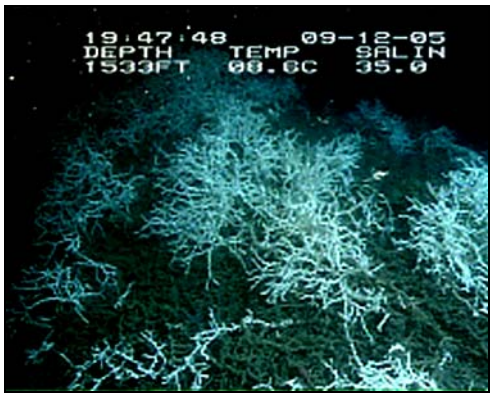

Figure 4.50. A 4.5-m high knob covered with either *L. pertusa* thickets or coppice on Knobby Knoll (VK826NE).

Chapter 5
Biological Characterization and Studies, Part I

Erik E. Cordes, Erin L. Becker, Stephanie Lessard-Pilon, Elizabeth L. Podowski, Michael P. McGinley, and Charles R. Fisher

Biological Characterization and Studies, Part I

- Photomosaics were assembled and analyzed for each alpha and beta site (except MC709).
- Fauna were collected with a Bushmaster device for community analyses.
- Stable isotopes were analyzed in *Lophelia* and associated fauna.
- Temperature probes were deployed within coral thickets at two sites (GC354 and VK862).
- Total petroleum hydrocarbon concentrations were measured in bottom water samples.

5.1 FIELD METHODS

5.1.1 Image Acquisition for Photomosaics

Photomosaics were assembled from successive overlapping images taken over a haphazardly selected target. Carbonate outcrops of less than 50 m^2 containing relatively high densities of *Lophelia pertusa* were selected for analysis. Photographs for the assembly of photomosaics were taken using a Canon PowerShot G2 digital camera contained within a pressure housing and mounted on the side of the submersible in a down-looking position. For the Cruise 1 series in 2004, two lasers spaced 10 cm apart were mounted on either side of the camera for size reference in each image. During the Cruise 2 series in 2005, the lasers were again mounted on the side of the camera, but spaced 25 cm apart. The submersible moved slowly over the top of the outcrop in a parallel transect pattern while photographs were obtained every 3 to 5 seconds. When the pattern was complete, the submersible was maneuvered over the top of the outcrop and a series of photographs was taken at increasing heights above the outcrop to ensure complete coverage of the target.

5.1.2 Bushmaster Collections

Quantitative physical samples of the coral thickets were obtained using the Bushmaster collection device (**Figure 5.1**). This device has an open diameter of approximately 60 cm and consists of a 63-µm mesh net suspended between Plexiglas rods that is closed with a series of hydraulic cylinders. *L. pertusa* colonies were sampled haphazardly, within the

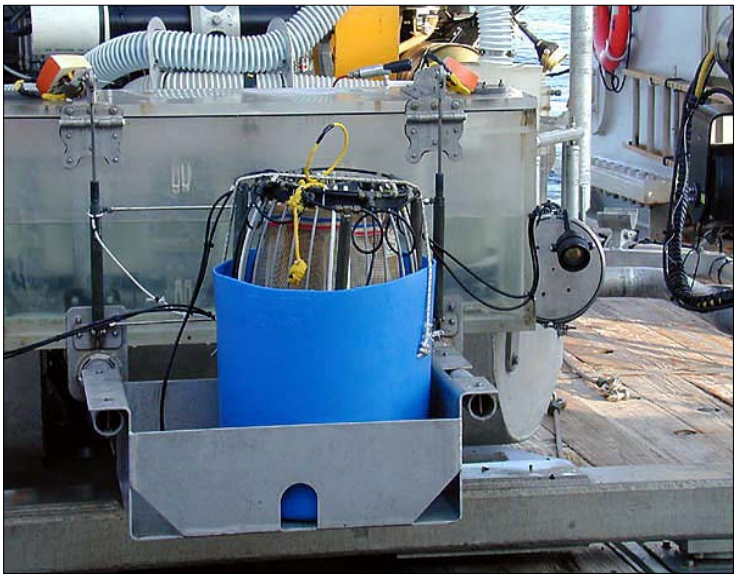

Figure 5.1. The Bushmaster collection device in its holster on the front of the submersible prior to launch.

photomosaic area if possible. The bottom of the Bushmaster was constricted around the base of the colony and the sample placed within a 63-μm mesh-lined container on the front of the submersible. Once retrieved, the collected material was washed out of the collection device and holster with filtered, cold seawater and placed in a basin. The material was sorted to remove all of the associated fauna from the coral framework. The coral was measured as detailed below, and the associated fauna identified to the lowest possible taxonomic level on board (if time allowed) or in the laboratory at The Pennsylvania State University (PSU).

5.1.3 Other Image and Specimen Collection

Additional specimens and photographs of unidentified species (particularly coral and gorgonian species) were collected along with the quantitative photographic and physical samples. Photographs of unidentified cnidarians were taken *in situ* when possible, and on deck following early collections. Upon collection, specimens of mobile fauna and cnidarians were fixed in 10% formalin and preserved in 70% ethanol or were frozen for genetics and stable isotope work.

5.1.4 Temperature Monitoring

At two of the sites (GC354 and VK862), HOBO-temp temperature probes were deployed within coral thickets. The probes recorded temperature every 5 h for 375 days. Upon recovery, the probes were removed from the pressure housings and the data downloaded from the probe using Boxcar® software (Onset Corporation).

5.1.5 Water Sampling

Samples of ambient water for TPH analysis were collected at near-bottom depths (approximately 2 m from the seafloor) during both cruises. During Cruise 1, two samples were collected at each of three sites (GC234, VK826, and VK862), and one sample was collected from each of two other sites (GC354 and MC885). During Cruise 2, one sample was collected from each of five sites (GC184/185, GC234, GC354, MC885, and MC929).

Samples were collected using a Niskin-type closing water sampling bottle, which was affixed to the submersible's forward vertical frame member and triggered during the dive using the manipulator arm. The interior bore and end caps of the Niskin bottle were cleaned before each collection using phosphate-free soap and distilled water. The bottle was left in the closed position until just prior to launching the submersible to prevent contamination. After the collection dive, a 1-L sample was decanted from the Niskin bottle directly into a precleaned amber glass sample bottle and stored at 2 °C. Sample blanks, using distilled water, were collected from the Niskin bottle and from the source of distilled water used for cleaning.

5.2 LABORATORY METHODS

5.2.1 Photomosaic Construction and Analyses

Each image was optimized in Adobe® PhotoShop® CS2 by using the automatic adjustments for lighting, contrast, and color before the construction and analysis of the photomosaics. Once the lighting for all images composing a particular mosaic was uniform, the images were saved with a

new file name and imported into a MatLab photomosaicking program written by Hanumat Singh, Tim Shank, and Jonathan Howland of the Woods Hole Oceanographic Institution. With sufficient overlap (about 25% to 50%), the program automatically aligned the images by matching common features in each. Manual selection of common features was necessary when overlap of images was less than approximately 25%. Once aligned, the program blended each image into the next, creating one final, seamless image.

Due to the large amount of computer memory necessary to run the mosaicking program, a maximum of six pictures could be automatically stitched together at one time. Individual lines of images were mosaicked to form intermediate mosaics. Each of these was aligned and connected to the adjacent lines using Photoshop CS2 to produce the final mosaic for each site.

To create a uniform scale for the entire mosaic, the distances between each pair of lasers present in any of the images were averaged together. This average was then used to create a scalar grid specific to each mosaic. Using PhotoShop CS2, the grids were overlaid on the mosaics and spaced according to each mosaic's spatial scale. The bottom left corner of each grid always signified the origin (0 m, 0 m).

Mosaics with the overlaid grid were then imported into ArcGIS 9.0 and, using the spacing between the grid points, were geo-referenced into a coordinate system created to specifically match each mosaic's spatial scale. The unit of measurement of the coordinate system was set to meters. Once the mosaic was geo-referenced, it was possible to use the software to estimate distance and area on the image.

All mosaics were analyzed within the framework of a geographic information system (GIS). The entire area of the mosaicked image was first digitized as a new polygon layer in the GIS. Then, referencing the original images, which were hyperlinked to the final mosaic, separate polygon layers were digitized for all non-sedimented substrate, including live *L. pertusa*, dead *L. pertusa*, mixed (50% live and 50% dead) *L. pertusa*, *Madrepora oculata*, antipatharians, gorgonians, stoloniferans, tubeworms, bacterial mats, and carbonate. All colonial cnidarians other than *L. pertusa* and *M. oculata* were combined in the subsequent statistical analyses. Point feature class layers were digitized for all mobile megafauna, sponges, and anemones. All fauna were identified to the lowest possible taxonomic level.

ArcGIS was used to calculate the areas of each polygon layer. Percent coverage of each non-sedimented substrate was determined by dividing the total area of a particular non-sedimented substrate by the total area of non-sedimented substrates. Densities of fauna were calculated by dividing the number of organisms in each individual point feature layer by the total area of the non-sedimented substrates (hardgrounds).

To assess how species distribution was related to the various non-sedimented substrates, the GIS was queried to determine the percent of different organisms found completely within polygons of each non-sedimented substrate (total number of a particular species directly within the polygons divided by total number of that species within the mosaic). Additionally, 10-cm buffers were created around all non-sedimented substrate polygons and the percent of each species within each

buffer was determined (total number of a particular species within a given buffer divided by total number of that species within the mosaic).

Three chi-square tests were designed to test a) whether species were evenly distributed across all substrates; b) which substrates had mobile fauna populations that were significantly different from random values; and c) which animals had populations that differed from random distributions in the 10-cm buffers around each of the substrates (α-value = 0.05). Chi-square tests were only applied to taxa that had more than five individuals in the mosaic.

5.2.2 Bushmaster Collection Processing and Analyses

Coral associated fauna were separated to "morphospecies," which are groups of individuals believed to represent separate species based on all morphological data. Each morphospecies was identified to the lowest possible taxonomic level in the laboratory using existing voucher collections at PSU and published taxonomic information. If the identification was ambiguous, representative individuals were sent to taxonomic experts for identification. Steve Cairns identified all cnidarians; Sabine Stohr, Roland Emson, and Gordon Patterson identified ophiuroids; Rich Mooi identified sea urchins; Anders Waren identified gastropods; and Stephane Hourdez identified polychaetes.

Following identification, all of the individuals were counted and weighed. In 2004, individuals were separated to the best of our ability on board, fixed in formalin, and transported to PSU where counts and preserved wet weights were determined. In 2005, counts were made on board and wet weights determined using a motion-compensated shipboard balance. Preserved and wet weights were converted to ash-free dry weight using existing conversion factors (Bergquist et al. 2003) or taxonomic-group specific conversion factors (Ricciardi and Bourget 1998).

Surface area of *L. pertusa* from Bushmaster collections was calculated from empirically measured average diameter and volume of coral skeleton. Portions of skeleton were placed in 25 cm by 30 cm dissecting trays so that they were one layer thick. Ten random points on the skeleton were selected, and the diameter of the coral was measured at each point. It was also noted whether the coral was live or dead for determination of proportion of live coral in the skeleton. The average diameter of coral skeleton in each collection was calculated as the average of all individual diameter measurements. Coral volume was determined by water displacement by placing the entire skeleton into a container filled with water and measuring the displaced volume with a graduated cylinder. Surface area (*SA*) was calculated as:

$$SA = \pi d \cdot L$$

where d = diameter and L = length of coral skeleton. Length was calculated from volume (V) as:

$$L = \frac{V}{\pi r^2}$$

where r is the radius calculated as $d/2$.

Diversity was assessed as species richness (number of species), the Shannon-Weaver diversity index (H'), and Pielou's evenness index (J'). Relationships between diversity and various measures of coral habitat (surface area, surface to volume ratio, proportion of live coral, and depth of collection) were evaluated using least-squares regression. For this analysis, habitat variables were standardized to a mean of 0 and a standard deviation of 1.

Similarity in associated fauna was analyzed for Bushmaster collections and for photomosaic samples. Similarity was assessed using the Bray-Curtis similarity index:

$$S_{jk} = 100\left(1 - \frac{\sum_{i=1}^{p}\left|y_{ij} - y_{ik}\right|}{\sum_{i=1}^{p}\left(y_{ij} + y_{ik}\right)}\right)$$

where S_{jk} is similarity between the j_{th} and k_{th} samples, y_{ij} is the density of the ith species in the jth sample, y_{ik} is the density of the ith species in the kth sample, and p is the total number of species. Species densities were calculated as the number of individuals per m^2 coral surface area or image area to provide a comparison among samples without the confounding variable of sample volume (Bushmaster) or area (mosaic). Since the Bushmaster device was used for all quantitative physical collections, collection size was fairly consistent.

Patterns of similarity among all *L. pertusa* community collections, mosaics, and among coral and tubeworm associated communities were assessed using multidimensional scaling (MDS) analyses. This ordination technique arranges communities such that their rank similarity in distance in two-dimensional space corresponds to their rank similarity in community structure determined by the Bray-Curtis index. The analysis proceeds through a series of iterations until the correlation between the community similarity matrix and the distance matrix is optimized. The Bray-Curtis similarity value used to designate similar community types (~35) is a somewhat arbitrary score and is intended to provide a relative assessment, rather than signify statistical significance. This value was based on the similarity of all previously collected tubeworm aggregations from the three main sites described here: GC234, GC354, and VK826. This similarity value therefore designates three different broad categories of community type within the coral-associated communities of the upper slope. A modified BIO-ENV procedure is then used to assess the relative importance of measured environmental factors on community similarity through correlation of similarity matrices. For the Bushmaster comparisons, the environmental factors tested included distance (latitude and longitude), depth, proportion of live coral, and habitat complexity (surface area/volume of coral skeleton). In the mosaic comparisons, distance, depth, and the proportion of each substrate type were examined.

5.2.3 Stable Isotope Sample Preparation and Analyses

Subsamples of suspension feeding species, *Lophelia* tissue and skeleton, and associated fauna from Bushmaster collections were obtained for stable isotope analyses. The $\delta^{13}C$ values of both tissue and skeleton of suspension feeding cnidarians (including *Lophelia*) were examined to determine if seep-derived productivity was entering the system. *Lophelia* skeleton was also

analyzed for $\delta^{18}O$ values to determine the potential for reconstructing temperature records from the skeleton. The $\delta^{13}C$, $\delta^{15}N$, and $\delta^{34}S$ values were determined from *Lophelia*-associated fauna from the Bushmaster collections to attempt to constrain the food web in the coral community. From the Bushmaster collections, between three and six individuals of each species that could be identified at sea were frozen at -20 °C in a plastic cryovial upon collection. For large individuals, muscle tissue was dissected from the specimen. For smaller individuals, the entire specimen was frozen, and in some cases it was necessary to pool individuals to obtain sufficient material. In the laboratory, samples were removed from the vials and homogenized in a new plastic weigh boat with a razor blade and a small volume of deionized water, if necessary. Homogenized samples were returned to the vials and placed in a 60 °C drying oven for 3 to 4 days until their weight stabilized and all water was removed. In 2004, samples were sent to the Marine Science Institute at the University of California (UC) Santa Barbara where they were acidified (for tissue samples) or bleached (for carbonate and coral skeleton samples) prior to analysis. Isotope values were determined by continuous-flow isotope ratio mass spectrometry using a Thermo-Finnigan Delta+ Advantage MS coupled with a Costech Technologies ECS 4010 Elemental Analyzer. In 2005, dried samples were crushed inside their cryovials using a glass plunger. The vials were shaken and tapped to ensure that no sample became packed in the pointed tip of the vial. Two or three drops of 10% HCl were added to remove any inorganic carbonate. It was noted that a few samples bubbled to the rim of the vial when the acid was added. All samples were dried for 2 days, after which the samples that had fizzed during the pretreatment were scraped off of the sides of the vial, and an additional drop of acid was added. All samples were then dried for an additional 5 days, until all water was removed. Samples were then sent to the University of Virginia, where stable isotope measurements were obtained using a Carlo Erba elemental analyzer coupled to a VG Optima isotope ration mass spectrometer (EA/IRMS) (Fry et al. 1992). Values are expressed using δ (delta) notation in parts per million (‰). Peedee belemnite (PDB) was used as the standard for carbon, air N_2 for nitrogen, and Cañon Diablo troilite (CDT) for sulfur.

Coral skeleton and authigenic carbonate samples were homogenized by placing the sample between two layers of 0.5-mm latex and crushing it with a hammer. The purpose of the latex was to keep the sample in one place and keep it from contacting the hammer. Although there was very little puncturing in the latex, both the work surface and hammer were washed with Terg-A-Zyme® enzyme detergent and rinsed with deionized water between samples. Homogenized samples were placed in 2-mL plastic cryovials. Samples were pretreated with 0.5 mL of bleach for 24 h. Samples were centrifuged for 3 min and the bleach removed using a disposable pipet. Samples were rinsed three times with deionized water using centrifuge and pipet techniques, then dried at 60 °C for 4 days until all water had evaporated.

Carbonate samples were sent to the geology department of UC Davis. Using a common 100% phosphoric acid bath at 90 °C, 20 to 50 µg of sample were reacted and analyzed in the directly coupled dual inlet of a GV Instruments Optima isotope ratio mass spectrometer. Isotope values were reported relative to Vienna PDB (VPDB) through the use of the UC Davis working standard, a carrara marble. Expected values of this standard are $^{13}C = +2.10$ and $^{18}O = -1.94$. It has been calibrated by repeated direct measurement against NBS-19. Long term external precision is ±0.04‰, one σ for ^{13}C and ±0.05‰, one σ for ^{18}O (David Winter, pers. comm.).

5.2.4 Total Petroleum Hydrocarbons Analysis

Water samples were shipped to the laboratory of TDI-Brooks International, Inc. for total petroleum hydrocarbons (TPH) analysis by B&B Laboratories. Samples were logged in according to B&B standard operating procedures (B&B SOP 1009). Water samples were analyzed for TPH by gas chromatography/flame ionization detection (GC/FID), using B&B 1011 extraction methods and B&B 1013 TPH analysis methods, with TPH method detection limits of 13 µg/L. Target compounds included a suite of aliphatic hydrocarbons (nC_{10} to nC_{34}, and pristane and phytane). Quality assurance/quality control (QA/QC) for this program included the analyses of a procedural blank and a blank spike/blank spike duplicate per analytical batch of samples. Procedural method blanks are used to determine that sample preparation and analyses are free of contaminants. The blank spike/blank spike duplicate is used to measure accuracy and precision of the analysis. All QC samples are subject to the identical preparation and analysis steps as samples. Additionally, a laboratory control sample consisting of a diesel sample for which controls are established was analyzed with the data set.

Surrogate solutions equivalent to 5 to 10 times the method detection limit were added to every sample, including QC samples. The data are corrected based on surrogate recovery up to 100%. The QC criteria for surrogate recoveries are between 40% and 120%.

5.3 RESULTS

5.3.1 Imaging and Photomosaics

Twelve mosaics were assembled from photographs obtained at the survey sites (**Appendix A**). The most common substrate types were dead *L. pertusa* and carbonate rubble, followed by live *L. pertusa* and solid carbonate (**Figure 5.2**). Deeper sampling locations contained greater proportions of dead coral in the images ($r = 0.651$, $p < 0.001$). Species considered to be foundation species and therefore included in the substrate area calculations were *L. pertusa*, *M. oculata*, other colonial cnidarians, and the tubeworm *Lamellibrachia luymesi*. The most common sessile fauna in the mosaics were sabellid polychaetes (most likely *Euratella* sp.), solitary corals, anemones (mostly due to their abundance at VK862), and sponges (**Table 5.1**). Commonly observed mobile megafauna in the mosaics included *Eumunida picta*, the large ophiuroid *Asteroschema* sp., *Munidopsis* spp., an unidentified crinoid (possibly *Comatonia cristata?)*, and fishes.

The most similar megafaunal communities were found at VK826 (**Figure 5.3**). The three mosaics from this site contained relatively high densities of crinoids and echinoids. The next most similar communities consisted of *Munidopsis* spp. and *E. picta* associated with numerous sponges, and were found at GC354. One of the Bush Hill (GC184) mosaics and one of the MC885 mosaics sampled similar communities dominated by sabellids and solitary corals. The most significant factor influencing the structure of the communities in the mosaics was the proximity of the samples to one another, both in terms of distance apart ($r = 0.411$, $p = 0.001$) and sampling depth ($r = 0.360$, $p = 0.003$). Community similarity was also influenced by the proportion of live ($r = 0.305$, $p = 0.013$) and dead ($r = 0.325$, $p = 0.008$) coral in the mosaic.

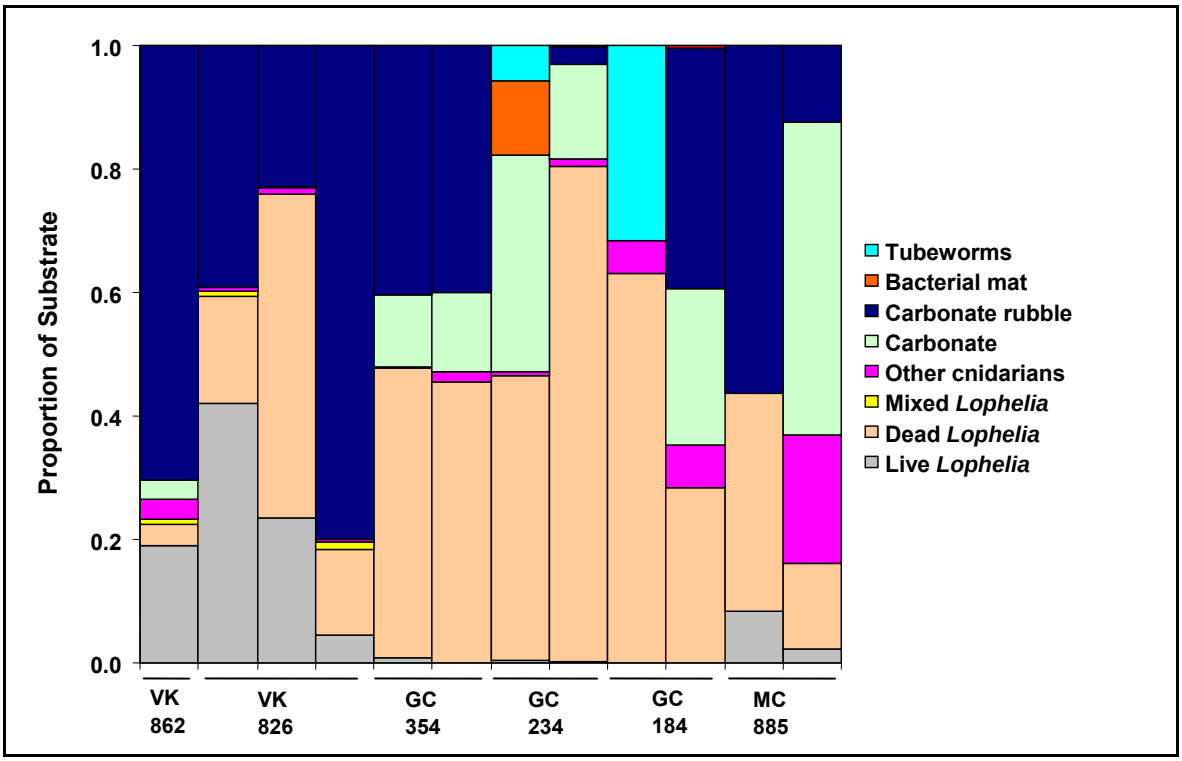

Figure 5.2. Summary of percent cover of each substrate type in each mosaic sample taken.

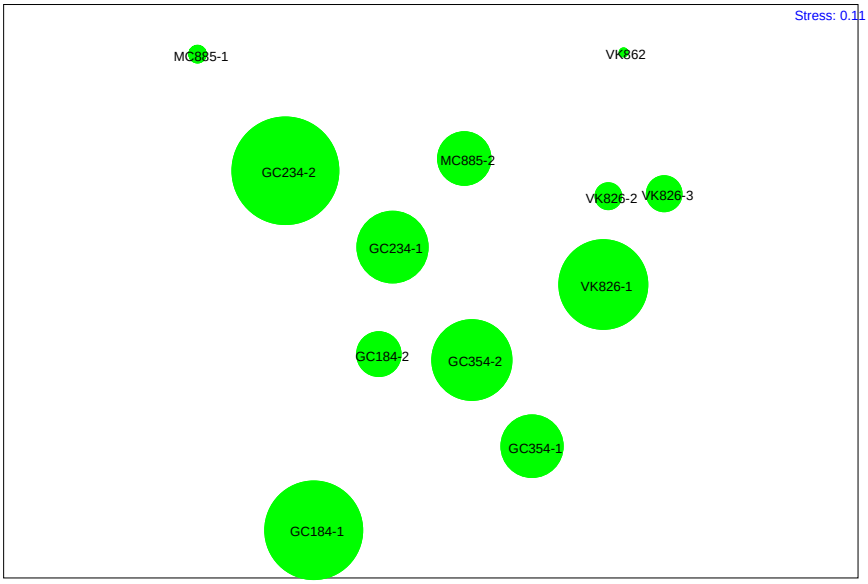

Figure 5.3. Multidimensional scaling plot of community similarity based on density of solitary fauna in the photomosaics. Position in the ordination reflects relative Bray-Curtis similarity in community structure to all other mosaic samples. Circles represent the proportion of dead coral substrate in the mosaic. Following distance between samples and depth of the site, this was the most significant factor explaining community similarity.

Table 5.1. Density of associated fauna within each photomosaic sample.

Taxon	Density (ind/m^2)													
Photomosaic:	VK862 4869	VK826-3 4736-2	VK826-1 4733	VK826-2 4736-1	GC354-2 4861	GC354-1 4726	GC234-1 4728	GC234-2 4740	GC184-1 4725	GC184-2 4862	MC885-2 4863	MC885-1 4738	Avg	SD
sabellids	0.51	0.09	0.94	2.56	4.39	0.70	26.67	0.00	25.43	31.20	6.77	0.00	8.27	12.00
solitary corals	0.01	0.40	0.00	0.17	0.00	0.00	9.63	1.48	0.00	0.58	1.56	16.23	2.51	5.10
anemones	3.59	0.03	0.19	0.17	8.10	0.00	0.37	6.67	0.00	0.42	4.17	1.30	2.08	2.86
Munidopsis sp.	0.00	0.00	0.27	0.00	1.35	2.30	0.00	3.33	8.48	0.92	0.52	1.30	1.54	2.42
Eumunida picta	0.20	0.64	0.90	0.94	6.07	0.91	2.22	1.11	0.00	0.00	0.00	0.00	1.08	1.70
brittle stars	0.00	0.00	0.00	0.00	0.00	0.00	2.22	0.37	0.00	0.00	0.00	9.09	0.97	2.63
sponges	0.00	0.64	0.53	0.34	4.05	2.51	0.37	0.00	0.00	0.08	0.52	0.00	0.75	1.25
crinoids	0.07	1.40	1.57	1.71	0.00	0.00	0.00	0.00	0.00	0.00	1.56	0.00	0.53	0.77
fishes	0.00	0.34	0.07	0.00	0.30	0.07	2.59	0.74	0.37	0.08	0.00	0.00	0.38	0.73
shrimp	0.00	0.00	0.02	0.00	0.67	0.14	2.22	0.00	0.00	0.08	0.00	0.00	0.26	0.65
other crabs	0.01	0.00	0.00	0.17	0.00	0.14	0.00	0.00	0.00	0.00	0.00	0.65	0.08	0.19
urchins	0.01	0.18	0.26	0.34	0.00	0.00	0.00	0.00	0.00	0.00	0.00	0.00	0.07	0.12
snails	0.04	0.09	0.03	0.00	0.00	0.00	0.00	0.00	0.00	0.00	0.00	0.00	0.01	0.03
sea star	0.01	0.00	0.00	0.00	0.00	0.07	0.00	0.00	0.00	0.00	0.00	0.00	0.01	0.02
basket star	0.00	0.06	0.00	0.00	0.00	0.00	0.00	0.00	0.00	0.00	0.00	0.00	0.01	0.02

There were a number of species that showed significant associations with specific substrate types (**Table 5.2**; **Figure 5.4**). *E. picta* was commonly found on dead *L. pertusa* or near live *L. pertusa* and carbonate. Species of *Munidopsis* (three species that were usually indistinguishable at the scale of the photographs and therefore analyzed together) were most commonly found associated with tubeworms, bacterial mats, and live *L. pertusa*, but away from dead *L. pertusa*. The ophiuroid *Asteroschema* sp. showed a strong association with gorgonians in the mosaics, occurring most commonly on *Callogorgia americana americana*. The fishes in the mosaics appeared to be associated with various types of vertical relief, including live coral, mixed coral, and carbonate. Crinoids were distributed most commonly on dead or mixed coral within 10 cm of live coral. Solitary corals settled on carbonate away from *L. pertusa* and anemones. Sabellid polychaetes showed an affinity for dead coral or carbonate away from live coral, tubeworms, and coral rubble.

5.3.2 Bushmaster Collections

A total of 68 species was identified in the 15 Bushmaster collections, with each collection containing between 6 and 23 species (**Table 5.3**). Collections with larger surface area of coral contained higher numbers of species ($r^2 = 0.536$, $p = 0.001$). The most common species in terms of frequency of occurrence were epifaunal organisms including the sabellid polychaete *Euratella* sp., an unidentified encrusting sponge, and hydroids (**Table 5.4**). Following these species were the predatory polychaetes *Glycera tesselata* and *Eunice* sp. and the shrimp *Periclemenes* sp. The species with the highest densities (in order from highest to lowest average density) were *Euratella* sp., a small unidentified ophiuroid, *G. tesselata*, the solitary coral *Laborynthocyathus* sp., and the polychaete *Proscoloplos* sp. The species with the highest average biomass in the collections were the galatheid *E. picta*, the brachyuran crab *Bathynectes* sp., and the sabellid polychaete *Euratella* sp. (**Table 5.5**). The most dominant species in terms of relative proportion of total biomass in each collection were *Euratella* sp., *E. picta*, and the tube-dwelling polychaete *Eunice* sp. The majority of the associated-fauna biomass in each collection was in either the suspension feeder or primary predator category, with occasional dominance by a large, mobile predator or scavenger (**Figure 5.5**). In general, higher order predators made up a larger proportion of the biomass in the Viosca Knoll sites than they did at the deeper Green Canyon sites.

There was a trend of more species in larger *L. pertusa* collections ($r^2 = 0.425$, $p = 0.008$), but other measures of diversity did not exhibit discernable trends with various measures of habitat complexity including coral surface area, surface area per liter of coral skeleton volume, and the proportion of live coral in the collection (**Figure 5.6**). The Shannon-Weaver diversity index (H') ranged from 0.67 to 2.54 (**Table 5.3**) and was not significantly related to the measures of habitat complexity examined, although the correlation to the proportion of live coral in the colony was nearly significant ($r^2 = 0.206$, $p = 0.051$). Similarly, Pielou's evenness index (J'), ranging from 0.371 to 0.976, was not significantly related to any of the factors examined.

Table 5.2. Tests for associations of species with substrate types by dive number and site. Shown are abundance and density of species, total area of mosaic, percent cover of substrate (includes abiotic substrate and colonial fauna), and percentages of occurrences in each substrate category. Rows in **bold** indicate that there were sufficient individuals of that species to satisfy the assumptions of the chi-square test. Cells with an asterisk indicate a significant departure from expected values. The first table in each pair presents the analysis of species occurrence in close proximity to (<10 cm from) a given substrate. The second table in each pair presents the occurrence of a species directly on a given substrate type.

(a) Dive 4725, GC184

Fauna	No. on Non-Sediment Substrate	% on Dead *Lophelia*	% on Tubeworms	% on *Callogorgia*
Total Area	2.71	1.81	0.90	0.16
sabellids	**69**	**42.0***	**27.5**	**8.7**
***Munidopsis* sp.**	**23**	**41.7***	**64.7***	**0**
fish	1	100	0	0

Fauna	Density/m^2	No. on Non-Sediment Substrate	% on Dead *Lophelia*	% on Tubeworms	% on *Callogorgia*	% on Carbonate Rubble
Percent Cover			40.18	7.48	1.22	40.51
sabellids*	**25.4**	**69**	**39.13**	**18.84***	**0**	**42.03**
Munidopsis* sp.	**8.5**	**23**	**21.7**	**39.1***	**0**	**39.1**
fish	*0.4*	1	0	0	0	100

(b) Dive 4726, GC354

Fauna	No. on Non-Sediment Substrate	% on Live *Lophelia*	% on Dead *Lophelia*	% on Carbonate	% on Other Colonial Cnidarians	% on Bacterial Mat
Total Area	14.35	1.05	12.34	5.30	14.30	2.72
Eumunida picta*	**13**	**7.69***	**15.38**	**15.38***	**7.69**	**7.69**
sea star	1	0	0	0	0	0
fish	1	0	0	0	0	0
Munidopsis* sp.	**33**	**0**	**9.09**	**9.09**	**12.12**	**9.09***
shrimp	2	0	0	0	0	0
sabellids	**10**	**30***	**10***	**0**	**0**	**0**
sponges*	**36**	**0**	**13.89**	**2.78**	**13.89**	**16.67***
other crabs	2	0	0	50	50	0

Fauna	Density/m^2	No. on Non-Sediment Substrate	% on Live *Lophelia*	% on Dead *Lophelia*	% on Carbonate	% on Other Colonial Cnidarians	% on Carbonate Rubble	% on Bacterial Mats
Percent Cover			0.05	45.47	12.97	1.58	39.96	0.08
Eumunida picta*	**0.9**	**13**	**0**	**38.46**	**38.46***	**0**	**15.38**	**7.69***
sea star	0.1	1	0	100	0	0	0	0
fish	0.1	1	0	0	100	0	0	0
Munidopsis* sp.	**2.3**	**33**	**0**	**45.45**	**12.12**	**3.03**	**27.27**	**12.12***
shrimp	0.1	2	0	100	0	0	0	0
sabellids	**0.7**	**10**	**0**	**90**	**0**	**0**	**10**	**0**
sponges*	**2.5**	**36**	**0**	**38.89**	**11.11**	**0**	**36.11**	**13.89***
other crabs	0.1	2	0	50	0	0	0	50

Table 5.2. (continued).

(c) Dive 4728, GC234

Fauna	No. on Non-Sediment Substrate	% on Live *Lophelia*	% on Dead *Lophelia*	% on Carbonate	% on Other Colonial Cnidarians	% on Bacterial Mat	% on Tubeworms
Total Area	2.7	4.07	48.52	25.19	10.37	104.07	68.15
Eumunida picta	**6**	**0**	**0**	**66.67***	**0**	**16.67**	**33.33**
anemones	1	0	0	100	0	100	0
brittle stars	**6**	**16.67**	**33.33***	**0**	**66.67***	**33.33**	**33.33**
sabellids	**72**	**0**	**15.28***	**13.89***	**0***	**18.06***	**72.22**
solitary coral	**26**	**3.85**	**30.77***	**3.85***	**19.23**	**11.50**	**19.23***
sponge	1	0	0	0	0	0	100
shrimp	**6**	**16.67**	**16.67***	**16.67**	**0**	**0**	**16.67***
fish	**7**	**0**	**17.65**	**35.29**	**5.88**	**23.53**	**23.53**

Fauna	Density/m^2	No. on Non-Sediment Substrate	% on Live *Lophelia*	% on Dead *Lophelia*	% on Carbonate	% on Other Colonial Cnidarians	% on Bacterial Mat	% on Tubeworms
Percent cover			0.33	46.2	35	0.56	12.2	5.63
Eumunida picta	**2.2**	**6**	**0**	**100**	**0**	**0**	**0**	**0**
anemones	0.4	1	0	100	0	0	0	0
brittle stars*	**2.2**	**6**	**0**	**33.3**	**33.3**	**33.3***	**0**	**0**
sabellids*	**26.7**	**72**	**0**	**15.3***	**81.9***	**0**	**2.8***	**0***
solitary coral*	**9.6**	**26**	**0**	**3.9***	**96.2***	**0**	**0**	**0**
sponge	0.4	1	0	0	100	0	0	0
shrimp	**2.2**	**6**	**0**	**33.3**	**66.7**	**0**	**0**	**0**
fish	**2.6**	**7**	**0**	**71.4**	**21.6**	**0**	**0**	**0**

(d) Dive 4733, VK826

Fauna	No. on Non-Sediment Substrate	% on Live *Lophelia*	% on Dead *Lophelia*	% on Carbonate	% on Other Colonial Corals	% on Bacterial Mat
Total Area	58.65	45.01	50.81	0.90	4.25	0.34
sea star	1	100	0	0	0	0
anemones	**11**	**18.18**	**54.55**	**0**	**0**	**0**
crinoids	**92**	**48.90**	**32.61***	**0**	**2.17**	**0**
Eumunida picta	**53**	**56.60**	**22.64***	**0**	**7.55**	**0**
fish	4	100	0	0	0	0
snails	2	0	0	0	0	0
***Munidopsis* sp.**	**16**	**31.30**	**43.75**	**0**	**6.30**	**0**
urchins	**15**	**46.67**	**20***	**6.67***	**0**	**0**
shrimp	1	0	100	0	0	0
sabellid	**55**	**7.27***	**12.73***	**0**	**0**	**0**
sponge	**31**	**9.68***	**41.94**	**0**	**0**	**0**

Fauna	Density/m^2	No. on Non-Sediment Substrate	% on Live *Lophelia*	% on Dead *Lophelia*	% on Carbonate	% on Carbonate Rubble	% on Other Colonial Corals	% on Bacterial Mat
Percent cover			23.53	52.33	0.10	22.93	1.10	0.01
sea star	0.02	1	0	100	0	0	0	0
anemones	**0.19**	**11**	**27.27**	**45.45**	**0**	**18.18**	**9.09**	**0**
crinoids*	**1.57**	**92**	**44.57***	**53.26**	**0**	**2.17***	**0**	**0**
Eumunida picta	**0.90**	**53**	**22.64**	**67.92**	**0**	**9.43**	**0**	**0**
fish	0.07	4	0	100	0	0	0	0
snails	0.03	2	0	100	0	0	0	0
Munidopsis* sp.	**0.27**	**16**	**68.75***	**12.5***	**6.25***	**12.5**	**0**	**0**
urchins	**0.26**	**15**	**6.67**	**73.33**	**0**	**20**	**0**	**0**
shrimp	0.02	1	0	0	0	100	0	0
sabellid*	**0.94**	**55**	**0***	**90.91***	**0**	**9.09***	**0**	**0**
sponge*	**0.53**	**31**	**51.61***	**29.03***	**0**	**19.35**	**0**	**0**

Table 5.2. (continued).

(e) Dive 4736-1, VK826

Fauna	No. on Non-Sediment Substrate	% on Live *Lophelia*	% on Dead *Lophelia*	% on Mixed *Lophelia*	% on other Colonial Corals	% on Carbonate
Total Area	11.70	28.55	26.75	7.78	1.51	0.66
solitary coral	2	0	50	0	0	0
crinoids	**20**	**60***	**45**	**20**	**5**	**0**
sabellids	**30**	**46.7***	**23.3**	**0**	**0**	**0**
anemones	2	0	100	100	0	0
sponges	4	50	0	25	0	0
Bathynectes	2	100	50	0	0	0
Eumunida picta	**11**	**54.6**	**36.4**	**36.4**	**0**	**0**
urchins	4	75	75	25	0	0

Fauna	Density/m^2	No. on Non-Sediment Substrate	% on Live *Lophelia*	% on Dead *Lophelia*	% on Mixed *Lophelia*	% on Other Colonial Cnidarians	% on Carbonate	% on Carbonate Rubble
Percent cover			4.44	14.02	1.18	0.35	0.05	79.97
solitary coral	*0.2*	2	50	0	0	0	0	50
crinoids*	**1.7**	**20**	**0**	**50***	**5**	**0**	**0**	**45***
sabellids*	**2.6**	**30**	**0**	**76.67***	**0**	**0**	**0**	**23.33***
anemones	*0.2*	2	100	0	0	0	0	0
sponges	0.3	4	0	50	25	0	0	25
Bathynectes	*0.2*	2	0	50	0	0	0	50
Eumunida picta*	**0.9**	**11**	**0**	**54.54***	**0**	**0**	**0**	**45.45***
urchins	0.3	4	0	25	0	0	0	75

(f) Dive 4736-2, VK826

Fauna	No. on Non-Sediment Substrate	% on Live *Lophelia*	% on Dead *Lophelia*	% on Mixed *Lophelia*	% on Other Colonial Cnidarians	% on Carbonate
Total Area	32.78	8.61	33.75	3.62	3.51	3.35
crinoids	**46**	**60.9***	**19.6***	**2.2**	**2.2**	**0**
anemones	1	0	0	0	0	0
basket star	2	100	0	0	0	0
urchins	**6**	**33.3***	**16.7**	**0**	**0**	**0**
solitary coral	**13**	**23.1**	**15.4**	**0**	**0**	**0**
fish	**11**	**27.3***	**18.2**	**18.2***	**9.1**	**36.4***
snail	3	66.7	0	0	0	0
sabellid	3	0	0	0	0	0
sponge	**21**	**28.6***	**28.6**	**0**	**0**	**0**
Eumunida picta	**21**	**61.9***	**14.3**	**0***	**0**	**0**

Fauna	Density/m^2	No. on Non-Sediment Substrate	% on Live *Lophelia*	% on Dead *Lophelia*	% on Mixed *Lophelia*	% on Other Colonial Cnidarians	% on Carbonate	% on Carbonate Rubble
Percent cover			42.10	17.30	0.72	0.60	0.16	39.11
crinoids*	**1.40**	**46**	**15.2***	**65.2***	**13.0***	**0**	**0**	**6.5***
anemones	0.03	1	100	0	0	0	0	0
basket star	0.06	2	0	100	0	0	0	0
urchins	**0.18**	**6**	**16.7**	**16.7**	**0**	**0**	**0**	**66.7**
solitary coral*	**0.40**	**13**	**7.69***	**7.69**	**0**	**0**	**0**	**84.6***
fish	**0.34**	**11**	**0**	**27.30**	**0**	**0**	**0**	**72.70**
snail	0.09	3	0	100	0	0	0	0
sabellid	0.09	3	0	66.7	0	0	0	33.3
sponge	**0.64**	**21**	**14.3**	**19.1**	**0**	**0**	**0**	**66.7**
Eumunida picta*	**0.64**	**21**	**28.6**	**47.62***	**4.76***	**4.76***	**0**	**14.3***

Table 5.2. (continued).

(g) Dive 4738, MC885

Fauna	No. on Non-Sediment Substrate	% on Live *Madrepora*	% on Dead *Madrepora*	% on Carbonate	% on Other Colonial Cnidarians
Total Area	1.54	24.81	21.90	63.36	67.18
brittle stars	**14**	**28.57**	**7.14**	**21.43***	**0***
galatheid	2	0	0	0	0
anemones	2	50	0	0	0
other crabs	1	0	0	100	100
solitary corals	**25**	**4***	**4***	**32***	**28***

Fauna	Density/m^2	No. on Non-Sediment Substrate	% on Live *Madrepora*	% on Dead *Madrepora*	% on Carbonate	% on Other Colonial Cnidarians	% on Carbonate Rubble
Percent cover			2.24	13.80	50.53	20.99	12.44
brittle stars*	**9.1**	**14**	**0**	**0**	**0***	**100***	**0**
galatheid	1.3	2	0	50	50	0	0
anemones	1.3	2	0	50	0	0	50
other crabs	0.6	1	0	0	0	0	100
solitary corals*	**16.2**	**25**	**0**	**0***	**52**	**12**	**36***

(h) Dive 4740, GC234

Fauna	No. on Non-Sediment Substrate	% on Live *Lophelia*	% on Dead *Lophelia*	% on Carbonate	% on Other Colonial Cnidarians	% on Tubeworms
Total Area	2.7	8.19	81.61	17.76	12.22	2.52
***Munidopsis* sp.**	**9**	**0**	**0***	**22.2**	**0**	**0**
Eumunida picta	3	66.7	0	0	33.3	0
anemones	**18**	**5.6**	**50***	**11.1**	**5.6**	**0**
solitary coral	4	50	0	0	25	0
fish	2	0	0	0	0	0
brittle star	1	0	0	100	0	0

Fauna	Density/m^2	No. on Non-Sediment Substrate	% on Live *Lophelia*	% on Dead *Lophelia*	% on Carbonate	% on Other Colonial Cnidarians	% on Carbonate Rubble	% on Tubeworms
Percent cover			0.13	80.23	15.24	1.26	2.88	0.25
***Munidopsis* sp.**	**3.3**	**9**	**0**	**100**	**0**	**0**	**0**	**0**
Eumunida picta	1.1	3	0	100	0	0	0	0
anemones*	**6.7**	**18**	**0**	**44.4***	**44.4***	**0**	**11.1***	**0**
solitary coral	1.5	4	0	100	0	0	0	0
fish	0.7	2	0	100	0	0	0	0
brittle star	0.4	1	0	0	0	100	0	0

Table 5.2. (continued).

(i) Dive 4861, GC354

Fauna	No. on Non-Sediment Substrate	% on Live *Lophelia*	% on Dead *Lophelia*	% on Carbonate	% on Other Colonial Cnidarians
Total Area	2.96	4.45	31.62	11.94	4.93
anemones	**24**	**8.3**	**4.17***	**0**	**12.5**
Eumunida picta	**18**	**0**	**22.2**	**16.7**	**5.6**
fish	2	0	0	0	0
Munidopsis sp.	4	0	0	25	0
sabellid	**13**	**0**	**0***	**7.7**	**61.5***
sponges	**12**	**0**	**16.7**	**33.3***	**16.7**
shrimp	2	0	0	0	0

Fauna	Density/m^2	No. on Non-Sediment Substrate	% on Live *Lophelia*	% on Dead *Lophelia*	% on Carbonate	% on Other Colonial Cnidarians	% on Carbonate Rubble
Percent cover			0.84	46.87	11.74	0.22	40.32
anemones*	**8.1**	**24**	**0**	**83.33***	**12.5**	**0**	**4.17***
Eumunida picta	**6.1**	**18**	**0**	**44.44**	**5.56**	**0**	**50**
fish	0.3	1	0	100	0	0	0
Munidopsis sp.	1.3	4	0	75	25	0	0
sabellid*	**4.4**	**13**	**0**	**100***	**0**	**0**	**0***
sponges*	**4.0**	**12**	**8.33***	**50**	**33.3***	**0**	**8.33***
shrimp	0.7	2	50	0	50	0	0

(j) Dive 4862, GC184

Fauna	No. on Non-Sediment Substrate	% on Live *Lophelia*	% on Dead *Lophelia*	% on Carbonate	% on *Callogorgia*	% on Tubeworms
Total Area	11.986	2.75	19.27	25.95	19.69	0.39
fish	1	0	0	0	0	1.5
anemones	**5**	**0**	**0**	**40**	**0**	**0**
solitary corals	**7**	**0**	**14.3**	**14.3**	**57.1***	**0**
galatheid	**11**	**0**	**0***	**9.1**	**9.1**	**0***
sponge	1	0	0	100	0	0
shrimp	1	0	0	100	0	0
sabellid	**374**	**3.2**	**10.2***	**21.7***	**21.7**	**0***

Fauna	Density/m^2	No. on Non-Sediment Substrate	% on Live *Lophelia*	% on Dead *Lophelia*	% on Carbonate	% on Carbonate Rubble	% on Other Colonial Cnidarians	% on Tubeworms
Percent cover			0.10	28.28	25.20	39.02	7.01	0.39
fish	0.08	1	0	0	0	100	0	0
anemones*	**0.42**	**5**	**0**	**100***	**0**	**0**	**0**	**0**
solitary corals	**0.58**	**7**	**0**	**0**	**42.9**	**42.9**	**14.3**	**0**
galatheid*	**0.92**	**11**	**0**	**9.1**	**0***	**27.3**	**9.1**	**54.5***
sponge	0.08	1	0	100	0	0	0	0
shrimp	0.08	1	0	0	0	100	0	0
sabellid*	**31.20**	**374**	**0**	**40.1***	**16.8***	**41.2**	**1.9***	**0**

Table 5.2. (continued).

(k) Dive 4863, MC885

Fauna	No. on Non-Sediment Substrate	% on Live *Madrepora*	% on Dead *Madrepora*	% on Other Colonial Cnidarians
Total Area	1.92	24.48	41.66	2.08
sponge	1	0	0	100
sabellid	**13**	**23.1**	**0***	**0**
anemones	**8**	**12.5**	**12.5**	**12.5***
solitary coral	3	66.7	33.3	0
galatheid	1	0	0	0
crinoid	3	0	0	0

Fauna	Density/m^2	No. on Non-Sediment Substrate	% on Live *Madrepora*	% on Dead *Madrepora*	% on Other Colonial Cnidarians	% on Carbonate Rubble
Percent cover			8.33	35.41	0.01	56.25
sponge	*0.5*	1	0	100	0	0
sabellid*	**6.8**	**13**	**0**	**100***	**0**	**0***
anemones	**4.2**	**8**	**0**	**62.5**	**0**	**37.5**
solitary coral	*1.6*	3	33.3	66.7	0	0
galatheid	0.5	1	0	100	0	0
crinoid	1.6	3	100	0	0	0

(l) Dive 4869, VK862

Fauna	No. on Non-Sediment Substrate	% on Live *Lophelia*	% on Dead *Lophelia*	% on Mixed *Lophelia*	% on Other Colonial Cnidarians	% on Carbonate
Total area		17.41	4.56	1.46	6.40	2.01
anemones	**369**	**10.0***	**2.2***	**0***	**8.4***	**1.4**
Eumunida picta	**21**	**47.6***	**9.5**	**0**	**0**	**0**
solitary corals	1	0	0	0	0	0
Bathynectes	1	0	0	0	0	0
crinoids	**7**	**71.4***	**42.9***	**0**	**0**	**0**
sabellids	**52**	**0***	**0**	**0**	**7.7**	**1.9**
snails	4	50	0	0	50	0
sea stars	1	0	0	0	100	0
urchins	1	0	0	0	0	0

Fauna	No. on Non-Sediment Substrate	Density	% on Live *Lophelia*	% on Dead *Lophelia*	% on Mixed *Lophelia*	% on Other Colonial Cnidarians	% on Carbonate	% on Carbonate Rubble
Total area	102.7		18.94	3.52	0.89	3.18	3.00	70.48
anemones*	**369**	**3.59**	**0***	**2.7**	**0**	**1.4**	**1.6**	**94.3***
Eumunida picta	**21**	**0.20**	**19.0**	**9.5**	**0**	**4.8***	**0**	**66.7**
solitary corals	1	0.01	0	0	0	0	0	100
Bathynectes	1	0.01	0	0	0	0	0	100
crinoids*	**7**	**0.07**	**28.6**	**14.3**	**14.3***	**0**	**0**	**42.9**
sabellids*	**52**	**0.51**	**0***	**0**	**0**	**1.9**	**7.7***	**90.4***
snails	4	0.04	0	0	0	0	0	100
sea stars	1	0.01	0	0	0	0	0	100
urchins	1	0.01	0	0	0	0	0	100

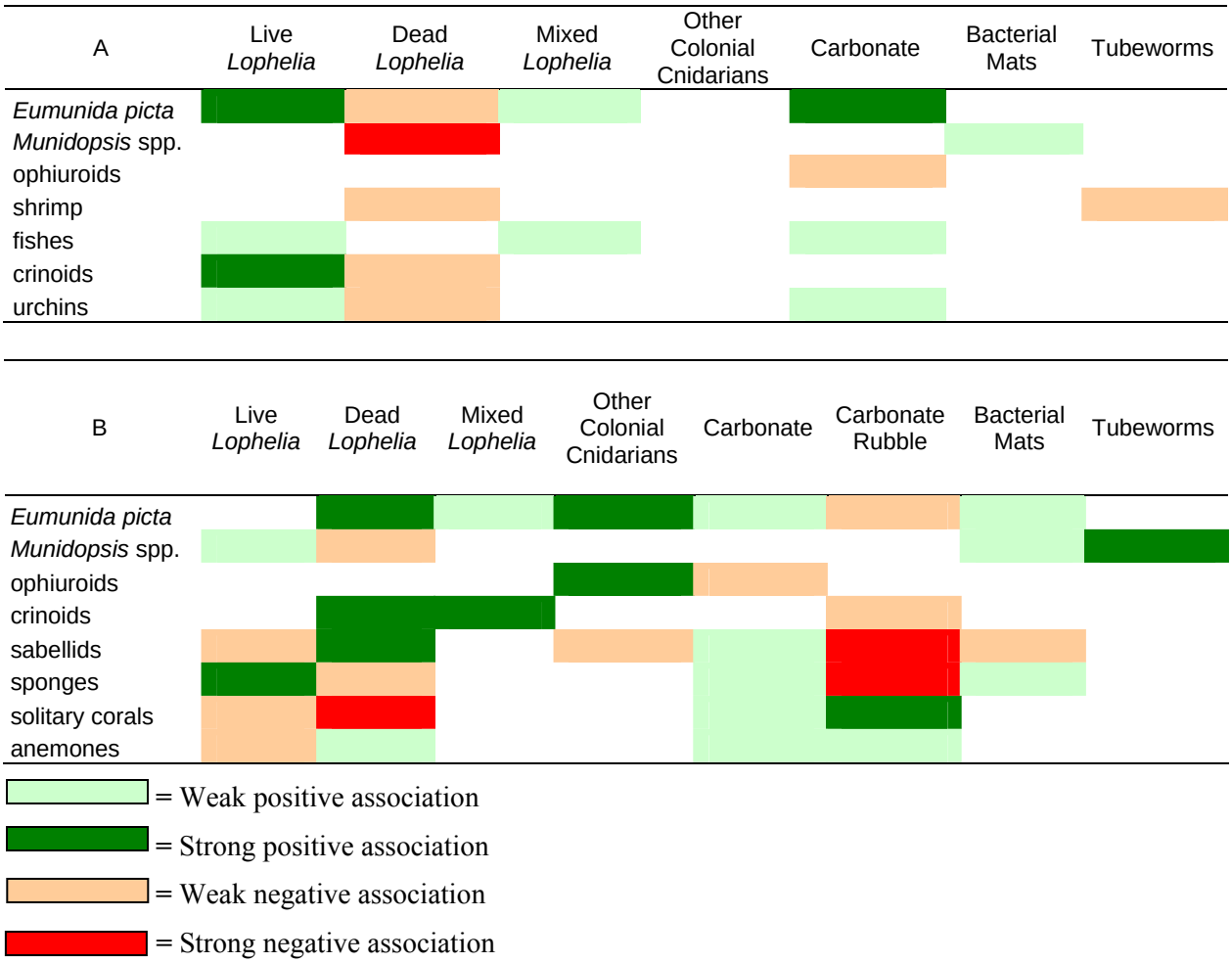

Figure 5.4. Positive and negative associations of species from photomosaic samples with specific substrate types (summary of Chi-square tests from all photomosaic samples). Weak associations were significant in only one mosaic analysis, positive associations were significant in multiple analyses. A. Mobile fauna in close proximity (<10 cm) to a given substrate. B. Direct association between species seen and substrate.

Table 5.3. Details of coral Bushmaster collections.

Sample	Site	Dive	Latitude (N)	Longitude (W)	Water Depth (m)	Coral Surface Area (m^2)	Coral Surface Area/Volume (m^2/L)	% Live Coral	No. of Species	Diversity H'	Evenness J'
G1a	GC234	4715	27°44.798'	91°13.450'	502	0.895	4.19	3.8	16	1.79	0.645
G1b	GC234	4724	27°44.817'	91°13.468'	502	0.270	3.79	0.0	15	2.21	0.815
G1c	GC234	4728	27°44.828'	91°13.437'	509	0.342	3.32	6.4	12	1.45	0.631
G1d	GC234	4740	27°44.805'	91°13.448'	507	1.302	3.94	2.2	20	1.07	0.371
G2a	GC354	4741	27°35.889'	91°49.595'	525	0.957	3.70	0.0	23	2.54	0.833
G2b	GC354	4577	27°35.893'	91°49.608'	524	0.847	6.30	9.6	13	2.01	0.873
G2c	GC354	4592	27°35.892'	91°49.579'	524	2.498	7.89	0.0	19	2.30	0.828
V1a	VK826	4736	29°09.495'	88°01.039'	464	0.181	3.73	50.0	6	1.55	0.963
V1b	VK826	4737	29°09.466'	88°01.049'	468	0.985	3.92	8.3	12	2.28	0.950
V1c	VK826	4733	29°09.527'	88°01.009'	465	0.209	3.93	5.3	6	1.75	0.976
V1d	VK826	4867	29°09.495'	88°01.037'	462	1.346	4.88	31.7	17	2.34	0.866
V2a	VK826NE	4868	29°10.215'	88°00.686'	470	0.676	4.97	14.7	16	1.72	0.651
V2b	VK826NE	4871	29°10.215'	88°00.704'	459	0.634	5.33	6.7	13	2.06	0.859
V3	VK826W	4872	29°09.642'	88°01.163'	453	1.566	5.64	21.2	20	2.52	0.891
V4	VK862	4869	29°06.355'	88°23.051'	313	0.761	7.61	80.0	8	0.67	0.413

Table 5.4. Abundance of coral associated fauna collected with the Bushmaster device. p = species present but not enumerated.

Taxon	Number in Sample														
	GC234				GC354			VK826				VK826NE		VK826W	VK862
	G1a	G1b	G1c	G1d	G2a	G2b	G2c	V1a	V1b	V1c	V1d	V2a	V2b	V3	V4
Porifera															
Sponge	--	--	p	--	p	p	p	p	p	--	p	p	--	p	p
Cnidaria															
Actinarian	1	--	--	--	--	--	7	--	--	--	--	--	--	--	1
Hydroid	--	--	p	p	p	p	p	--	--	--	p	p	p	p	p
Zoanthid	--	--	--	--	--	p	p	--	--	--	--	--	p	p	p
Callogorgia	--	--	--	p	--	--	--	--	--	--	--	--	--	--	--
Caryophyllia	1	1	1	19	2	--	--	1	--	--	--	--	--	--	--
Labyrinthocyathus	1	9	2	9	4	--	--	--	--	--	--	--	--	--	--
Tethocyathus	--	1	3	11	--	--	--	2	--	--	--	--	--	--	--
Nemertea															
Nemertean	--	--	1	--	--	--	11	--	--	--	--	--	--	--	--
Sipuncula															
Phascolosoma	--	--	--	1	--	--	--	--	--	--	--	--	--	--	--
Annelida: Polychaeta															
Branchinotogluma	--	1	--	--	--	--	--	--	--	--	--	--	--	--	--
Chloeia	--	--	--	--	--	--	1	--	--	--	5	1	--	--	--
Eteone	--	--	--	--	--	1	--	--	--	--	1	--	--	--	--
Eumida	--	--	--	--	--	--	--	--	--	--	1	--	--	--	--
Eunice sp.	3	2	--	--	--	1	--	--	2	--	5	1	1	4	--
Euratella	39	17	30	272	23	1	--	--	4	--	2	26	3	9	--
Glycera capitata	--	3	--	1	--	--	--	--	--	--	--	--	1	--	--
Glycera tesselata	11	13	1	8	5	2	--	--	5	2	3	--	--	8	--
Harmothoe	--	--	--	--	2	3	4	--	--	--	--	--	--	--	--
Hesionid	--	--	--	--	--	--	--	--	1	--	--	--	--	1	--
Iphioninoe	--	--	--	--	--	--	1	--	--	--	--	--	--	--	--
Lumbrineris	--	--	--	--	--	--	2	--	--	--	--	--	--	--	--
Lysidice	--	2	--	3	2	--	--	--	--	--	2	--	--	4	--

Table 5.4. (continued).

Taxon	Number in Sample														
	GC234				GC354			VK826				VK826NE		VK826W	VK862
	G1a	G1b	G1c	G1d	G2a	G2b	G2c	V1a	V1b	V1c	V1d	V2a	V2b	V3	V4
Neoamphitrite	--	2	--	--	--	--	--	--	--	--	--	--	--	--	--
Onuphidae	--	--	--	--	--	--	--	--	--	--	1	--	--	--	--
Pholoe	2	--	--	--	--	--	--	--	--	--	--	--	--	--	--
Phyllodoce	--	--	--	--	--	--	--	--	1	--	--	1	1	1	--
Proscoloplos	1	3	--	--	--	--	--	--	--	--	--	6	8	--	--
Sabellid	--	--	--	--	--	--	--	--	--	--	--	--	--	--	15
Serpulid	--	--	--	--	--	--	--	--	1	--	--	--	--	--	--
Sigalionid	1	--	--	--	--	--	--	--	--	--	--	--	--	--	--
Syllid	1	--	--	1	8	--	--	--	--	--	--	--	--	1	2
Terebellid	--	--	--	--		--	--	--	3	1	2	1	7	2	3
Unid. polychaete 1	--	--	--	--	3	--	--	--	--	--	--	--	--	--	--
Unid. polychaete 2	--	--	--	--	--	--	--	--	--	--	--	--	1	--	--
Unid. polychaete 3	--	--	--	--	--	--	--	--	--	--	--	1	--	--	--
Mollusca: Aplacophora															
Aplacophoran	--	--	--	--	1	--	--	--	--	--	--	--	--	--	--
Mollusca: Polyplacophora															
Leptochiton	--	1	--	--	--	--	--	--	--	--	--	--	--	--	--
Mollusca: Gastropoda									--						
Bathynerita	--	2	--	--	--	--	--	--	--	--	--	--	--	--	--
Coralliophila	2	--	3	1	--	--	2	1	--	--	--	1	--	2	--
Diodora	--	--	--	--	--	--	1	--	--	--	--	--	--	--	--
Emarginula	--	--	--	--	--	--	1	--	--	--	--	--	1	--	--
Prolipidium	--	--	--	--	1	--	--	--	--	--	--	--	--	--	--
Provanna	--	--	2	--	--	--	--	--	--	--	--	--	--	--	--
Mollusca: Bivalvia															
Arca	--	--	--	--	2	--	--	--	--	--	--	--	--	--	--
Arthropoda: Pycnogonida															
Anopylodactylus	1	--	--	--	--	--	--	--	--	--	--	--	--	--	--
Pentacolossendeis	1	--	--	--	--	--	--	--	--	--	--	--	--	--	--

Table 5.4. (continued).

Taxon	Number in Sample														
	GC234				GC354			VK826				VK826NE		VK826W	VK862
	G1a	G1b	G1c	G1d	G2a	G2b	G2c	V1a	V1b	V1c	V1d	V2a	V2b	V3	V4
Arthropoda: Crustacea															
Amphipod	--	--	--	--	1	--	--	--	--	--	2	--	5	--	--
Bathynectes	--	--	--	--	--	--	--	--	--	--	--	1	--	--	--
Bathynomous giganteus	--	--	--	--	--	--	1	--	--	--	--	--	--	--	--
Costatoverruca floridana	--	--	3	--	--	4	--	--	--	--	--	--	1	1	--
Eumunida	--	--	--	1	--	--	--	1	--	1	--	1	--	2	--
Isopod	--	--	--	--	--	--	--	--	--	--	1	3	6	2	--
Munidopsis 1	2	4	--	--	--	9	6	--	--	--	--	--	--	--	--
Munidopsis 2	2	--	2	2	5	--	--	--	--	--	1	2	--	1	--
Munidopsis 3	--	--	--	5	1	--	15	--	--	--	--	--	--	1	--
Nibilia	--	--	--	2	1	--	--	--	--	--	--	--	--	--	--
Periclemenes	5	--	--	--	1	2	1	--	3	2	2	--	--	3	--
Plesionika	--	--	--	--	1	--	--	--	--	--	--	--	--	--	--
Stenopus	--	--	--	11	4	1	1	--	3	--	--	1	--	--	--
Unid. bresilid	--	--	--	--	--	--	2	--	--	--	--	--	--	--	--
Unid. galatheid	--	--	--	--	4	--	--	--	--	--	--	1	--	--	--
Echinodermata															
Crinoid	--	--	--	--	--	--	--	2	3	--	1	--	--	1	--
Ophionerid	--	--	--	2	--	--	--	--	2	--	--	--	--	--	--
Ophiotreta valenciennesi rufescens	--	--	--	2	3	3	12	--	--	2	--	--	--	--	--
Ophiuroid sp. 1	--	1	--	--	--	--	--	--	--	--	--	--	--	--	--
Ophiuroid sp. 2 (6 arms)	--	--	--	--	1	--	--	--	--	2	12	--	--	2	87
Chordata															
Bellotia	--	--	--	1	--	--	--	--	--	--	--	--	--	--	--

Table 5.5. Biomass of associated fauna in each Bushmaster collection. Trophic level designations are as follows: 1 – suspension feeder; 2 – detritus feeder/grazer; 3 – first-order predator; 4 – higher-order predator.

Trophic Level	Taxon	Biomass (ash-free dry wt, g/m^2)														
		GC234				GC354			VK826				VK826NE		VK826W	VK862
		G1a	G1b	G1c	G1d	G2a	G2b	G2c	V1a	V1b	V1c	V1d	V2a	V2b	V3	V4
	Cnidaria															
1	Actinarian	0.11	--	--	--	--	--	0.88	--	--	--	--	--	--	--	0.24
	Nemertea															
3	Nemertean	--	--	0.23	--	--	--	0.32	--	--	--	--	--	--	--	--
	Sipuncula															
2	*Phascolosoma*	--	--	--	0.60	--	--	--	--	--	--	--	--	--	--	--
	Annelida: Polychaeta															
3	*Branchinotogluma*	--	0.84	--	--	--	--	--	--	--	--	--	--	--	--	--
3	*Chloeia*	--	--	--	--	--	--	0.30	--	--	--	0.47	0.32	--	--	--
3	*Eteone*	--	--	--	--	--	0.10	--	--	--	--	0.17	--	--	--	--
3	*Eumida*	--	--	--	--	--	--	--	--	--	--	0.30	--	--	--	--
3	*Eunice* sp.	0.40	0.57	--	--	--	0.25	--	--	0.66	--	0.45	0.98	0.48	0.24	--
1	*Euratella*	0.44	0.24	0.33	3.55	0.16	0.15	--	--	0.28	--	0.29	0.39	0.78	0.20	--
3	*Glycera capitata*	--	0.37	--	0.23	--	--	--	--	--	--	--	--	0.72	--	--
3	*Glycera tesselata*	0.13	0.22	0.19	0.25	0.18	0.10		--	0.53	0.18	0.18	--	--	0.49	--
3	*Harmothoe*	--	--	--	--	0.48	0.18	0.22	--	--	--	--	--	--	--	--
2	Hesionid	--	--	--	--	--	--		--	0.17	--	--	--	--	0.36	--
2	*Iphioninoe*	--	--	--	--	--	--	0.10	--	--	--	--	--	--	--	--
3	*Lumbrineris*	--	--	--	--	--	--	0.13	--	--	--	--	--	--	--	--
3	*Lysidice*	--	0.48	--	0.12	0.22	--	--	--	--	--	0.13	--	--	0.49	--
2	*Neoamphitrite*	--	0.39	--	--	--	--	--	--	--	--	--	--	--	--	--
2	Onuphidae	--	--	--	--	--	--	--	--	--	--	0.14	--	--	--	--
2	*Pholoe*	0.19	--	--	--	--	--	--	--	--	--	--	--	--	--	--
2	*Phyllodoce*	--	--	--	--	--	--	--	--	0.59	--	--	0.14	0.18	0.18	--
3	*Proscoloplos*	0.19	0.12	--	--	--	--	--	--	--	--	--	0.44	0.46	--	--
1	Sabellid	--	--	--	--	--	--	--	--	--	--	--	--	--	--	0.23
1	Serpulid	--	--	--	--	--	--	--	--	0.10	--	--	--	--	--	--

Table 5.5. (continued).

Trophic Level	Taxon	Biomass (ash-free dry wt, g/m^2)														
		GC234				GC354			VK826				VK826NE		VK826W	VK862
		G1a	G1b	G1c	G1d	G2a	G2b	G2c	V1a	V1b	V1c	V1d	V2a	V2b	V3	V4
3	Sigalionid	0.48	--	--	--	--	--	--	--	--	--	--	--	--	--	--
2	Syllid	0.60	--	--	0.36	0.61	--	--	--	--	--	--	--	--	0.36	0.72
1	Terebellid	--	--	--	--	--	--	--	--	0.32	0.60	0.59	0.24	0.12	0.12	0.18
2	Unid polychaete 1	--	--	--	--	0.12	--	--	--	--	--	--	--	--	--	--
2	Unid polychaete 2	--	--	--	--	--	--	--	--	--	--	--	--	0.12	--	--
2	Unid polychaete 3	--	--	--	--	--	--	--	--	--	--	--	0.36	--	--	--
	Mollusca: Aplacophora															
2	Aplacophoran	--	--	--	--	0.48	--	--	--	--	--	--	--	--	--	--
	Mollusca: Polyplacophora															
2	*Leptochiton*	--	0.19	--	--	--	--	--	--	--	--	--	--	--	--	--
	Mollusca: Gastropoda															
2	*Bathynerita*	--	0.47	--	--	--	--	--	--	--	--	--	--	--	--	--
3	*Coralliophila*	0.80	--	0.30	0.17	--	--	0.80	0.13	--	--	--	0.74		0.19	
2	*Diodora*	--	--	--	--	--	--	0.40	--	--	--	--	--	--	--	--
2	*Emarginula*	--	--	--	--	--	--	0.25	--	--	--	--	--	0.68	--	--
2	*Prolipidium*	--	--	--	--	0.20	--	--	--	--	--	--	--	--	--	--
2	*Provanna*	--	--	0.10	--	--	--	--	--	--	--	--	--	--	--	--
	Mollusca: Bivalvia															
1	*Arca*	--	--	--	--	0.16	--	--	--	--	--	--	--	--	--	--
	Arthropoda: Pycnogonida															
3	*Anopylodactylus*	0.16	--	--	--	--	--	--	--	--	--	--	--	--	--	--
3	*Pentacolossendeis*	0.70	--	--	--	--	--	--	--	--	--	--	--	--	--	--
	Arthropoda: Crustacea															
2	Amphipod	--	--	--	--	0.32	--	--	--	--	--	0.19	--	0.96	--	--
4	*Bathynectes*	--	--	--	--	--	--	--	--	--	--	--	5.66	--	--	--
4	*Bathynomous giganteus*	--	--	--	--	--	--	0.12	--	--	--	--	--	--	--	--
1	*Costatoverruca floridana*	--	--	0.14	--	--	0.19	--	--	--	--	--	--	0.44	0.50	--
4	*Eumunida*	--	--	--	0.25	--	--	--	4.19	--	3.55	--	5.23	--	8.28	--
3	Isopod	--	--	--	--	--	--	--	--	--	--	0.44	0.54	0.47	0.20	--
3	*Munidopsis* 1	0.70	0.53	--	--	--	0.38	0.12	--	--	--	--	--	--	--	--

Table 5.5. (continued).

Trophic Level	Taxon	Biomass (ash-free dry wt, g/m^2)														
		GC234				GC354			VK826						VK826NE	VK826W	VK862
		G1a	G1b	G1c	G1d	G2a	G2b	G2c	V1a	V1b	V1c	V1d	V2a	V2b	V3	V4
3	*Munidopsis* 2	0.12	--	0.24	0.22	0.59	--	--	--	--	--	0.98	0.84	--	0.42	--
3	*Munidopsis* 3	--	--	--	0.26	0.73	--	0.93	--	--	--	--	--	--	0.46	--
3	*Nibilia*	--	--	--	0.44	0.21	--	--	--	--	--	--	--	--	--	--
3	*Periclemenes*	0.39	--	--	--	0.91	0.70	0.17	--	0.10	--	0.21	--	--	0.23	--
3	*Plesionika*	--	--	--	--	0.49	--	--	--	--	--	--	--	--	--	--
3	*Stenopus*	--	--	--	0.14	0.83	0.60	0.40	--	0.60	--	--	0.46	--	--	--
3	Unid. bresilid	--	--	--	--	--	--	0.90	--	--	--	--		--	--	--
3	Unid. galatheid	--	--	--	--	0.75	--	--	--	--	--	--	0.16	--	--	--
	Echinodermata															
1	Crinoid	--	--	--	--	--	--	--	0.12	0.37	--	0.88	--	--	0.18	--
1	Ophionerid	--	--	--	0.18	--	--	--	--	0.18	--	--	--	--	--	--
2	*Ophiotreta valenciennesi rufescens*	--	--	--	0.67	0.23	0.14	0.44	--	--	0.67	--	--	--	--	--
2	Ophiuroid sp. 1	--	0.35	--	--	--	--	--	--	--	--	--	--	--	--	--
2	Ophiuroid sp. 2 (6 arms)	--	--	--	--	0.70	--	--	--	--	0.56	0.53	--	--	0.59	0.62
	Chordata															
4	*Bellotia*	--	--	--	1.58	--	--	--	--	--	--	--	--	--	--	--

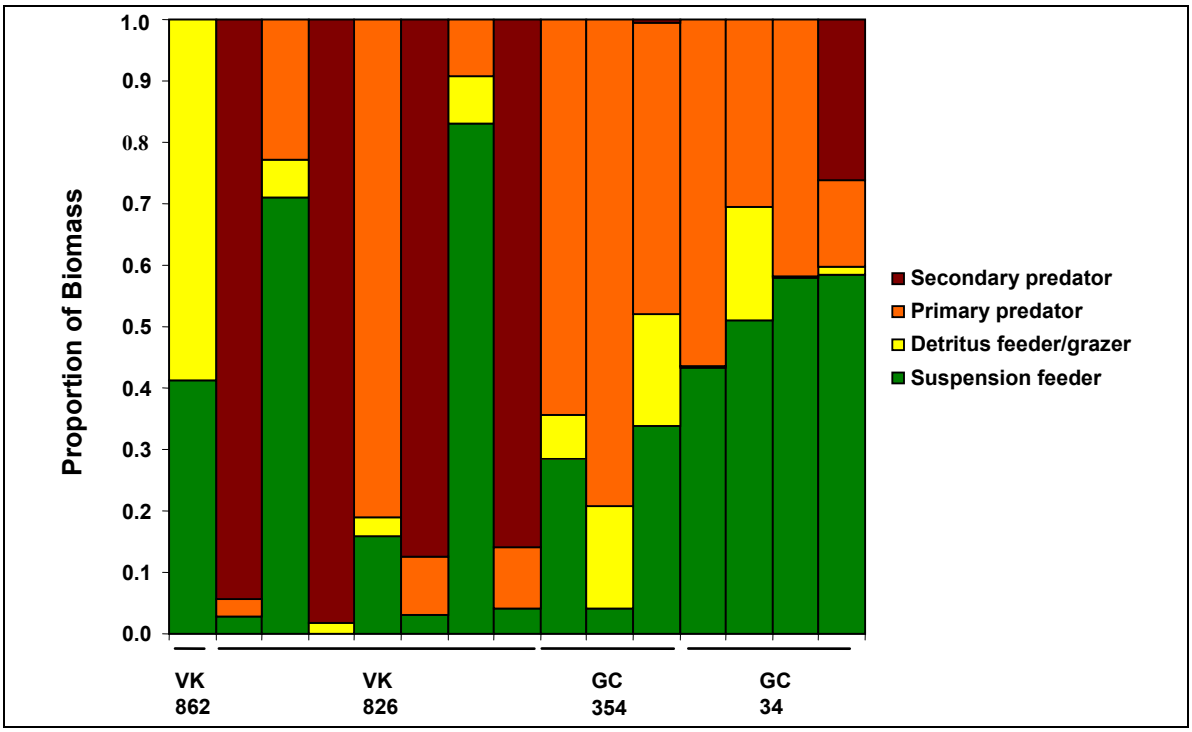

Figure 5.5. Proportion of biomass by trophic level in each Bushmaster collection. Refer to **Table 5.5** for the trophic level designations of each species.

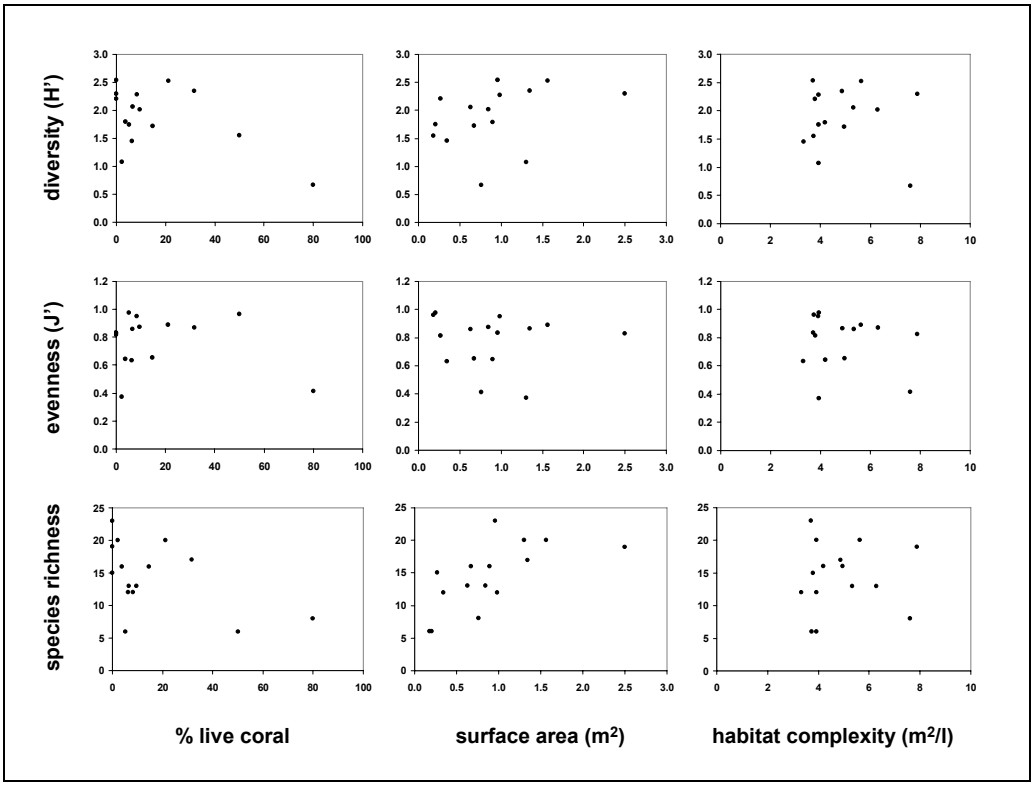

Figure 5.6. Correlations between measures of diversity and characteristics of Bushmaster collections.

Communities were generally more similar within sites than they were among sites. Three groups of communities were identified to have a Bray-Curtis similarity index of greater than 40 (**Figure 5.7**). The most similar group consists of three communities from two nearby portions of the Viosca Knoll site, V1b and V1d from VK826 and V3 from VK826W. The similarity in this group was mainly attributed to the commonality of the polychaete fauna. The next group consisted of two collections from the VK826NE area of Viosca Knoll, V2a and V2b. These two communities shared an abundance of a rarely sampled isopod species and contained relatively high numbers of the polychaete *Proscoloplos* sp. The third group comprised G1a, G1c, and G1d from GC234 and G2a from GC354. These collections contained relatively high densities of solitary corals, the corallivorous gastropod *Coralliophila* sp., and the galatheid *Munidopsis* sp. 2. In addition, one collection from Viosca Knoll, V1a, was more similar to the Green Canyon collections than it was to any of the Viosca Knoll collections, primarily due to secondary settlement of solitary corals, not seen in the other Viosca Knoll collections.

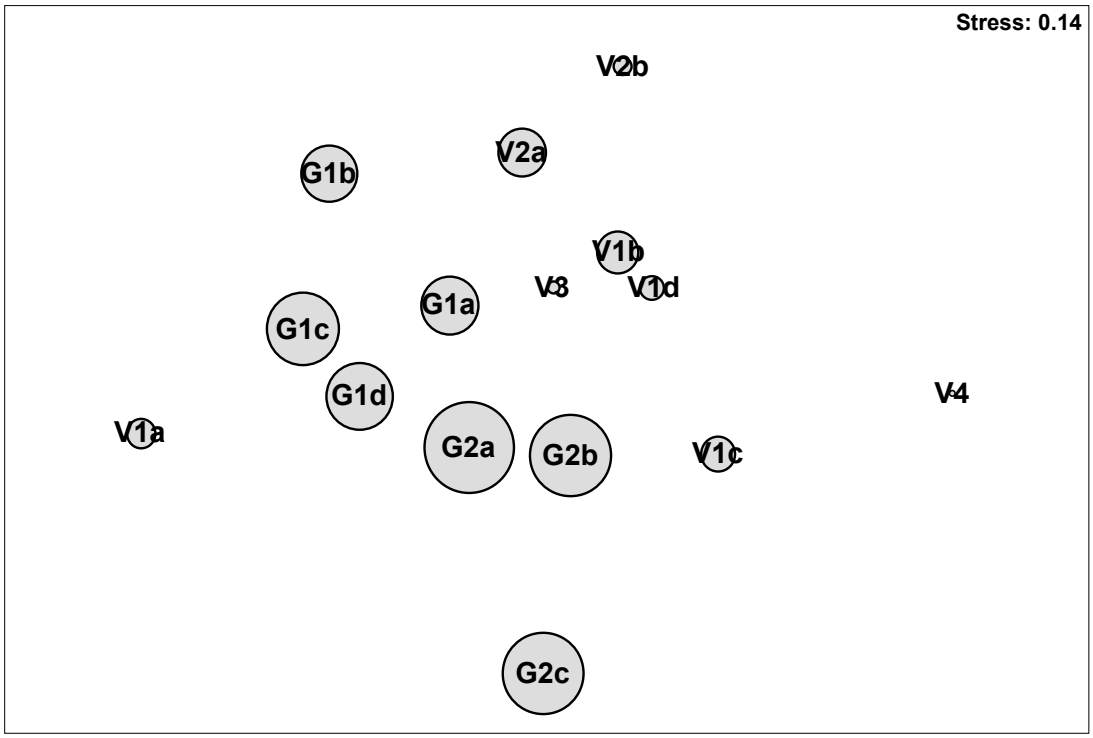

Figure 5.7. Multidimensional scaling plot of community similarity among Bushmaster collections. The circles represent the depth of collection, which was the most significant factor explaining the relative position of communities within the figure.

The observed pattern in community similarity between collections was best explained by the depth of collection and the proportion of live coral in the collection. Bray-Curtis similarity between pairs of community collections was most strongly correlated to pairwise Euclidean distance in depth ($r = -0.479$, $p < 0.001$, $n = 106$) where spatially distant communities (increasing distance) exhibited lower degrees of similarity. Communities were also similar in collections that contained similar proportions of live coral ($r = 0.423$, $p < 0.001$, $n = 106$). Habitat structure (surface area of coral per mL coral volume) ($r = 0.390$, $p < 0.001$, $n = 106$) and distance between

collections (r = 0.294, p = 0.002, n = 106) also were significant factors in this analysis, but explained lower proportions of the variability in community similarity.

5.3.3 Stable Isotopes

Lophelia Skeleton Analyses

Samples of *L. pertusa* skeleton from different portions of the coral thicket failed to detect consistent changes in the dissolved inorganic carbon (DIC) source pool over time (**Table 5.6**). Proceeding from the basal to distal portions of coral skeleton, over the range of distances measured (10 to 30 cm), the change in carbon isotopic signature ($\Delta\delta^{13}C$) was both positive and negative, ranging from +4‰ to nearly -5‰ (**Figure 5.8**). In targeted collections of basal, middle, and live portions of an *L. pertusa* skeleton from within a thicket at VK826, there also were no significant differences detected in the $\delta^{13}C$ values measured (**Figure 5.9**).

There was a significant relationship between $\delta^{18}O$ and $\delta^{13}C$ in *L. pertusa* skeleton (**Table 5.6**, **Figure 5.10**). This relationship differed slightly at the three sites where it was estimated:

VK826: $\delta^{18}O = 0.35 \cdot \delta^{13}C + 3.14$, $r^2 = 0.756$, $p = 0.015$
VK826NE: $\delta^{18}O = 0.41 \cdot \delta^{13}C + 3.14$, $r^2 = 0.966$, $p < 0.001$
VK862: $\delta^{18}O = 0.45 \cdot \delta^{13}C + 2.96$, $r^2 = 0.989$, $p = 0.047$

Table 5.6. $\delta^{13}C$ and $\delta^{18}O$ values for *Lophelia pertusa* skeleton.

Site	Dive	Position	$\delta^{13}C$	$\delta^{18}O$
VK826	4867	base	-3.7	2.6
VK826	4867	base	0.0	3.0
VK826	4867	dead	-1.1	2.6
VK826	4867	dead	-3.5	1.5
VK826	4867	live	1.0	3.7
VK826	4867	live	-4.6	1.3
VK826NE	4871	base	-3.5	1.7
VK826NE	4871	base	-1.3	2.5
VK826NE	4871	base	-2.2	2.2
VK826NE	4871	dead	-2.9	2.0
VK826NE	4871	dead	-7.1	0.3
VK826NE	4871	dead	-1.8	2.4
VK826NE	4868	live	-1.8	2.8
VK826NE	4868	live	-0.1	3.1
VK826NE	4868	live	-2.1	2.3
VK826NE	4871	live	-1.9	2.3
VK826NE	4871	live	-1.3	2.5
VK826NE	4871	live	-3.4	1.7
VK862	4869	live	-2.4	1.9
VK862	4869	live	-4.5	0.8
VK862	4869	live	-6.5	0.1

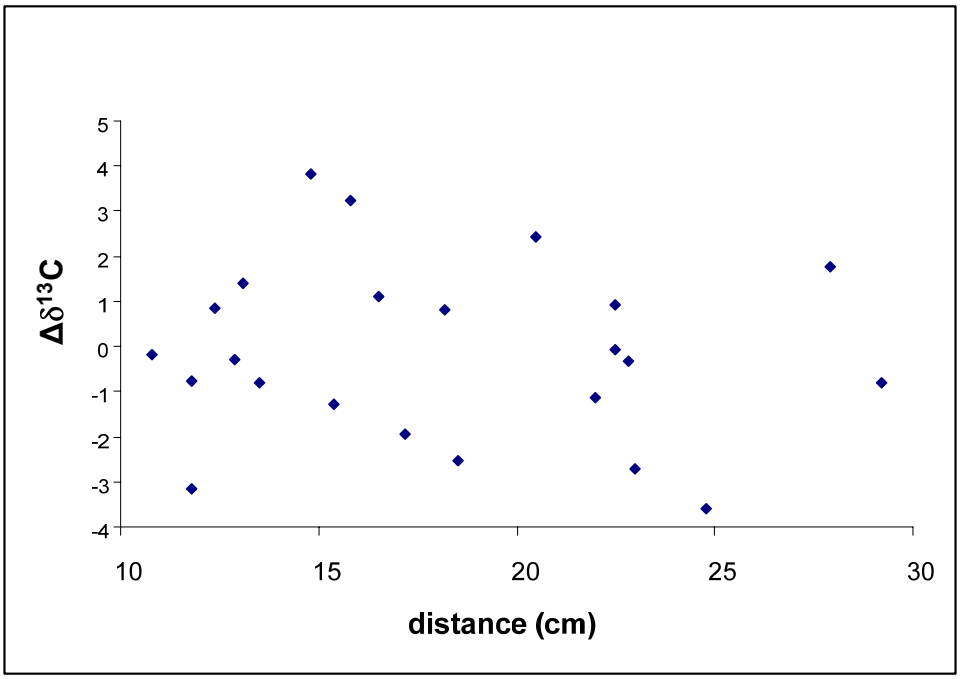

Figure 5.8. Change in skeletal $\delta^{13}C$ ($\Delta\delta^{13}C$) vs. distance (cm) in *Lophelia pertusa* from Bushmaster collections in 2004. The change in $\delta^{13}C$ was obtained by calculating the difference between the two endpoints of a given distance along the skeleton (distal point $\delta^{13}C$ – basal point $\delta^{13}C$).

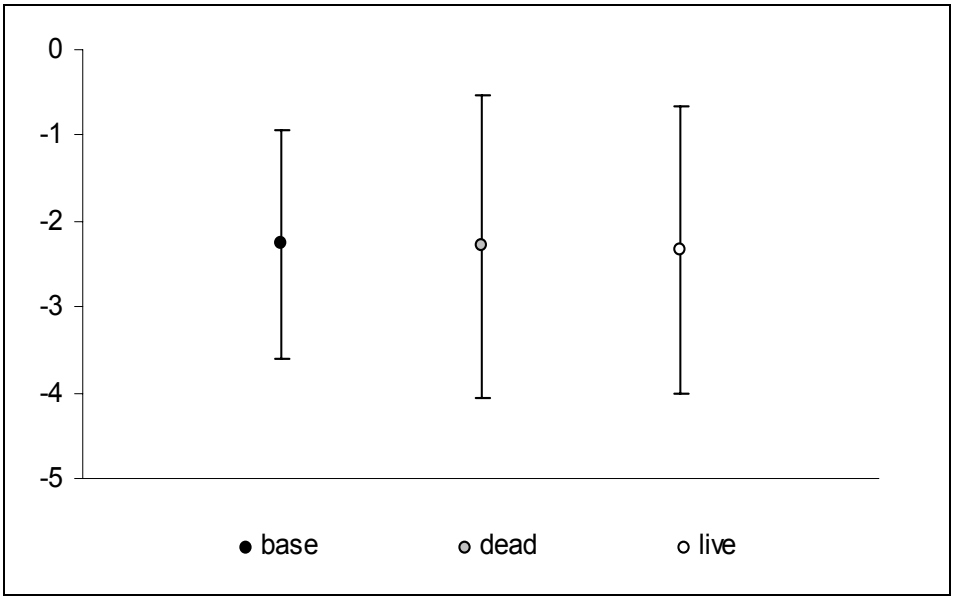

Figure 5.9. Average $\delta^{13}C$ for *Lophelia pertusa* skeleton grouped by location along the skeleton: base, middle, and live.

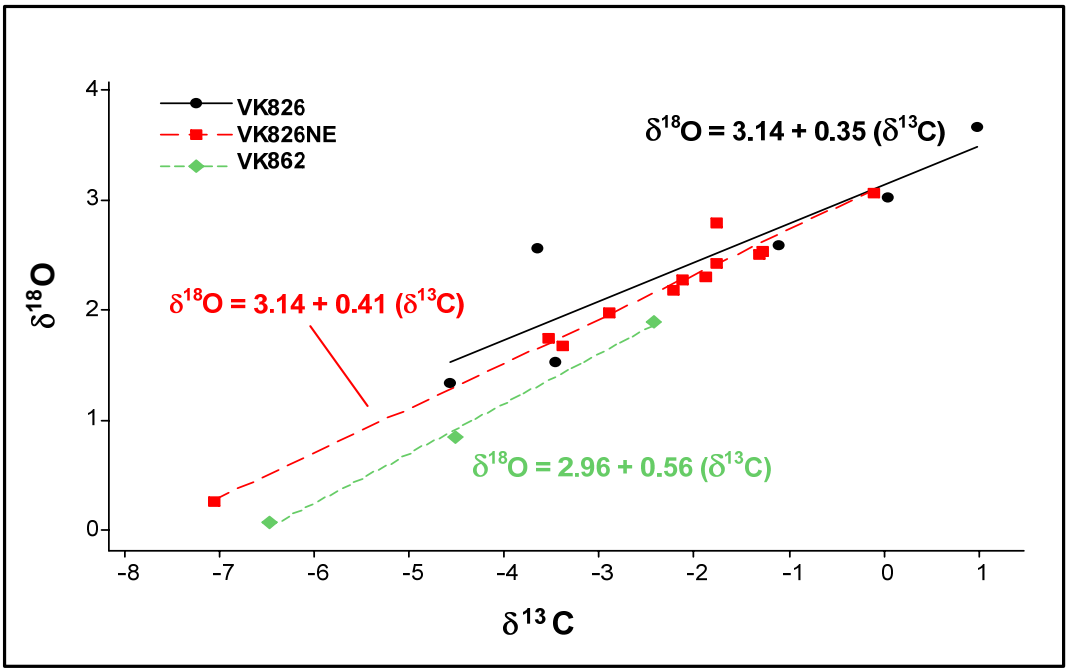

Figure 5.10. Plot of $\delta^{18}O$ vs. $\delta^{13}C$ in live *Lophelia pertusa* skeleton at three sites in the Gulf of Mexico. Regression lines are included for each site.

The tight correlation between $\delta^{13}C$ and $\delta^{18}O$ indicates that the skeleton was in isotopic disequilibrium with seawater and exhibits significant biological fractionation (Mikkelsen et al. 1982). Therefore, temperature at the time of the skeleton secretion was estimated using the method of Smith et al. (2000) derived from 18 species of deepsea coral. Briefly, the intercept of the plot of $\delta^{13}C$ vs. $\delta^{18}O$ provides an estimate of the fractionation from seawater to aragonite, and this value (the y-intercept in **Figure 5.10**) is used to calculate the temperature at the time of skeletal formation where $\delta^{18}O = -0.25T + 4.97$. For y-intercepts of 3.14 and 2.96 (**Figure 5.10**), this gives estimates of 7.32 °C at VK826 and VK826 NE, and 8.04 °C at the shallower VK862 station, respectively. For different portions of the skeleton from VK826 (**Figure 5.11**), the temperature estimates are 8.34 °C at the base, 7.64 °C in the middle, and 7.14 °C in the live portion.

Cnidarian Tissue and Skeleton Analyses

Different groups of corals had different relationships between tissue and skeleton $\delta^{13}C$ values (**Figure 5.12**, **Table 5.7**). *L. pertusa* tissue carbon was generally between -21‰ and -23‰ and skeleton between 0 and -6‰. The octocoral *Callogorgia americana americana* and an unidentified bamboo coral (Octocorallia, Family Isididae) were in a similar range, approximately -21‰ for tissue and -4‰ to -8‰ for skeleton. An unidentified antipatharian measured had a tissue $\delta^{13}C$ signature ranging from -21‰ to -19‰, but skeletal values were more depleted than the other species, from -16‰ to -20‰ (**Figure 5.13**, **Table 5.8**).

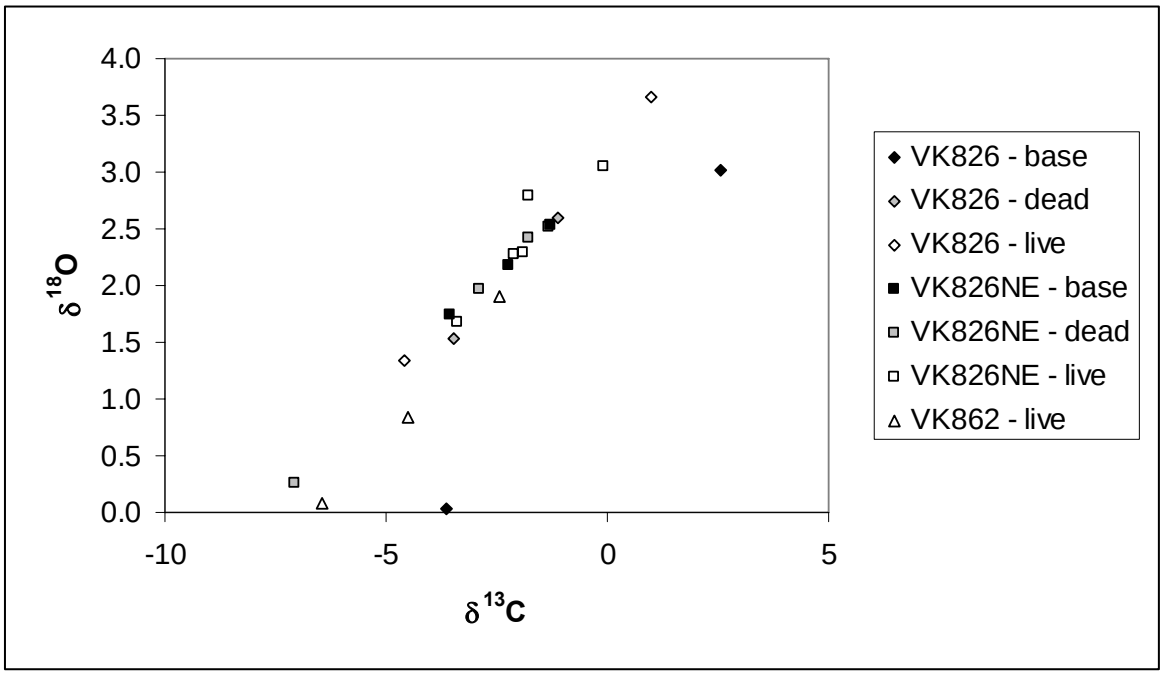

Figure 5.11. *Lophelia pertusa* skeleton $\delta^{18}O$ vs. $\delta^{13}C$ for samples collected from three sites in the Gulf of Mexico. Base samples are those taken from the bottom of the aggregation, where skeleton appears dark brown and has abundant hydroid growth. Dead samples are toward the center of aggregation, where the skeleton is lighter brown and has less hydroid growth. Live samples are at the growing tips of the aggregation (farthest from the sediment), where the skeleton is pure white and live tissue is present.

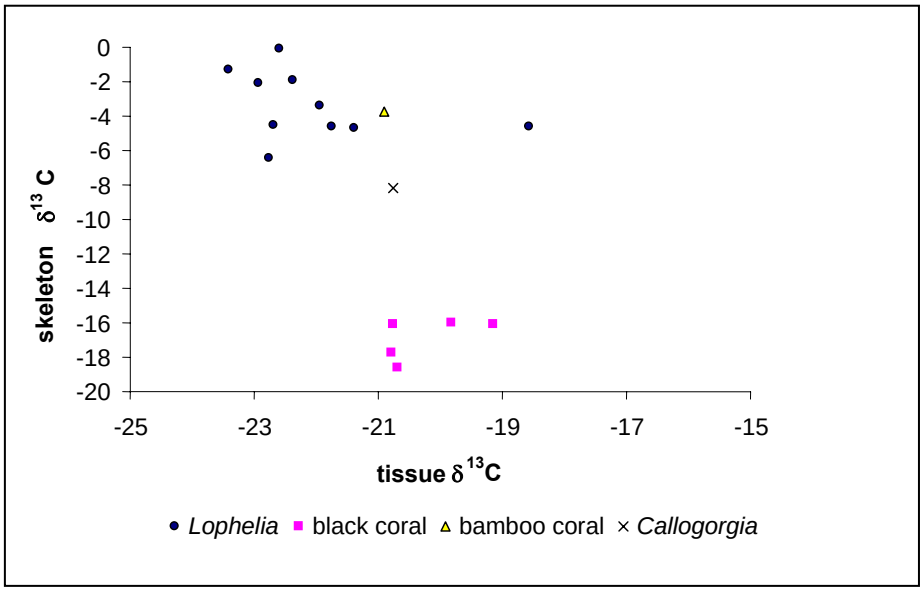

Figure 5.12. $\delta^{13}C$ for paired skeleton and tissue samples from cnidarians collected from VK826, VK826NE, and VK862.

Table 5.7. Stable carbon, nitrogen, and sulfur isotope ratios for all non-Bushmaster tissue collections.

Taxon	Site	Dive	$\delta^{13}C$	$\delta^{15}N$	$\delta^{34}S$
Anthopodium rubens	GC354	4741	-18.5	9.9	ND
Anthothela	VK826	4737	-20.8	10.8	20.4
Antipatharian	GC354	4741	-19.5	9.9	ND
Antipathes	VK862	4732	-20.8	9.7	20.4
Antipathes	VK862	4732	-20.7	9.9	19.4
Antipathes 1	VK826	4731	-20.8	9.8	20.4
Antipathes 2	VK826	4731	-19.8	10.1	20.1
Bamboo coral	VK862	4734	-20.9	10.6	14.9
Black coral	VK862	4734	-19.2	10.5	18.8
Bulbous sponge	VK862	4732	-20.0	14.1	18.6
Bulbous sponge	VK862	4734	-20.2	14.5	19.1
Bulbous sponge	VK826	4735	-19.7	9.4	20.3
Bulbous sponge	VK826	4734	-20.1	14.3	ND
Callogorgia	VK826	4737	-20.8	9.6	23.0
Callogorgia	MC885	4738	-23.9	8.9	18.8
Calyptrophora	GC354	4741	-20.6	9.3	ND
Demosponge	VK826	4735	-19.5	14.9	21.7
Demosponge	VK862	4734	-19.0	15.7	ND
Demosponge 2	VK862	4734	-16.7	10.4	20.4
Demosponge lg	VK862	4734	-17.8	10.7	20.0
Echinmuricea atlantica	GC354	4741	-17.9	10.3	ND
Encrusting sponge	VK862	4732	-18.1	12.5	20.5
Encrusting sponge	VK862	4734	-20.3	13.9	20.9
Green glass sponge	VK826	4736	-17.9	15.7	21.0
Hexactinellid sponge	MC885	4738	-17.1	9.9	17.3
Lophelia	VK826	4737	-20.0	10.6	21.3
Lophelia	MC885	4738	-20.1	9.5	ND
Lophelia	GC354	4741	-19.9	9.3	ND
Lophelia	VK826	4733	-19.5	10.8	20.6
Lophelia	VK862	4734	-17.5	10.2	23.3
Lophelia	VK862	4734	-21.4	9.5	20.2
Lophelia	VK862	4734	-18.6	11.4	18.6
Lophelia	GC354	4741	-19.9	9.3	ND
Lophelia	MC885	4738	-23.9	8.9	ND
Lophelia	VK826	4737	-20.0	10.6	ND
Lophelia tissue+skeleton	VK862	4732	-26.1	-5.0	13.2
Madrepora	MC885	4738	-21.0	4.5	13.1
Plate sponge	VK862	4732	-18.3	15.5	19.7
Sponge	GC354	4741	-17.6	8.5	ND
Tubular sponge	VK862	4732	-19.1	12.0	21.9
Vase hexactinellid sponge	VK826	4737	-18.8	15.6	16.9

ND = no data.

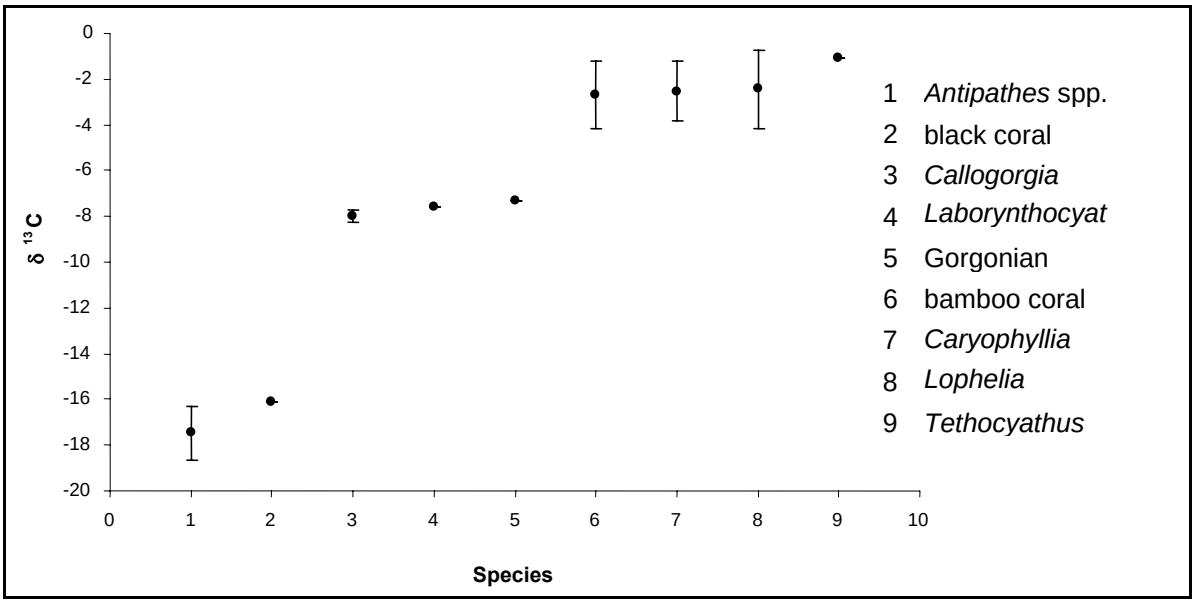

Figure 5.13. Average and standard deviation for $\delta^{13}C$ values of all cnidarian skeleton samples collected.

Table 5.8. Stable carbon isotope ratios for all non-Bushmaster coral skeleton collections.

Taxon	Site	Dive	$\delta^{13}C$
Antipathes	VK826	4732-2	-17.8
Antipathes	VK826	4732-10	-18.6
Bamboo coral	VK826	4735-7	-1.6
Callogorgia	MC885	4738-4	-7.8
Lophelia	VK826	4734-12	-5.5
Lophelia base	MC885	4738-10	-4.4
Unidentified gorgonian base holdfast	MC885	4738-6	-7.3

Suspension-feeding Species Analyses

The suspension-feeding species collected here exhibited a wide range of carbon, nitrogen, and sulfur stable isotopic values (**Figure 5.14**). The isotope signature of the gorgonian, antipatharian, and scleractinian tissues ranged from -25‰ to -17‰ $\delta^{13}C$, 5‰ to 12‰ $\delta^{15}N$, and 10‰ to 25‰ $\delta^{34}S$ with the exception of one hydroid sample with a very light sulfur signature of approximately 2‰. The one *Madrepora oculata* individual measured from MC885 has a more depleted $\delta^{15}N$ value (4.45‰) than the range measured for *L. pertusa* (8.94‰ to 10.64‰), suggesting that it may feed at lower trophic levels than *L. pertusa*. There were no species collected with the Bushmaster that could serve as prey for the suspension feeders. This suggests that their prey may include small swimming amphipods that are commonly observed in the area but rarely collected.

Coral-associated Fauna Analyses

The majority of the stable isotope signatures of the coral-associated fauna range from -25‰ to -13‰ $\delta^{13}C$, 6‰ to 14‰ $\delta^{15}N$, and 10‰ to 25‰ $\delta^{34}S$ (**Figures 5.15** through **5.21**). Species lying outside of this range include *Provanna sculpta* from GC234 (-30.5‰ $\delta^{13}C$, 3.9‰ $\delta^{15}N$, -5.4‰ $\delta^{34}S$, **Figure 5.15**), *Stenopus* sp. from VK826 (-28‰ $\delta^{34}S$, **Figure 5.16**), *Eumunida picta* from GC354 (5.7‰ $\delta^{15}N$, **Figure 5.18**), and one sample of hydroids from GC354 (1.9‰ $\delta^{34}S$, **Figure 5.18**). Many of the species that fell within the typical range of stable isotope values had high intraspecific variability in their carbon isotope values in particular (**Figures 5.22** to **5.28**, **Table 5.9**).

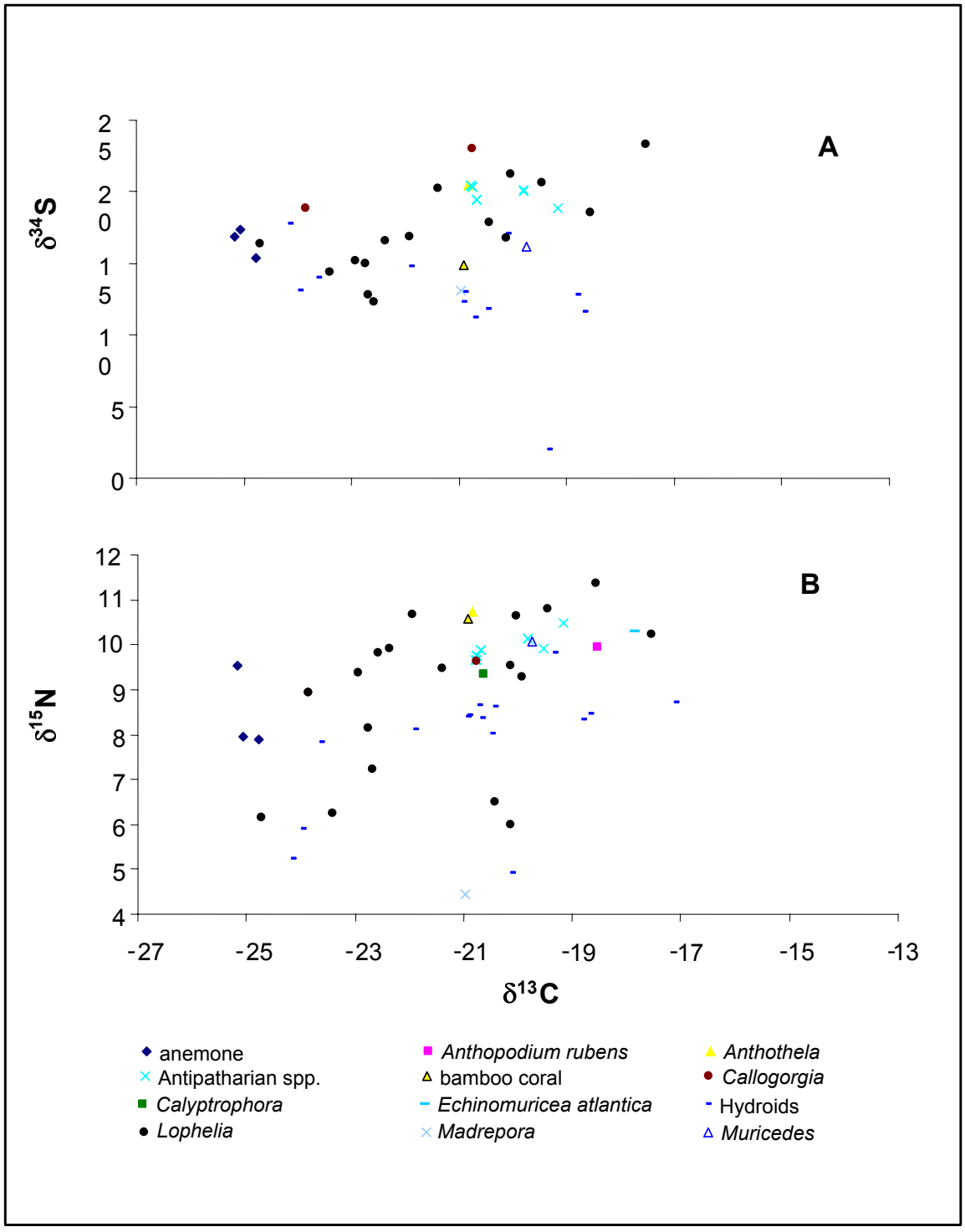

Figure 5.14. (A) $\delta^{34}S$ vs. $\delta^{13}C$ and (B) $\delta^{15}N$ vs. $\delta^{13}C$ for all suspension feeding species collected in this study.

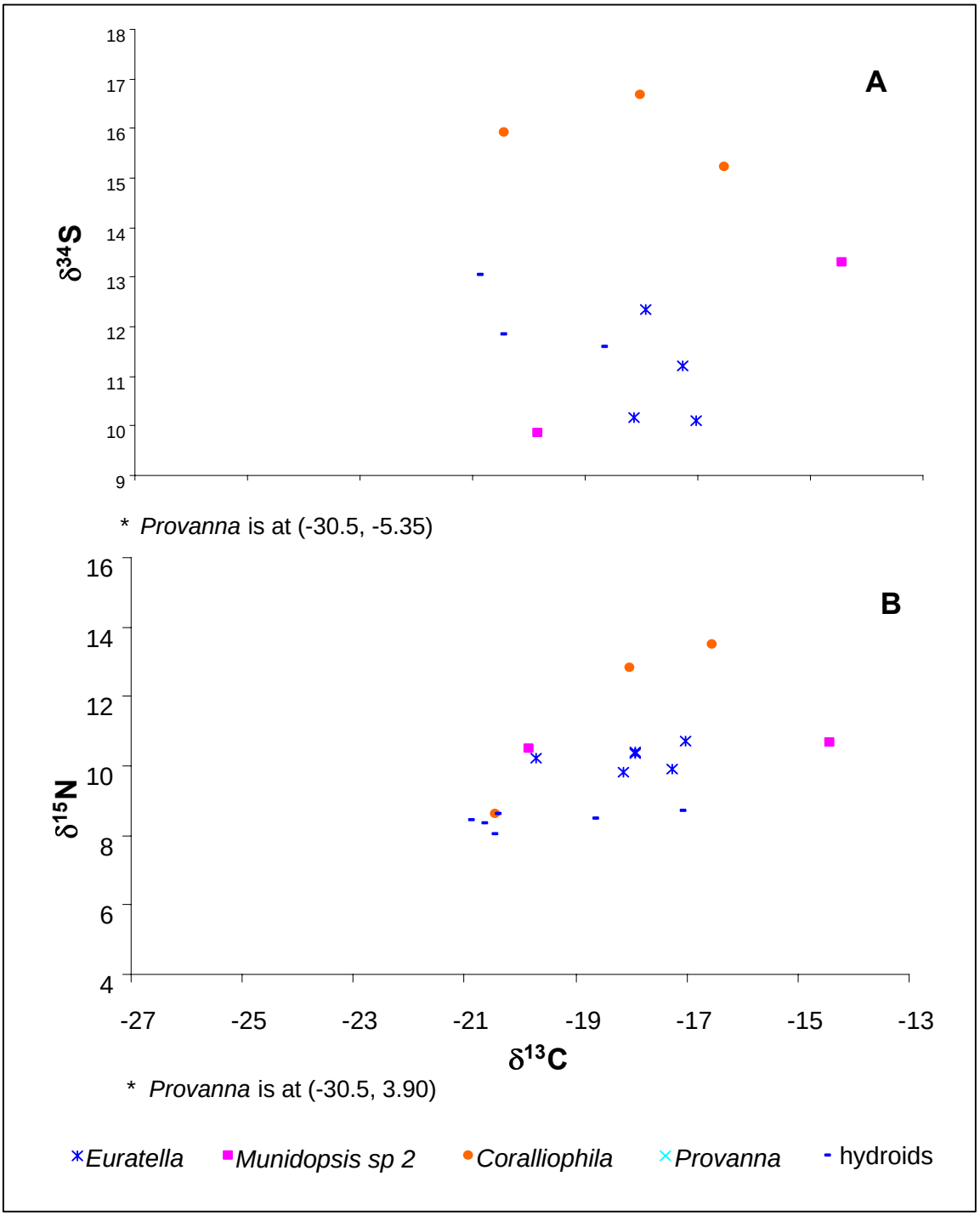

Figure 5.15. (A) $\delta^{34}S$ vs. $\delta^{13}C$ and (B) $\delta^{15}N$ vs. $\delta^{13}C$ for *Lophelia pertusa* and coral-associated fauna in a Bushmaster collection taken on Dive 4728 at GC234 in 2004.

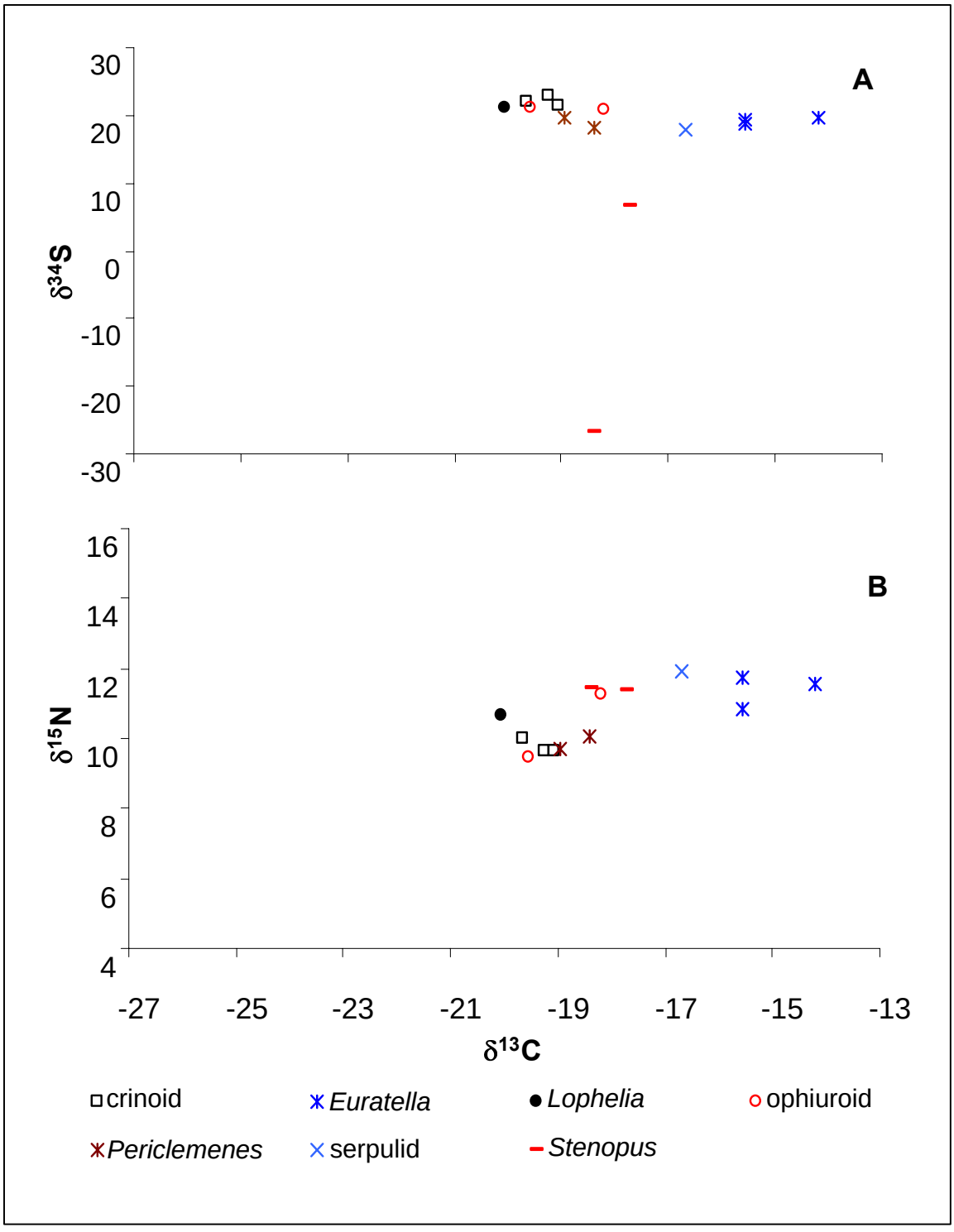

Figure 5.16. (A) $\delta^{34}S$ vs. $\delta^{13}C$ and (B) $\delta^{15}N$ vs. $\delta^{13}C$ for *Lophelia pertusa* and coral-associated fauna in a Bushmaster collection taken on Dive 4737 at VK826 in 2004.

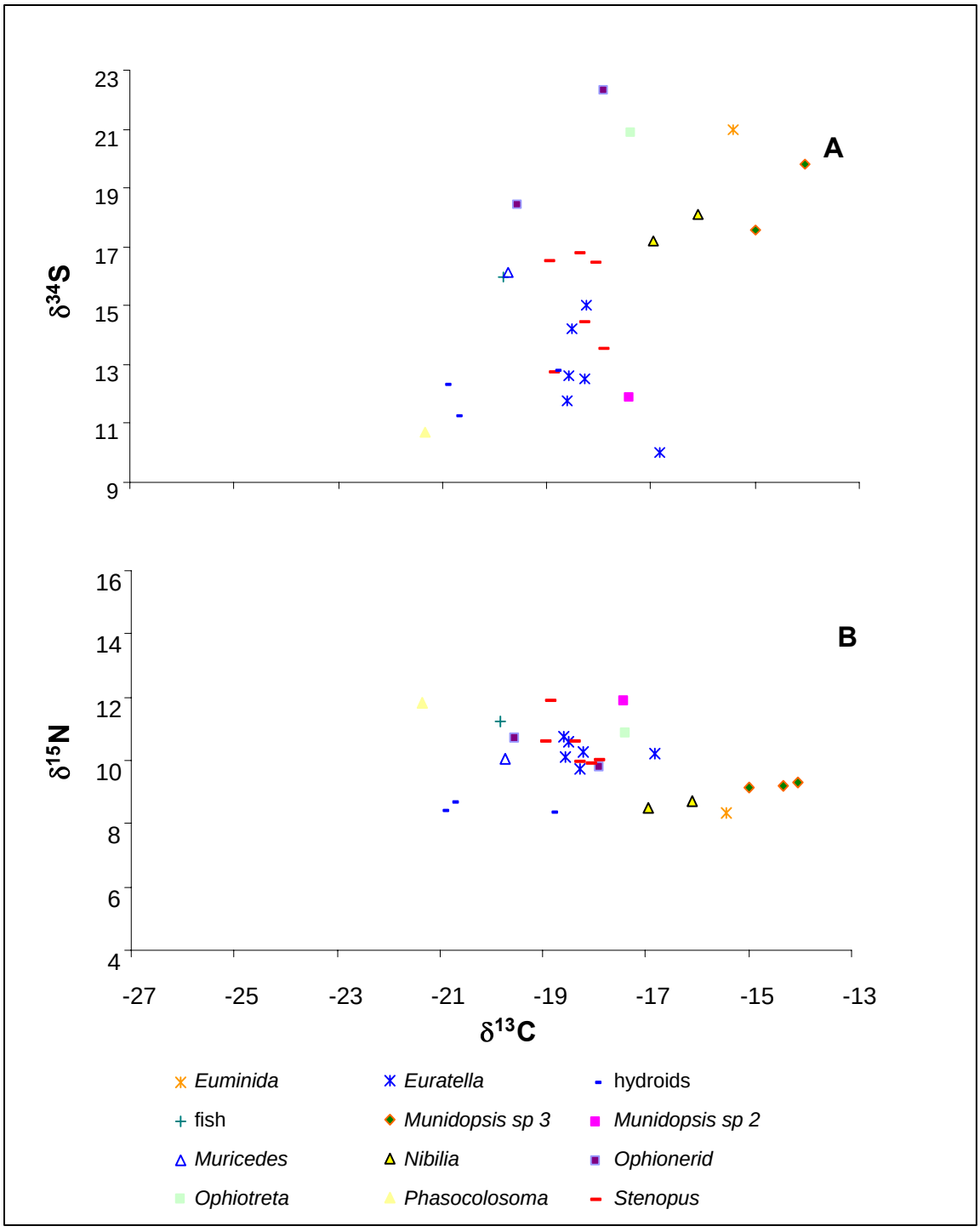

Figure 5.17. (A) $\delta^{34}S$ vs. $\delta^{13}C$ and (B) $\delta^{15}N$ vs. $\delta^{13}C$ for *Lophelia pertusa* and coral-associated fauna in a Bushmaster collection taken on Dive 4740 at GC234 in 2004.

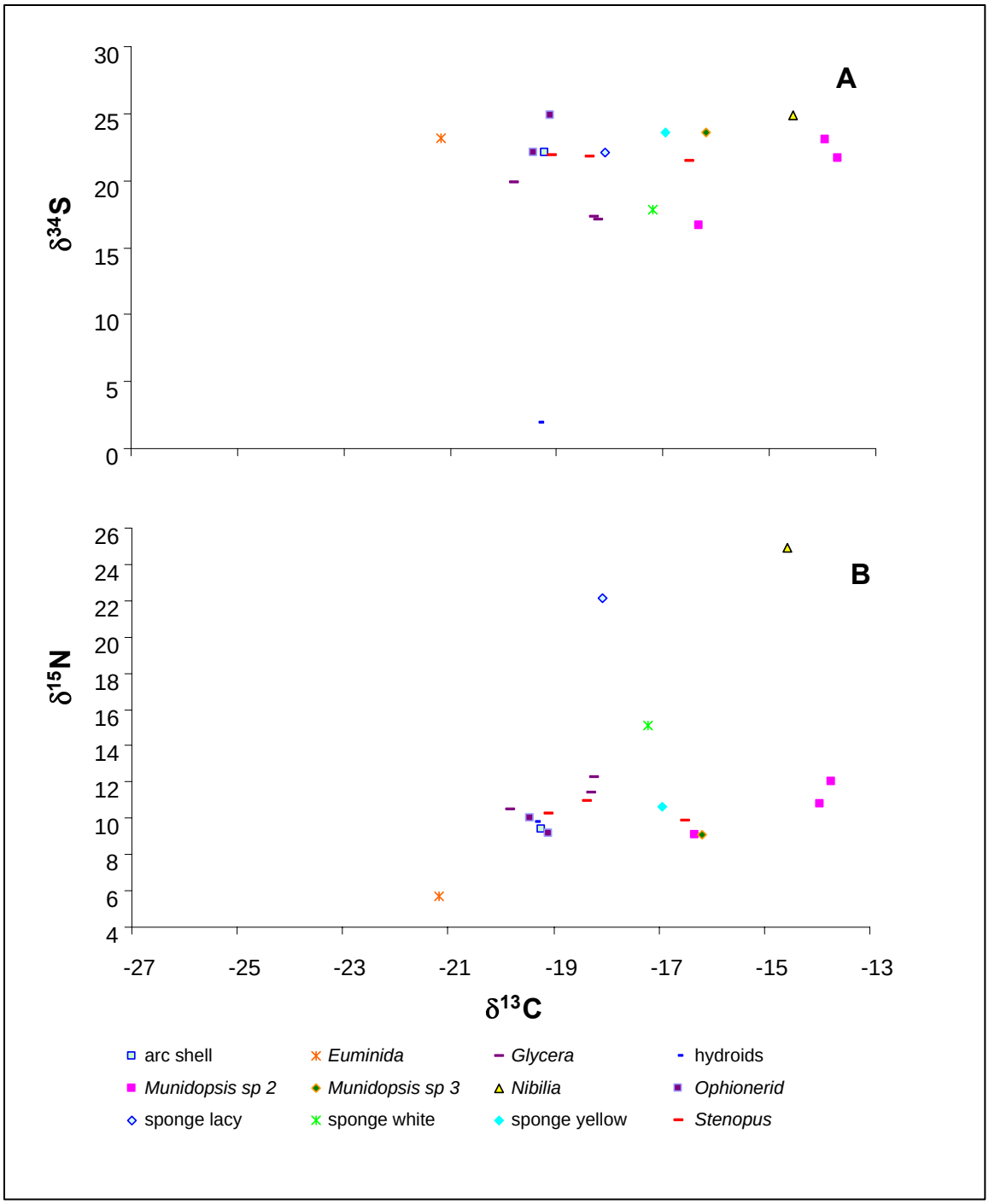

Figure 5.18. (A) $\delta^{34}S$ vs. $\delta^{13}C$ and (B) $\delta^{15}N$ vs. $\delta^{13}C$ for *Lophelia pertusa* and coral-associated fauna in a Bushmaster collection taken on Dive 4741 at GC354 in 2004.

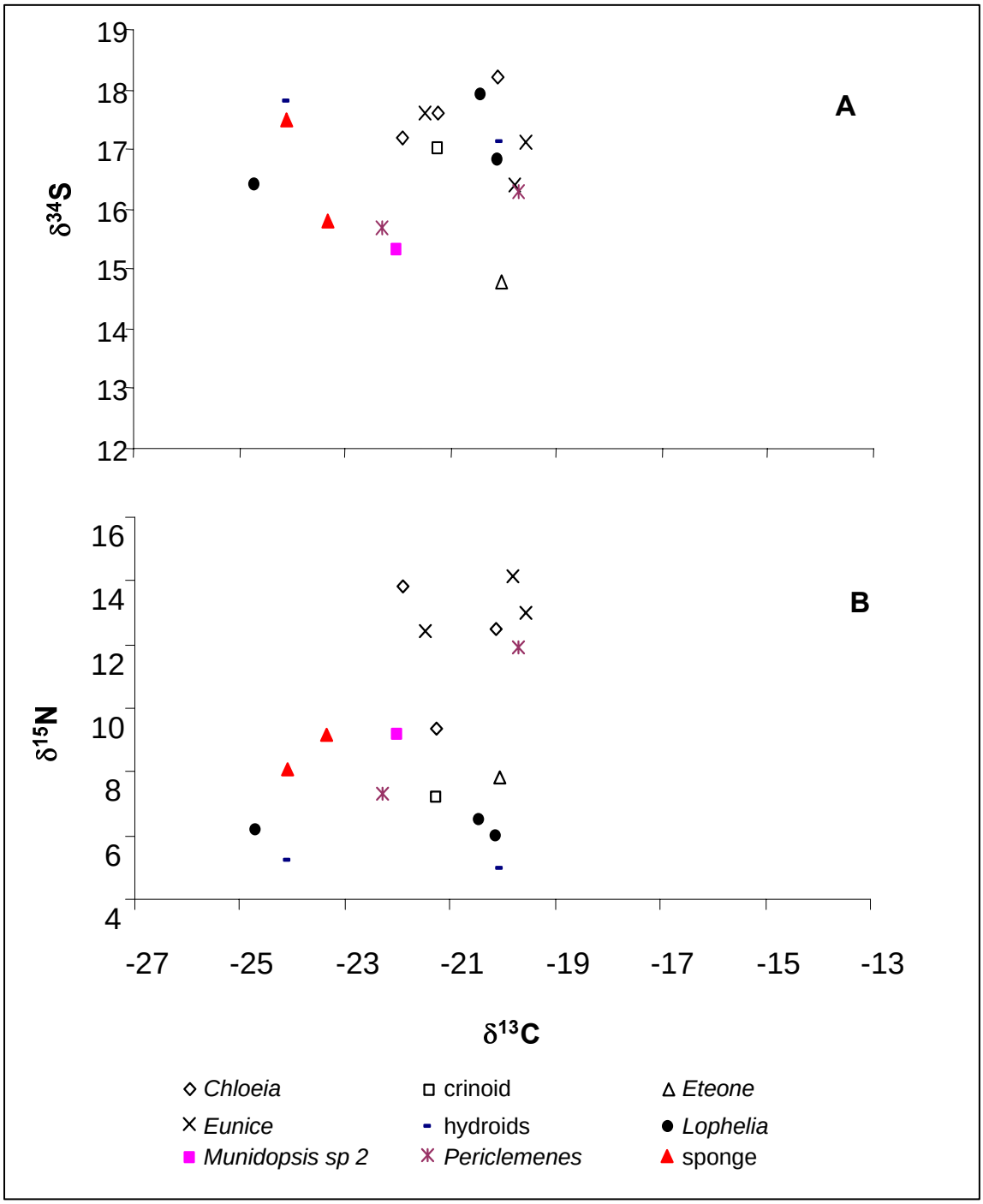

Figure 5.19. (A) $\delta^{34}S$ vs. $\delta^{13}C$ and (B) $\delta^{15}N$ vs. $\delta^{13}C$ for *Lophelia pertusa* and coral-associated fauna in a Bushmaster collection taken on Dive 4867 at VK826.

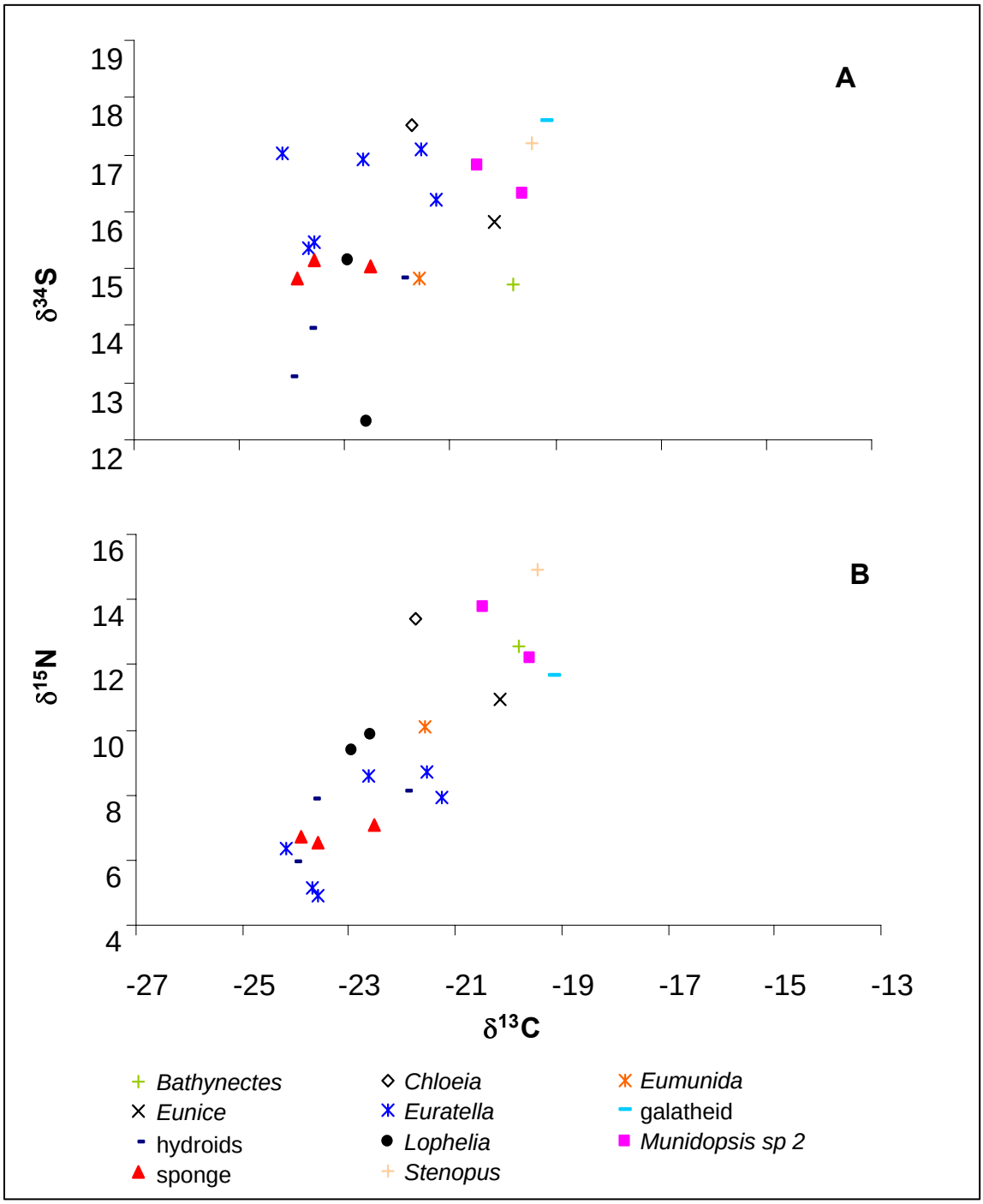

Figure 5.20. (A) $\delta^{34}S$ vs. $\delta^{13}C$ and (B) $\delta^{15}N$ vs. $\delta^{13}C$ for *Lophelia pertusa* and coral-associated fauna in a Bushmaster collection taken on Dive 4868 at VK826NE in 2005.

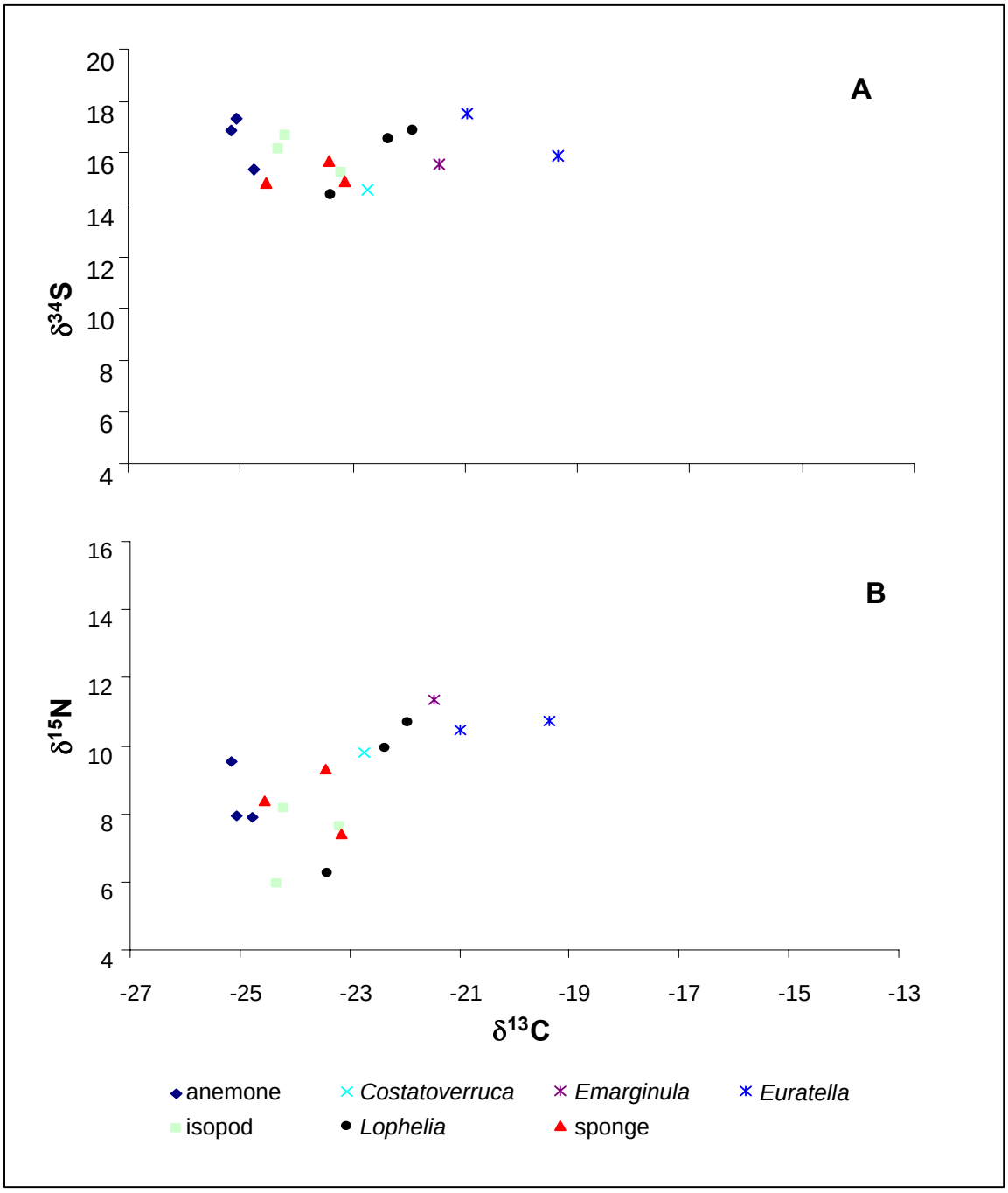

Figure 5.21. (A) $\delta^{34}S$ vs. $\delta^{13}C$ and (B) $\delta^{15}N$ vs. $\delta^{13}C$ for *Lophelia pertusa* and coral-associated fauna in a Bushmaster collection taken on Dive 4871 at VK826NE in 2005.

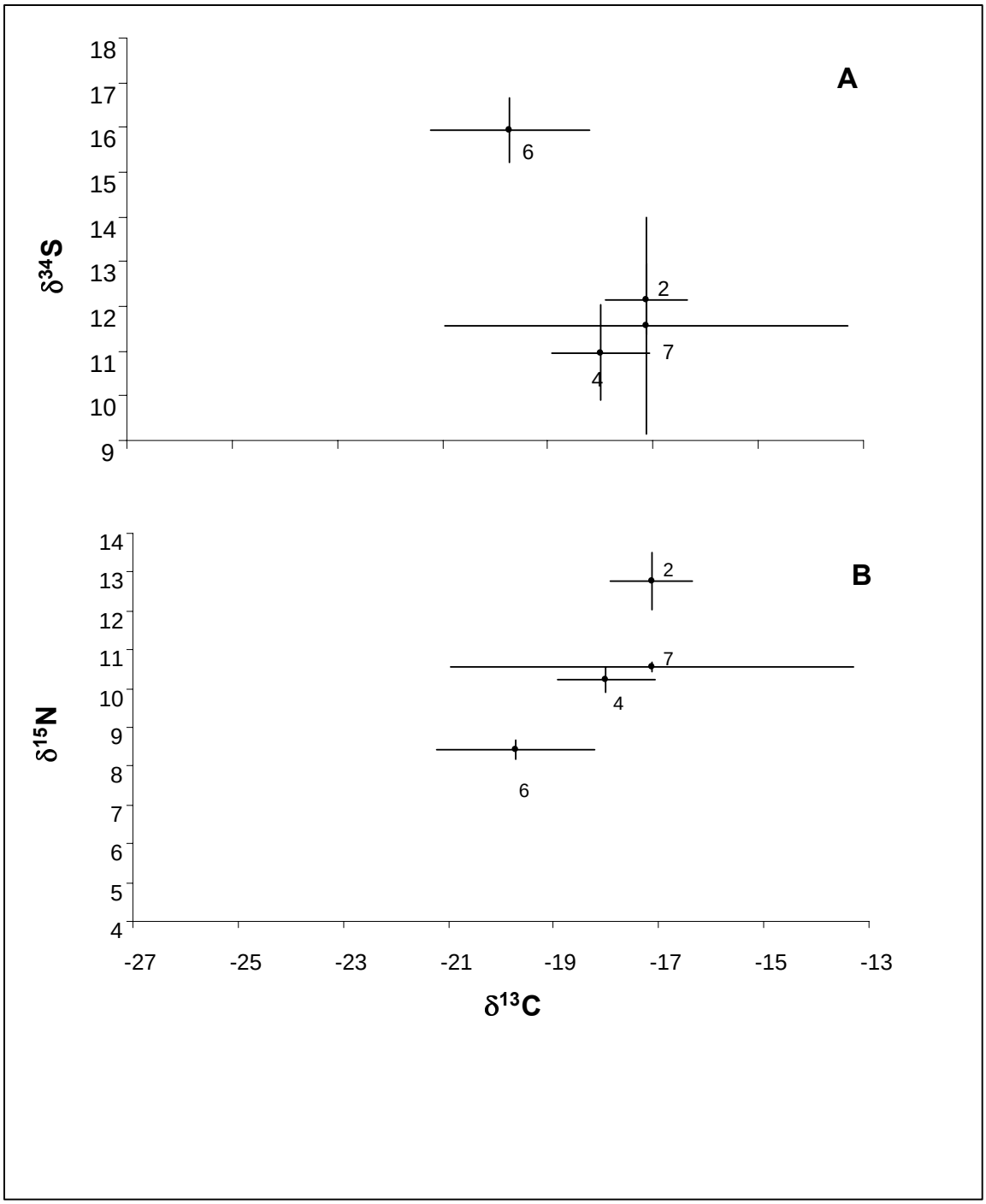

Figure 5.22. Average (A) $\delta^{34}S$ vs. $\delta^{13}C$ and (B) $\delta^{15}N$ vs. $\delta^{13}C$ for *Lophelia pertusa* and coral-associated fauna in a Bushmaster collection taken on Dive 4728 at GC234. Only species for which there was more than one individual were included.

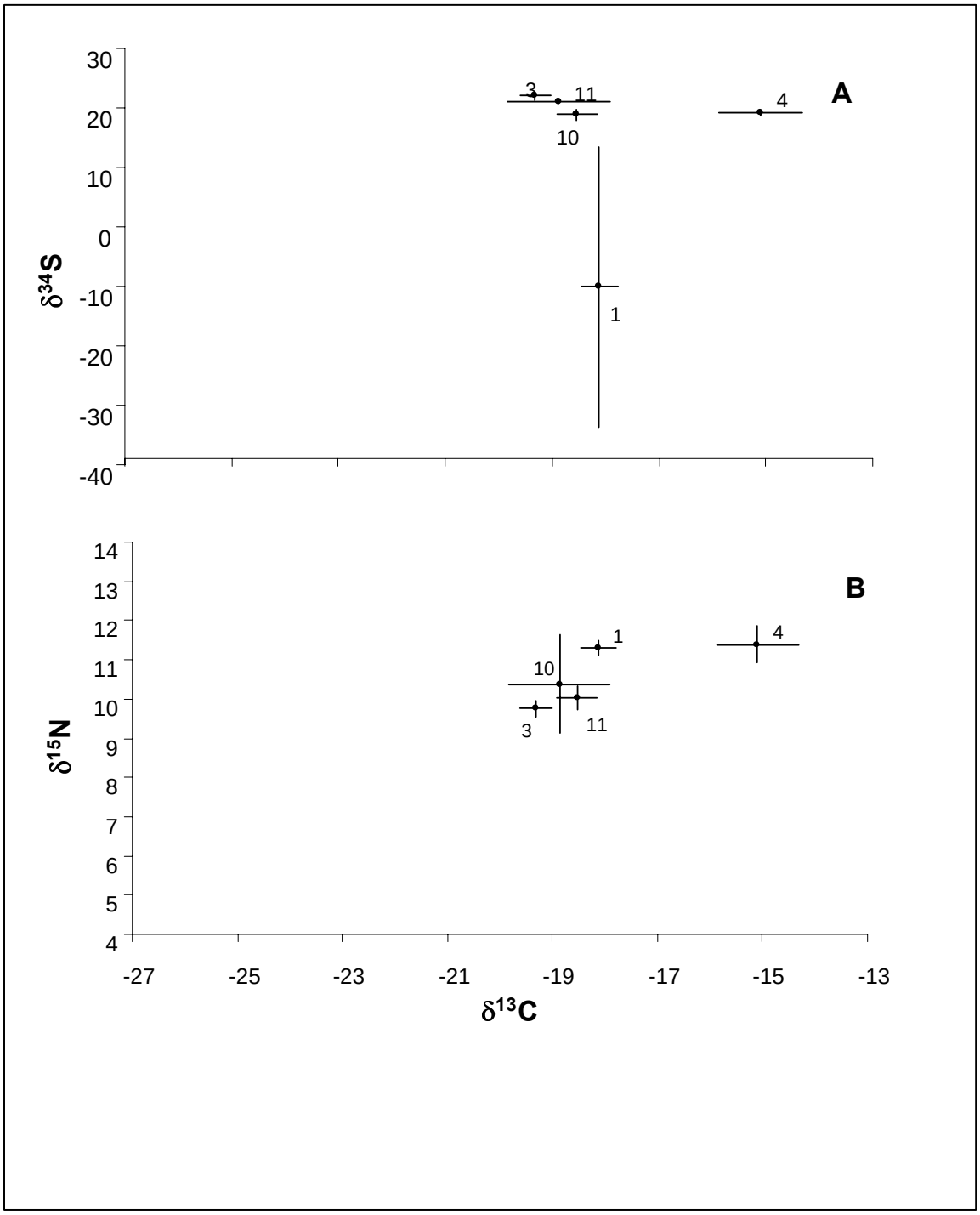

Figure 5.23. Average (A) $\delta^{34}S$ vs. $\delta^{13}C$ and (B) $\delta^{15}N$ vs. $\delta^{13}C$ for *Lophelia pertusa* and coral-associated fauna in a Bushmaster collection taken on Dive 4737 at VK826. Only species for which there was more than one individual were included.

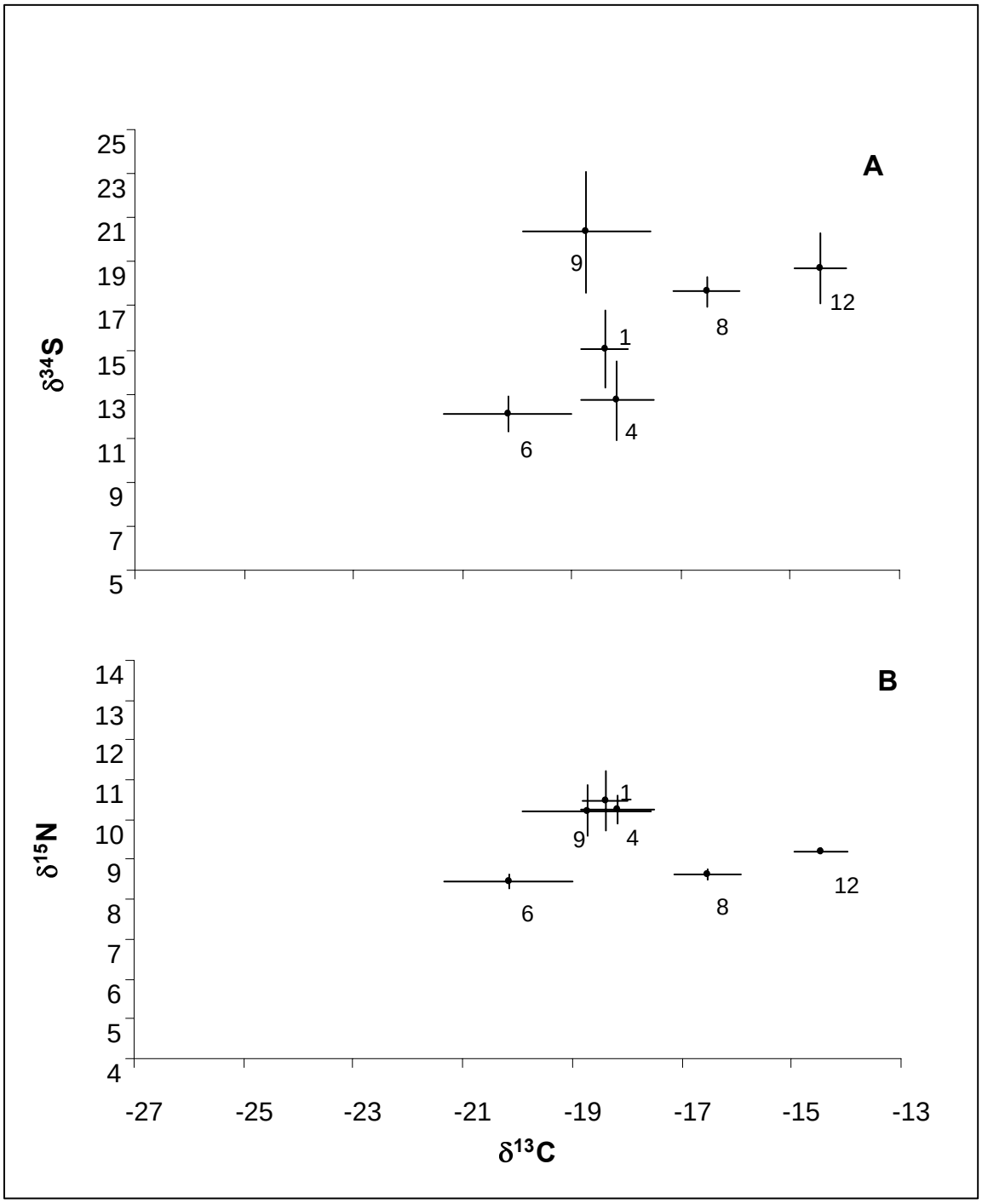

Figure 5.24. Average (A) $\delta^{34}S$ vs. $\delta^{13}C$ and (B) $\delta^{15}N$ vs. $\delta^{13}C$ for *Lophelia pertusa* and coral-associated fauna in a Bushmaster collection taken on Dive 4740 at GC234. Only species for which there was more than one individual were included.

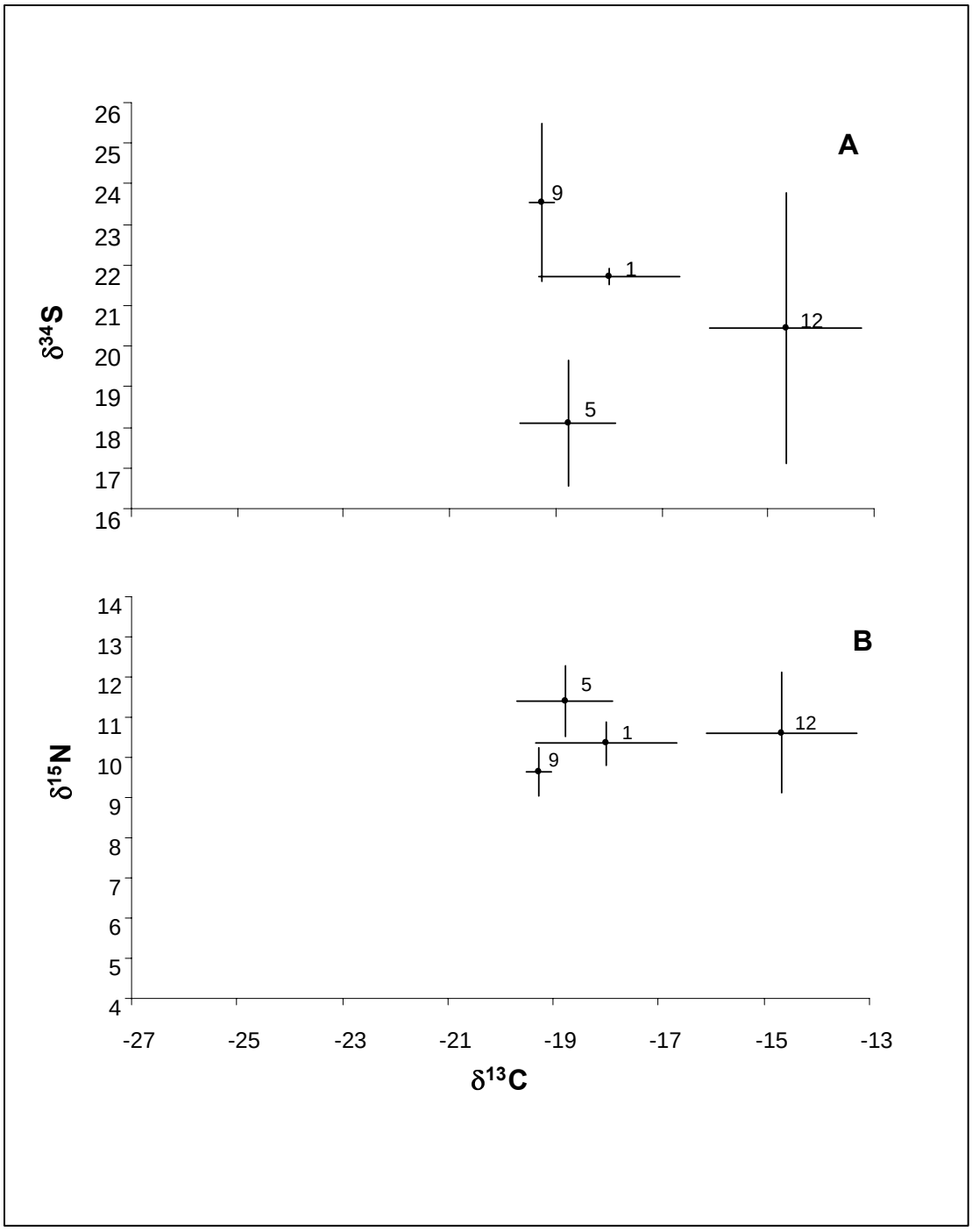

Figure 5.25. Average (A) $\delta^{34}S$ vs. $\delta^{13}C$ and (B) $\delta^{15}N$ vs. $\delta^{13}C$ for *Lophelia pertusa* and coral-associated fauna in a Bushmaster collection taken on Dive 4741 at GC354. Only species for which there was more than one individual were included.

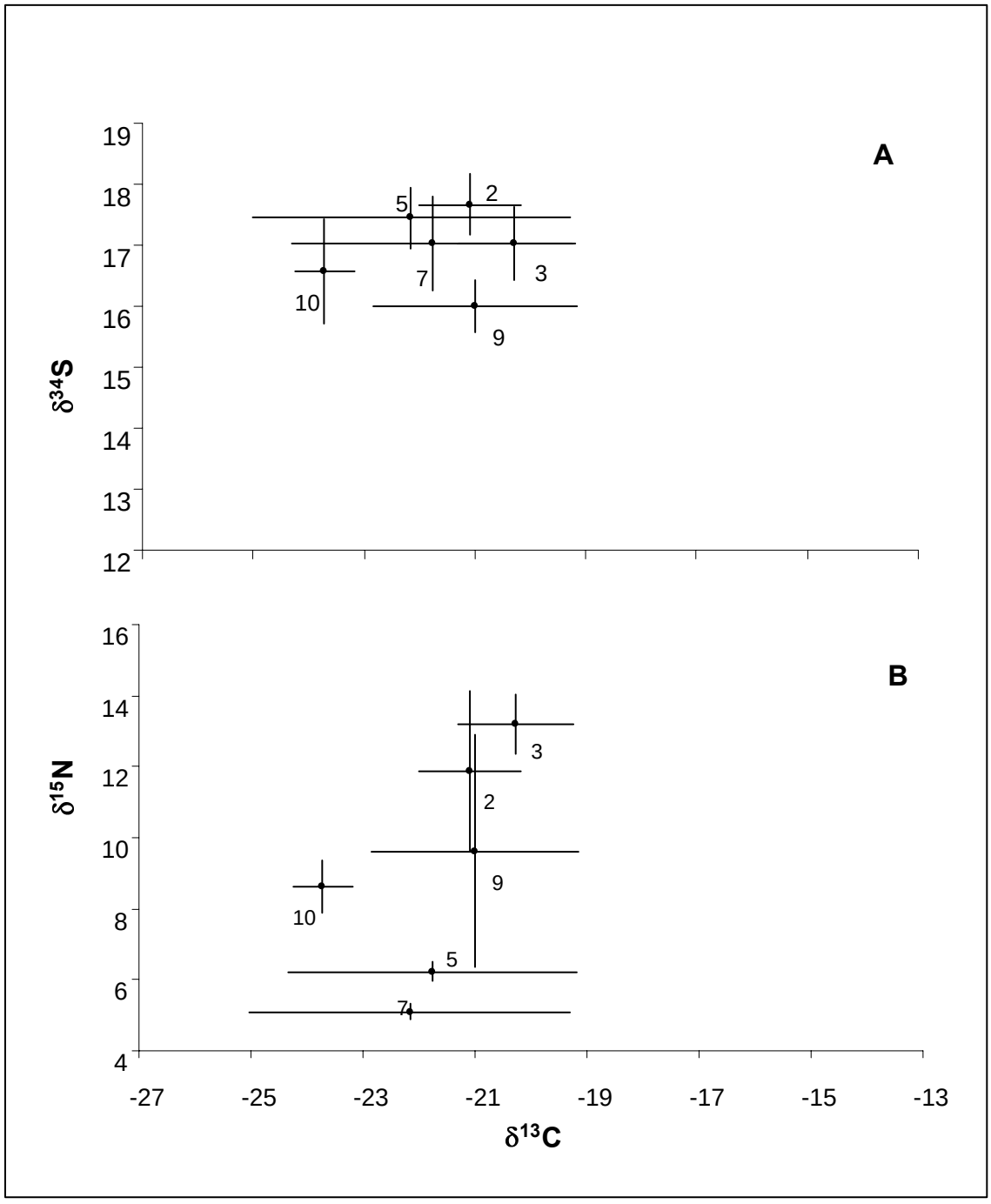

Figure 5.26. Average (A) $\delta^{34}S$ vs. $\delta^{13}C$ and (B) $\delta^{15}N$ vs. $\delta^{13}C$ for *Lophelia pertusa* and coral-associated fauna in a Bushmaster collection taken on Dive 4867 at VK826. Only species for which there was more than one individual were included.

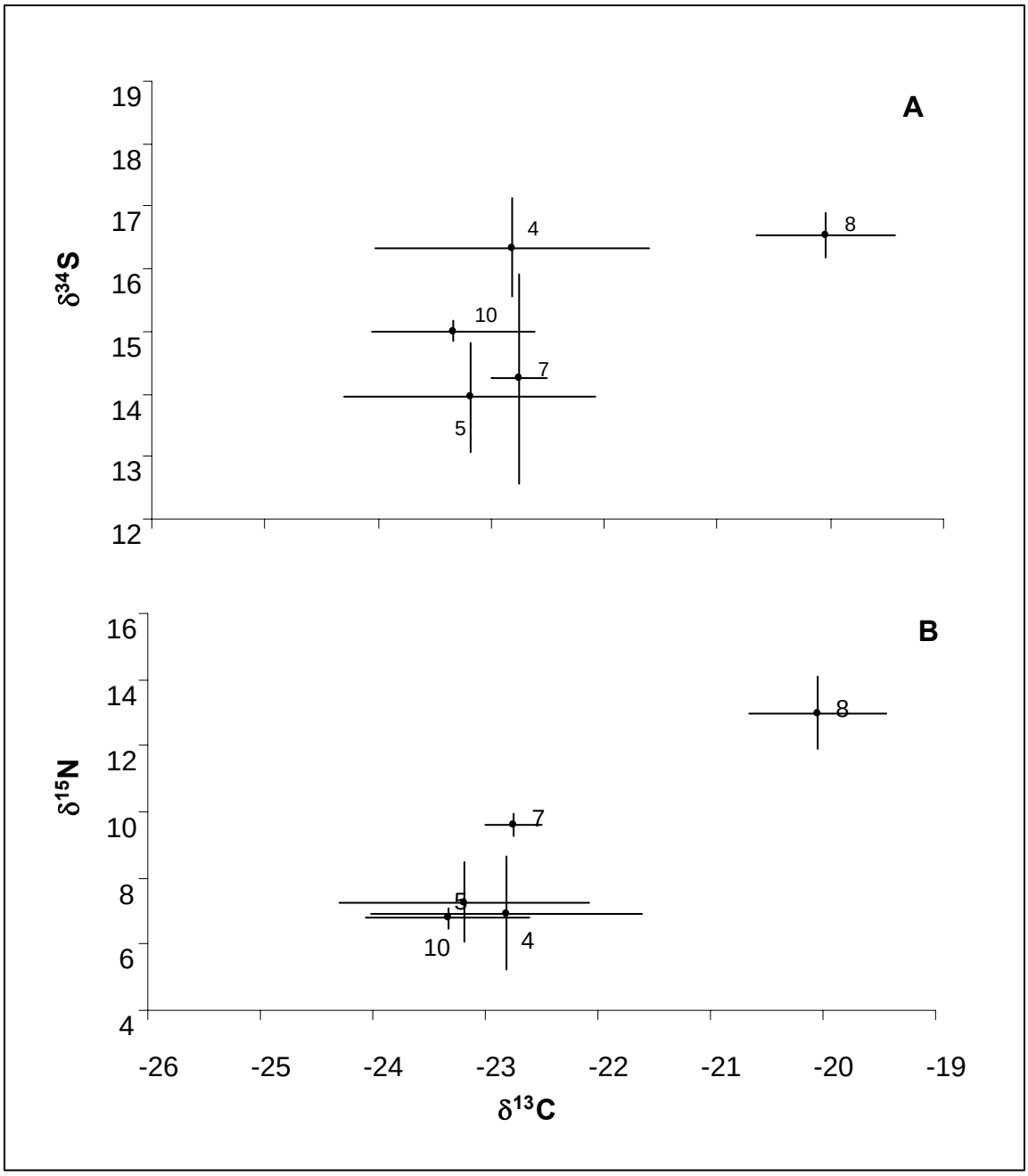

Figure 5.27. Average (A) $\delta^{34}S$ vs. $\delta^{13}C$ and (B) $\delta^{15}N$ vs. $\delta^{13}C$ for *Lophelia pertusa* and coral-associated fauna in a Bushmaster collection taken on Dive 4868 at VK826NE. Only species for which there was more than one individual were included.

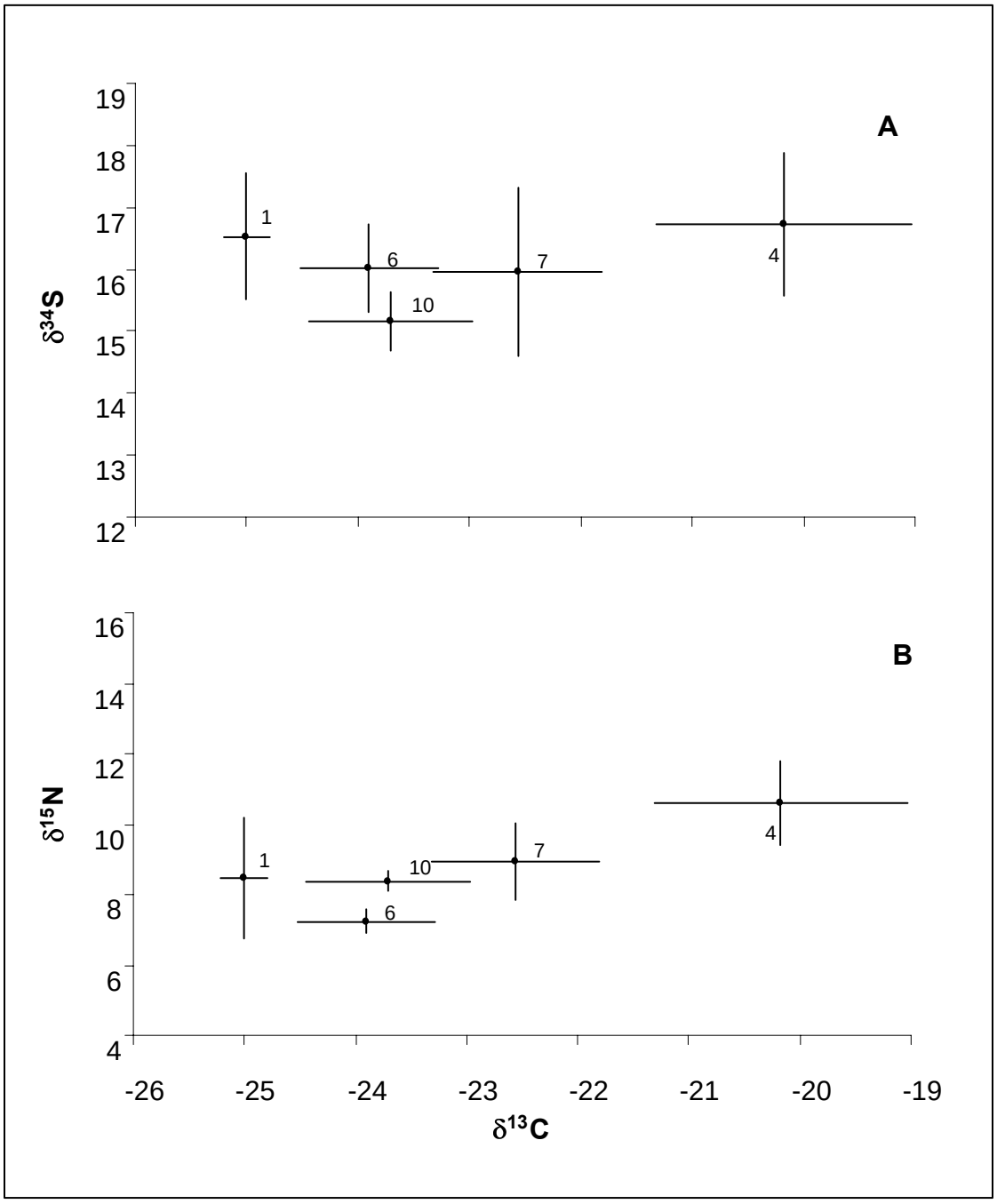

Figure 5.28. Average (A) $\delta^{34}S$ vs. $\delta^{13}C$ and (B) $\delta^{15}N$ vs. $\delta^{13}C$ for *Lophelia pertusa* and coral-associated fauna in a Bushmaster collection taken on Dive 4871 at VK826NE. Only species for which there was more than one individual were included.

Table 5.9. Average and standard deviations for all Bushmaster tissue $\delta^{13}C$, $\delta^{15}N$, and $\delta^{34}S$ values.

Site	Dive	Label	Taxon	Average			Standard Deviation		
				$\delta^{13}C$	$\delta^{15}N$	$\delta^{34}S$	$\delta^{13}C$	$\delta^{15}N$	$\delta^{34}S$
GC234	4728								
		2	*Coralliophila*	-17.1	12.8	12.2	0.8	0.8	0.8
		4	*Euratella*	-18.0	10.2	11.0	0.9	0.3	1.1
		6	Hydroids	-19.7	8.4	15.9	1.5	0.2	0.7
		7	*Munidopsis* sp. 2	-17.1	10.6	11.6	3.8	0.1	2.4
VK826	4737								
		1	*Stenopus*	-18.1	11.3	-10.1	0.3	0.2	23.5
		3	Crinoid	-19.3	9.8	22.0	0.3	0.2	0.7
		4	*Euratella*	-15.1	11.4	19.2	0.8	0.5	0.4
		10	Ophiuroid	-18.9	10.4	21.0	1.0	1.3	0.2
		11	*Periclemenes*	-18.5	10.0	18.9	0.4	0.3	1.0
GC234	4740								
		1	*Stenopus*	-18.4	10.5	15.1	0.4	0.7	1.7
		4	*Euratella*	-18.2	10.3	12.7	0.7	0.4	1.8
		6	Hydroids	-20.2	8.5	12.1	1.2	0.2	0.8
		12	*Munidopsis* sp. 3	-14.5	9.2	18.7	0.5	0.1	1.6
		8	*Nibilia*	-16.5	8.6	17.6	0.6	0.1	0.6
		9	*Asteroschema*	-18.7	10.2	20.4	1.2	0.6	2.8
GC354	4741								
		1	*Stenopus*	-18.0	10.3	21.7	1.3	0.5	0.2
		5	*Glycera*	-18.8	11.4	18.1	0.9	0.9	1.6
		12	*Munidopsis* sp. 3	-14.7	10.6	20.4	1.4	1.5	3.3
		9	*Asteroschema*	-19.3	9.6	23.5	0.2	0.6	2.0
VK826	4867								
		2	*Chloeia*	-21.1	11.9	17.7	0.9	2.3	0.5
		3	*Eunice*	-20.3	13.2	17.0	1.0	0.9	0.6
		5	Hydroids	-22.2	5.1	17.5	2.9	0.2	0.5
		7	*Lophelia*	-21.8	6.2	17.0	2.6	0.3	0.8
		9	*Periclemenes*	-21.0	9.6	16.0	1.8	3.3	0.4
		10	Sponge	-23.7	8.6	16.6	0.5	0.7	0.9
VK826NE	4868								
		4	*Euratella*	-22.8	6.9	16.3	1.2	1.7	0.8
		5	Hydroids	-23.2	7.3	14.0	1.1	1.2	0.9
		7	*Lophelia*	-22.8	9.6	14.2	0.3	0.3	1.7
		8	*Munidopsis* sp. 2	-20.1	13.0	16.6	0.6	1.1	0.4
		10	Sponge	-23.3	6.8	15.0	0.7	0.3	0.2
VK826NE	4871								
		1	Anemone	-25.0	8.5	16.5	0.2	0.9	1.0
		4	*Euratella*	-20.2	10.6	16.7	1.2	0.2	1.2
		6	Isopod	-23.9	7.2	16.0	0.6	1.2	0.7
		7	*Lophelia*	-22.6	8.9	16.0	0.8	2.4	1.4
		10	Sponge	-23.7	8.4	15.2	0.7	0.9	0.5

5.3.4 Total Petroleum Hydrocarbons in Seawater

TPH concentrations in bottom water samples are listed in **Table 5.10**. Values ranged from below the method detection limit to 29 µg/L. About half of the values were below or near the detection limit. There are too few samples to conduct a meaningful statistical analysis of differences among sites and cruises. However, values are within the typical range for seawater TPH in the Gulf of Mexico (T. McDonald, personal communication, TDI-Brooks International, Inc.) and do not provide any indication of elevated hydrocarbon concentrations.

Table 5.10. Total petroleum hydrocarbon (TPH) concentrations in near-bottom water samples.

Site	Cruise Number	Sample Number	TPH Concentration (µg/L)[a]
GC184/185	2	1	<13.5[b]
GC234	1	1	18
	1	2	29
	2	1	13.3
GC354	1	1	25
	2	1	<14.4[b]
MC885	1	1	26
	2	1	<13.8[b]
MC929	2	1	<14
VK826	1	1	13[b]
	1	2	26
VK862	1	1	27
	1	2	19

[a] TPH values are surrogate-corrected to 100%.
[b] Below method detection limit.

5.4 DISCUSSION

L. pertusa plays a significant role in the ecology of hard-ground habitats on the upper slope of the northern Gulf of Mexico. *L. pertusa* colonizes hard substrates following the decline of seepage, relying on the seeps as a source of hard substrate in the form of authigenic carbonate but not incorporating significant amounts of seep productivity into its diet. The role of *L. pertusa* in structuring the surrounding slope community appears to be through the provision of habitat rather than direct provision of nutrition by *L. pertusa*, with the possible exception of the gastropod *Coralliophila* sp. *L. pertusa* creates habitat for a number of associated species, many of which show significantly higher densities in proximity to coral or have been found only in tight association with *L. pertusa* in the Gulf of Mexico. *L. pertusa* therefore plays a similar role to tubeworm aggregations at active seeps, although the fauna attracted to these two types of biogenic habitat are quite different.

Measured $\delta^{13}C$ values of *L. pertusa* skeleton suggest that they do not settle in an area until seepage has largely subsided. The vast majority of the carbon serving as the source of the coral skeleton comes from the DIC in the surrounding seawater. There was no significant trend in

increasing $\delta^{13}C$ values over time in the skeleton, suggesting that light carbon from methane oxidation is not a significant input to the local DIC pool when the corals settle. It is still possible that methane oxidation is occurring in the vicinity of the corals when they settle, and this small input is diluted by the much larger pool of seawater DIC. However, if methane oxidation rates were high at the site of settlement, some small change in $\delta^{13}C$ should have been detected. In addition, *L. pertusa* tissue $\delta^{13}C$ signatures indicate that they are largely feeding off of the background fauna, with little apparent link to seep productivity in their nutrient supply. Comparisons of the isotopic signature of particulate organic matter and *L. pertusa* tissues from areas off the coast of Spain (Duineveld et al. 2004), Norway, and the UK (Kiriakoulakis et al. 2005) also indicate that the main food source of *L. pertusa* is zooplankton, although they have also been observed to ingest large resuspended sediment particles (Mortensen 2001; Freiwald et al. 2002). The majority of carbonates serving as attachment for the coral larvae is seep-derived and provides a link between *L. pertusa* distribution and the seep habitat (see Hovland and Thomsen 1997), but it appears that in the Gulf of Mexico *L. pertusa* prefers areas where seepage has almost completely subsided prior to settlement.

Temperature estimates derived from the coral skeleton are similar to those measured during the course of the study. Estimated temperatures fall into the expected range and are higher in shallower water, as would be expected. This demonstrates that *L. pertusa* may be used as a record of temperature in the Gulf of Mexico and suggests that additional efforts be made to obtain targeted collections for this purpose in the future.

On the scale of an individual carbonate outcrop or *L. pertusa* thicket (tens of square meters), the proportion of live and dead coral significantly influenced the structure of the associated community. This influence is apparent in the associations with *L. pertusa* structure detected in the spatial analysis. These include *Eumunida picta*, comatulid crinoids, the ophiuroid *Asteroschema* sp, and fishes. Many of these species are common members of the background community, having been previously collected in trawls away from hard substrates (Pequegnat et al. 1990; Carney 1994). However, when near a hard substrate, they tend to aggregate near coral structure. The ophiuroid *Asteroschema* sp. preferentially inhabited *C. americana americana*. In fact, it was only found on this species of gorgonian. The anemones at VK862 were found away from *L. pertusa* and other cnidarians, occurring most commonly on carbonate more than 10 cm away from other species. This is possibly a method of avoiding direct competition for food or contact with other species' nematocysts. Species of *Munidopsis* exhibited a skewed distribution favoring bacterial mats and tubeworms, when present. This suggests that these species may be a casual associate of coral structure, and only when it is found near a seepage source.

In a similar study of *L. pertusa* associates based on ROV video surveys from Norway, a number of other species were found in close association with the coral (Mortensen et al. 1995). Sponges occurred in higher densities on dead *L. pertusa* or on the surrounding carbonate and coral rubble. Gorgonians occurred in higher densities on *L. pertusa* structure, often on live *L. pertusa* as well as dead skeleton, in contrast to the findings here. Galatheids occurred preferentially on coral rubble. The bivalve *Acesta excavata* was observed on live *L. pertusa*. There are two species of *Acesta* on the upper slope, and previous observations indicate that the species growing on *L. pertusa* is different from the species on tubeworms at the same sites, although neither was observed growing on *L. pertusa* in this study. The crinoid *Hathrometra sarsii* was also found to

be most abundant on live *L. pertusa* in Norway, as was the case for the crinoid in this study, although low numbers of observations precluded statistical treatment of this observation.

Species in more close association with *L. pertusa* were sampled in the Bushmaster collections. These collections primarily contained species from the background fauna, as well as a few species that appear to be coral-endemic and a few species that were previously described as seep-endemic. The potential coral-endemic species include the gastropod *Coralliophila* sp., the shrimp *Stenopus* sp., and the polychaete *Eunice* sp., all of which have been previously observed in tight associations with other corals. *Coralliophila* species are known coralliovores from tropical coral reefs in the Caribbean, Red Sea, and Indo-Pacific (Hayes 1990). They have been observed to do significant damage to *Acropora* colonies in the Caribbean. Their feeding rates in deep water and their potential role in limiting the extent of live *L. pertusa* within a thicket are unknown.

The polychaete *Eunice* sp. is likely to be similar in habit to the species *Eunice norvegica* on the *L. pertusa* reefs of Norway. Both species are found in burrows or tubes surrounded by *L. pertusa* skeleton. *E. norvegica* has been shown to play a role in joining pieces of coral skeleton together by building a parchment-like tube that is subsequently calcified by *L. pertusa* (Mortensen 2001; Roberts 2005). In aquaria, *E. norvegica* was observed to physically move pieces of broken coral skeleton (Mortensen 2001; Roberts 2005) and attach them with its tube (Roberts 2005). This behavior could enhance rates of thicket formation and assist in recovery from disturbance (Mortensen 2001; Roberts 2005). It is possible that this polychaete plays a similar role in the formation and maintenance of *L. pertusa* thickets in the Gulf of Mexico.

The shrimp *Stenopus* sp. belongs to the crustacean Family Stenopodidae, many of which are common cleaner shrimp on tropical coral reefs. It is unknown whether this species fills this niche in the Gulf of Mexico, as such a relationship has not, to our knowledge, been reported for deepwater reef systems. It also is notable that members of the genus *Periclimenes*, a species of which was found in this study and in previous investigations of Gulf of Mexico tubeworm aggregations (Cordes et al. 2005), is also reported as being a cleaner species on tropical reefs.

Some of the species associated with *L. pertusa* have been previously reported in association with tubeworm aggregations at these same sites on the upper slope. Most of these species are from the background Gulf communities and are probably simply attracted to the increased habitat heterogeneity provided by these biogenic structures. However, some of these species have been reported as seep-endemics (Carney 1994; Bergquist et al. 2003; Cordes et al. 2005; Cordes et al. in press). These species include the polychaetes *Branchinotogluma* sp. and *Harmothoe* sp., the gastropods *Bathynerita naticoidea* and *Provanna sculpta*, and the galatheid crabs *Munidopsis* sp. 1 and 2. These species occurred only in collections with low proportions of live coral (<10%) from GC234 and GC354 where tubeworm aggregations were nearby. These species may be indicators of the presence of seepage, including more hypoxic conditions and low levels of sulfide and methane, particularly if they were located near the sediment surface and associated with dead coral. Although they have now been reported from another habitat, without discreet water chemistry samples and knowledge of their exact position within the coral framework, it is premature to remove them from the list of seep-endemic species.

The main factors controlling the similarity of coral communities sampled in the Bushmaster collections were location, depth, the proportion of live coral in the collection, and the relative complexity of the coral framework. At the most broad level of similarity, the main clusters of communities in the MDS analysis were by location. Distance between samples was also significant in the mosaic analyses. At the level of pairwise collection similarity, depth was the most important factor followed by proportion of live coral and complexity. The collections with the highest proportion of live coral were similar to one another and contained lower levels of diversity. On *L. pertusa* reefs in Norway, the highest-diversity communities were contained within dead and mixed live and dead portions of the thickets (Mortensen et al. 1995). Coral associates taking advantage of the complex structure for shelter are likely to avoid damage or consumption by the live coral in a thicket. The avoidance of live coral was also apparent in the spatial association analyses of the mosaic data, where most species occupied areas of dead coral adjacent to live coral. It is still unknown whether species avoid live coral or if the presence of large numbers of associates actually causes damage to the coral and increases the amount of dead coral in a thicket.

The majority of the fauna sampled among the coral framework comprised members of the regional species pool found in other Gulf of Mexico continental slope habitats. These background communities have been shown to change with distance and depth along the Louisiana slope at the macrofaunal (Pequegnat et al. 1990) and meiofaunal levels (Baguley et al. 2006). There was also a break in the community at approximately 500 m depth. This would separate the Viosca Knoll sites (315 to 470 m depth) from the Green Canyon sites (500 to 525 m depth). Because the bathymetric and spatial distribution of our sites are somewhat confounded (eastern sites are shallower than western sites), it is difficult to assess which of these variables is the most significant.

Differences between background and coral communities are likely due to the added degree of habitat complexity provided by the coral structure. The simple addition of a vertical profile above a flat bottom will provide a first order shelter for associated fauna. This may be provided by carbonate outcrops, tubeworms, *L. pertusa*, and other colonial cnidarians. The addition of gaps in this structure, present in tubeworms and corals but not as common in abiotic substrate, provides a secondary spatial niche to occupy. The highly complex structure of the three-dimensional network of anastomosing branches in *L. pertusa* provides a variety of different sized voids, and theoretically should support the most diverse (at least morphologically) communities. Complexity had a significant effect on the similarity between coral communities in both the mosaic and Bushmaster samples, although correlations between complexity and diversity were not significant. In addition, *L. pertusa* communities (H' = 0.67 to 2.54) were generally less diverse than tubeworm communities (H' = 1.37 to 3.12) collected with the Bushmaster at the same sites.

Coral-associated communities shared a few species with tubeworm-associated communities collected at nearby sites with the same sampling gear. Species commonly occurring in both forms of biogenic habitat included the polychaetes *Euratella*, *Glycera tesselata*, the galatheids *Munidopsis* sp. 1 and sp. 2, and the shrimp *Periclemenes*. Even though many species were shared between habitats, the community composition and structure was sufficiently different that all tubeworm-associated communities were more similar to each other than they were to any of the coral-associated communities at the three alpha sites where both types were observed (**Figure 5.29**).

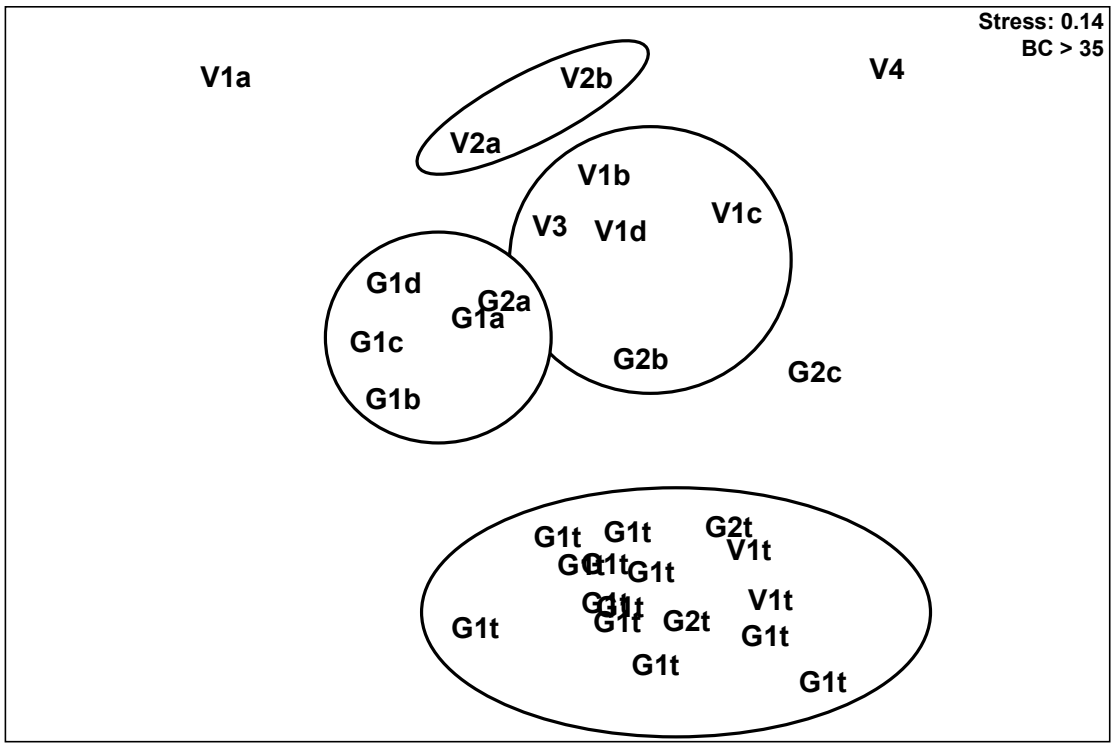

Figure 5.29. Multidimensional scaling plot of coral-associated communities and tubeworm-associated communities collected with the Bushmaster from the same sites.

The low numbers of species associated with both coral and tubeworm collections led to the separation of these two habitat types in the community ordination. Because depth and distance between collections were not significant factors in a similar analysis of tubeworm-associated communities from the same sites (Cordes et al. 2005; Cordes et al. in press), the effect these factors had on the background communities could explain some of the differences in the patterns observed. However, the most significant factor influencing community structure is likely to be habitat chemistry. The presence of sulfide and methane in conjunction with lower oxygen levels in tubeworm aggregations would select for a set of seep-endemic species adapted to this environment. Even in older tubeworm aggregations where sulfide concentrations are near or below detection limits, there are relatively high proportions (25% to 30%) of seep-endemic species (Bergquist et al. 2003; Cordes et al. 2005). The higher diversity of tubeworm aggregations is likely a result of the combination of endemic species with the background species of the upper slope. The absence of this selective factor in coral communities allows background species to colonize and dominate the coral structure. This would almost entirely eliminate the seep-endemic species from the *L. pertusa* habitat, except for deeper layers of coral structure embedded in or just above the sediment where sulfide may be present and/or oxygen concentrations may be low. The dominance of background species in the coral-associated community in addition to the limited number of potential coral-endemics results in the dissimilarity between associated fauna in these two types of biogenic habitats.

There were few trophic links that were congruent among the three stable isotope values measured and practical considerations of taxonomic feeding constraints (e.g., hydroids cannot possibly feed on fishes). Expected shifts in isotopic signature from prey to predator are +3.4 for nitrogen, +1 for carbon, and approximately 0 for sulfur (Rau et al. 1983; McCutchan et al. 2003). Using these values, there was only one collection where a possible food source for *L. pertusa* could be identified: small isopods collected at VK826NE on Dive 4871 (**Figure 5.21**). Other potential feeding relationships include *Munidopsis* spp. preying on hydroids (**Figures 5.15** and **5.17**) and on the sabellid *Euratella* (**Figure 5.20**), *Eumunida* feeding on sponge or *Euratella* (**Figure 5.20**), *Eunice* on the small polychaete *Chloeia* (**Figure 5.19**) and the sabellid *Euratella* (**Figure 5.20**), and *Periclemenes* feeding on the small polychaete *Eteone* (**Figure 5.19**). Although paired samples were not available within a single collection, the range of values for the corallivorous snail *Coralliophila* sp. (-21‰ to -17‰ $\delta^{13}C$, 8‰ to 13‰ $\delta^{15}N$, 15‰ to 16.5‰ $\delta^{34}S$, **Figure 5.15**) support a trophic link with *L. pertusa* (-25‰ to -18‰ $\delta^{13}C$, 6 to 11‰ $\delta^{15}N$, 12‰ to 20‰ $\delta^{34}S$, **Figure 5.14**).

Most of the associated species for which multiple individuals were measured had consistent nitrogen isotope ratios but variable carbon values (**Figures 5.22** to **5.28**, **Table 5.9**). This is an indication of a generalist feeding strategy within a single trophic level. These species were mostly suspension feeders, including *L. pertusa*, *Euratella*, and the hydroids, but also included *Periclemenes* sp. (**Table 5.9**).

The species occupying the coral habitat derive little to none of their nutrition from seep productivity. The suspension feeding organisms, including gorgonians, antipatharians, sabellid polychaetes, hydroids, and *L. pertusa*, had $\delta^{13}C$, $\delta^{15}N$, and particularly $\delta^{34}S$ values that were more positive than would be expected for food source derived mainly from seep productivity. This indicates that if there is seep productivity in the area, it is not resuspended in significant quantities, or into large enough particles to be captured by these taxa. However, the range of isotope values in these species could be explained by a mixture of seep and photosynthetic productivity entering the base of the food web. If seep productivity is entering this trophic web, it may be through the presence of small mobile crustaceans that were not sampled here. Generalist feeding on a variety of prey, some of which may be occasionally feeding within the seep habitat, could produce the broad isotopic patterns observed in this study.

The *L. pertusa*-associated fauna from the Bushmaster collections exhibited a wide range of $\delta^{13}C$ values but a narrow range of $\delta^{15}N$ values. The narrow range of nitrogen isotope values suggests that most species occupy relatively few trophic levels. Species occupying similar trophic positions may be partitioning resources to avoid competition, leading to the wide range of carbon signatures. Specialization on different resource pools containing different proportions of seep productivity would produce the large spread in carbon isotopic values observed. This could lead to a disconnection between two alternate trophic pathways. However, broad intraspecific variability in carbon isotope values suggests that most species are generalists. The range in carbon values may reflect the mixing of the resource end-member values and a dilution of the seep stable-isotopic signature as it progresses from one trophic level to the next.

Some individuals exhibited isotope values overlapping those observed in tubeworm associates and could therefore incorporate significant proportions of seep productivity into their diet. Species with low sulfur isotope ratios included *Provanna sculpta*, *Stenopus* sp., and the hydroids from GC354. It is possible that these values reflect a certain degree of reliance on seep productivity. However, the relatively positive $\delta^{13}C$ and $\delta^{15}N$ values of *Stenopus* sp. and the hydroids suggest that if they are incorporating seep productivity, that their reliance on this food source is minor. The isotope values of *Provanna sculpta*, a known tubeworm associate, do support the conclusion that this individual was incorporating a certain proportion of seep productivity. It is possible that it was occupying a narrow zone at or below the sediment water interface where sulfide- or methane- oxidizing microbes are abundant and serving as a food source. Other individuals of this species (potentially missed in the sampling due to their presence at the very base of the skeletal framework) could serve as prey for other higher-order consumers within the *L. pertusa* thicket and explain the trend of some of the isotope signatures falling within the range of those measured in tubeworm associated communities.

In an examination of the stable isotope values of the foundation species of the hardgrounds of the upper slope, including corals, mussels, tubeworms, and their associated fauna, it appears that the coral communities may represent a final stage of succession (**Figure 5.30**). The inhabitants of the coral framework exhibit more positive carbon, nitrogen, and sulfur stable isotope values than young and middle aged tubeworm aggregations. These values fall within the range of the oldest tubeworm aggregation-associated fauna, although nitrogen is even more positive. This is a result of the increasing dominance of higher-order predators and the reliance of the lowest trophic levels on allochthonous photosynthetic productivity rather than local seep productivity.

Stable isotope values support the concept of *L. pertusa* thickets as the end point of the seep community succession pathway. In all three isotope signatures measured, there is a general progression from light (negative) signatures in young tubeworm aggregations, to heavier (more positive) signatures in older aggregations. This has been inferred to result from the decline in seepage over time and the colonization of the tubeworm habitat by additional non-endemic species. This continues into the *L. pertusa* community, with an increasing elevation of nitrogen values and similar carbon and sulfur values at the oldest tubeworm aggregations examined. This implies that there is little to no seepage evident at the time of settlement and greater proportions of background, non-endemic species dominating the associated community. The presence of a few coral-endemic species complicates this progression and introduces a second round of primary colonization to the succession pathway. Because the majority of seep-endemic species occupy lower trophic levels (Bergquist et al. 2003; Cordes et al. 2005), their absence creates a number of potential niches for coral-endemic species to occupy. These endemic species all appear to have tight associations with the coral either by feeding on them (*Coralliophila*), contributing to framework assembly (*Eunice*), or by establishing symbioses with other coral associates (*Stenopus*). These relationships are all based on previous investigations of similar species and require additional investigation in the Gulf of Mexico *L. pertusa* community.

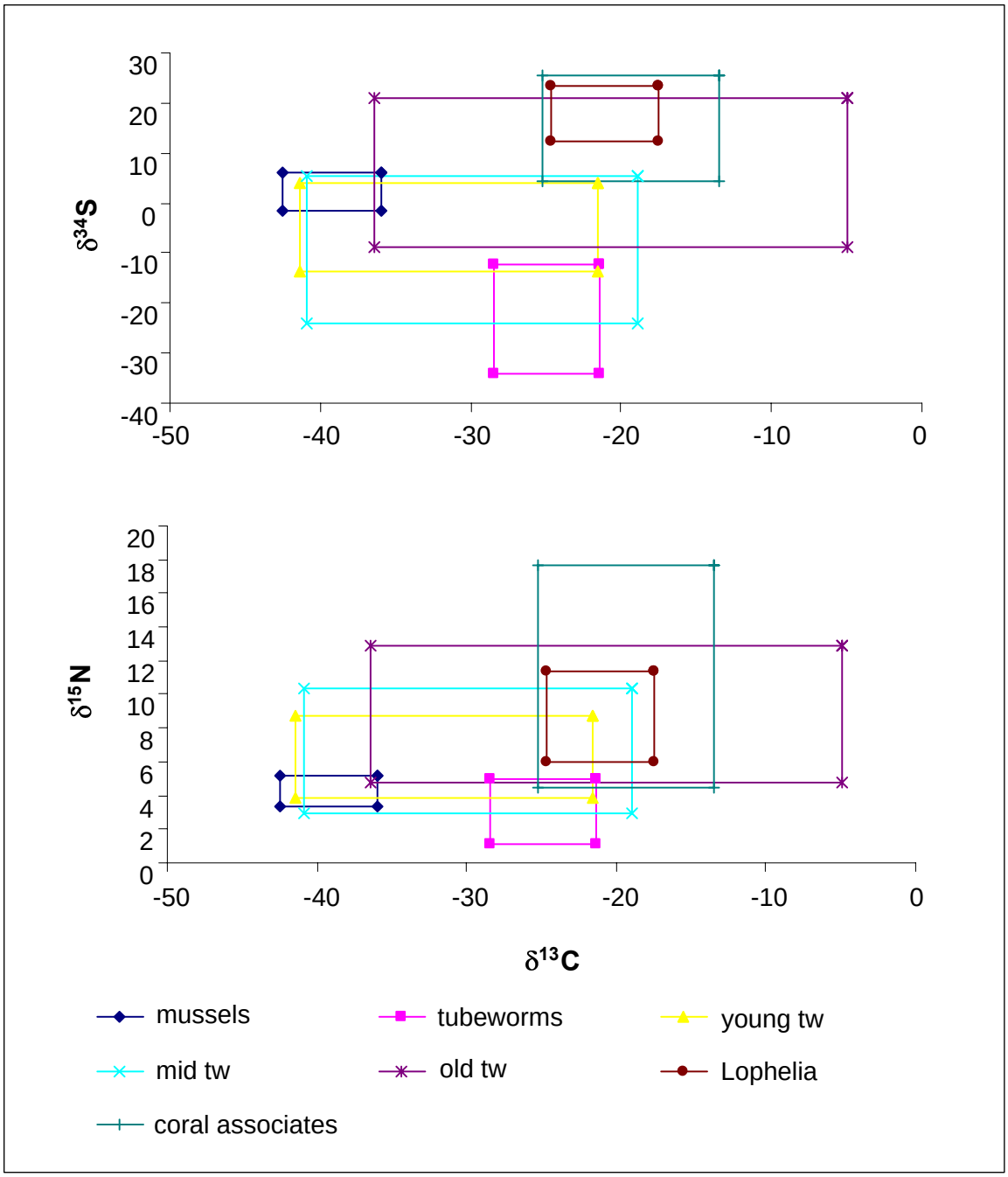

Figure 5.30. Comparison of the range in isotope values of foundation species (corals, tubeworms, and mussels) and associated fauna in young, middle aged, and old tubeworm aggregations and the coral communities collected in this study.

Chapter 6
Biological Characterization and Studies, Part II

Sandra D. Brooke, Craig M. Young, and Michael Holmes

6.1 METHODS – FIELD STUDIES

6.1.1 Biological Characterization

Biological Characterization and Studies, Part II

- Sites were characterized based on video, photographs, samples.
- Sediment traps were deployed to estimate sediment flux and zooplankton availability.
- A *Lophelia* transplantation experiment was conducted at VK826.
- Laboratory studies focused on *Lophelia* morphology and skeletal density; reproduction; temperature and sediment tolerance; and feeding.

The *JSL* submersible was used to collect photographic, video, and sample data used for habitat characterization. Integrated positioning system (IPS) software integrated the submersible's position relative to the ship and calculated the submersible's real time DGPS position throughout each dive. The *JSL* was equipped with a manipulator arm (including a 20-cm clam-shell grab for sediment samples, jaw, and suction hose), 12 plexiglas buckets, and a CTD data recorder (Seabird SBE 25 Sealogger) that continuously recorded time, temperature, conductivity, salinity, oxygen, and depth. Video footage was recorded continuously during each dive with an external pan and tilt videocamera (Sony DX2 3000A), with parallel lasers (25 cm apart) for scale reference. The video data overlay provided information on time, date, depth (feet), salinity, and temperature (°C). Video transect data were collected at each of the study sites during cruises in 2004 and 2005 and were supplemented with additional information from other cruises in 2002 (*R/V Seward Johnson II*/*JSL*, funded by the National Science Foundation) and 2003 (*R/V Ron Brown*/*SONSUB ROV*, funded by NOAA OE). At each site, five video transects were conducted, each approximately 100 m in length and 20 m apart, along parallel bathymetric contour lines to provide an area of ~10,000 m^2 for analysis. The submersible, where possible, maintained a constant distance above the substrate with an area of approximately 8 m^2 visible through the videocamera. The video footage was split into consecutive image frames, which were labeled with the video time stamp. For each image the total frame area, salinity, depth, and temperature were entered into a data sheet. For sites dominated by *Lophelia pertusa* (VK826, GC234, and GC354), the percentage cover of live and dead coral was measured and other visible fauna counted. For the other sites (VK862, GC184/185 [Bush Hill], and MC885), all visible components of the benthic fauna were counted and identified. The scientist in the sphere provided audio descriptions of the habitat and biota throughout the dive on the video. Samples of invertebrate species (primarily cnidarians) were collected opportunistically using the submersible manipulators, to verify taxonomy, since most benthic taxa (especially sponges and gorgonians) cannot be identified to the species level from videotapes. The samples were photographed *in situ* prior to collection and again on deck with a calibration ruler and sample number. Polyp detail was photographed under a dissecting microscope with a Nikon Coolpix digital camera. Museum voucher specimens were taken from each sample and stored in 70% ethanol; these were subsequently shipped to appropriate taxonomists for identification. The video transects were

used to document the benthic habitat and estimate distributions, densities, and sizes of dominant fauna.

6.1.2 Sediment Flux and Zooplankton Availability

Each sediment trap was constructed from a piece of PVC pipe (30 cm in length with 4.5 cm inside diameter), which was sealed with an end cap and attached to a 2.3 kg disc weight. Dense brine with mercuric chloride fixative (1 g/L) and fluorescein dye was added to the tube prior to deployment. The tops were sealed with plastic cling film and a rubber band to retain the fixative solution during deployment. The submersible removed the plastic film after the traps were placed on the substrate. The dense fixative remains at the base of the tube where it kills and preserves any living organisms that enter (Yund et al. 1991). Six sediment traps were initially deployed in July 2004 at each of the alpha sites, three within the coral complex (high coral) and three outside the reef (no coral), to investigate the effect of the coral structure on particulate deposition. Since the beta sites do not have high coral density regions, only three traps were deployed at beta sites VK862 and MC885. An additional three traps were deployed in no coral and high coral areas of VK826, and a high coral area of VK862 later in the cruise (following a request by the MMS). The traps outside the reef provided a comparison of sediment and zooplankton delivery between sites. The traps were recovered by the *JSL* submersible in September 2005, and the contents were transferred to 5% formalin in seawater and transported to the laboratory for further processing. The contents of each trap were filtered through 300-µm sieves to separate the zooplankton from the sediment. The sediment then was analyzed for grain size distribution using a series of sieves between 20 and 200 µm. The dry weight (DW) was measured after drying each sediment fraction for 72 hours at 67 °C. The samples then were transferred to a muffle furnace (550 °C) for 24 hours to obtain the ash-free dry weight (AFDW), and organic content was determined by subtracting AFDW from DW. Zooplankton samples were divided by class, and each sample was then analyzed for DW and organic content using the methods described above.

6.1.3 *Lophelia* Transplantation

This experiment was deployed at the primary alpha site, VK826, which has areas of dense coral cover and areas of hard substrate with no coral. The objective of this experiment was to determine whether the uncolonized areas are unsuitable for adult coral survival, or whether some other factor (recruitment limitations, juvenile mortality, etc.) may be responsible for the absence of coral colonies on apparently suitable hard substrate. Fragments of healthy *L. pertusa* were collected in July 2004 from VK826 and placed in the submersible "biobox" for transport to the surface where they were transferred to the shipboard cold room and maintained at 8 °C. Transplant fragments were stained with Alizarin Red for 48 hours at a concentration of 10 mg/L (ppm). A colored cable tie was placed at the base of the terminal polyp on each fragment. The same colors were used to mark the ¾-in. polyvinyl chloride (PVC) union or compression fitting to which the transplants were secured. Colors used were yellow, green, red (or black), and white. The fragments were all photographed after the cable tie was attached and Image Tool (UTHSCA) image analysis program was used to measure distance from cable tie to rim of calyx to create pre-deployment baseline data for growth measurements. Fragments were placed in quick-setting cement in the PVC fittings and left to set for approximately 3 minutes in air (**Figure 6.1**). Fragments were then transferred to clean water at 8 °C and deployed the following day. Before attaching to transplant bases, the numbers of live, dead, and broken polyps were recorded.

Broken polyps with live tissue in the calyx were counted as live but broken (or buried if the polyp was partly covered with cement). For deployment, the transplant modules were placed in the submersible biobox, which had been filled with cold (8 °C) seawater (**Figure 6.2**). A total of eight transplant blocks was deployed, each with four replicate fragments attached. Four blocks were placed within coral thickets at VK826 to serve as controls for the artifacts of manipulation, and the remaining four were deployed in an area with no coral. After recovery in September 2005, the fragments were photographed and removed from the cement fittings. Survival and growth data were collected for each fragment, and the average and standard deviation generated for each of the replicate transplant blocks. Growth was measured as distance from cable tie to tip of calyx, and any new additional growth (including new polyps) was recorded. Pieces of the skeleton that showed evidence of additional growth were embedded in plastic casting resin, cut into thin slices with a diamond saw, and polished to enable visualization of the dye lines.

Figure 6.1. Stained fragments of *L. pertusa* set in compression fittings prior to attachment to transplant blocks. Note the color-coded ties on the fragment polyps.

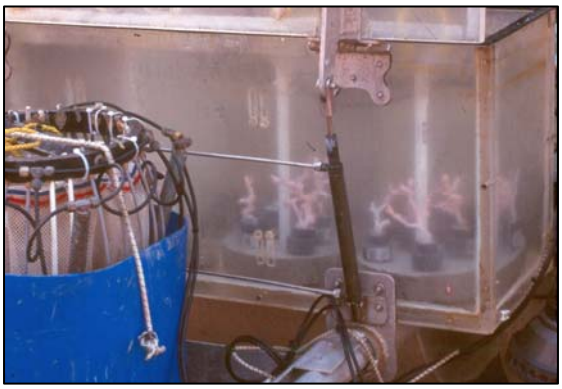

Figure 6.2. Transplant blocks in submersible biobox ready for deployment.

6.1.4 *Lophelia in situ* Staining

In order to calibrate the transplants and account for any handling artifact, two small colonies of *L. pertusa* were stained *in situ* in July 2004 using a plastic dome apparatus with a quick release connection to the submersible. A concentrated solution (25 ppm) of Alizarin Red, contained in a 5-gallon cubitainer, was attached to the outside of the submersible with a hose connection to the staining dome. The dome was placed over the colony and secured by a heavy flexible skirt around the base. The stain was pumped into the apparatus, displacing the seawater through a flapper valve at the top. The hose connection was then severed and the dome was left in place for 48 hours, after which time it was removed by the submersible and the colonies remained *in situ* until September 2005. On recovery, the colony was broken apart and the linear extension of each stained polyp was measured. Representative stained polyps from each of the transplanted fragments were embedded in plastic casting resin, and 2-mm transverse and longitudinal slices were cut with a circular diamond blade. Images were taken under a Zeiss dissection microscope using an Optronics digital camera system. These images were imported into Image Tool and the distance from the stain band to the outer edge of the calyx was measured. In combination, these techniques will provide measurements of linear extension, age, and ring deposition rate.

6.2 METHODS – LABORATORY STUDIES

6.2.1 *Lophelia* Morphology and Skeletal Density

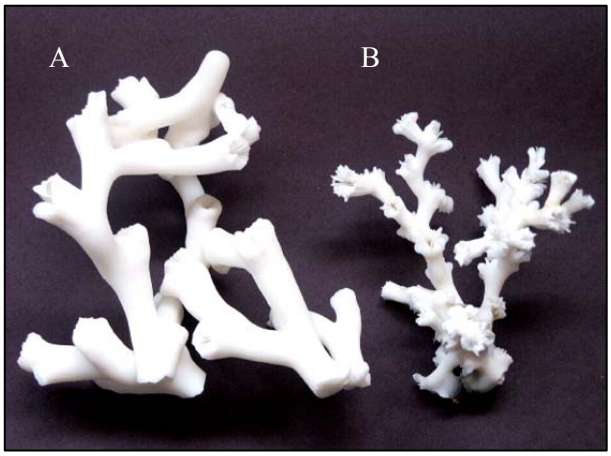

Figure 6.3. Samples of *L. pertusa* colonies collected from the Gulf of Mexico: A) heavily calcified morphology ("*brachycephala*") with large polyps from VK826; B) fragile morphology ("*gracilis*") from GC354.

Colonies of *L. pertusa* found in the deep Gulf of Mexico exhibit two distinct growth forms or "morphotypes" originally described by Newton et al. (1987). One is very heavily calcified with thick branches and very large calices, termed "*brachycephala*" (**Figure 6.3A**), and the other, "*gracilis*" (**Figure 6.3B**), is more fragile with smaller branches and very prominent septal ridges. The heavier form comprises the extensive colonies at VK826, and the more delicate morphotype is found at all of the other study sites. This section examines differences in skeletal characteristics between the two morphotypes. Skeletal density measurements were taken for 10 paired fragments of *L. pertusa* colonies collected from the Gulf of Mexico. Each pair had one representative of the heavily calcified morphotype ("*brachycephala*") with large polyps and one of the fragile form ("*gracilis*"). Processing protocols were taken from methods outlined in Bucher et al. (1998) and provided values for bulk density, micro-density, and porosity. Bulk density is the density of the skeleton, where the volume includes the pore spaces within the skeleton. Micro-density is a density measurement of the skeletal matrix excluding the pore spaces, and therefore calculates the density of the mineral matrix and will always be higher than the bulk density. The porosity value indicates the quantity of air spaces within the skeleton.

Calculations for skeletal parameters:

δ_m	Density of fluid medium
DW_{clean}	Dry weight (g) of clean skeletal material dried to a constant weight at 60 °C
BW_{sat}	Saturated buoyant weight (g) of the clean skeletal material (skeletal voids filled with the fluid medium)
$V_{matrix} = (DW_{clean} - BW_{sat})* \delta_m$	Skeletal matrix volume (cm^3)
DW_{wax}	Dry weight of waxed coral skeletons (g)
BW_{wax}	Buoyant weight of waxed coral skeletons (g)
$V_{enclosed} = (DW_{wax} - BW_{wax})* \delta_m$	Total (enclosed) volume (cm^3)
$V_{enclosed} - V_{matrix}$	Volume of skeletal voids (cm^3)

Formulae for calculation of skeletal parameters:

Micro-density (g/cm^3)	DW_{clean} / V_{matrix}
Bulk density (g/cm^3)	$DW_{clean} / V_{enclosed}$
Porosity (%)	$100*[V_{enclosed} - V_{matrix}]/V_{enclosed}$ (skeletal void volume as % total enclosed volume)

Small fragments of each morphotype were embedded in plastic casting resin, cut into thin slices with a diamond saw, and polished to enable visualization of the growth bands and comparison of the two morphotypes.

6.2.2 Histological Processing for Reproduction in *Lophelia* Coral

Fragments were decalcified in 10% hydrochloric acid, then polyps were dehydrated through a series of ethanol concentrations, embedded in paraffin wax, cut into 8-µm sections, and stained using Mayer's haematoxylin/eosin B staining techniques. Images of oocytes were taken using an Optronics digital camera attached to an Olympus BX50 compound microscope. The area of each oocyte was measured and recorded using Image Tool (UTHSCSA) image analysis software. Oocyte "feret" diameter was calculated, which estimates the diameter of a hypothetical circle with the same area as the object measured.

$$\text{Diameter} = \sqrt{\frac{4 \times \text{area}}{\pi}}$$

Information on oocyte feret diameter and size frequency distribution was used to infer the timing of the gametogenic cycle. Oocyte size-frequency distributions were generated using the oocyte diameter data.

6.2.3 Temperature Tolerance of *Lophelia* Coral

These experiments were conducted in replicate (n = 5) re-circulating systems, each with one to two coral fragments composed of approximately 20 polyps per replicate (**Figure 6.4**). The five experimental temperatures: 5 °C, 10 °C, 15 °C, 20 °C, and 25 °C, plus a control system at 8 °C (ambient temperature at the coral collection site) were maintained using temperature-controlled incubators under dark conditions. Experimental fragments were transferred from the main tanks (8 °C) in 1-L glass jars and left to acclimate to the experimental temperatures over 1 to 2 hours before being placed in the experimental tanks. Mortality was recorded after 24 hours (short term) and at the termination of the experiment after 7 days (long term). After 3 days, the corals were fed freshly hatched *Artemia* nauplii (thereby maintaining the pre-experimental feeding schedule) to avoid the effects of experimental artifacts.

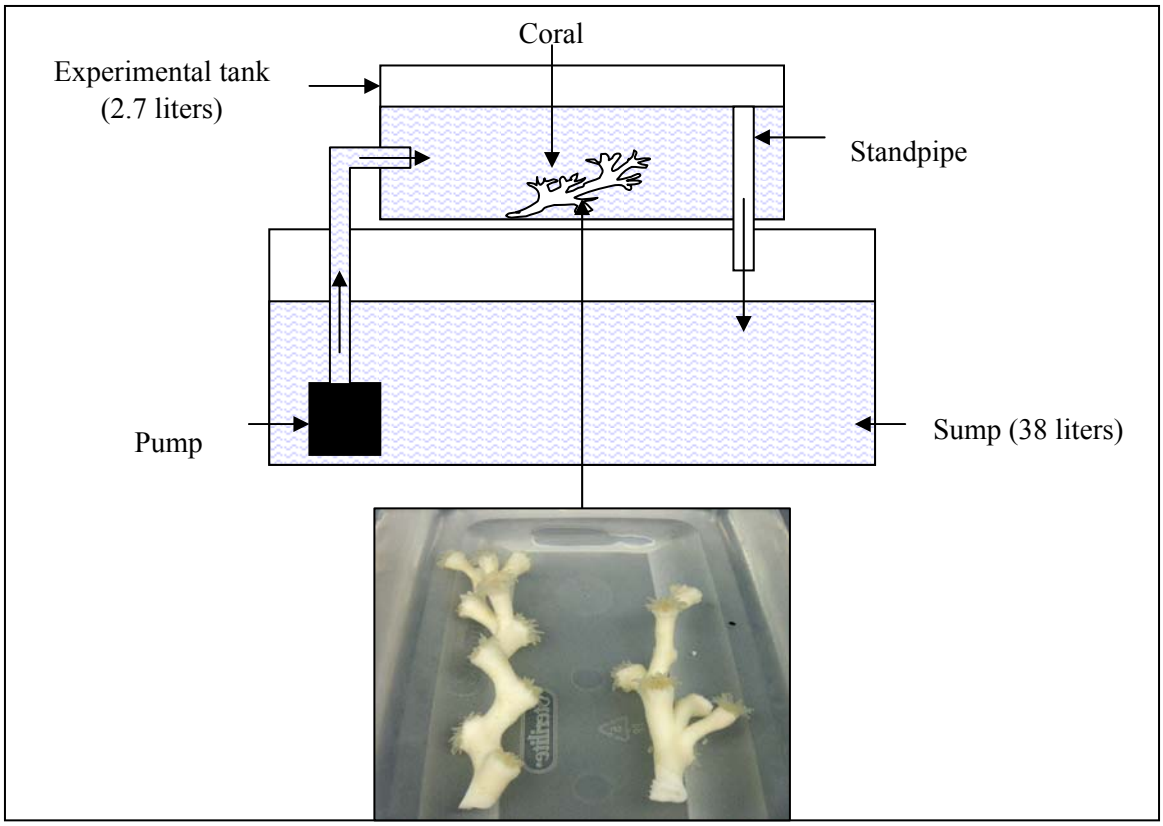

Figure 6.4. Aquaria design for the temperature tolerance experiments, with five replicate systems per treatment. Treatments were 5 °C, 10 °C, 15 °C, 20 °C, and 25 °C.

6.2.4 Sediment Tolerance of *Lophelia* Coral

The first experiment investigated tolerance of *L. pertusa* fragments to a range of sediment loads. Experimental sediments were collected from non-chemosynthetic sites in the deep (600 m) Gulf of Mexico, and were sieved (5 mm) and autoclaved prior to introduction into the experiment. Small coral fragments (10 to 15 polyps) of each morphotype were exposed to a range of sediment concentrations in individual 19-L experimental systems (**Figure 6.5**). Five target suspended sediment concentrations (0, 50, 150, 250, and 350 mg/L) were selected. The treatment levels were chosen to represent a continuum between the control (no sediment) and the highest concentration that could be maintained in the experimental system. Subsamples (50 mL) of suspension were taken daily from each treatment for the duration of the experiment to track any changes in sediment concentration that may have occurred. After 14 days under treatment conditions, the fragments were removed and placed into re-circulating recovery tanks (8 °C). Survival was assessed 4 days later.

A second experiment tested the response of *L. pertus*a fragments to complete burial over treatment periods of 1, 2, 4, and 7 days. Fragments of each morphotype were placed in individual containers, covered in Gulf of Mexico sediment and assigned a treatment and replicate (n = 3) number. They were then distributed randomly within a re-circulating tank of seawater at 8 °C for the designated treatment period. After removal, each fragment was scored for polyp mortality.

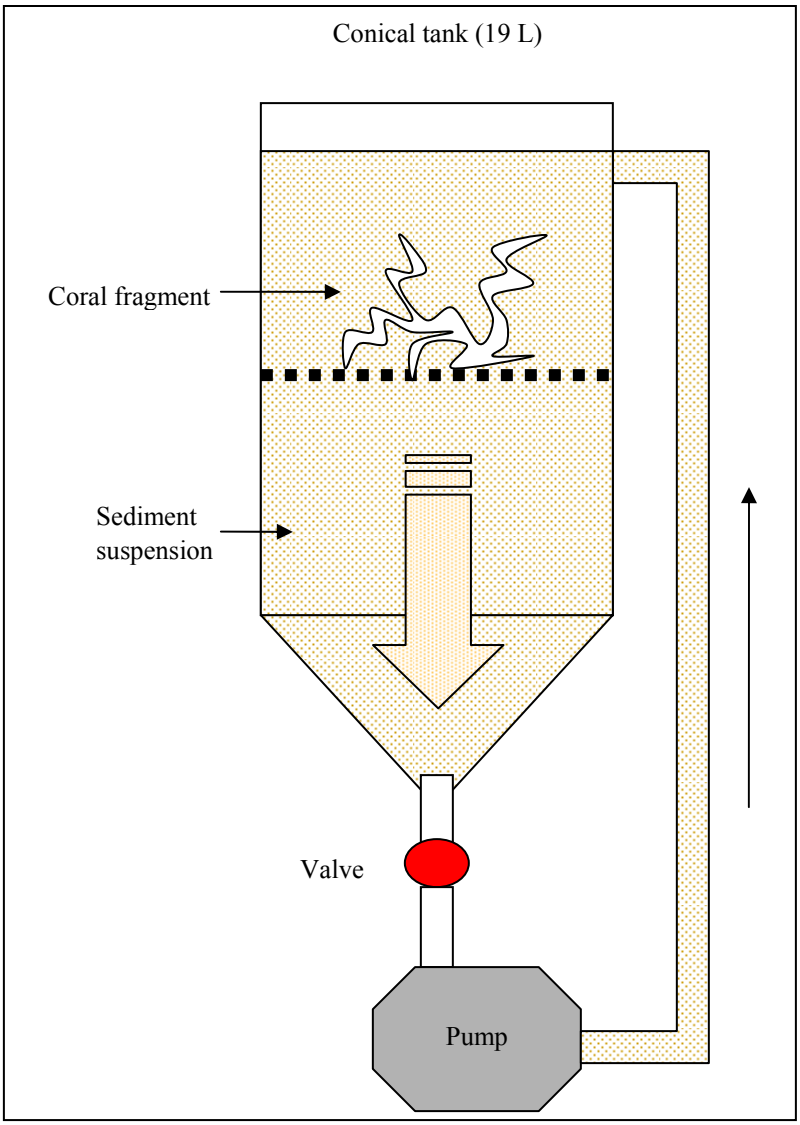

Figure 6.5. Experimental apparatus used to investigate sediment tolerance of *Lophelia* coral.

6.2.5 Feeding Experiments for *Lophelia* Coral

This experiment was designed to investigate the effect of various food rations on the survival, calcification rate, and lipid content of *L. pertusa* fragments. At the beginning of the experiment, each fragment (approximately 20 polyps) was weighed using the buoyant weight technique (Davies 1989) and placed in an individual re-circulating system filled with 0.2 µm-filtered seawater at 8 °C in a cold room. At each feeding event the re-circulation pumps were closed, and the corals were fed to satiation with freshly hatched *Artemia* nauplii over a period of several hours. The water then was replaced with clean filtered seawater, which prevented fouling of the water from unconsumed *Artemia.* For each treatment, a different time interval elapsed between feeding events (2 days, 4 days, 6 days, 8 days, unfed), therefore each treatment received a different food ration over the 30-day experimental period. The trial was repeated twice to increase statistical power. At the end of the experiment, the fragments were weighed again and processed for lipid content; they were preserved in 5% formaldehyde for 48 hours then washed in distilled water and decalcified in 10% hydrochloric acid for 8 hours. The polyps were washed

again in distilled water to remove the remains of the acid, transferred to small plastic pans, and placed in a drying oven at 56 °C for 48 hours (or until the weight was constant). The polyps were weighed on a fine balance, then transferred to a 1:2 methanol:chloroform solution for 48 hours to extract the lipid. The polyps were removed from the extraction solution, dried in the oven for 24 hours, and weighed once more. The average percentage lipid was then calculated for each treatment. Food ration for each treatment was translated into caloric content using estimates of nauplii consumed at each feeding and caloric content of freshly hatched nauplii (Paffenhofer 1967).

6.3 RESULTS – FIELD STUDIES

6.3.1 Biological Characterization – Alpha Sites

Viosca Knoll 826

A total of 16 transects was surveyed in the Viosca Knoll region; seven of these were at the primary alpha site for this project (VK826), and the others were on a small feature to the northeast of the primary site, which was designated VK826 NE. Transects surveyed at VK826 ranged from 46 to 181 m in length and covered a combined area of nearly 1,600 m^2 (**Table 6.1**). Transects were all surveyed within an area bounded by 29°09.5'N and 88°01'W. The transect layout is shown in **Appendix B.1a**. The average transect depth ranged from 452 to 484 m, with temperatures between 8.23 °C and 9.47 °C. There is a difference of >1 °C between transects surveyed in 2003 and those surveyed in 2005; this is probably a temporal phenomenon rather than being attributable to depth differences between transects. The percentage of live coral cover varies between 2.1% and 15.6% of the frame area and is consistently less than the percentage of dead coral. The ratio of live:dead coral cover lies between 0.18 and 0.74 (**Table 6.1**), with an average of 0.39 over the whole transect area. Coral colonies were not evenly distributed along transects; dense aggregations of large colonies were interspersed with areas of sediment and coral rubble, shell hash, and occasionally chemosynthetic communities. The diversity of coral-associated fauna visible on the video footage was low, but some species were consistently observed in high coral areas. These included an echinoid urchin (*Echinus tyloides*), a comatulid crinoid (*Comatonia cristata*), the "venus fly trap" anemone (Actinoschyphiidae), and two common galatheid crabs (*Eumunida picta* and *Munidopsis* sp.). Transects surveyed at VK826 NE encompassed most of the coral habitat, which was limited to the top and upper flanks of the feature (29°10'N, 88°00'W) at depths of 459 to 475 m (**Appendix B.1b**). All transects were surveyed in the same year (2005) and showed similar average temperatures (~8.5 °C). The overall coral cover (live plus dead) on this feature was similar to the primary site; however, the percentage of live *L. pertusa* was much higher on this feature (16.88%, SE: 4.85) than on the main area (8.76%, SE: 1.90). Consequently, the ratio of live:dead coral was also higher (0.91, SE: 0.27). The associated faunal community visible on the video footage appears to be very similar to the main VK826 site. The distribution of live and dead coral is presented graphically in **Appendix B.2** for VK826 and **Appendix B.3** for VK826 NE.

Table 6.1. Summary of transect data for each alpha site. For each transect, the table shows total length, total area covered, average depth, average temperature, percent cover of live and dead *Lophelia pertusa*, and the live: dead coral ratio.

Transect	Year	Length (m)	Area (m^2)	Depth (m)	Temp. (°C)	*Lophelia pertusa*		
						% Live	% Dead	Live: Dead
VK826								
1	2003	92.33	216.60	461.90	9.44	10.63	34.62	0.31
2	2003	72.30	168.87	No Data	No Data	15.60	29.80	0.52
3	2003	46.57	117.78	453.61	9.47	12.61	37.31	0.34
4	2003	48.78	105.19	454.24	9.53	10.99	31.96	0.34
5	2003	67.87	191.20	452.02	9.61	6.26	8.44	0.74
6	2005	181.00	612.69	470.65	8.30	3.15	9.90	0.32
7	2005	129.81	177.63	484.25	8.23	2.10	11.71	0.18
VK826NE								
1	2005	20.51	69.71	459.60	8.54	31.04	10.64	2.92
2	2005	38.56	158.55	461.69	8.58	22.76	25.94	0.88
3	2005	71.79	200.17	465.68	8.50	12.90	25.27	0.51
4	2005	79.54	196.69	476.83	8.50	0.19	0.51	0.37
5	2005	99.21	138.11	470.03	8.53	12.08	36.62	0.33
6	2005	45.77	133.62	461.50	8.58	17.30	27.29	1.00
7	2005	53.50	178.00	461.18	8.55	45.45	46.85	0.97
8	2005	45.38	199.54	464.37	8.53	10.19	12.04	0.85
9	2005	31.82	59.59	472.64	8.5	0.05	0.13	0.38
GC234								
1	2004	44.13	83.63	502.22	8.01	1.70	60.47	0.03
2	2004	111.97	225.91	501.30	8.15	0.08	21.36	0.00
3	2005	37.84	82.26	507.77	7.70	0.50	13.48	0.04
GC354								
1	2004	68.45	144.07	522.88	7.84	4.48	51.60	0.09
2	2004	10.94	25.87	525.28	7.84	0.00	50.37	0.00
3	2005	47.38	89.34	525.62	8.25	1.24	48.12	0.03

GC = Green Canyon; VK = Viosca Knoll.

Green Canyon 234

Three transects were taken at this site, two in 2004 (44 and 112 m in length), and a third in 2005 (38 m) (**Appendix B.1c**). The total transect area (392 m^2) was considerably smaller than at Viosca Knoll, since *Lophelia* habitat at this site is limited to a single ridge, approximately 150 m in length. Coral colonies can be large and abundant along the ridge, but are predominantly composed of dead coral (**Table 6.1**, **Appendix B.4**). The average coverage of live coral observed along all transects was 0.76% (SE 0.49), which is less than 10% of average live coral cover at the Viosca Knoll sites. All transects were taken at approximately the same depth (500 m); however, there was a temperature difference of ~0.5 °C between transects taken in 2004 and 2005. This is probably due to interannual variation rather than a consistent depth related difference. On the southwestern side of this ridge, there are dense fields of the gorgonian *Callogorgia americana delta*. These gorgonians can be large (>1 m across) and almost invariably have fleshy ophiuroids (*Asteroschema* sp.) attached to the branches, sometimes in large numbers. Scatterings of small to medium sized old tubeworm aggregations also were observed at this site.

Green Canyon 354

In total, 13 transects were taken at this site during 2004 and 2005. Ten of these transects were taken over 90% sediment substrate and were therefore not analyzed for coral distribution. The locations of these transects are included in the transect plot for this site (**Appendix B.1d**), since they illustrate the boundaries of the coral habitat. Three transects were analyzed for coral habitat, one of which (T2) was very short (11 m), and T1 and T3 were 68.45 and 47.38 m respectively, covering a total area of 260 m^2. The coral and no coral transects all fall within a similar depth range, and the average temperature for transects was 7.8 °C in July 2004 and 8.3 °C for September 2005, which is consistent with observations from other sites. The distribution of coral cover at this site was limited and localized. Large intact *L. pertusa* colonies were observed on the carbonate outcrops, sometimes completely obscuring the substrate. The average percentage dead coral cover was 50% of the transect area, which was higher than for the other alpha sites; however, the occurrence of live coral was very low (0% to 5%) (**Table 6.1**, **Appendix B.5**). Large demosponges (Lithistiidae) are common on the exposed carbonate and clumps of tubeworms, and associated communities occur in some areas of this site.

6.3.2 Biological Characterization – Beta Sites

Viosca Knoll 862

The benthic community in this area is very different from any of the other study sites; small *L. pertusa* colonies were observed on the exposed carbonate boulders, but there was no evidence of coalescing colonies and thickets, and none of the standing dead colonies observed at GC354. In 2004, five transects were taken at this site over a depth range of 303 to 320 m (**Appendix B.1e**). This is the shallowest of all the study sites, with the warmest temperatures (~11.5 °C) and highest anthozoan diversity. The numerically dominant benthic organisms at this site were small white anemones (probably belonging to several different species), with average densities of 7 to 24 individuals m^{-2} observed in the transects (**Appendix B.6**), and small localized areas of approximately 100 individuals m^{-2}. The bamboo coral *Keratoisis flexibilis* is a common component of the benthos and grows in dense patches of up to 10 colonies m^{-2}; these are

interspersed with colonies of black coral, which occur as white, orange, or red colonies and can be >1 m height. These have been identified as *Leiopathes* sp., but it is unknown whether the colors represent different species or different color morphs of the same species. Other common benthic fauna include "venus fly trap" anemones, cerianthid anemones, echinoid and cidaroid urchins, hexactinellid sponges, and galatheid crabs. Schools of barrelfish (*Hyperoglyphe perciformes*) also were seen at this site on multiple occasions.

Mississippi Canyon 885

This site is mostly soft sediment interspersed with large holes (burrows or slumps) at depths of 620 to 645 m. The most notable feature is the occurrence of large dense fields of *C. americana delta,* which were documented in various parts of this site during a previous cruise (Brooke, personal observation, 2003, NOAA's Office of Ocean Exploration). These gorgonians were large (>1 m across) and supported communities of the ophiuroid *Asteroschema* sp. Other fauna were also observed in association with the gorgonian colonies at this site; these included small colonies of *L. pertusa*, solitary cup corals, large asteroids, possibly *Coronaster briareus*, and large egg cases, probably from a species of skate. There were also some seep areas observed within this site with small tubeworm colonies, *Beggiatoa* bacterial mats, and shell hash from vesicomyid clams. There were four transects taken at this site in 2005 at depths of 626 to 643 m (7.3 °C), which showed mostly soft sediment, with occasional small groups of *C. americana delta* colonies. The distribution of *C. americana delta* (taken from 2003 NOAA OE cruise) is presented in **Appendix B.1f**, with the coordinates from transects taken in 2005 included to illustrate soft sediment areas.

Green Canyon 184/185

This is a well-studied chemosynthetic site commonly known as "Bush Hill" for the abundant tubeworm colonies. There are large boulders of exposed carbonate at 540 m, which extend as a steep ridge along the southeastern side of the hill. The boulders were colonized with large *C. americana delta* colonies, with the ophiuroid *Asteroschema* sp. attached. There was a small colony of mostly dead *L. pertusa* on the ridge at 544 m, but this was the only evidence of colonization on natural substrate; there were however, several small colonies of *L. pertusa* attached to a tetrahedral metal mooring buoy that had been deployed since 1991. There also were large numbers of tinselfish (*Grammicolepis brachiusculus*) observed amongst the boulders. Video transects were not taken at this site.

The gorgonian and antipatharian samples were sent to Dr. Stephen Cairns (National Museum of Natural History) and Dr. Dennis Opresko (Oakridge National Laboratory) for identification, and are catalogued in **Appendix C**.

6.3.3 Sediment Flux and Zooplankton Availability

Sediment traps were recovered from all of the alpha sites: VK826 high coral (5) and no coral (3), GC234 high coral (3) and no coral (3), and GC354 high coral (3). However, VK862 no coral (3) was the only beta site from which sediment traps were recovered. These data can be used to compare sediment characteristics from within and outside coral stands and across a geographic range, but they do not provide sufficient information to permit comparison between our

designated alpha and beta sites. The single beta site also has a confounding depth factor since it is shallower than the alpha sites. The average sediment load at VK826 was 22.47 g (SE: 2.22) for traps deployed in dense coral and 21.42 g (SE: 2.21) for those deployed on bare substrate. Sediment deposition was similar in the no coral traps at VK862 (21.96 g). The sediment load was lower at the Green Canyon sites; traps recovered from high coral density areas of GC234 contained an average of 9.93 g (SE: 1.44), and those recovered from bare substrate contained 8.84 g (SE: 0.37) of sediment. Three traps were recovered from dense coral habitat at GC354 and contained an average of 6.24 g (SE: 0.4) of sediment. There is therefore a trend of increasing sediment load from the western to the eastern sites. A two-factor analysis of variance (ANOVA) was used to analyze the total dry weight of sediment deposition across regions and at different coral densities. Sediment load at the Viosca Knoll sites was significantly higher than the Green Canyon sites (F: 32.96, p = 0.00), however, there was no difference in sediment load between traps placed close to dense coral, and those deployed on bare substrate (F: 0.84, $p = 0.38$) (**Figure 6.6**).

The average organic content at VK826 was 16.95% (SE: 1.19) for traps deployed in dense coral and 21.85% (SE: 5.60) for those deployed on bare substrate, with slightly lower values for the VK862 no coral traps (16.01%). Sediment from high coral traps at GC234 contained an average of 21.04% (SE: 2.32) organic material. Similarly, sediment recovered from bare substrate traps contained an average of 18.13% (SE: 3.21) organic content. Three traps were recovered from dense coral habitat at GC354 and had an average organic content of 12.75% (SE: 0.52). The organic fraction data had a non-homogeneous variance distribution, even after transformation (arcsin and natural log), therefore a non-parametric test was used in the place of ANOVA. Kruskal-Wallis analysis showed no significant difference between sites (Chi Sq: 6.17, $p = 0.10$) or between traps placed in high coral vs. no coral sites (Chi Sq: 0.74, $p = 0.39$) (**Figure 6.7**). Grain size analysis shows that the dominant size fraction was <20 μm by percentage dry weight (>80%), with very little contribution (<10%) from other fractions (**Figure 6.8**). A two-factor ANOVA showed no significant difference in grain size distribution between sites (F: 0.41, $p = 0.53$) or between traps deployed in high vs. no coral density (F: 0.04, $p = 0.85$).

The zooplankton fraction was divided into four major groups: crustaceans, molluscs, polychaetes, and miscellaneous others. The overall quantity of zooplankton was low at all sites and in both high coral and no coral areas (**Figure 6.9**). The counts of total plankton were averaged over the number of traps at each location. At GC234, 1.33 (SE: 1.52) individuals were found in the no coral traps at GC234, and the high coral traps at this site contained no plankton. At GC354, the average number of individuals was 11.0 (SE: 3.0) from the high coral traps. Traps recovered from the no coral substrate at VK862 contained an average of 5.33 (SE: 0.88) individuals. At VK826, the no coral traps and high coral traps contained an average of 12.67 (SE: 14.84) and 7.8 (SE: 5.81) individuals, respectively. The data showed non-homogeneous variance (Levenes test, $p = 0.00$), therefore a non-parametric Kruskal-Wallis analysis was applied to the data. The test showed a significant difference between the total number of zooplankton between sites (Chi sq: 15.09, $p = 0.00$), with VK826 having the highest values, and GC234 the lowest.

The distribution of different plankton groups between sites (**Figure 6.10A,B**) also was analyzed using Kruskal-Wallis analysis, and no significant difference was found between sites (Chi Sq: 4.59, $p = 0.21$) or from traps deployed in high coral vs. no coral areas (0.18, $p = 0.67$).

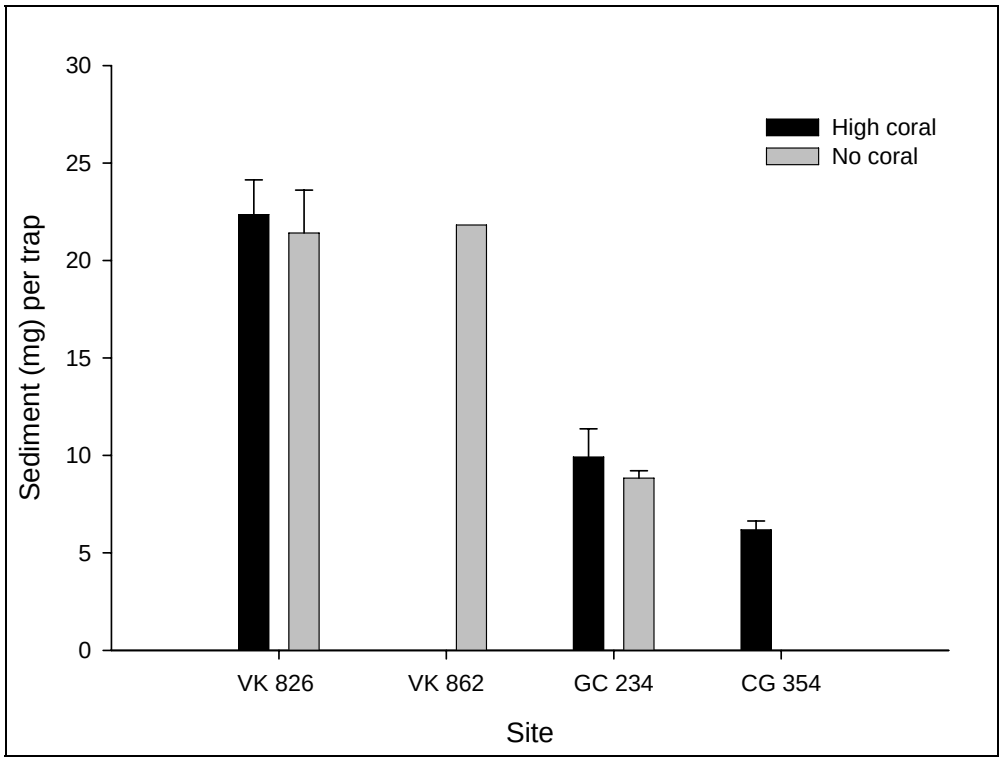

Figure 6.6. Dry weight of sediment (mg) recovered from traps deployed between July 2004 and September 2005. Error bars represent standard error of the mean.

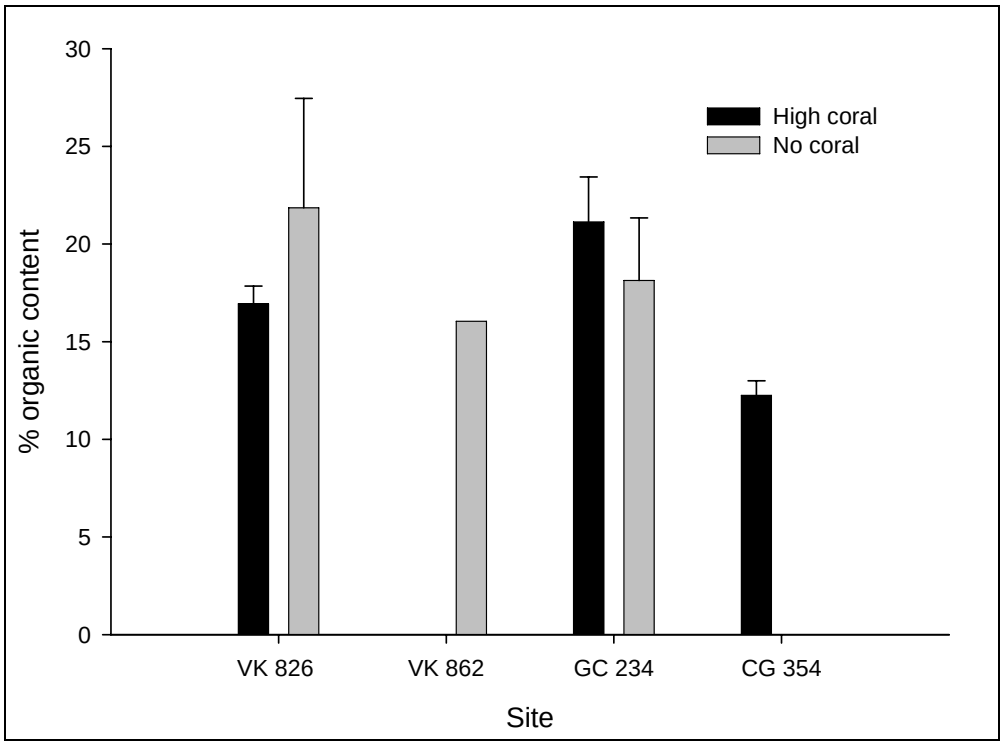

Figure 6.7. Percentage organic content of sediment recovered from traps deployed between July 2004 and September 2005. Error bars represent standard error of the mean.

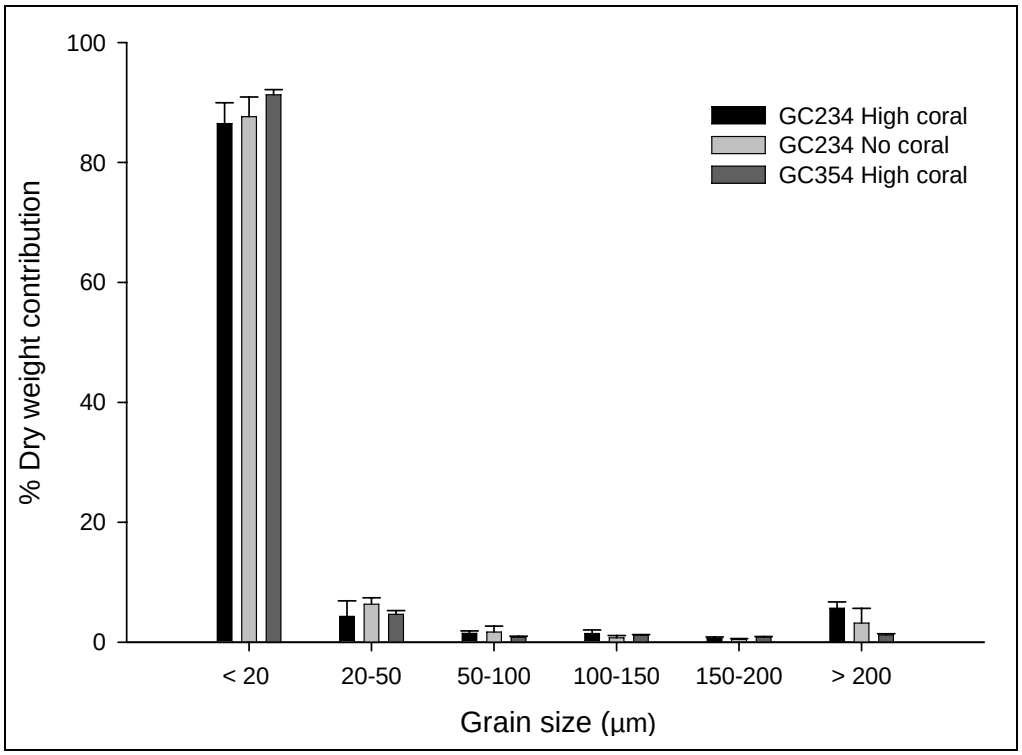

Figure 6.8. Grain size distribution of sediment collected in traps deployed at Green Canyon between July 2004 and September 2005. Error bars represent standard error of the mean.

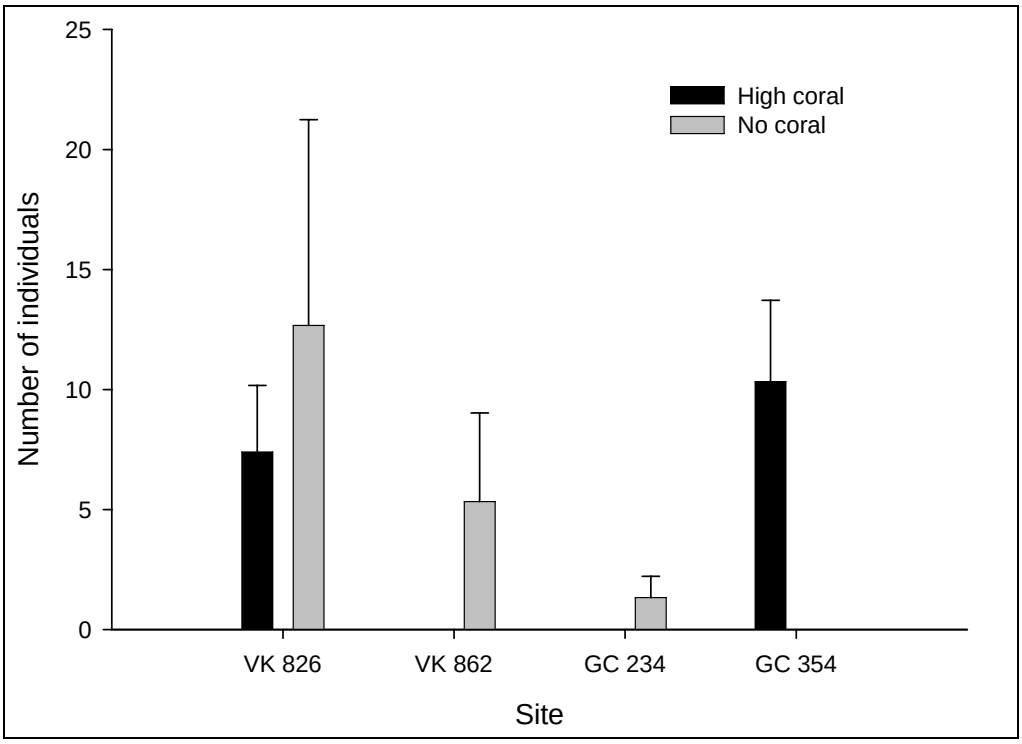

Figure 6.9. Distribution of total zooplankton from sediment traps deployed in areas of high coral and no coral at different sites. Error bars represent standard error of the mean.

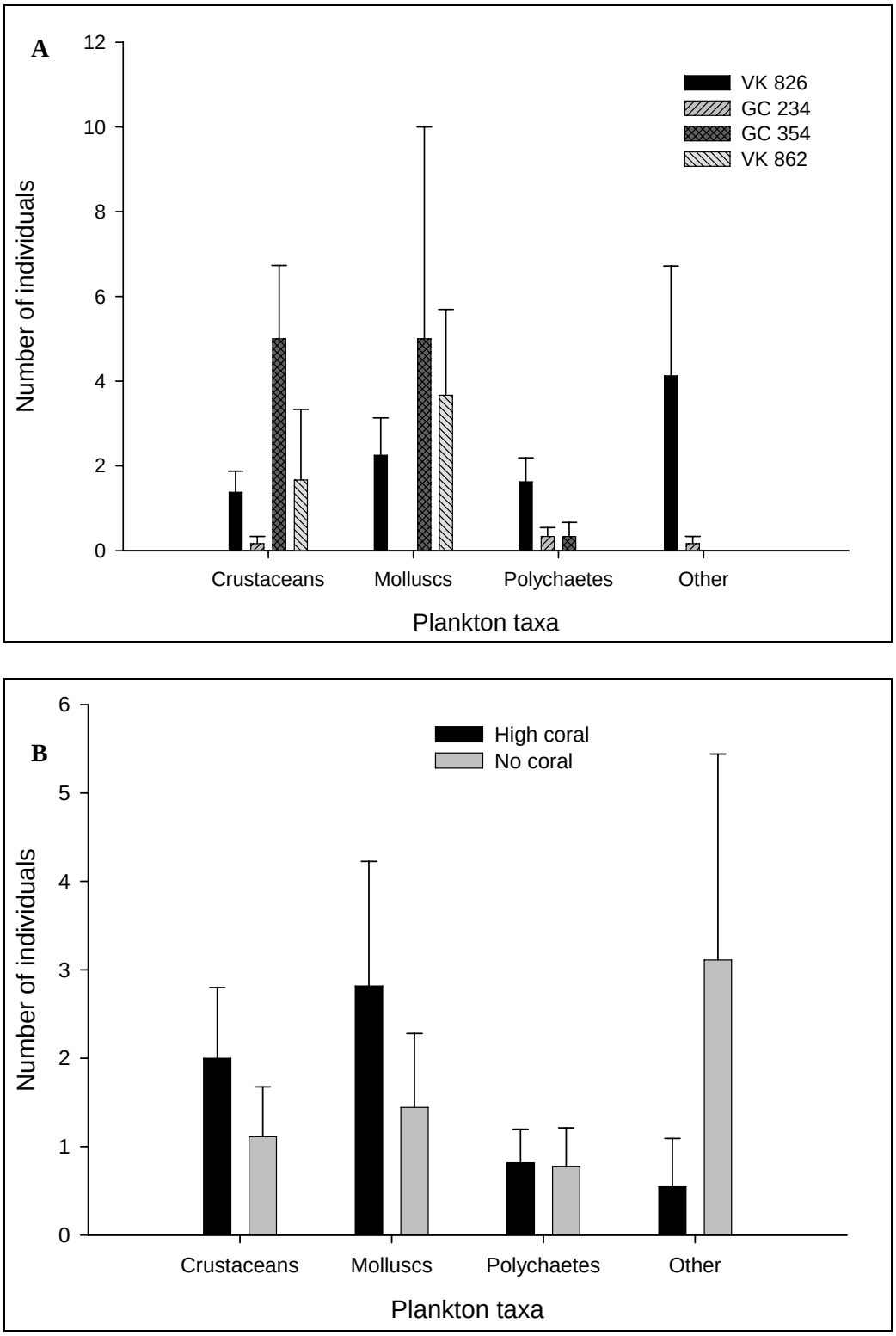

Figure 6.10. Distribution of four main zooplankton groups found in sediment traps A) deployed at the different study sites, and B) deployed at high coral and no coral areas across all sites between July 2004 and September 2005. Error bars represent standard error of the mean.

6.3.4 *Lophelia* Transplantation

All of the transplant blocks deployed in the no coral area (**Appendix D**; Transplants 5 through 8) were recovered, but only three of the four placed within high coral habitat were found (**Appendix D;** Transplants 1 through 3). Each fragment was photographed after recovery and visually compared with the pre-deployment images. There was no significant difference between percentage survival of transplants deployed in dense coral habitat (91.2, SE: 5.05) and those placed on exposed substrate (91.9, SE: 1.33) (**Figure 6.11**) (F: 0.02, $p = 0.97$). The amount of new (linear) growth (visible from the dye line) was measured with calipers for each fragment. In several cases, the polyps with the cable tie had broken off, therefore these data were not used separately, but where growth was visible on the marked polyp, the increment was included in the linear growth data. The total linear growth was 19.55 mm (SE: 4.64) and 10.85 mm (SE: 4.03), and average growth was 4.27 mm (SE: 0.51) and 2.76 mm (SE: 1.07) for the transplants deployed in high coral and no coral, respectively (**Figure 6.12**). These values translate into monthly total growth increments of 1.4 and 0.78 mm, and average growth of 0.28 and 0.2 mm for high and no coral areas, respectively. The data were analyzed using one-way ANOVA, which showed no significant difference between total (F: 2.00, $p = 0.21$) or average (F: 0.71, $p = 0.44$) linear growth. The average number of new polyps per fragment in the high coral area (3.08, SE: 0.85) was similar to the no coral area (3.52, SE: 0.83) (**Figure 6.13**), and a one-way ANOVA showed no significant difference (F: 0.03, $p = 0.86$) between the areas. The stained growth bands from the plastic sections were clearly visible in the smaller polyps, (**Figure 6.14**), and it is apparent that there are two growth centers; one on the outer edge of the calyx, and another on the inner edge near the septae. The average outer growth increment was 278.3 μm (SE: 20.33), and the inner growth was 99.89 μm (SE: 7.13). This translates into monthly lateral increments of 19.88 and 7.14 μm, respectively.

6.3.5 *Lophelia in situ* Staining

One of the stained colonies was recovered but the other was not located. The recovered colony was photographed (**Figure 6.15**) and separated into individual polyps. The stain was not taken up by the entire colony, but an average linear growth of 3.46 mm (SE: 2.86) was calculated from those polyps with a visible stain line, which translates to an annual growth increment of approximately 2.97 mm. This falls within the observed average growth range for the coral transplants.

6.4 RESULTS – LABORATORY STUDIES

6.4.1 *Lophelia* Morphology and Skeletal Density

The bulk density and micro-density of the skeleton were calculated for both morphotypes (**Figure 6.16**). The heavily calcified "*brachycephala*" morphotype had an average bulk density of 1.98 g/cm^3 (SE: 0.06), microdensity of 2.35 g/cm^3, and porosity of 15.53 (SE: 1.99). For the more fragile "*gracilis*" morphotype, the average bulk density, micro-density, and porosity values were 1.49 g/cm^3 (SE: 0.04), 2.22 g/cm^3 (SE: 0.04), and 23.87 (SE: 2.11), respectively. ANOVA showed significantly higher micro-density (F: 6.1, $p = 0.02$), and bulk density (F: 49.76, $p = 0.00$) values for the heavy "*brachycephala*" form than the fragile "*gracilis*" fragments. There was also a significant difference in the porosity values (F: 35.68, $p = 0.00$), but the trend was reversed (**Figure 6.17**). The cross-section of the "*brachycephala*" morphology shows a much denser skeleton with closer growth bands (**Figure 6.18A**) than in the "*gracilis*" section (**Figure 6.18B**).

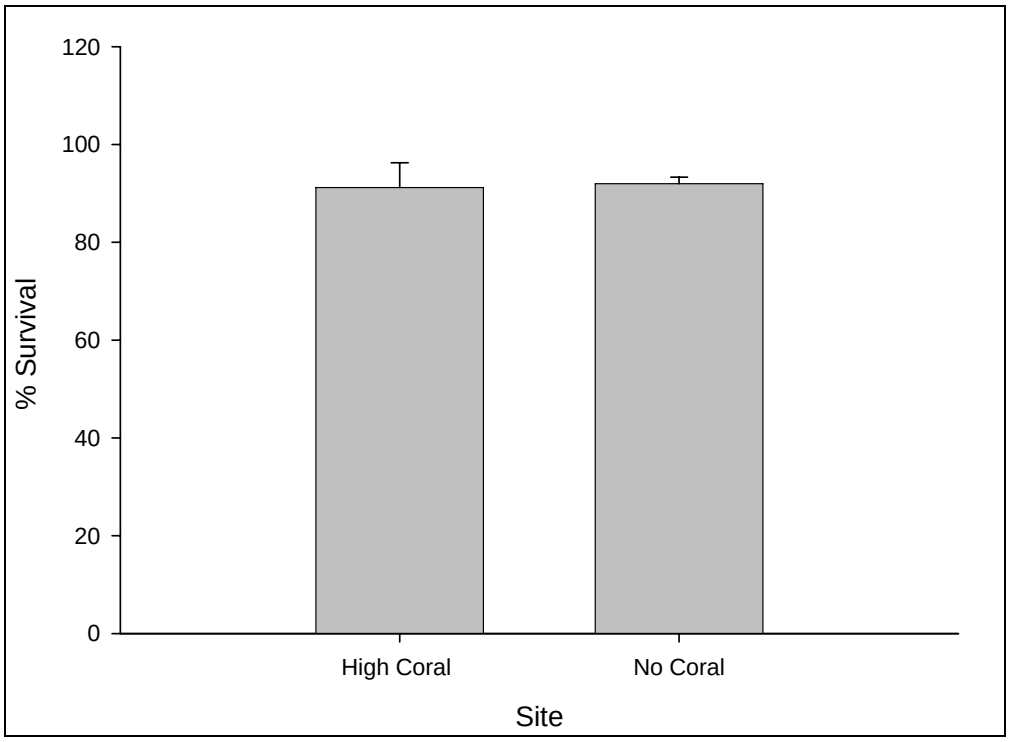

Figure 6.11. Mean survival of transplants in high coral and no coral sites. Error bars represent standard error of the mean (n = 3 for high coral site; n = 4 for no coral site).

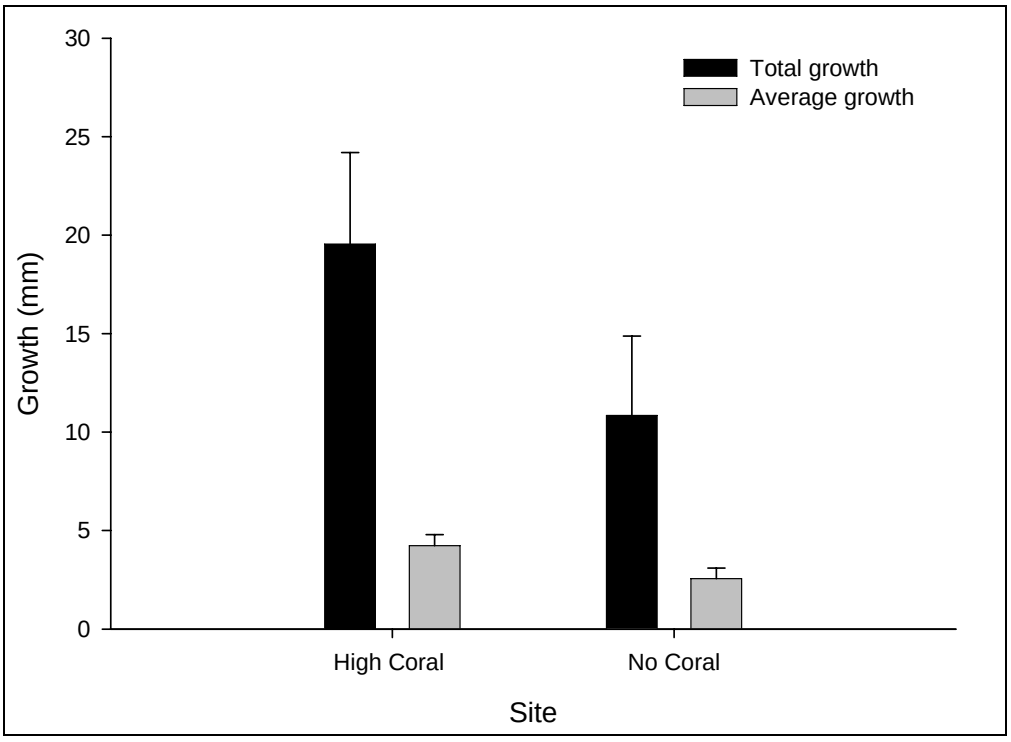

Figure 6.12. Total and average linear growth in transplants deployed in high coral and no coral sites between July 2004 and September 2005. Error bars represent standard error of the mean (n = 3 for high coral site; n = 4 for no coral site).

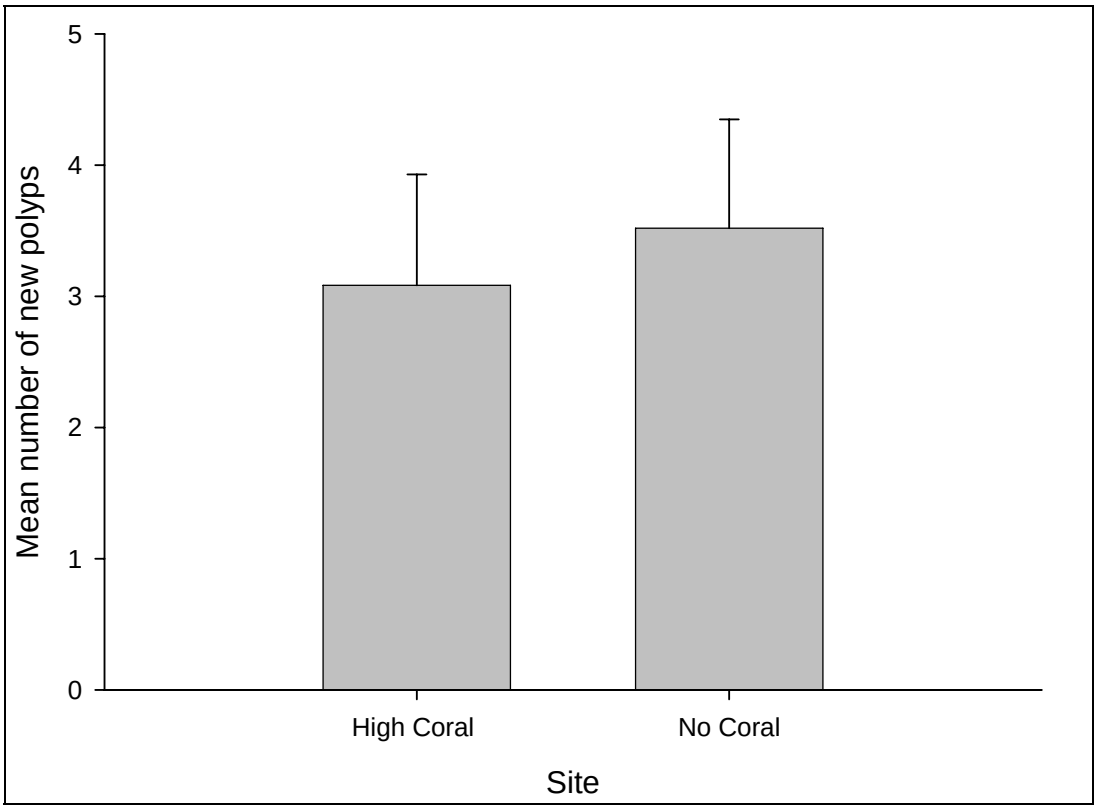

Figure 6.13. Mean number of new polyps found in transplants in high coral and no coral sites. Error bars represent standard error of the mean (n = 3 for high coral site; n = 4 for no coral site).

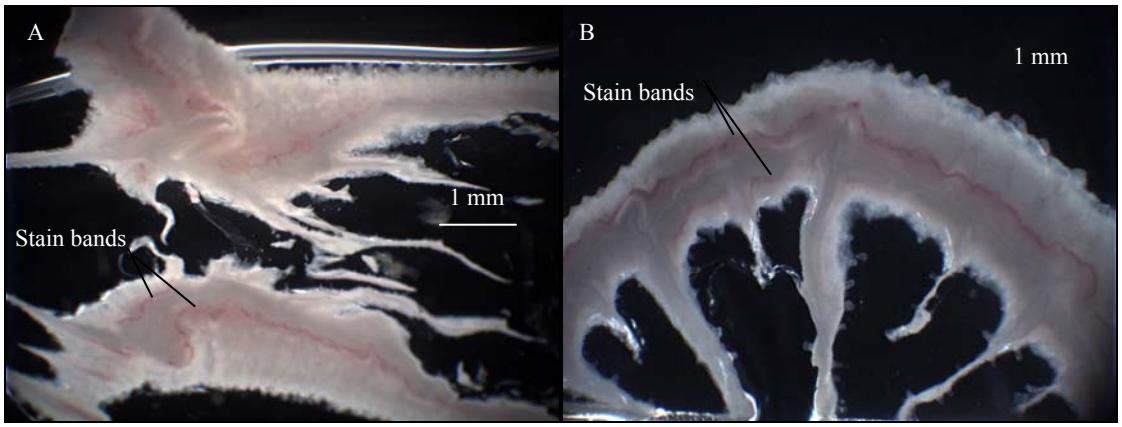

Figure 6.14. A) Lengthwise and B) transverse sections of stained transplant fragments showing two growth centers (stain bands) for each section.

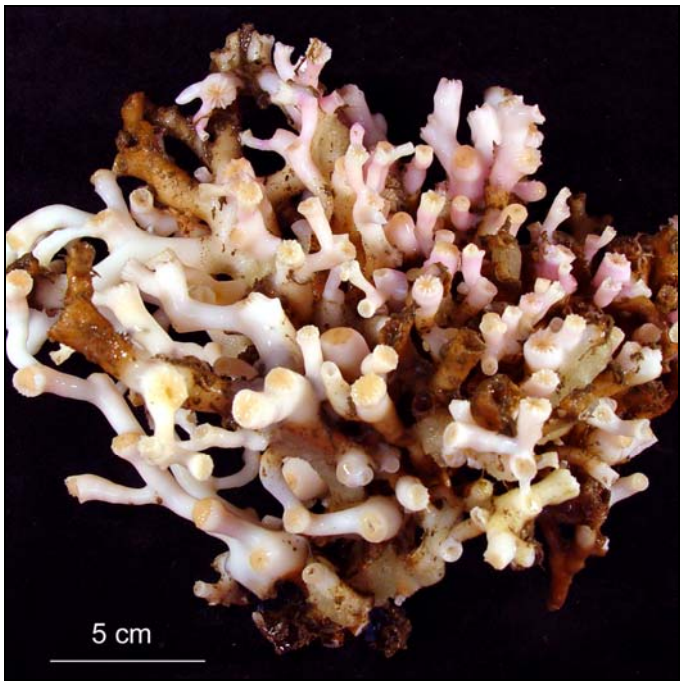

Figure 6.15. Small colony of *L. pertusa* that was stained *in situ* during the cruise in July 2004 and recovered in September 2005. The stain is visible in the top right section, but was not taken up throughout the colony.

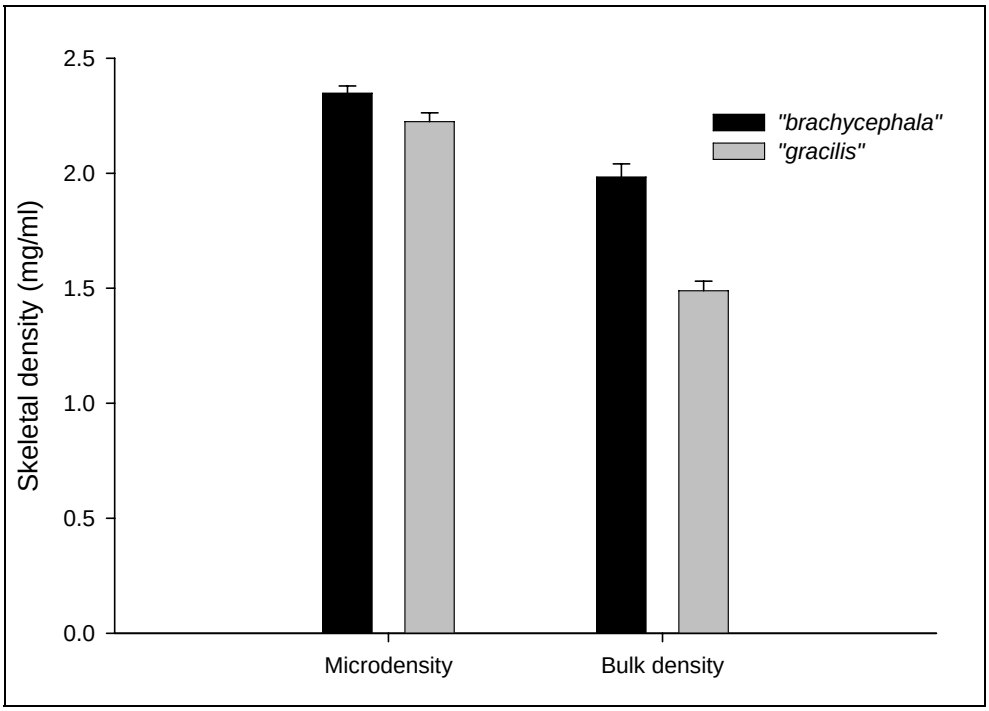

Figure 6.16. Skeletal density characteristics of different morphotypes of *L. pertusa*. Micro-density represents the aragonite skeleton; bulk density is total skeletal density, including the pore spaces in the matrix. Bars represent averages of replicate fragments (n = 10) of each morphotype.

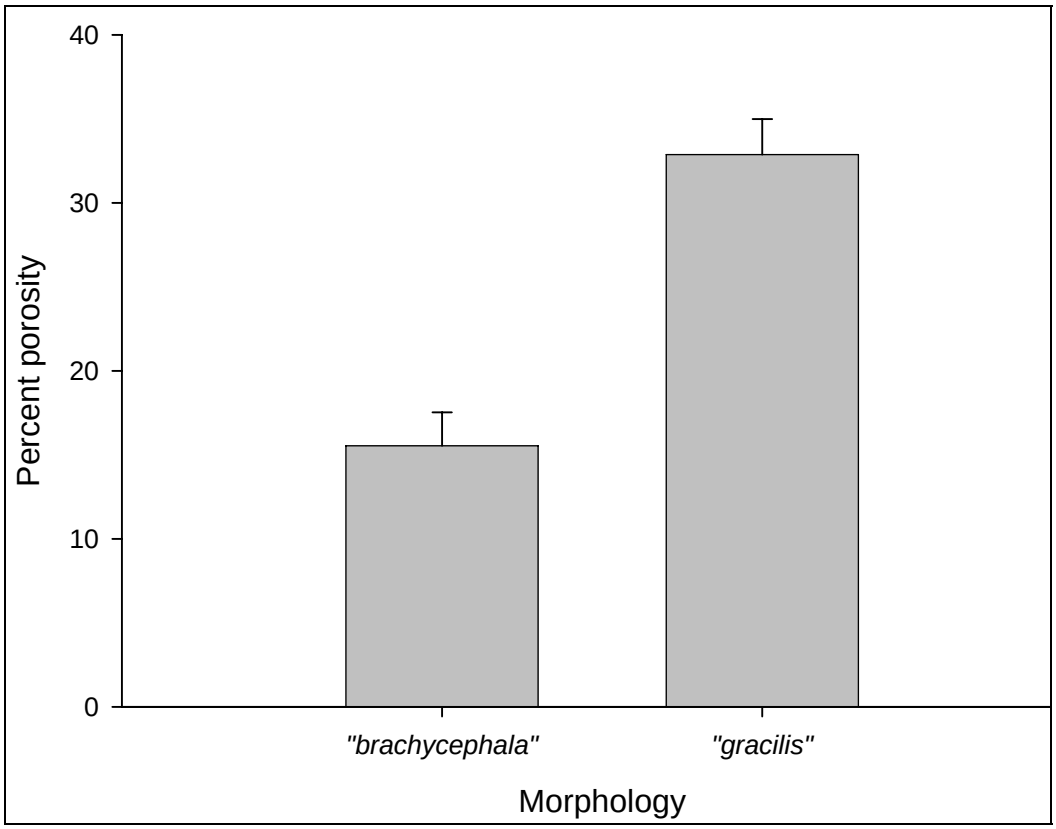

Figure 6.17. Porosity values for different morphotypes of *L. pertusa*. Bars represent averages of replicate fragments (n = 10) of each morphotype.

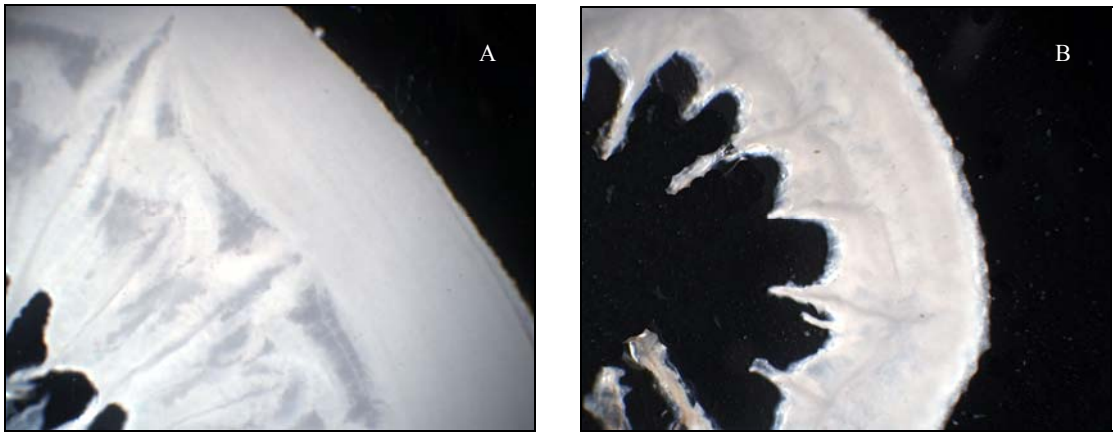

Figure 6.18. Resin embedded sections (2 mm) of A) "*brachycephala*" and B) "*gracilis*" morphotypes showing the higher number and more closely spaced bands in the "*brachycephala*" morphotype.

6.4.2 *Lophelia* Reproduction

Samples for analysis of reproduction were collected during the cruises in July 2004 and September 2005, and additional samples were supplied from other cruises in November 2002 and October 2003. The July and September collections included three and six female colonies, respectively. A single female was identified from the November samples but colonies collected in October had no reproductive material, therefore gender could not be determined. Females collected in July contained vitellogenic oocytes with an average diameter of 73.4 µm (SE: 1.22), which increased to 88.1 µm in September as the eggs matured, then decreased substantially in November. These data, together with the absence of reproductive material in the October samples, indicates that the gametogenic cycle of *L. pertusa* begins in the spring, with vitellogenesis commencing through the summer and mature oocytes observed in September (**Figure 6.19**). The size frequency distributions for July and September (**Figure 6.20**) show a wide spread, but with a definite single peak in the distribution, which indicates that spawning is probably not synchronous but occurs over a seasonal time period.

6.4.3 Temperature Tolerance of *Lophelia* Coral

After 24 h, the numbers of live and dead polyps were counted on each fragment and percentage survival calculated. All of the fragments in the 5 °C, 8 °C (ambient), 10 °C, and 15 °C treatments were alive and healthy (polyps extended and retracted rapidly on contact), but at 20 °C, survival was reduced to 68.3% (SE: 13.07). At the highest temperature (25 °C), there was complete mortality after 24 h and this treatment was terminated. After 7 days, the survival was reassessed and as previously, the 5 °C, 8 °C, and 10 °C treatments showed no mortality; however, survival in the 15 °C treatment was reduced to 81.2% (SE: 7.9), and the polyps responded slowly to tactile stimulation. In the 20 °C treatment, survival was 32.9% (SE: 20.8) after 7 days (**Figure 6.21**).

6.4.4 Sediment Tolerance of *Lophelia* Coral

The average experimental sediment concentrations were 362 mg/L (SE: 3.67), 245 mg/L (SE: 5.96), 103 mg/L (SE: 1.94), 54 mg/L (SE: 0.77), and 0 mg/L (SE: 0.76). The standard errors in parentheses represent variation between three replicate trials. Survival of *Lophelia* fragments (both morphotypes) was scored after 14 days of exposure to the different treatments. There was 100% survival in the control treatment for both morphotypes, with decreasing survival (as the treatment sediment level increased) to an average of 6.67% (SE: 6.67) survival for the heavily calcified "*brachycephala*" growth form, and complete mortality of the fragile "*gracilis*" morphotype (**Figure 6.22**). The data from replicate trials were arcsin transformed to remove heteroscedastic variance, and a two-factor ANOVA was applied to determine effects of sediment concentration and morphotype on the survival of the experimental fragments. The different morphotypes showed no significant difference in their response to sediment exposure (F: 0.12, $p = 0.73$), nor was there significant interaction between treatment and morphotype (F: 0.24, $p = 0.91$). There was however a significant difference in survival between the different treatments (F: 48.03, $p = 0.00$). A Tukey's Honestly Significant Difference (HSD) test showed no significant differences between effects of the two highest concentrations (T1, T2) and the two intermediate concentrations (T3, T4), with differences between each group and the control (T5).

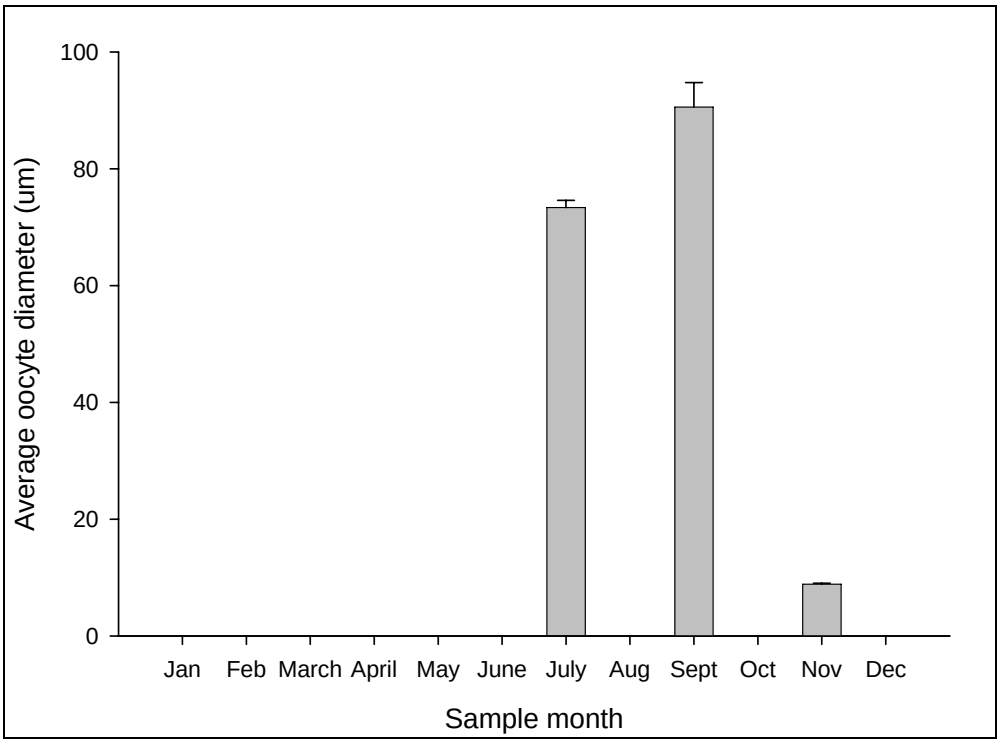

Figure 6.19. Seasonal changes in *L. pertusa* oocyte diameter, indicating that spawning occurs in late September or October. Error bars represent standard error of the mean number of samples.

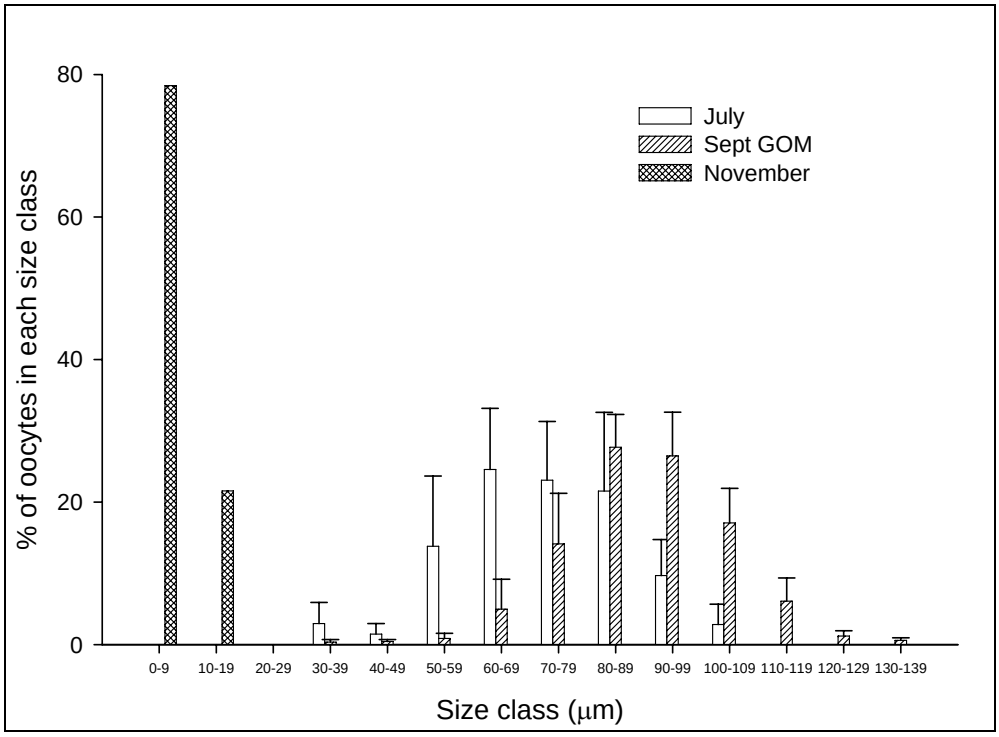

Figure 6.20. Oocyte size frequency distribution showing percentage size distribution of oocytes from different months. Error bars represent standard error of the mean number of samples.

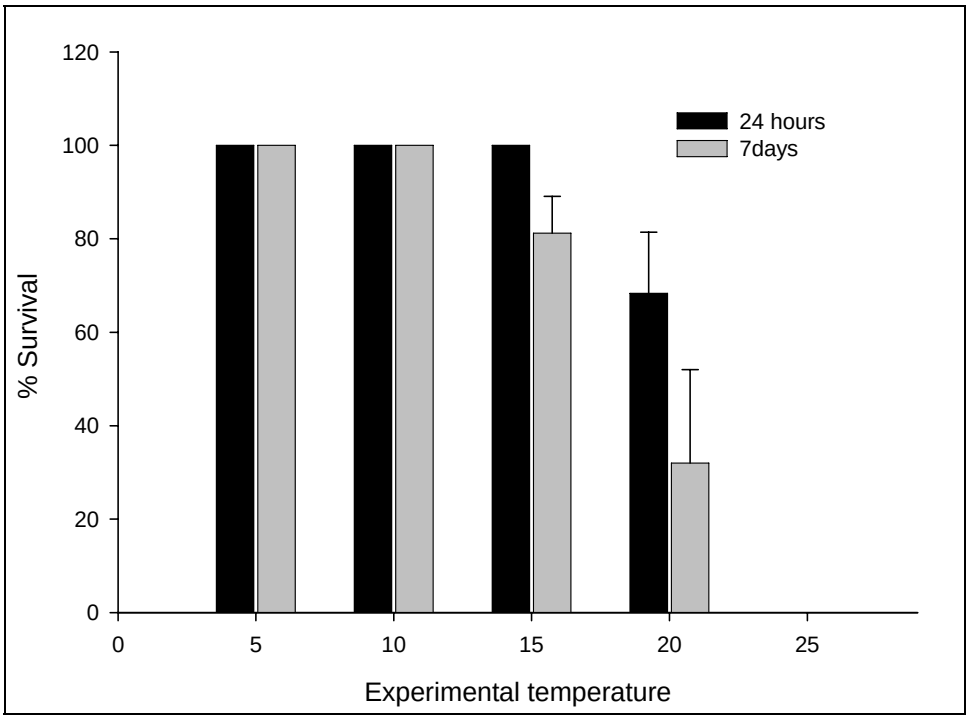

Figure 6.21. Percent survival of *L. pertusa* exposed to different experimental temperatures for 24 hours and 7 days (n = 20 polyps per replicate, with 5 replicate tanks per treatment).

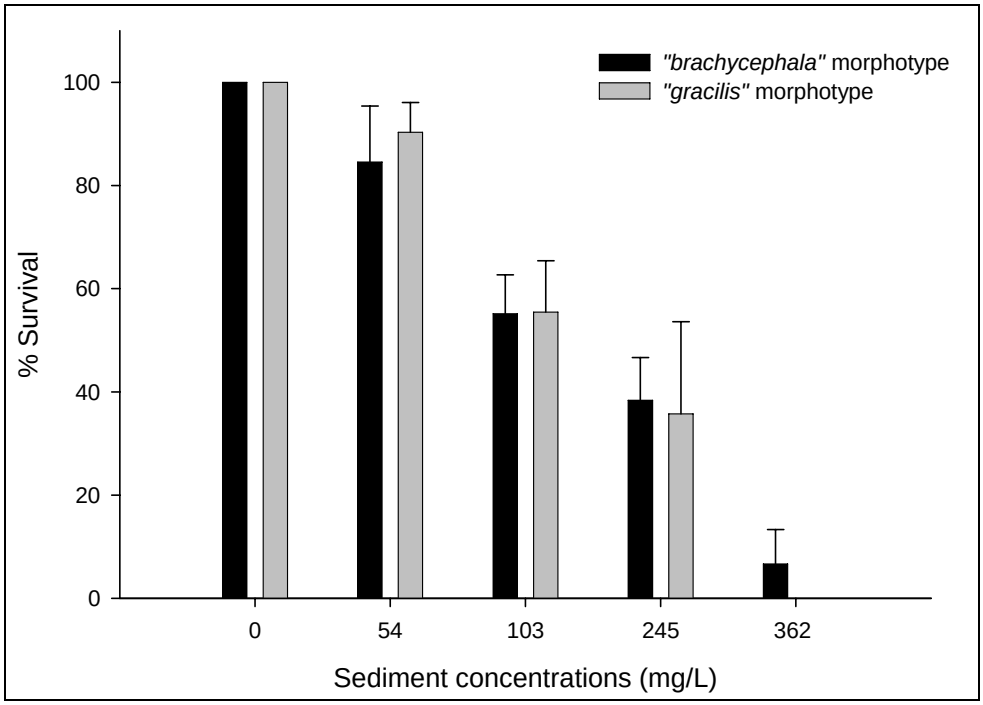

Figure 6.22. Mean percentage survival of two morphotypes of *L. pertusa* after exposure to a range of sediment suspensions for 14 days. Error bars represent standard error of three replicate trials.

Results from the burial experiment show almost complete survival for fragments of both morphotypes after 24 h, dropping to an average of 89.47% (SE: 9.53) after 2 days for the heavily calcified growth form and 73.33% (SE: 15.27) for the fragile morphotype. After 4 days, almost all the polyps had died, and mortality was complete after 7 days (**Figure 6.23**). The survival data showed non-homoscedastic variance (Levenes test: $p = 0.00$), even after arcsin transformation. A non-parametric Kruskall-Wallace test showed no significant difference between the responses of the different morphotypes (Chi-Sq: 0.24, $p = 0.62$), however there was a significant treatment effect (Chi-Sq: 19.98, $p = 0.00$). The greatest differences occurred between the effects of 1 and 2 days of burial versus 4 and 7 days.

6.4.5 Feeding Experiments for *Lophelia* Coral

Results of this experiment indicate that lipid content increases in response to increased food supply (**Figure 6.24**). Those polyps fed the highest ration contained an average of 25.2% (SE: 1.65) lipid over two trials, whereas the starved fragments contained only 13.1% (SE: 0.58). A field sample collected in September 2003 from VK826 was analyzed at the same time as the experimental fragments and had a lipid content of 21.5%, which fell between the values obtained for experimental corals fed every 2 days and every 4 days. Regression analysis shows a significant relationship between food ration and lipid content (r^2: 0.96, F = 73.03, $p = 0.00$). Calories consumed were calculated for each treatment using 9.24×10^{-4} calories per nauplius (Paffenhofer 1967). The total calories consumed by each treatment during the course of the experiment were translated into daily consumption rates. A regression of lipid content on caloric consumption produced the relationship: % lipid = 0.80 x daily caloric consumption + 14.187. When the lipid content of the field sample was entered into this equation, the caloric consumption was calculated to be 9.1 calories/day.

6.5 DISCUSSION – FIELD STUDIES

6.5.1 Biological Characterization

VK826 is the only known region of the Gulf of Mexico that supports well developed and extensive *L. pertusa* habitat. Some thicket development was observed at the Green Canyon sites, but despite initial colonization and growth, the colonies did not expand to form the type of habitat seen at VK826, and a large percentage of the coral colonies were dead. The Viosca Knoll *Lophelia* is also unique in that most of the colonies are composed of the heavily calcified "*brachycephala*" growth form, and in some cases calcification around the calyx is so extensive that it has obscured the septal ridges. The cnidarian diversity at VK826 is quite low with few antipatharians and gorgonians, which were present at other sites, sometimes in large numbers. There was some evidence of seepage at VK826, but this was localized and was identified by small colonies of tubeworms, some *Beggiatoa* mats, and areas of vesicomyid and lucinid shell hash. These areas generally had less coral cover than those without seep fauna. The Green Canyon alpha sites have well developed seep communities and less *Lophelia* than VK826. They do however support dense populations of *Callogorgia americana delta* (Primnoidae), a large branching octocoral with abundant associated communities of ophiuroids, asteroids, and occasionally *Lophelia* colonies. These gorgonians are orientated perpendicular to the prevailing current to take advantage of food passing by in the water column. There is no information on the age, growth, and reproduction of this species, but deepwater gorgonians can be extremely long-lived and slow growing, and as vulnerable to disturbance as *Lophelia* colonies.

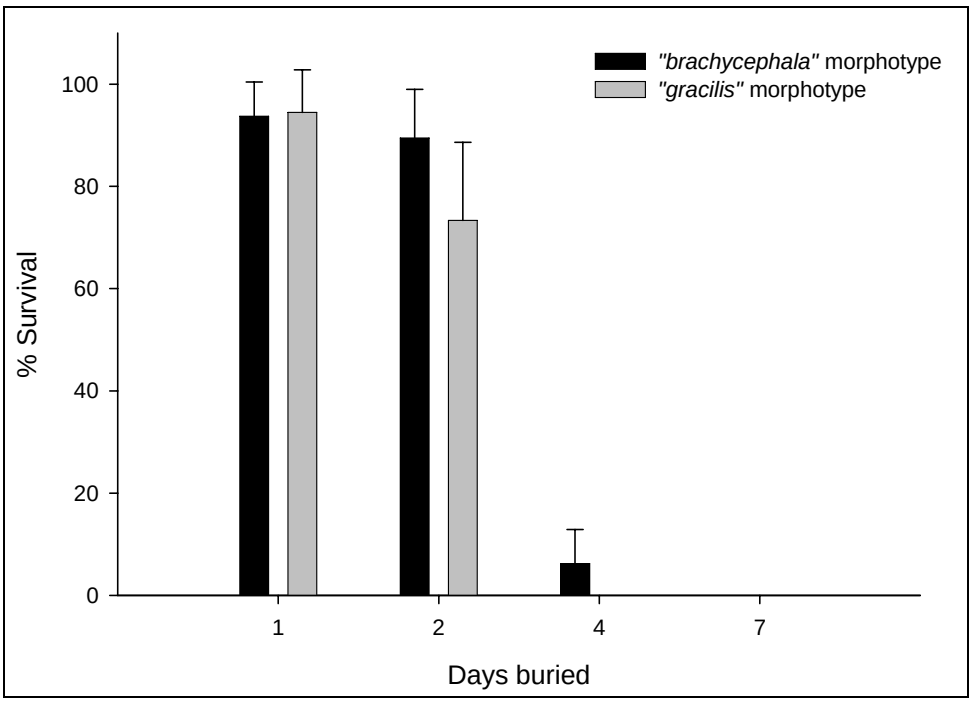

Figure 6.23. Mean percentage survival of two morphotypes of *L. pertusa* after burial for different periods of time in Gulf of Mexico sediment. Error bars represent standard error of three replicate fragments.

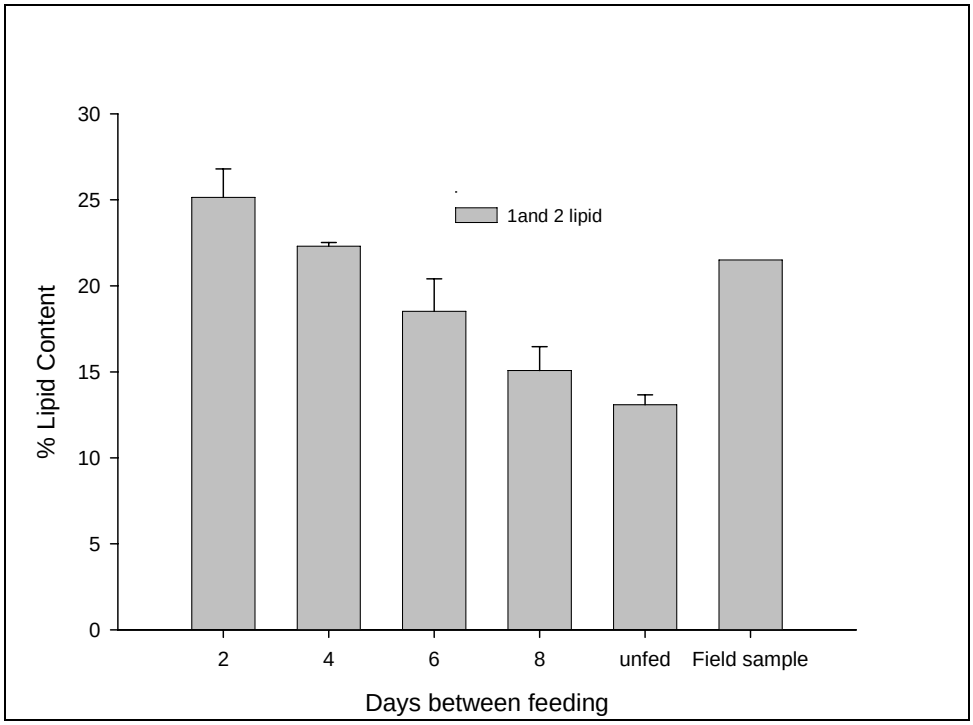

Figure 6.24. Percentage lipid content of *L. pertusa* fragments fed five different food rations over a 1-month period. Error bars represent standard error of two trials. A field sample collected from VK826 in September 2005 was also included.

VK862 is much shallower and warmer than the other study sites and supports a very different fauna from the other beta sites. There was very little *L. pertusa* present, but the highest cnidarian diversity and abundance was observed here. The substrate was covered with dense patches of small white anemones, and large colonies of antipatharians and bamboo coral provided structure for other animals. These antipatharian and gorgonian species may also be slow growing, long-lived, and vulnerable to human impact, but very little is currently known about their biology or ecology. Some of the large carbonate boulders support *Lophelia* colonies, however these are isolated and do not form coalescing thickets. Large schools of barrel fish were often seen here; but there is currently no fishery for this species in the Gulf of Mexico. There also was no indication of active seepage at VK862, and dense mono-specific stands of *C. americana delta* also were absent. The other beta sites however had both seepage communities and extensive *C. americana delta* communities. Past discussions have suggested a positive correlation may exist between *L. pertusa* and seep environments; however, in the Gulf of Mexico it appears that *L. pertusa* does not thrive in active seep areas and does not develop extensive habitat where seepage is still occurring. Once the seeps have expired or diminished, however, the carbonate remains to provide substrate for corals and other species with low tolerance for seep chemicals. Seepage may limit the development of diverse cnidarian communities, but the production of authigenic carbonate provides abundant substrate for those species that can tolerate the seep environment, such as *C. americana delta.*

6.5.2 Sediment Flux and Zooplankton Availability

The sediment trap data showed a regional difference in sediment load between Viosca Knoll and Green Canyon. These data were integrated over the deployment period (14 months), therefore seasonal deposition information is not available. Viosca Knoll is located approximately 120 miles southeast from the mouth of the Mississippi River, which releases a large amount of sediment into the Gulf of Mexico. During the deployment time period, Hurricanes Katrina, Ivan, and Rita made landfall in the Gulf of Mexico, potentially increasing outflow from the Mississippi River. The sediment load data could represent a real and consistent difference between the sites, but it could also have been due to localized increases in sediment caused by the hurricanes. There was no difference between the sediment loads in traps close to high-density coral versus those outside coral areas. Therefore, the coral distribution is neither controlled by sediment load nor mediating sediment deposition. The quantity of sediment varied between regions, but grain size distribution and organic content was similar across the entire study region. The Viosca Knoll sites are potentially under the influence of the outflow from the Mississippi River, however the nature of the sediment was the same for this area as for Green Canyon, which is far beyond the influence of the river. The sediment is primarily composed of fine particles (<20 μm), which would be resuspended at lower current speeds than heavy sandy particulates.

6.5.3 *Lophelia* Transplantation

Transplant survival was high in both dense coral and no coral locations, and amount of new growth and number of new polyps showed no significant difference between sites. This experiment was designed to test the hypothesis that coral distribution on VK826 is driven by habitat suitability and that the bare substrate areas are not good habitat for adult *Lophelia*. This experiment shows however that adult corals can survive and grow equally well in both habitat types, therefore some other factor must be responsible for the absence of corals in habitat that

appears suitable for colonization. The growth observed in these experimental fragments was extremely variable, as was the degree to which each fragment incorporated the Alizarin stain. The terminal polyps that were marked with a cable tie were missing from many of the recovered fragments, but it is unclear whether this is an artifact of handling or whether the terminal polyps are frequently broken off *in situ*. The stain bands on the coral sections illustrated the double growth center, which introduces an additional level of complexity when assessing growth through lateral banding patterns; six visible bands may be interpreted as 6 years of growth, when it represents only 3 years of growth. It also is apparent from the stain bands that lateral skeletal deposition is not equal, but the causes of this variability are unknown. Linear extension is a more reliable growth rate estimate than lateral banding, but given the highly variable growth between fragments (i.e., growth of existing polyps and production of new polyps), extrapolation from branch growth to whole colony expansion should be performed with caution.

6.5.4 *Lophelia in situ* Staining

The *in situ* staining technique was successful in that the small colony that was recovered (the other stained colony could not be located) had incorporated the stain into the skeleton; however although the linear extension was similar, the type of growth exhibited by the small colony was markedly different from the growth of the transplants, which produced many more new polyps than the stained colony, and had larger and apparently healthier polyps. This is another example of the high degree of variability in the growth of these coral colonies.

6.6 DISCUSSION – LABORATORY STUDIES

6.6.1 *Lophelia* Morphology and Skeletal Density

Superficial observations reveal a denser, more tightly packed skeletal structure in the heavily calcified growth form, and since bulk density and porosity are inversely related, differences between the morphotypes were expected for these characteristics. In shallow water corals, the bulk density has been found to vary with latitude, depth, temperature, and different growth forms (Schneider and Smith 1982; van Veghel and Bosscher 1995). Several studies have highlighted the effect that high porosity (i.e., reduced bulk density) would have on the corals and hence their tolerance to physical damage (Chamberlain 1978; Jimenez and Cortes 1993). Increased bulk density in the "*brachycephala*" morphotype may be a response to an environment with high physical stress. The micro-density was also significantly different for the two morphotypes. Published estimates of the density of pure aragonite vary from 2.92 to 2.94 g/cm^2 (Kinsman and Holland 1969; Hughes 1987), and measured micro-densities for shallow corals range from 2.62 g/cm^2 for *Acropora humilis* to 2.82 g/cm^2 for *Porites porites* (Bucher et al. 1998). The micro-densities measured for *Lophelia* were lower than either of the shallow water values. This difference may represent an organic component to the skeletal matrix or may be caused by differences in the crystal lattice between the coral skeleton and pure aragonite. All of these skeletal characteristics may be affected by environmental factors such as nutrient availability, current speed, and pH. The differences observed between the morphotypes may be indicators of a fundamental environmental difference between Viosca Knoll and the more westerly sites where the fragile "*gracilis*" growth form is found. The causes of the different skeletal characteristics are unknown but warrant further investigation.

6.6.2 *Lophelia* Reproduction

The full gametogenic cycle cannot be described without a full set of seasonal samples; however, the available data shows that *L. pertusa* spawns in late September or October in the Gulf of Mexico. Primary oocytes were observed in November, which indicates concurrent gametogenesis, with little or no break between cycles. This has also been observed in *L. pertusa* from the Norwegian fjords, but the gametogenic cycle is offset from the Gulf of Mexico populations by several months (Brooke and Jarnegren, unpublished). Investigation into environmental differences between the Gulf of Mexico and fjord habitats (e.g., food supply, temperature cycles, current speeds) will provide insight into the factors driving gametogenesis in this species. The size frequency distributions for oocyte diameter show that egg development is not highly synchronized in these corals as with many shallow water species. This asynchronous but seasonal reproduction was also observed in *L. pertusa* from Norwegian fjords and deepwater populations of *Oculina varicosa* (Brooke and Young 2003).

6.6.3 Temperature Tolerance of *Lophelia* Coral

The temperature tolerance experiments show that *L. pertusa* can survive for short periods of time (up to 24 h) at 15 °C, but mortality occurs if the corals remain at this temperature for a week. From these experiments, it appears that the upper thermal threshold for long-term survival lies between 10 °C and 15 °C, but there was no mortality observed at the lowest experimental temperature of 5 °C. An upper temperature threshold of 12 °C has been suggested for *L. pertusa* from other geographic locations (Freiwald et al. 1997; Rogers 1999), and this seems to hold true for the Gulf of Mexico populations, implying a physiological constraint on distribution. The temperatures recorded during the VK862 transects fluctuated around 11.5 °C, which is close to the temperature threshold. Sublethal stress effects can occur when organisms are living close to their environmental limits, so VK862 could provide an interesting site for further investigations into this aspect of *Lophelia* biology.

6.6.4 Sediment Tolerance of *Lophelia* Coral

Standing dead coral colonies are a characteristic feature of many *Lophelia* habitats. The reasons for the coral mortality and the age of the dead coral are unknown. Suggested causes include temperature fluctuations, disease or parasites, and sediment load or burial. In the Gulf of Mexico, temperatures fluctuate over time, but in all but VK862, they most likely remain below the mortality threshold temperature. There are currently no known pathogens of deepwater corals, but since most deepwater scleractinian reefs are composed of a single keystone species, a disease outbreak could cause widespread mortality. Similarly, a benthic storm or slumping event could smother large areas of coral, leaving standing dead colonies. The sediment load experiment showed survival of >50% after 2 weeks of exposure to ~100 mg/L of Gulf of Mexico sediment, or after complete burial for 2 days; however, although *Lophelia* can tolerate fairly severe sediment conditions, mortality increases rapidly with longer burial or higher sediment loads. Information on duration and severity of sediment events in the Gulf of Mexico are required to put these results in context.

6.6.5 Feeding Experiments for *Lophelia* Coral

The feeding experiment data are preliminary and serve to demonstrate appropriate techniques for calculation of *Lophelia* energy consumption in the field. Lipid content appears to be a reliable estimator of different energetic regimes, and calories per treatment can be calculated with reasonable accuracy if sufficient care is taken to count food consumption during the experiment. This experiment indicates that corals in the field might be energy limited, since fragments show higher lipid content in laboratory experiments than in the field; however, this study should be expanded to include replicate samples from different seasons and different locations before drawing firm conclusions. Seasonal fluctuations in lipid content are possible, particularly for female colonies since *Lophelia* eggs contain lipid. This phenomenon was observed in *Oculina varicosa*, an ahermatypic coral that inhabits both deep (100 m) and shallow (6 m) ledges off the east coast of Florida (Brooke 2002). This experiment used a food source that is not available *in situ* to *Lophelia*, and although crustacean larvae were one of the primary constituents of the zooplankton in the sediment traps, a more extensive study should include deepwater plankton tows, preferably seasonally, to estimate food supply in the field.

Chapter 7
Synthesis

Neal W. Phillips
with contributions from
Project Team Investigators

7.1 SITE SUMMARY

Ten sites on the northern Gulf of Mexico continental slope were visited during the study (**Table 7.1**). Three alpha sites were designated for intensive study and three beta sites were selected for more limited characterization (one additional beta site, MC709, is listed in the table but not discussed because only soft bottom substrata were seen). A grant from the NOAA-OE program allowed three additional sites to be visited.

Table 7.1. Study sites. Within categories, sites are ordered by water depth.

Study Site	Water Depth (m)	Ratio of Live:Dead Coral (Phototransects)	% Live Coral (Bushmaster)	Notes
Alpha Sites				
VK826	472	0.18-0.74	5.3-50.0	The most highly developed coral site visited, with abundant thickets of living *L. pertusa* and scattered tubeworm aggregations.
GC234	501	0.00-0.04	0-6.4	Limited *L. pertusa* development, mostly dead framework in colonies. Populations of *Callogorgia americana delta* and highly developed seep communities in the area.
GC354	525	0.00-0.09	0-9.6	Similar to GC234 with respect to *L. pertusa* colonies, but more extensive octocoral communities and more limited seep communities.
Beta Sites				
VK862	310	--	80	Very different from other sites; high cnidarian diversity, cover dominated by white anemones; some *L. pertusa*.
GC184/185	528	--	--	Small colony of mostly dead *L. pertusa*. Locally abundant seep fauna and *C. americana delta*.
MC885	634	--	--	Mostly soft bottom, a few *Madrepora oculata* colonies and occasional dense colonies of *C. americana delta*.
MC709	686	--	--	Only soft bottom was seen during the dive.
NOAA-OE Sites				
VK862S	335	--	--	Fauna similar to main VK862 site.
VK826NE	457	0.33-2.92	6.7-14.7	Fauna similar to main VK826 site.
MC929	650	--	--	Interspersed patches of seep fauna, *C. americana delta*, and small *L. pertusa* colonies.

GC = Green Canyon; MC = Mississippi Canyon; VK = Viosca Knoll; NOAA-OE = National Oceanic and Atmospheric Administration, Office of Ocean Exploration.

Lophelia community development at the study sites can be summarized as follows:

- VK826, an alpha site, supported the most-developed and extensive *L. pertusa* colonies. *L. pertusa* aggregations provided the dominant biogenic habitat for other fauna at this site. VK826 also was unique in that most of the colonies sampled were composed of the heavily calcified ("*brachycephala*") growth form. Cnidarian diversity at VK826 was quite low, although some large antipatharian and gorgonian colonies were interspersed with the *L. pertusa*. There was some evidence of seepage at VK826, but it was localized and identified by scattered white *Beggiatoa* mats, symbioses such as aggregations of tubeworms, and patches of vesicomyid and lucinid shell hash.

- The Green Canyon alpha sites (GC234 and GC354) had both seep communities and much less *L. pertusa* than VK826. These sites supported locally dense populations of *Callogorgia americana delta*, a large branching octocoral with associated communities of ophiuroids and galatheids. Some *Lophelia* thicket development was observed, but the colonies did not expand to form the type of habitat seen at VK826, and a large percentage of the coral colonies were dead. The main seep site at GC234, approximately 250 m to the east of the coral ridge, supported one of the most spatially extensive and active seep communities known on the upper slope, with numerous aggregations of tubeworms, mussels, gas hydrates, and both white and red bacterial mats. The seep community at GC354 may be in a later stage of development, as no mussel aggregations or gas hydrates, and relatively few tubeworm aggregations have been documented at this site.

- MC885, MC929, and GC184/185 had both seep communities and well developed *C. americana delta* communities, but little or no living *L. pertusa*. MC885 was mostly soft sediment interspersed with large holes (burrows or slumps) and locally dense areas of *C. americana delta* on exposed hard substratum. The MC929 site was mostly soft sediment with shell fragments, partially exposed hard grounds, and low-relief outcrops with large *C. americana delta* and/or small *L. pertusa* colonies, as well as mussel beds and small brine pools. At GC184/185 (the well known "Bush Hill" seep site with mussel beds, tubeworms, and exposed gas hydrates), there were a few small colonies of mostly dead *L. pertusa* on the ridge on the western edge of the active seep area, and several small colonies attached to a metal mooring buoy. Large colonies of *C. americana delta* occurred on carbonate outcrops on the north and northwest edges of the active seep area.

- The VK862 beta site and the VK862S OE site were much shallower (310 to 335 m) and warmer (~11.5 °C) than the other study sites, and supported a very different fauna from the other sites. The *L. pertusa* thickets present were composed of mainly live coral. The highest cnidarian diversity and abundance was observed here. The substratum was covered with dense patches of small white anemones, and large colonies of antipatharians and bamboo coral provided structure for other animals. Some of the large carbonate boulders supported *Lophelia* colonies; however, these were isolated and did not form coalescing thickets. There also was no seep fauna identified at VK862 or VK862S, and dense stands of *C. americana delta* were also absent.

Bushmaster collections provided detailed information about community composition (*Chapter 5*). Key findings included the following:

- At least 68 species of invertebrates were closely associated with *L. pertusa* aggregations in the Gulf of Mexico.

- Matrix correlation analyses (the BIO-ENV procedure) indicate that on the scale of an individual carbonate outcrop or *L. pertusa* thicket (tens of square meters), the depth of collection followed by the proportion of live and dead coral were the most significant factors correlated with the composition of the associated communities.

- The other important factors controlling the similarity of coral communities were the relative complexity of the coral framework and the location of collection.

- Communities associated with *L. pertusa* were generally more similar within sites than they were among sites.

- While *L. pertusa* communities were easily distinguished from tubeworm-associated communities, there consistently was overlap in species composition.

7.2 ENVIRONMENTAL FACTORS

Factors potentially affecting the distribution and development of *Lophelia* communities include water depth, substratum availability, hydrocarbon seepage, sedimentation rate, water temperature, current regime, and food availability. This study addressed some of these environmental factors through observations and field and laboratory experiments.

7.2.1 Water Depth

Lophelia has been recorded from depths ranging from 50 m in the fjords of Norway (Rogers 1999) to 3,600 m near the Mid-Atlantic Ridge (Bett 1997). Bathymetric limits to distribution in the Gulf of Mexico are most likely related to confounding variables such as temperature, current speed, sedimentation, and other factors discussed below. In this study, the sites studied ranged in depth from 310 m (VK862) to 650 m (MC929). The shallowest site (VK862) may be near the upper temperature threshold for *Lophelia (Chapter 6)*. The lower depth limit in the Gulf of Mexico is unknown; however, since seep-derived authigenic carbonates provide the substratum for attachment, the depth range for *Lophelia* communities may be similar to that of hydrocarbon seepage, which extends to the edge of the lower continental slope (~3,400 m) in the northern Gulf of Mexico.

7.2.2 Substratum Availability

Lophelia requires hard substrata for attachment. Below depths of 300 m in the Gulf of Mexico, the surficial sediment regime is dominated by fine-grained pelagic and hemipelagic material (Coleman et al. 1991). However, on the continental slope, authigenic carbonate is produced as a by-product of coupled methane oxidation and sulfate reduction by microbial consortia (Boetius et

al. 2000; Aharon and Fu 2000). This seafloor lithification is a regular component of hydrocarbon seep sites (Roberts and Aharon 1994; Sager et al. 1999) and provides a substratum for establishment of coral and other hard-bottom communities.

Isotope analysis of rock samples from several study sites confirms that the hard substrata consist of authigenic carbonate produced as a result of hydrocarbon seepage (*Chapter 4*). Authigenic carbonates are depleted in heavy carbon isotopes (^{13}C) and enriched in heavy oxygen isotopes (^{18}O), indicating incorporation of seep derived carbon and biological fractionation of isotopes during carbonate formation. The relationship to seepage is important because many seep areas have been mapped and there are protective measures in place that require offshore oil and gas operators to evaluate the possible presence of seep communities (see *Section 7.3.2*).

Within sites, *L. pertusa* distribution is patchy, with some areas of bare substratum and substratum colonized by other colonial cnidarians. We conducted a transplantation experiment (*Chapter 6*) to test the hypothesis that coral distribution at VK826 is driven by habitat suitability and that areas of bare substratum are not good habitats for adult *L. pertusa*. However, the results indicate that adult corals can survive and grow equally well on substratum colonized by *L. pertusa* as on bare substratum at VK826. Therefore, some other factors including recruitment, predation on new recruits, differential sensitivity of young colonies to environmental factors, and/or random chance may be responsible for the absence of corals on areas of apparently suitable exposed substratum.

7.2.3 Hydrocarbon Seepage

Whether the distribution of *L. pertusa* in the Gulf of Mexico is linked to local hydrocarbon seepage is a key question for ecology and management. Results of this study indicate that, although the carbonate substratum at *Lophelia* sites is seep-derived, the corals derive little or no nutrition from seep productivity. Apparently, *L. pertusa* prefers areas where seepage has almost completely subsided prior to settlement. *L. pertusa* thickets may represent the end point of seep community succession. As seepage declines over time, tubeworm habitat is colonized by non-endemic species and eventually the *L. pertusa* community (Bergquist et al. 2003; Cordes et al. 2005; Cordes et al. in press).

The present study did not include any direct measurements of seepage. Water samples were analyzed for TPH, but this gross measure provided no indication of seepage, even at sites such as GC234 and GC184/185 where previous MMS work has identified release of crude oil from the seafloor and the presence of exposed gas hydrates. However, because isotopically light methane and discrimination against ^{13}C by seep autotrophs is reflected in both organic and inorganic carbon in the seep environment, stable carbon isotope data can provide information on the extent of seepage and seep-produced organics in *L. pertusa* habitats. Stable carbon isotope data from old coral skeletons may also provide information on the presence of seep carbon in the dissolved inorganic carbon (DIC) pool in epibenthic seawater at the time of settlement.

Measured $\delta^{13}C$ values of *L. pertusa* skeleton suggest that the corals do not settle in an area until seepage has subsided to the point that it is not reflected in the epibenthic DIC pool (*Chapter 5*). One possible explanation is that during periods of seepage, elevated concentrations of methane

and hydrogen sulfide, as well as low oxygen concentrations, may exclude larvae from otherwise suitable hard substrata. There was no significant trend of increasing $\delta^{13}C$ values over time in the skeleton, suggesting that light carbon from methane oxidation was not a significant input to the local DIC pool even during early growth of the coral colonies. In addition, stable carbon, nitrogen, and sulfur content of *L. pertusa* tissue indicate that there has been little or no input of seep productivity to their nutrient supply in the recent past.

Most of the other species occupying the coral habitat also derive little to none of their nutrition from seep productivity (*Chapter 5*). The suspension feeding organisms, including gorgonians, antipatharians, sabellid polychaetes, and hydroids had carbon, nitrogen, and sulfur isotope values that were more positive than would be expected for food sources derived mainly from seep productivity. Some species collected along with *L. pertusa* were previously considered seep endemics. These species were found in collections made from areas near to tubeworm aggregations and that contained low proportions of live coral (<10%). Examples include the polychaetes *Branchinotogluma* sp. and *Harmothoe* sp., the gastropods *Bathynerita naticoidea* and *Provanna sculpta*, and the galatheid crabs *Munidopsis* sp. 1 and 2. These species may indeed be "seep endemics," and their presence in the *L. pertusa* collections simply may be a reflection of the nearby populations associated with tubeworm aggregations. On the other hand, these species perhaps may be more generally adapted to hypoxic conditions likely to exist near the sediment surface in the midst of dead coral.

7.2.4 Water Temperature

Temperatures at most sites ranged from about 7 °C to 9 °C (**Table 7.2**). Data sources include the current meter deployments at GC234 and VK826 (*Chapter 3*), HOBO-temp probe deployments at GC354 and VK862 (*Chapter 3*), and measurements during submersible transects (*Chapter 6*). The results are similar to previous data from two Green Canyon chemosynthetic sites reported by MacDonald (2002).

VK862 is the exception. Temperatures observed during the submersible transects were about 11.5 °C, and temperatures recorded by the HOBO data loggers ranged from 9 °C to 13 °C (*Chapter 3*). The highest temperatures recorded during the year-long deployment of the data loggers exceed the hypothesized upper temperature threshold of 12 °C for *L. pertusa* (Frederiksen et al. 1992; Freiwald 1998). Temperature tolerance experiments reported in *Chapter 6* similarly indicated a threshold between 10 °C and 15 °C for *L. pertusa* from the Gulf of Mexico. In the laboratory, *L. pertusa* tolerated short term (up to 24 hours) exposure to 15 °C but experienced reduced survival (81.2%) after exposure to 15 °C for 1 week. At the VK862 site, temperatures remained above 12 °C for 2 weeks on one occasion and for several days at other times during the year. This site may be near the upper temperature limit for *Lophelia* distribution. The lower thermal limit for *L. pertusa* was not observed in the laboratory, but there was no mortality after 1 week at 5 °C, which is lower than temperatures observed during this study.

7.2.5 Currents

In general, *Lophelia* and other corals are found where current speeds are sufficient to deliver food and oxygen, but not so fast that the feeding structures are inhibited or the branches broken. Frederiksen et al. (1992) suggested a threshold current speed of 1 m/s for *L. pertusa*.

Table 7.2. Summary of near-bottom temperatures measured at study sites.

Study Site	Water Depth (m)	Water Temperature (°C)		
		Current Meters (*Chapter 3*)[a]	HOBO-Temp Probes (*Chapter 3*)[b]	Submersible Transects (*Chapter 6*)[c]
Alpha Sites				
VK826	472	7.5 – 9	--	8.3 – 9.6
GC234	501	7 – 9	--	7.7 – 8.2
GC354	525	--	6.8 – 8.8	7.8 – 8.2
Beta Sites				
VK862	310	--	9 – 13	~ 11.5
GC184/185	528	--	--	--
MC885	634	--	--	~ 7.3
NOAA-OE Sites				
VK862S	335	--	--	--
VK826NE	457	--	--	8.5 – 8.6
MC929	650	--	--	--

GC = Green Canyon; MC = Mississippi Canyon; VK = Viosca Knoll; NOAA-OE = National Oceanic and Atmospheric Administration, Office of Ocean Exploration.

[a] Data record consisted of 11 days for VK862 and 9 months for GC234.

[b] Temperatures recorded every 5 hours for 375 days; 40-hour low pass filter was applied.

[c] Temperatures recorded during submersible transects.

Current speeds measured at GC234 and VK826 during this study are well below the hypothesized threshold for polyp extension of 1 m/s (*Chapter 3*). Over the entire 9-month data record from the lower instrument at GC234, the maximum speed was 44 cm/s. A shorter data record (11 days) from VK826 indicated a maximum speed of 18.3 cm/s. Mean vector speeds were 6.7 cm/s over the 9-month record at GC234 and 5.8 cm/s from the 11-day deployment at VK826. Therefore, it seems unlikely that current speeds were high enough to inhibit feeding at any of the study sites.

Aside from direct mechanical effects, currents may also influence deepwater coral distribution by controlling the distribution of zooplankton and detritus sinking from the euphotic zone, transporting larvae (see *Section 7.3.3*), and resuspending bottom sediments (see *Section 7.2.6*).

7.2.6 Sedimentation

Sedimentation can pose a stress for *Lophelia* and other corals and therefore is a potential factor affecting distribution. Sources of sediment deposition in the region include river-derived particulates sinking through the water column and bottom sediments resuspended by currents. Benthic storms might have a tremendous impact on sediment concentration in the water column and subsequent deposition.

Experimental results from *Chapter 6* suggest that *Lophelia* can tolerate fairly severe sediment conditions for short periods, but that mortality increases rapidly with longer periods of burial or higher sediment loads. Under laboratory conditions, over half of the *L. pertusa* polyps survived 2 weeks exposure to ~100 mg/L of sediment. However, in burial experiments, nearly all polyps buried for 2 days had died after 4 days, and mortality was 100% after 7 days.

Within sites, sediment trap data (*Chapter 6*) indicate that coral distribution was not correlated with sediment load. There was no difference between the sediment loads in traps positioned in high-density coral stands and those positioned away from living coral.

Regionally, the Viosca Knoll and Green Canyon sites are exposed to quite different levels of sedimentation (*Chapter 6*). The average sediment load in sediment traps at the Viosca Knoll sites (VK826 and VK862) was about two to three times higher than at two Green Canyon sites (GC234 and GC354) (22 g vs. 6 to 10 g). Viosca Knoll is located approximately 120 miles southeast of the mouth of the Mississippi River, which releases a large amount of terrigenous sediment into the Gulf of Mexico. During the deployment period, Hurricanes Katrina, Ivan, and Rita made landfall in the Gulf of Mexico, potentially increasing the outflow from the Mississippi River. The sediment load data could represent a consistent difference among the sites, which has been noted in previous studies (Trefry et al. 2006). If this is the case, then it appears that sediment load over the ranges present at the sites studied does not hinder coral settlement or survival. The differences among sites could also have been due partly to localized and short-lived increases in sediment load caused by the hurricanes. In this case, the differences among sites and the relation to coral occurrence is not clear. The grain-size distribution and organic content of trapped sediments was similar across the entire study region.

Bottom sediments at all sites are composed mainly of clay and silt (*Chapter 4*), which can resuspend at relatively low current speeds (Hjulstrom 1939). The limited current meter observations from the present study indicate similar current regimes for the two sites studied (GC234 and VK826).

7.2.7 Organic Input

Previous studies have indicated that the main food source of *L. pertusa* is zooplankton, although this species has also been observed to ingest large resuspended sediment particles (Mortensen 2001; Freiwald et al. 2002; Duineveld et al. 2004; Kiriakoulakis et al. 2005).

Based on the sediment trap data, there are differences among sites in zooplankton availability (*Chapter 6*). The overall quantity of zooplankton in the traps was low at all sites, with the average number of individuals ranging from 1.33 to 12.67. The number of zooplankton was highest at VK826 and lowest at GC234. Within sites, there was no difference between "high coral" and "no coral" areas in quantity of zooplankton or the distribution of different plankton groups.

The observed higher zooplankton quantity in the VK826 traps may be due to higher productivity in this region. As discussed in *Chapter 3*, a high-chlorophyll tongue-like pattern extends eastward over De Soto Canyon and southeastward offshore of the West Florida Shelf during the summer. The Viosca Knoll area exists in the heart of the summertime high chlorophyll tongue, whereas the Green Canyon area lies outside of this region.

7.3 ISSUES AND QUESTIONS

7.3.1 Ecological Importance of Deepwater Corals

Deepwater corals can provide habitat for diverse communities of organisms, including commercially important fisheries species (Koslow et al. 2001; Andrews et al. 2002; Hall-Spencer et al. 2002). In addition, macrofauna and megafauna may occur in numbers that are orders of magnitude higher in deepwater coral habitats than on the surrounding seafloor (Mortensen et al. 1995). Species diversity may also be higher in coral thickets than on the surrounding soft bottom (Jensen and Frederiksen 1992; Mortensen et al. 1995), emphasizing the importance of this habitat to the ecology of the deep benthos. Accordingly, efforts are underway to protect deepwater coral areas including *Lophelia* "Darwin Mounds" off the coast of Ireland, Norwegian *Lophelia* banks, Australian seamount corals, and *Primnoa* off the eastern coast of Canada. Within the U.S., Alaska has protected coral habitat in the Aleutian Islands and *Primnoa* (a deepwater octocoral) stands in the Gulf of Alaska. The South Atlantic Fisheries Management Council recently declared all known deepwater coral habitat in the southeast U.S. region to be a Habitat Area of Particular Concern (HAPC), with protective measures to be instated. Moreover, the United Nations is currently considering a ban on high-seas trawling that is designed to protect deepwater corals on seamounts and other hard bottom areas.

Results of this study suggest that *L. pertusa* plays a significant role in the ecology of hard bottom habitats on the upper slope of the northern Gulf of Mexico. *L. pertusa* colonizes hard substrata, following the decline of seepage. Corals therefore rely on seeps as a source of hard substratum in the form of authigenic carbonate but do not incorporate significant amounts of seep productivity into their diet. *L. pertusa* appears to structure the surrounding slope community largely through the provision of habitat rather than food. *L. pertusa* creates habitat for a number of associated species, many of which show significantly higher densities near coral. A number of species have only been found in tight association with *L. pertusa* in the Gulf of Mexico. *L. pertusa* therefore plays a similar role to tubeworm aggregations, although the fauna attracted to these two types of biogenic habitat are mostly different.

7.3.2 Detection

This study examined selected sites where geophysical or visual records and/or previous sampling indicated either the presence or likelihood of *L. pertusa* and associated communities. Various sources have confirmed, either through direct observations, video records, or specimen collections, the presence of *Lophelia* or *Madrepora* colonies at a number of locations in the northern Gulf of Mexico (e.g., Moore and Bullis 1960; Cairns 1979; Newton et al. 1987; Viada and Cairns 1987; MacDonald et al. 1989; Schroeder 2002). However, there has been no prior comprehensive effort to map these areas.

Since seep-derived authigenic carbonates provide the substratum for attachment, the distribution of *Lophelia* communities in the Gulf of Mexico will overlap that of chemosynthetic communities. Under Notice-to-Lessees (NTL) 2000-G20, MMS requires deepwater operators to analyze high-resolution seismic data and map the seafloor and shallow geologic features such as hydrocarbon-charged sediments associated with surface faulting, acoustic void zones associated with surface faulting, mounds or knolls, and gas or oil seeps. Side-scan sonars also have the

ability to show differences in seafloor properties (e.g., hard bottom features) and thus may be useful in imaging deepwater hard bottom communities. However, since *Lophelia* communities can exist in areas where seepage has subsided, it is uncertain whether existing methods used to identify chemosynthetic communities will also detect (and protect) *Lophelia*. Additional analyses aimed specifically at detection of hard substratum should also be required for protection of the hard and soft corals that routinely colonize these substrata.

7.3.3 Reproduction and Larval Transport

While asexual reproduction (via fragmentation and breakage) is probably important for spreading of *Lophelia* within established reef areas, colonization of new areas depends on dispersive planktonic larvae and sexual reproduction. The same is true for recolonization of disturbed areas where all the corals have died.

Laboratory studies in *Chapter 6* indicate that *L. pertusa* spawns in late September or October in the Gulf of Mexico. Primary oocytes were observed in November, which indicates concurrent gametogenesis, with little or no break between cycles. The size-frequency distributions for oocyte diameter show that egg development is not highly synchronized in these corals as with many shallow water species.

Chapter 3 included simulations of larval dispersion from two sites, VK826 and GC234. The experiment was designed to yield information on how far larvae may travel during their lifespan, and to test hypotheses that larvae distributions may vary from season to season, or year to year. Particles were assumed to be released at a depth of 400 m, and densities were computed using particle positions 5, 10, 15, 20, and 25 days after release. It should be emphasized, however, that the actual dispersal time of *L. pertusa* remains unknown, since the embryos and larvae of this species have not been reared in the laboratory. Larvae of *Oculina varicosa*, another deepwater structure-forming coral with a similar egg size, have been shown to survive between 2 and 3 weeks in the laboratory (Brooke and Young 2003); this encompasses most of the time periods used in the simulations.

Currents in the area flow predominantly along isobaths. Accordingly, particles released from the VK826 site were distributed primarily along the continental slope, and preferentially eastward. The eastward drifting particles travel around the De Soto Canyon and southward along the West Florida shelf slope. Few particles find their way west of the Mississippi Canyon. Some particles are transported out into deeper water. The particles released from the GC234 site initially spread nearly symmetrically east and west along isobaths. After the initial few days, dispersion of particles to the west slows and the eastward extent of the particle distribution expands past the Mississippi Canyon, similar to the pattern of particle distribution from Viosca Knoll. Based on climatology maps, little interseasonal or interannual variability in the distribution patterns is expected. The modeling indicates that currents are sufficient to widely disperse larvae and allow genetic exchange among sites studied here.

7.3.4 Dead Corals

Standing dead coral colonies and partially dead colonies are a characteristic feature of *Lophelia* habitats and were frequently observed during this study. The reasons for the coral polyp

mortality and the age of the colonies are unknown. Possible causes include temperature fluctuations, disease or parasites, and sediment load or burial. In the Gulf of Mexico, temperatures fluctuate over time, but at all but one of the study sites (VK862), they most likely remain below the coral's upper temperature limit. There are currently no known pathogens of deepwater corals, but since most deepwater scleractinian reefs are composed of a dominant foundation species, a disease outbreak could cause widespread mortality and have a devastating effect on the habitat. Similarly, a benthic storm or slumping event could smother large areas of coral, leaving standing dead colonies. There is insufficient information to determine the cause of polyp and colony mortality at our study sites. Regardless of the cause, the dead portions of the *L. pertusa* colonies are important to the structure of the associated communities as they provide substrata for settlement of other cnidarians as well as habitat for numerous other invertebrates.

7.3.5 Growth Form and Skeletal Density

Colonies of *L. pertusa* found in the deep Gulf of Mexico exhibit two distinct growth forms or "morphotypes." One ("*brachycephala*") is very heavily calcified with thick branches and very large calices, and the other ("*gracilis*") is more fragile with smaller branches and very prominent septal ridges. The heavier form comprises the extensive colonies at VK826, and the more delicate morphotype is found at all of the other study sites. Superficial observations revealed a denser, more tightly packed skeletal structure in the heavily calcified growth form, and since bulk density and porosity are inversely related, differences between the morphotypes were expected for these characteristics (*Chapter 6*). In shallow water corals, the bulk density has been found to vary with latitude, depth, temperature, and different growth forms (Schneider and Smith 1982; van Veghel and Bosscher 1995). Several studies have highlighted the effect that high porosity (i.e., reduced bulk density) would have on the corals and hence their tolerance to physical damage (Chamberlain 1978; Jimenez and Cortes 1993). The differences observed between the morphotypes may be indicators of environmental differences such as nutrient availability, current speed, or pH between Viosca Knoll and the more westerly sites where the fragile growth form occurs.

7.3.6 *Lophelia* Feeding

A preliminary feeding experiment was conducted (*Chapter 6*). Although the experiment served mainly to develop appropriate techniques, results indicate that lipid content increases in response to increased food supply. Corals in the field might be energy limited, since fragments show higher lipid content in laboratory experiments than in the field. However, the lack of seasonal replication or use of food sources available to *L. pertusa in situ* prevents firm conclusions from this portion of the study.

7.3.7 Coral Skeleton as Temperature Record

Temperature estimates derived from the coral skeleton (*Chapter 5*) demonstrate that *L. pertusa* may be used as a record of temperature in the Gulf of Mexico and suggest that additional efforts be made to obtain targeted collections for this purpose in the future. Temperatures at the time of the skeleton secretion were estimated to be 7.32 °C at VK826 and VK826NE and 8.04 °C at the shallower VK862 station.

7.4 RECOMMENDATIONS FOR FURTHER STUDY

This was the first comprehensive study of the distribution of *L. pertusa*, its biology, and community ecology in the Gulf of Mexico. This study has significantly advanced understanding of *L. pertusa* in all of these areas, but many questions remain unanswered and several productive new avenues of study have been illuminated by the project. For example, this study has been effective in describing the distribution of *L. pertusa* from a subset of the known coral sites associated with known chemosynthetic sites between 330 and 640 m depths, but it also indicated how little is known of *L. pertusa* distribution Gulf-wide. This study also clearly demonstrates that other colonial cnidarians are important and abundant components of deepwater hard grounds should be studied in concert with *L. pertusa* communities. Investigations of productive deepwater cnidarian communities should include study of remotely detected hard grounds in areas not associated with geophysical or geochemical indicators of active seepage, as well as investigations at greater depths. Additional work is required to develop a predictive model for *L. pertusa* distribution that would allow more confidence in using ship-based geophysical measurements as predictors of hard ground community development.

To better understand the linkage between *L. pertusa* and seeps, studies of the coral's tolerance of seep conditions could be quite productive. We have demonstrated that laboratory investigations with live *L. pertusa* can provide considerable insight into its biology, and studies of coral tolerance to hydrocarbons and low oxygen may provide insight into why *L. pertusa* is seldom found closely associated with areas of very active seepage and seems to appear in seep communities only during the later successional stages of the sites.

The experimental work and growth studies also provide important baseline information that will be necessary to fully understand the sensitivity of *L. pertusa* communities to disturbance. Additional studies are necessary to further understand their sensitivity to high temperatures and sediment loads, as well as to anthropogenic substances such as drilling mud and refined petroleum. The skeletal density study also provides a baseline for investigations into how changes in pH and other environmental factors may affect the skeletal structure of deepwater corals. Physical disturbance is also a threat to *L. pertusa* worldwide, and to understand recovery trajectories of affected populations and colonies, studies are needed to better estimate their growth rates, understand the limitations on larval dispersal, and quantify reproductive output in relation to colony size and age.

The deployment of artificial structures to investigate recruitment would be a useful and inexpensive addition to future studies. One of the World War II wrecks in the deep Gulf shows extensive *L. pertusa* colonization; therefore, this species will settle and develop on artificial structures. With an increase in deepwater exploration and production, abandoned structures may play an ecological role similar to that of shallower structures in the northern Gulf.

Further studies of the relationship between *L. pertusa* and *Coralliophila* sp., *Stenopus* sp., and *Eunice* sp. are recommended to evaluate the positive or negative nature of each interspecific interaction. Studies should include a description of these species, monitoring of their interactions *in situ* and in the laboratory, and possibly manipulative experiments.

This study has begun the characterization of the communities associated with *L. pertusa* at different spatial scales and established their role as a significant foundation species on hard bottoms in the Gulf of Mexico. However, the number of sites surveyed precluded adequate replication, so additional transect, mosaic, and physical samples at high-density sites are required to fully assess the diversity of the coral-associated communities, make valid comparisons across a depth or latitudinal transect, and provide more robust comparisons to surrounding chemosynthetic communities. In addition, the inherent limitations of the expeditionary approach that dominated this study prevented gathering information on events that occurred between cruises and in the absence of submersible lights and noise. Subsequent studies that include long-term *in situ* observations will provide valuable information on the coral community response to potentially important transient environmental events as well as utilization of the habitat by mobile fauna including larger fish species.

Chapter 8
Literature Cited

Aharon, P. and B. Fu. 2000. Microbial sulfate reduction rates and sulfur and oxygen isotope fractionations at oil and gas seeps in deepwater Gulf of Mexico. Geochim. Cosmochim. Acta. 64(2):233-246.

Aharon, P., H.P. Schwarcz, and H.H. Roberts. 1997. Radiometric dating of submarine hydrocarbon seeps in the Gulf of Mexico. Geol. Soc. Amer. Bull. 109:568-579.

Aharon, P., D. Van Gent, B. Fu, and L.M. Scott. 2001. Fate and Effects of Barium and Radium-Rich Fluid Emissions from Hydrocarbon Seeps on the Benthic Habitats of the Gulf of Mexico Offshore Louisiana. Prepared by the Louisiana State University, Coastal Marine Institute. U.S. Department of the Interior, Mineral Management Service, Gulf of Mexico OCS Office, New Orleans, LA. OCS Study MMS 2001-004. 142 pp

Andrews, A.H., E.E. Cordes, M.M. Mahoney, K. Munk, K.H. Coale, G.M. Cailliet, and J. Heifetz. 2002. Age, growth and radiometric age validation of a deep-sea, habitat-forming gorgonian (*Primnoa resedaeformis*) from the Gulf of Alaska. Hydrobiologia 471:101-110.

Baguley, J.G., P.A. Montagna, L.J. Hyde, R.D. Kalke, and G.T. Rowe. 2006. Metazoan meiofauna abundance in relation to environmental variables in the northern Gulf of Mexico deep sea. Deep-Sea Research I 53:1,344-1,362.

Barnes, D.J. and J.M. Lough. 1989. The nature of skeletal density banding in scleractinian corals: Fine banding and seasonal patterns. J. Exp. Mar. Biol. Ecol. 126:119-134.

Barnes, D.J. and J.M. Lough. 1993. On the nature and cause of density banding in massive coral skeletons. J. Exp. Mar. Biol. Ecol. 167:91-108.

Bergquist, D.C., T. Ward, E.E. Cordes, T. McNelis, S. Howlett, R. Kosoff, S. Hourdez, R. Carney, and C.R. Fisher. 2003. Community structure of vestimentiferan-generated habitat islands from upper Louisiana slope cold seeps. J. Exp. Mar. Biol. Ecol. 289:197-222.

Bett, B.J. 1997. Atlantic Margin Environmental Survey: Seabed Survey of the Shelf Edge and Slope West of Shetland. Published by Challenger Division for Seafloor Processes: Southampton Oceanography Centre, NERC/ University of Southampton. 165 pp.

Boetius, A., K. Ravenschlag, C. Schubert, D. Rickert, F. Widdel, A. Gieseke, R. Amann, B.B. Jørgensen, U. Witte, and O. Pfannkuche. 2000. A marine microbial consortium apparently mediating anaerobic oxidation of methane. Nature 407:623-626.

Brooke, S.D. 2002. Reproductive ecology of a deep-water scleractinian coral, *Oculina varicosa*, from the South East Florida Shelf. Ph.D. Dissertation. School of Ocean and Earth Science, University of Southampton.

Brooke, S.D and J. Jarnegren (unpublished). Asynchronous reproduction in *Lophelia pertusa* populations from the Norwegian Fjords and the Gulf of Mexico.

Brooke, S. and C.M. Young. 2003. Reproductive ecology of a deep-water scleractinian coral, *Oculina varicosa*. Cont. Shelf Res. 23:847-858.

Brooks, J.M., M.C. Kennicutt, R.R. Fay, T.J. McDonald, and R. Sassen. 1984. Thermogenic gas hydrates in the Gulf of Mexico. Science 225:409–411.

Bryant, W.R., J. Lugo, C. Cordova, and A. Salvado. 1991. Physiography and Bathymetry, pp. 13-30. In: A. Salvador (ed.), The Geology of North America, Vol. J, The Gulf of Mexico Basin. The Geological Society of America, Boulder, CO.

Bucher, D., V. Harriott, and L. Roberts. 1998. Skeletal bulk density, micro-density and porosity of acroporid corals. J. Exper. Mar. Biol. Ecol. 228(1):117-135.

Cairns, S.D. 1979. The deep-water Scleractinia of the Caribbean Sea and adjacent waters. Stud. Fauna Curaçao 57:1-34.

Cairns, S.D. 1994. Scleractinia of the Temperate North Pacific. Smithsonian Contrib. Zool. No. 557. 150 pp.

Cairns, S.D. 1995. New records of azooxanthellate stony corals (Cnidaria: Scleractinia and Stylasteridae) from the Neogene of Panama and Costa Rica. Proc. Biol. Soc. Wash. 108(3):533-550.

Cairns, S.D., D.M. Opresko, T.S. Hopkins, and W.W. Schroeder. 1994. New records of deep-water Cnidaria (Scleractinia & Antipatharia) from the Gulf of Mexico. Northeast Gulf Sci. 13(1):1-11.

Carney, R.S. 1994. Consideration of the oasis analogy for chemosynthetic communities at Gulf of Mexico hydrocarbon vents. Geo-Mar. Lett. 14:149-159.

Chamberlain, J.A. 1978. Mechanical properties of coral skeleton: Compressive strength and its adaptive significance. Paleobiology 4:419-435.

Coleman, J.M., H.H. Roberts, and W.R. Bryant. 1991. Late Quaternary sedimentation, pp. 325-352. In: A. Salvador (ed.), The Geology of North America, Vol. J, The Gulf of Mexico Basin. The Geological Society of America, Boulder, CO.

Cordes, E.E., S. Hourdez, B.L. Predmore, M.L. Redding, and C.R. Fisher. 2005. Succession of hydrocarbon seep communities associated with the long-lived foundation species *Lamellibrachia luymesi*. Mar. Ecol. Prog. Ser. 305:17-29.

Cordes, E.E., D.C. Bergquist, B.L. Predmore, C. Jones, P. Deines, G. Telesnicki, and C.R. Fisher. In press. Alternate unstable states: Convergent paths of succession in hydrocarbon-seep tubeworm-associated communities. J. Exp. Mar. Biol. Ecol.

DaSilva, A., A.C. Young, and S. Levitus. 1994. Atlas of Surface Marine Data 1994, Volume 1: Algorithms and Procedures. NOAA Atlas NESDIS 6. U S. Department of Commerce, Washington, DC.

Davies, P.S. 1989. Short-term growth measurements of corals using an accurate buoyant weighing technique. Mar. Biol. 101:389-395.

Duineveld, G.C.A., M.S.S. Lavaleye, and E.M. Berghuis. 2004. Particle flux and food supply to a seamount coldwater coral community (Galicia Bank, NW Spain). Mar. Ecol. Prog. Ser. 277:13-23.

Folk, R.L. 1954. The distinction between grain size and mineral composition in sedimentary rock nomenclature. J. Geol. 62:344-359.

Folk, R.L. 1974. The Petrology of Sedimentary Rocks. Hemphill Publishing Co., Austin, TX. 182 pp.

Fosså, J.H., P.B. Mortensen, and D.M. Furevik. 2002. The deep-water coral *Lophelia pertusa* in Norwegian waters; distribution and fishery impacts. Hydrobiologia 417:1-12.

Frederiksen, R., A. Jensen, and H. Westerberg. 1992. The distribution of the scleractinian coral *Lophelia pertusa* around the Faroe Islands and the relation to internal tidal mixing. Sarsia 77:157-171.

Freiwald, A. 1998. Geobiology of *Lophelia pertusa* (Scleractinia) reefs in the North Atlantic. Habilitationsschrift zur Erlangung der venia legendi am Fachbereich Geowissenschaften der Universität Bremen. 116 pp.

Freiwald, A., R. Henrich, and J. Pätzold. 1997. Anatomy of a deep-water coral reef mound from Stjernsund, West-Finnmark, Northern Norway. SEPM Special Volume 56:141-162.

Freiwald, A., V. Huhnerbach, B. Lindberg, J.B. Wilson, and J. Campbell. 2002. The Sula Ridge Complex, Norwegian Shelf. Facies 47:179-200.

Fry, B., W. Brand, F.J. Mersch, K. Tholke, and R. Garritt. 1992. Automated-analysis system for coupled delta-c-13 and delta-n-15 measurements. Anal. Chem. 64:288-291.

Fugro-McClelland. Undated. Bathymetry Survey of Blocks 825, 826, 869, and 870 Viosca Knoll Area, Gulf of Mexico.

Gage, J.D. 2001. Deep-sea benthic community and environmental impact assessment at the Atlantic Frontier. Cont. Shelf Res. 21:957-986.

Goodwin, R.H. and D.B. Prior. 1989. Geometry and Deposition Sequences of the Mississippi Canyon, Gulf of Mexico. J. Sed. Pet. 59:318-329.

Hall-Spencer, J., V. Allain, and J.H. Fosså. 2002. Trawling damage to Northeast Atlantic ancient coral reefs. Proc. R. Soc. Lond. B. 269:507-511.

Hayes, J.A. 1990. Distribution, movement and impact of the corallivorous gastropod *Coralliophila abbreviata* (Lamark) on a Panamanian patch reef. J. Exp. Mar. Biol. Ecol. 142:25-42.

Hjulstrom, F. 1939. Transportation of detritus in moving water, pp. 5-31. In: P.D. Trask (ed.), Recent marine sediments. Amer. Assoc. Petrol. Geol., Tulsa, OK.

Hovland, M. and E. Thomsen. 1997. Cold-water corals – are they hydrocarbon seep related? Mar. Geol. 137:159-164.

Hovland, M., P.F. Croker, and M. Martin. 1994. Fault associated seabed mounds (carbonate knolls?) off western Ireland and north-west Australia. Mar. Petrol. Geol. 11:233–246.

Hovland, M., P.B. Mortensen, E. Thomsen, and T. Brattegard. 1997. Substratum-related ahermatypic corals on the Norwegian continental shelf, pp. 1,203-1,206. In: Proceedings of the 8th International Coral Reef Symposium, Vol. 2. Panama 1996.

Hovland, M., P.B. Mortensen, T. Brattegard, P. Strass, and K. Rokoengen. 1998. Ahermatypic coral banks off mid-Norway: Evidence for a link with seepage of light hydrocarbons. Palaios 13:189-200.

Hughes, T.P. 1987. Skeletal density and growth form of corals. Mar. Ecol. Prog. Ser. 35:259-266

Huntley, D.A. 1988. A modified inertial dissipation method for estimating seabed stresses at low Reynolds numbers, with application to wave/current boundary layer measurements. J. Phys. Oceanogr. 18:339-346.

Jensen, A. and R. Frederiksen. 1992. The fauna associated with the bank forming deepwater coral *Lophelia pertusa* (Scleractinaria) on the Faroe shelf. Sarsia 77:53-69.

Jimenez, C. and J. Cortes. 1993. Density and compressive strength of the coral *Siderastrea siderea* (Scleractinia: Siderastreidae): Intraspecific variability. Rev. Biol. Trop. Suppl. 41(1):39-43.

Kennicutt, M.C., J.M. Brooks, R.R. Bidigare, and G.J. Denoux. 1988. Gulf of Mexico hydrocarbon seep communities: I. Regional distribution of hydrocarbon seepage and associated fauna. Deep-Sea Res. 35:1,639-1,651.

Kinsman, D.J.J. and H.D. Holland. 1969. The co-precipitation of cations with $CaCO_3$. IV. The co-precipitation of Sr^{2+} with aragonite between 16°C and 96°C. Geochim. Cosmochim. Acta 33:1-17.

Kiriakoulakis, K., E. Fisher, G.A. Wolff, A. Freiwald, A. Grehan, and J.M. Roberts. 2005. Lipids and nitrogen isotopes of two deep-water corals from the North-East Atlantic: Initial results and implications for their nutrition, pp. 715-729. In: A. Freiwald and J.M. Roberts (eds.), Cold-water Corals and Ecosystems. Springer-Verlag, Berlin.

Koenig, C.C., F.C. Coleman, C.B. Grimes, G.R. Fitzhugh, C.T. Gledhill, K.M. Scanlon, and M.A. Grace. 2000. Protection of fish spawning habitat for the conservation of warm temperate reef fish fisheries of shelf-edge reefs of Florida. Bull. Mar. Sci. 66(3):593-616.

Koslow, J.A., K. Gowlett-Holmes, J.K. Lowry, T. O'Hara, G.C.B. Poore, and A. Williams. 2001. Seamount benthic macrofauna off southern Tasmania: Community structure and impacts of trawling. Mar. Ecol. Prog. Ser. 213:111-125.

Krupp, D.A. 1983. Sexual reproduction and early development of the solitary coral *Fungia scutaria* (Anthozoa: Scleractinia). Coral Reefs 2:159-164.

Le Tissier, M. D'A.A., B. Clayton, B.E. Brown, and P. Spencer Davis. 1994. Skeletal correlates of density banding and an evaluation of radiography as used in sclerochronology. Mar. Ecol. Prog. Ser. 110:29-44.

LeDanois, E. 1948. Les Profondeurs de la Mer. Payot, Paris. 303 pp.

MacDonald, I.R. (ed.). 2002. Stability and change in Gulf of Mexico chemosynthetic communities. Volume II: Technical Report. Prepared by the Geochemical and Environmental Research Group, Texas A&M University. U.S. Department of the Interior, Minerals Management Service, Gulf of Mexico OCS Region, New Orleans, LA. OCS Study MMS 2002-036. 456 pp.

MacDonald, I.R., G.S. Boland, J.S. Baker, J.M. Brooks, M.C. Kennicutt, II, and R.R. Bidigare. 1989. Gulf of Mexico chemosynthetic communities II: Spatial distribution of seep organisms and hydrocarbons at Bush Hill. Mar. Biol. 101:235-247.

MacDonald, I.R., N.L. Guinasso Jr., J.F. Reilly, J.M. Brooks, W.R. Callender, and S.G. Gabrielle. 1990. Gulf of Mexico hydrocarbon seep communities; VI. Patterns in community structure and habitat. Geo-Mar. Lett. 10:244-252.

MacDonald, I.R., W.W. Schroeder, and J.M. Brooks. 1995. Chemosynthetic ecosystems studies final report. U.S. Department of the Interior, Minerals Management Service, Gulf of Mexico OCS Region, New Orleans, LA. OCS Study MMS 95-0021.

MacDonald, I.R., W.W Sager, and M.B. Peccini. 2003. Gas hydrate and chemosynthetic biota in mounded bathymetry at mid-slope hydrocarbon seeps: northern Gulf of Mexico. Mar. Geol. 198:133-158.

Martin, P.J. 2000. A description of the Navy Coastal Ocean Model Version 1.0. NRL Report: NRL/FR/7322-009962. Naval Research Laboratory, Stennis Space Center, MS. 39 pp.

Martin, R.G. and A.H. Bouma. 1978. Physiography of the Gulf of Mexico, pp. 3-19. In: A.H. Bouma, G.T. Moore, and J.M. Coleman (eds.), Framework, facies, and oil-trapping characteristics of the upper continental margin. AAPG Studies in Geology 7.

McCutchan, J.H., W.M. Lewis, Jr., C. Kendall, and C.C. McGrath. 2003. Variation in trophic shift for stable isotope ratios of carbon, nitrogen and sulfur. Oikos 102:378-390.

Mikkelsen, N., H. Erlenkauser, J.S. Killingley, and W.H. Berger. 1982. Norwegian corals: Radiocarbon and stable isotopes in *Lophelia pertusa*. Boreas 5:163-171.

Moore, D.R. and H.R. Bullis. 1960. A deep-water coral reef in the Gulf of Mexico. Bull. Mar. Sci. 10(1):125-128.

Morey, S.L., P.J. Martin, J.J. O'Brien, A.A. Wallcraft, and J. Zavala-Hidalgo. 2003a. Export pathways for river discharged fresh water in the northern Gulf of Mexico. J. Geophys. Res. 108(C10), 3303, doi:10.1029/2002JC001674.

Morey, S.L., W.W. Schroeder, J.J. O'Brien, and J. Zavala-Hidalgo. 2003b. The annual cycle of riverine influence in the eastern Gulf of Mexico basin. Geophys. Res. Let, 30(16), 1867, doi: 10.1029/2003GL017348.

Mortensen, P.B. 2000. *Lophelia pertusa* (Scleractinia) in Norwegian waters. Distribution, growth, and associated fauna. Dr. scient. Thesis, Department of Fisheries and Marine Biology, University of Bergen, Norway.

Mortensen, P.B. 2001. Aquarium observations on the deep-water coral *Lophelia pertusa* (L., 1758) (Scleractinia) and selected associated invertebrates. Ophelia 54:83-104.

Mortensen, P.B. and H.T. Rapp. 1998. Oxygen- and carbon isotope ratios related to growth line patterns in skeletons of *Lophelia pertusa* (L) (Anthozoa: Scleractinia): Implications for determination of linear extension rates. Sarsia 83:433-446.

Mortensen, P.B., M. Hovlund, T. Brattegard, and R. Farestveit. 1995. Deep water bioherms of the scleractinian coral *Lophelia pertusa* (L.) at 64° N on the Norwegian shelf: Structure and associated megafauna. Sarsia 80:145-158.

Mullins, H.T., C.R. Newton, K. Heath, and H.M. Vanburen. 1981. Modern deep-water coral mounds north of Little Bahama Bank: Criteria for recognition of deep-water coral bioherms in the rock record. J. Sed. Petrol. 51:999-1013.

Nagelkerken, I., G. Van der Velde, and P.H. Van Avessaath. 1997. A description of the skeletal development pattern of the temperate coral *Carophyllia smithii* based on internal growth lines. J. Mar. Biol. Ass.UK 77:375-387

Neumann, A.C., J.W. Kofoed, and G.H. Keller. 1977. Lithoherms in the Straits of Florida. Geology 5:4-10.

Newton, C.R., H.T. Mullins, and A.F. Gardulski. 1987. Coral mounds on the west Florida slope: Unanswered questions regarding the development of deep-water banks. Palaios 2:359-367.

Nowlin, W.D., Jr., A.E. Jochens, S.F. DiMarco, R.O. Reid, and M.K. Howard. 2001. Deepwater Physical Oceanography Reanalysis and Synthesis of Historical Data: Synthesis Report. OCS Study MMS 2001-064. U.S. Department of the Interior, Minerals Management Service, Gulf of Mexico OCS Region, New Orleans, LA. 528 pp.

Opresko, D.M. and S.D. Cairns. 1992. New species of black coral (Cnidaria: Antipatharia) from the Northern Gulf of Mexico. N.E. Gulf Sci. 12:93-97.

Paffenhofer, G.A. 1967. Caloric content of larvae of the brine shrimp *Artemia salina*. Helgoland Marine Research (Historical archive) 16(1-2):130-135.

Pequegnat, W.E., B.J. Gallaway, and L.H. Pequegnat. 1990. Aspects of the ecology of the deep-water fauna of the Gulf of Mexico. Am. Zool. 30:45-64.

Rau, G.H., A.J. Mearns, D.R. Young, R.J. Olsen, H.A. Schafer, and I.R. Kaplan. 1983. Animal $^{13}C/^{12}C$ correlates with trophic levels in pelagic food webs. Ecology 64:1,314-1,318.

Reilly, Jr., J.F., I.R. MacDonald, E.K. Biegert, and J.M. Brooks. 1996. Geologic controls on the distribution of chemosynthetic communities in the Gulf of Mexico, pp. 39-62. In: D. Schumacher and M.A. Abrams (eds.), Hydrocarbon migration and its near-surface expression. AAPG Memoir 66.

Reyss, D. 1971. Les canyons sous-marins de la mer Catalane: Le rech du Cap et le rech Lacaze-Duthiers. III. Les peuplements de la macrofaune benthique. Vie Milieu 22:529-613.

Ricciardi, A. and E. Bourget. 1998. Weight to weight conversion factors for marine benthic invertebrates. Mar. Ecol. Prog. Ser. 163:245-251.

Roberts, H.H. and P. Aharon. 1994. Hydrocarbon-derived carbonate buildups of the northern Gulf of Mexico continental slope: A review of submersible investigations. Geo-Marine Lett. 14:135-148.

Roberts, H.H., R. Sassen, R. Carney, and P. Aharon. 1989. ^{13}C-depleted authigenic carbonate buildups from hydrocarbon seeps, Louisiana continental slope. Gulf Coast Assoc. Geol Soc. Trans. 39:523-530.

Roberts, J.M. 2005. Reef-aggregating behaviour by symbiotic eunicid polychaetes from cold-water corals: Do worms assemble reefs? J. Mar. Biol. Assoc. UK 85:813-819.

Roberts, J.M. and R.M. Anderson. 2002. A new laboratory method of monitoring deep-sea coral polyp behaviour. Hydrobiologia 471:143-148.

Rogers, A.D. 1999. The biology of *Lophelia pertusa* (Linnaeus 1758) and other deep-water reef forming corals and impacts from human activities. Int. Rev. Hydrobiol. 844:315-406.

Rowe, G.T. and M.C. Kennicutt II. 2002. Deepwater program: Northern Gulf of Mexico continental slope habitat and benthic ecology. Year 2: Interim Report. U.S. Department of the Interior, Minerals Management Service, Gulf of Mexico OCS Region, New Orleans, LA. OCS Study MMS 2002-063. 158 pp.

Sager, W.W., C.S. Lee, I.R. Macdonald, and W.W. Schroeder. 1999. High-frequency near-bottom acoustic reflection signatures of hydrocarbon seeps on the northern Gulf of Mexico continental slope. Geo-Marine Letters 18:267-276.

Sammarco, P.W. 1982. Polyp bail-out: An escape response to environmental stress and a new means of reproduction in corals. Mar. Ecol. Prog. Ser. 10:57-65.

Schneider, R.C. and S.V Smith. 1982. Skeletal Sr content and density in *Porites* spp in relation to environmental factors. Mar. Biol. 66:121-131.

Schroeder, W., S. Brooke, J. Olson, B. Phaneuf, J. McDonough, and P. Etnoyer. 2005. Occurrence of deep-water *Lophelia pertusa* & *Madrepora oculata* in the Gulf of Mexico, pp. 297-307. In: Freiwald and Roberts (eds.), Cold-water Corals & Ecosystems. Springer-Verlag, Berlin.

Schroeder, W.W. 1992. Authigenic carbonates at hydrocarbon seeps: A review of published material, pp. 3-1 to 3-14. In: I.R. MacDonald (ed.), Chemosynthetic Ecosystem Study Literature Review and Data Synthesis, Volume II: Technical Report. U.S. Department of the Interior, Minerals Management Service, Gulf of Mexico OCS Region, New Orleans, LA. OCS Study MMS 92-0034.

Schroeder, W.W. 2002. Observations of *Lophelia pertusa* and the surficial geology at a deep-water site in the northeastern Gulf of Mexico. Hydrobiol. 471:29-33.

Schroeder, W.W. 2006. Mapping and habitat characterization of deepwater coral sites: Northern Gulf of Mexico. Final Report to the NOAA Office of Ocean Exploration, Silver Spring, MD. Grant No NA05OAR4601062. 10 pp.

Smith, J.E., H.P. Schwarcz, M.J. Risk, T.A. McConnaughey, and N. Keller. 2000. Paleotemperatures from deep-sea corals: Overcoming “vital effects.” Palaios 15:25-32.

Stetson, T.R., D.F. Squires, and R.M. Pratt. 1962. Coral banks occurring in deep water on the Blake Plateau. American Museum Noviates 2114:39.

Stoddart, J.A. 1983. Asexual production of planulae in the coral *Pocillopora damicornis*. Mar. Biol. 76:279–284.

Stull, R.B. 1988. An Introduction to Boundary Layer Meteorology. Kluwer Academic Publishers, The Netherlands. 666 pp.

Taylor, L.A., T.L. Holcomb, and W.R. Bryant. 2000. Bathymetry of the northern Gulf of Mexico and the Atlantic Ocean east of Florida. Report MGG-16, 17, 18 National Geophysical Data Center, Boulder, Boulder, CO.

Taylor, R.B., D.J. Barnes, and J.M. Lough. 1993. Simple models of density band formation in massive corals. J. Exp. Mar. Biol. Ecol. 167:109-125.

Trefry, J.H., R.P. Trocine, R.D. Rember, and M.L. McElvaine. 2006. Metals, total organic carbon, and redox conditions in sediments. Chapter 8. In: Continental Shelf Associates, Inc., Effects of Oil and Gas Exploration and Development at Selected Continental Slope Sites in the Gulf of Mexico. Volume II: Technical Report. U.S. Department of the Interior, Minerals Management Service, Gulf of Mexico OCS Region, New Orleans, LA. OCS Study MMS 2006-045.

van Veghel, M.L.J. and H. Bosscher. 1995. Variation in linear growth and skeletal density within the polymorphic reef building coral *Montastrea annularis*. Bull. Mar. Sci. 56:902-908.

Viada, S.T. and S.D. Cairns. 1987. Range extensions of ahermatypic Scleractinia in the Gulf of Mexico. Northeast Gulf Sci. 9:131-134.

Waller, R.G. and P.A. Tyler. 2005. The reproductive biology of two deep-water, reef-building scleractinians from the NE Atlantic Ocean. Coral Reefs 24:514-522.

Weatherly, G.L. 1972. A study of the bottom boundary layer of the Florida Current. J. Phys. Oceangr. 2:54-72.

Wilson, J.B. 1979a. The distribution of the coral *Lophelia pertusa* (L) (*L. prolifera* (Pallas)) in the north-east Atlantic. J. Mar. Biol. Assoc. UK 59:149-164.

Wilson, J.B. 1979b. Patch development of the deep-water coral *Lophelia pertusa* (L.) on Rockall Bank. J. Mar. Biol. Assoc. U.K. 59:165-177.

Yund, P.O., S.D. Gaines, and M.D. Bertness. 1991. Cylindrical tube traps for larval sampling. Limnol. Oceanogr. 36:1,167-1,177.

Zavala-Hidalgo, J., S.L. Morey, and J.J. O'Brien. 2003. Seasonal circulation on the western shelf of the Gulf of Mexico using a high-resolution numerical model. J. Geophys. Res. 108(C12), 3389, doi:10.1029/2003JC001879.

Zibrowius, H. 1980. Les Scléractiniaires de la Méditerranée et de l'Atlantique nord-oriental. Mémoires de l'Institut Océanographique, Monaco 11:1–284.

Appendices

Appendix A

Photomosaic Images of Exposed Hard Bottom Communities at Study Sites During Cruises 1 and 2

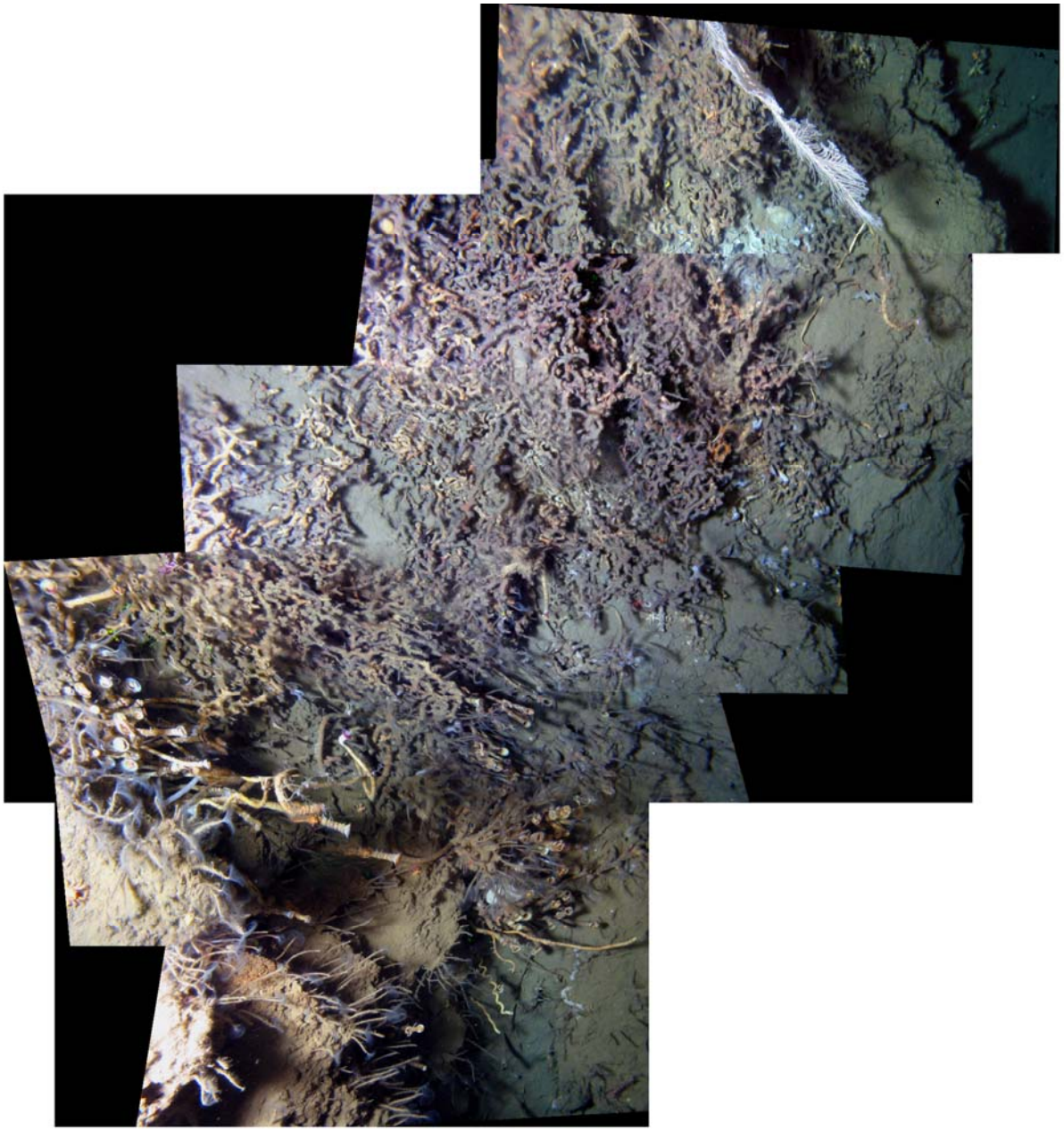

A.1. Green Canyon 184/185 – JSL Dive No. 4725.

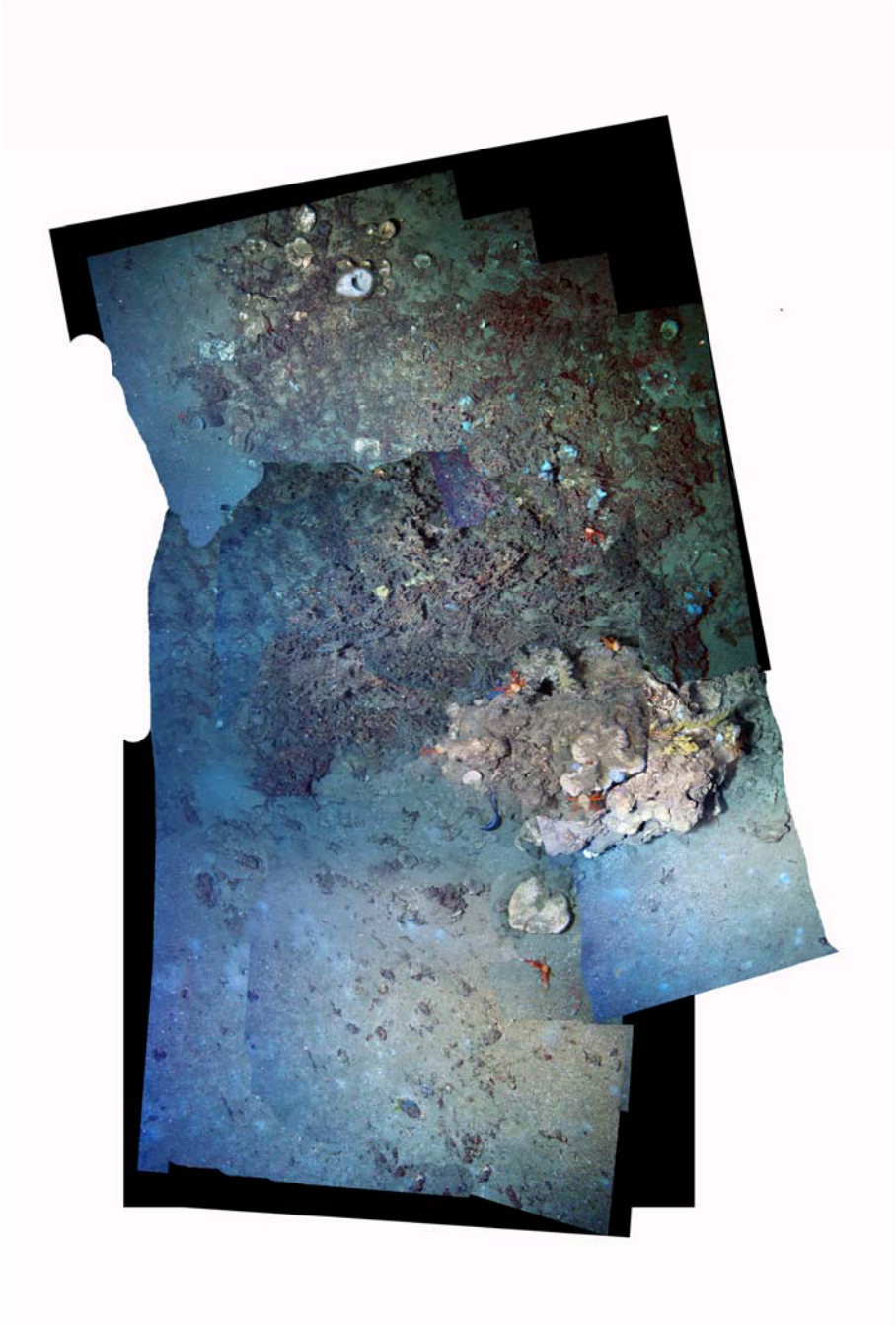

A.2. Green Canyon 354 – JSL Dive No. 4726.

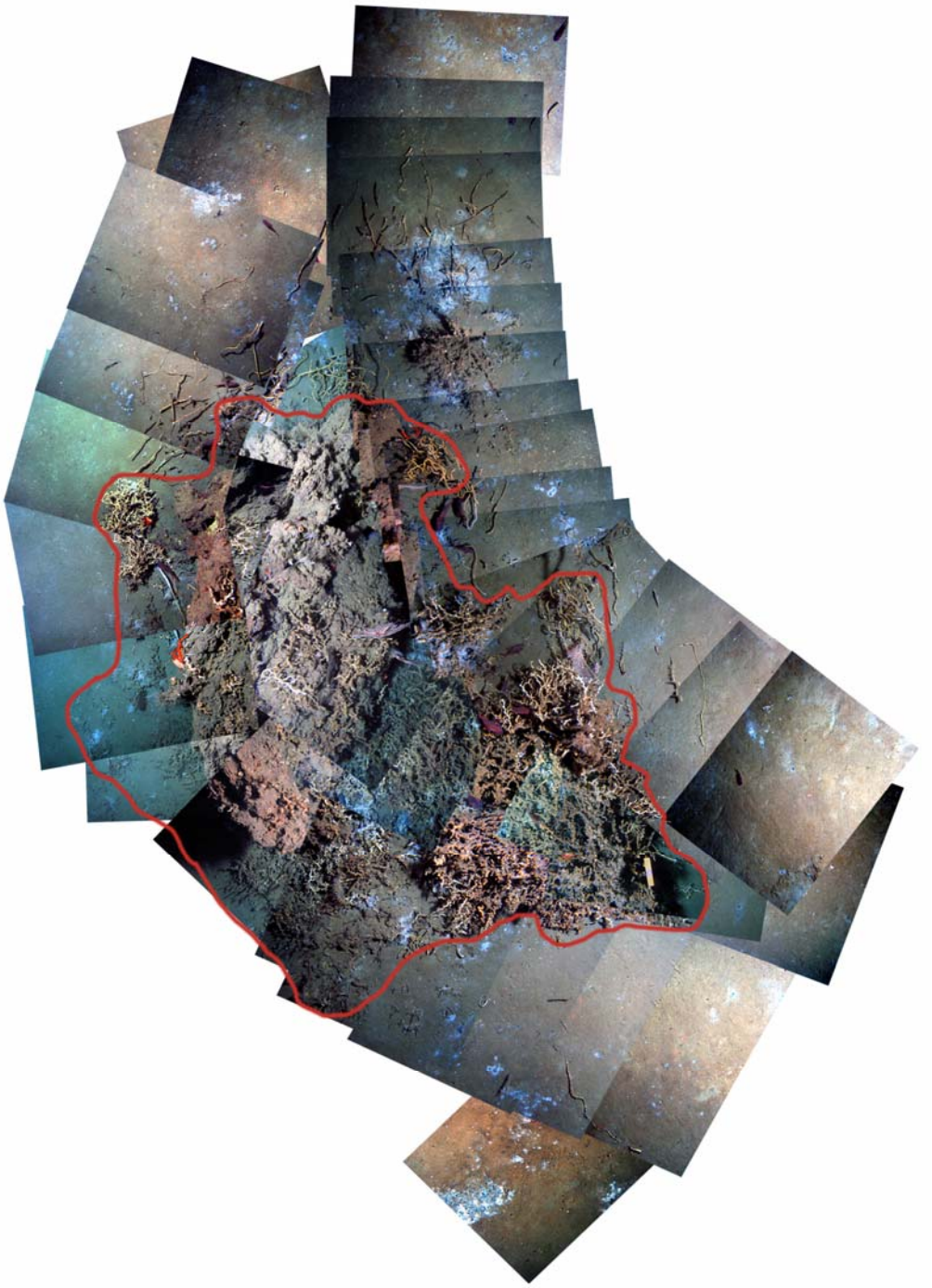

A.3. Green Canyon 234 – JSL Dive No. 4728.

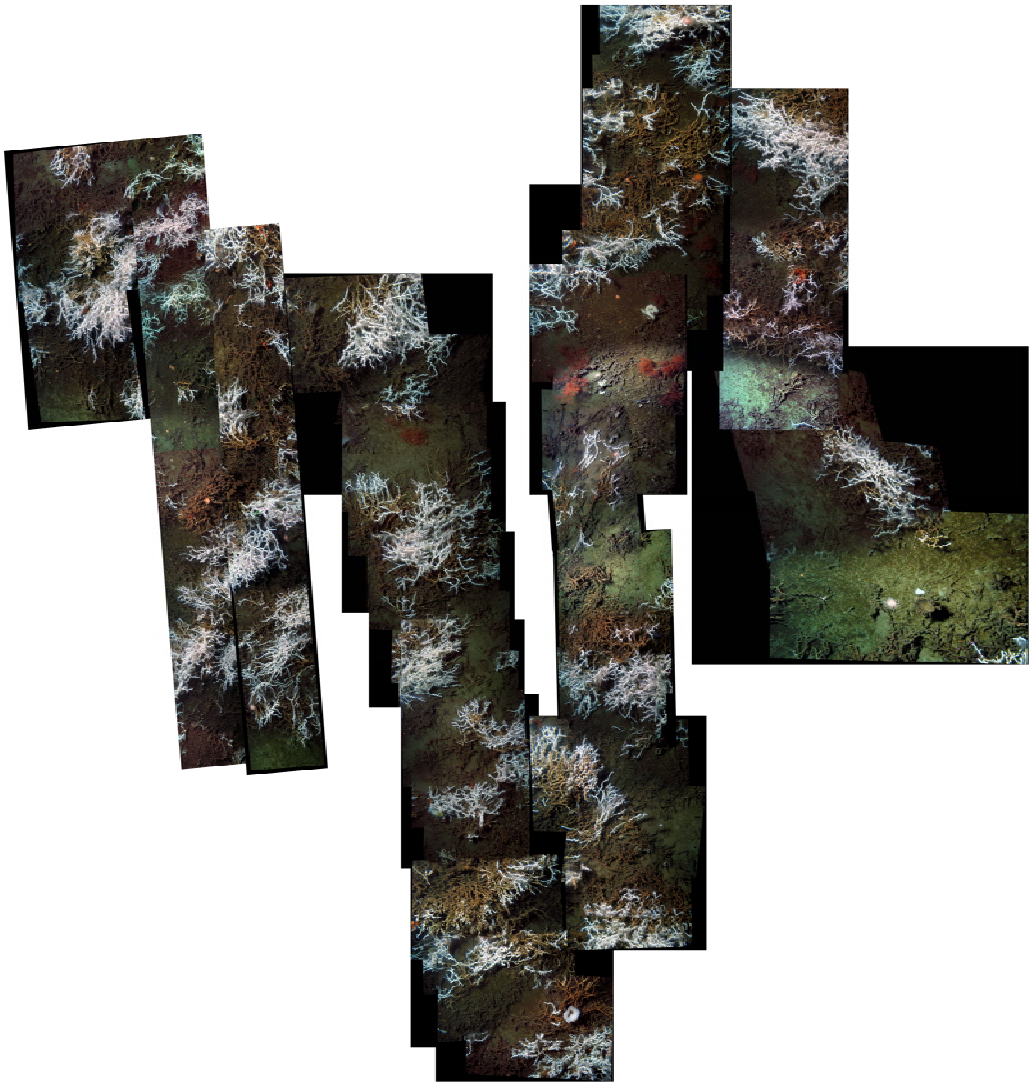

A.4. Viosca Knoll 826 – JSL Dive No. 4733.

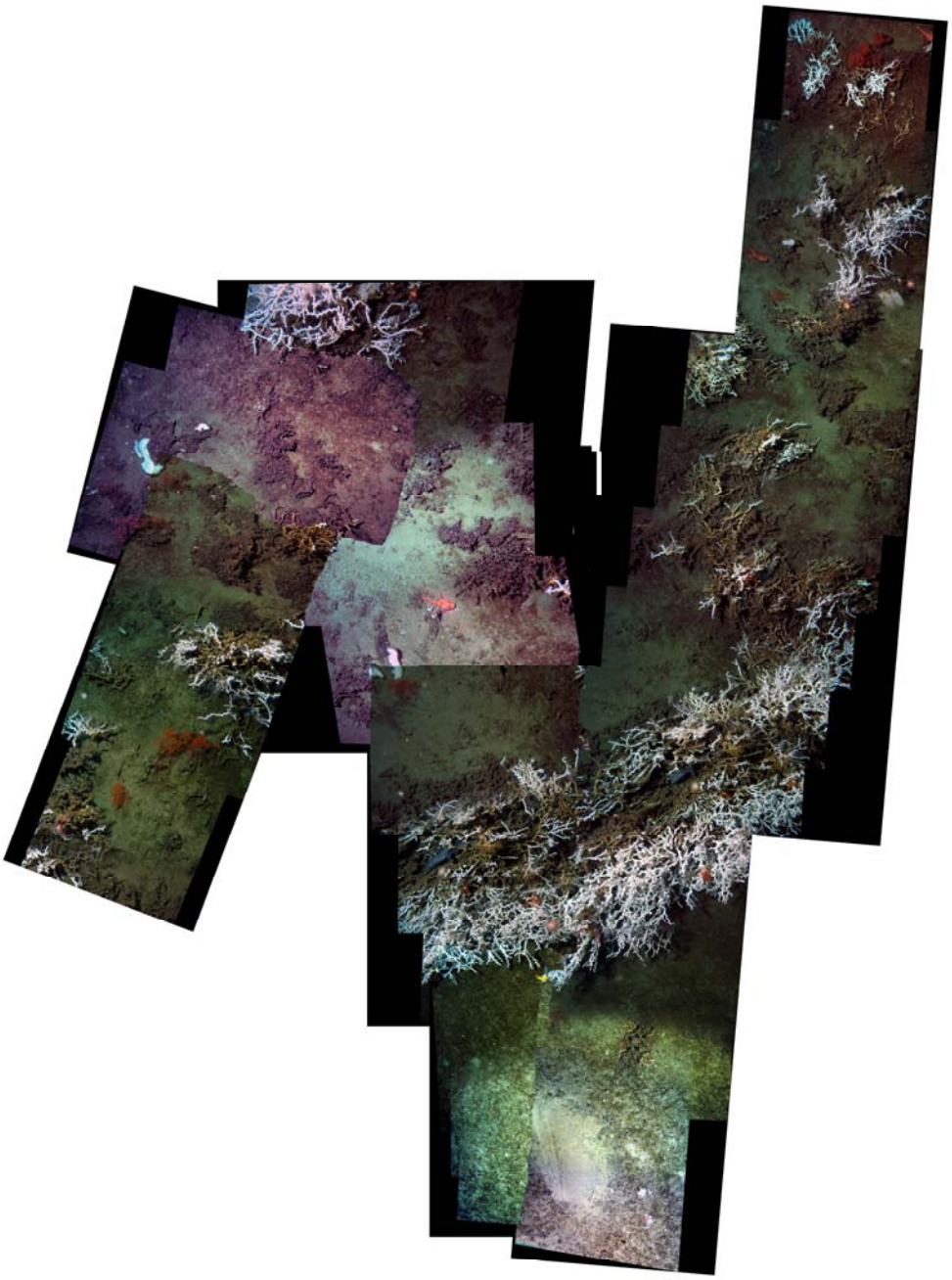

A.5. Viosca Knoll 826 – JSL Dive No. 4736. Segment 1 of 2.

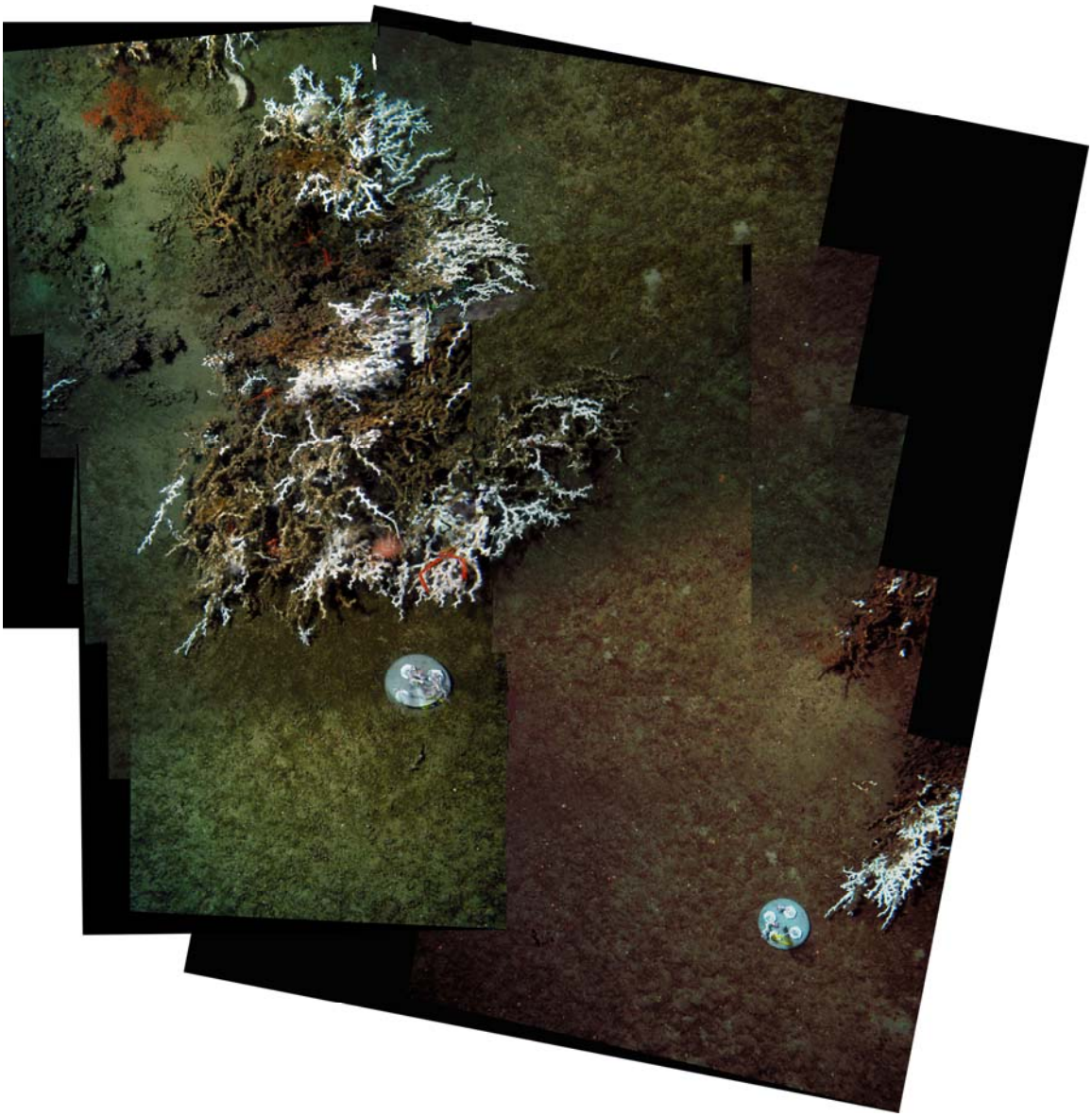

A.6. Viosca Knoll 826 – JSL Dive No. 4736. Segment 2 of 2.

A.7. Mississippi Canyon 885 – JSL Dive No. 4738.

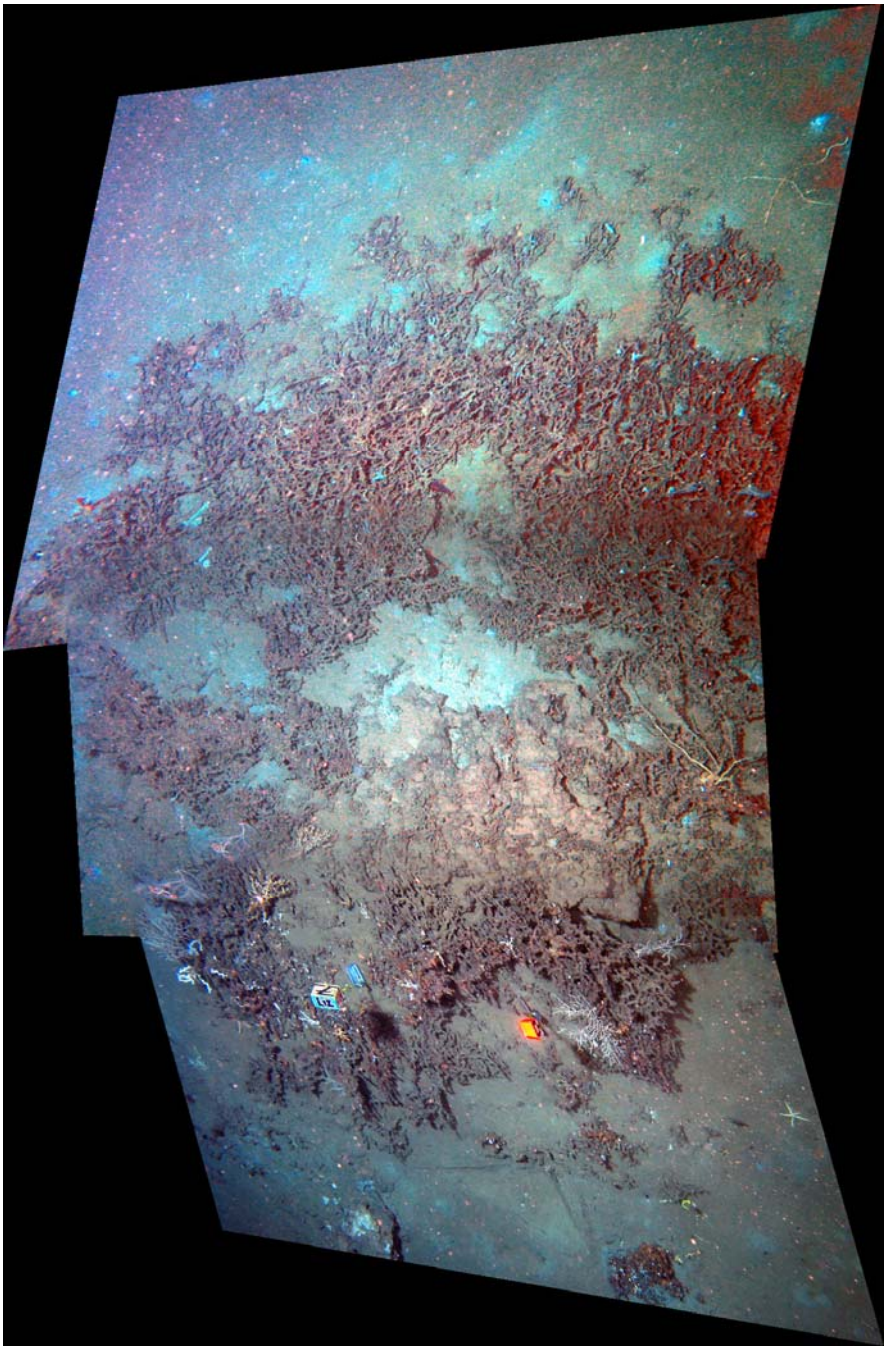

A.8. Green Canyon 234 – JSL Dive No. 4740.

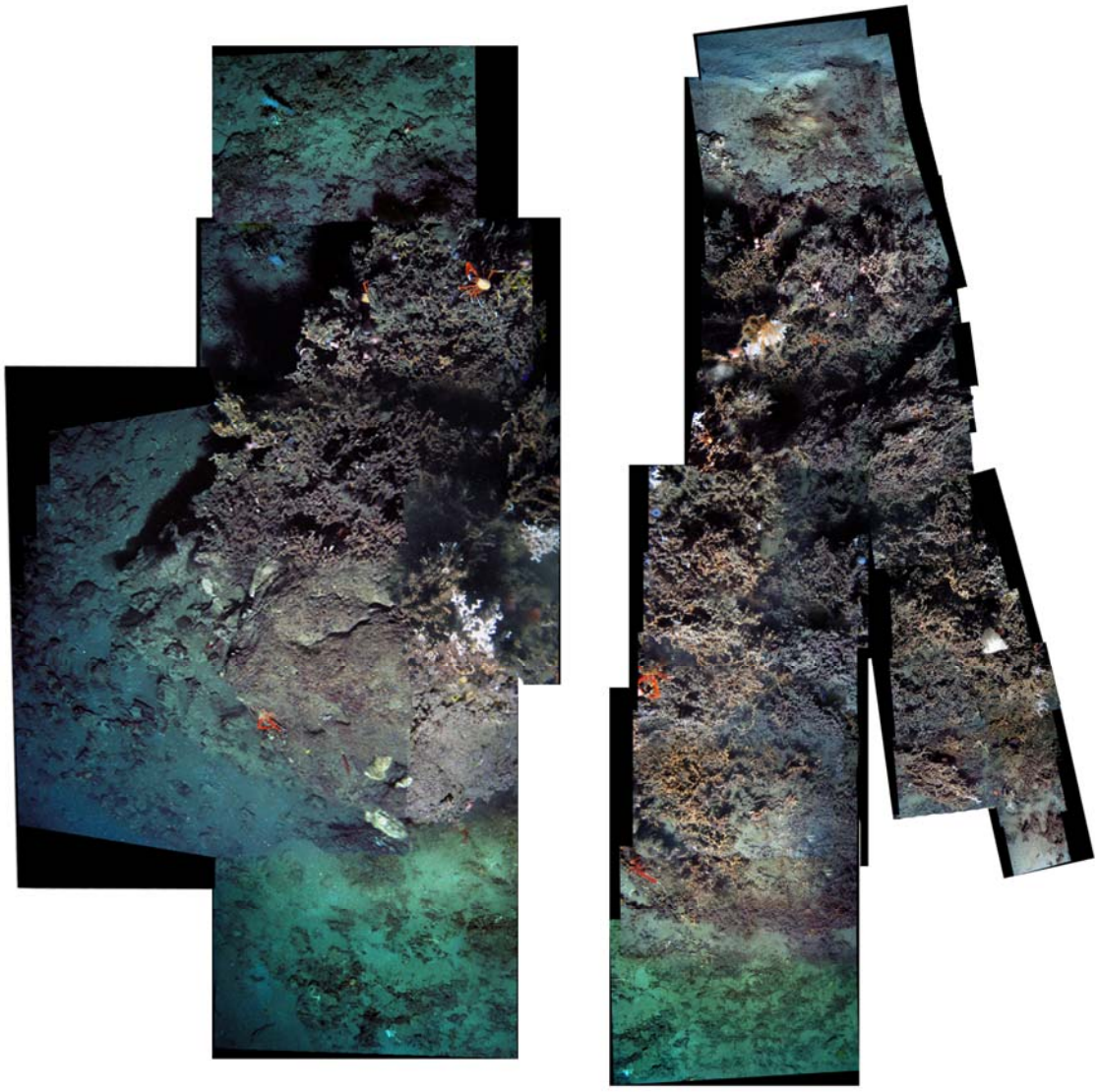

A.9. Green Canyon 354 – JSL Dive No. 4861.

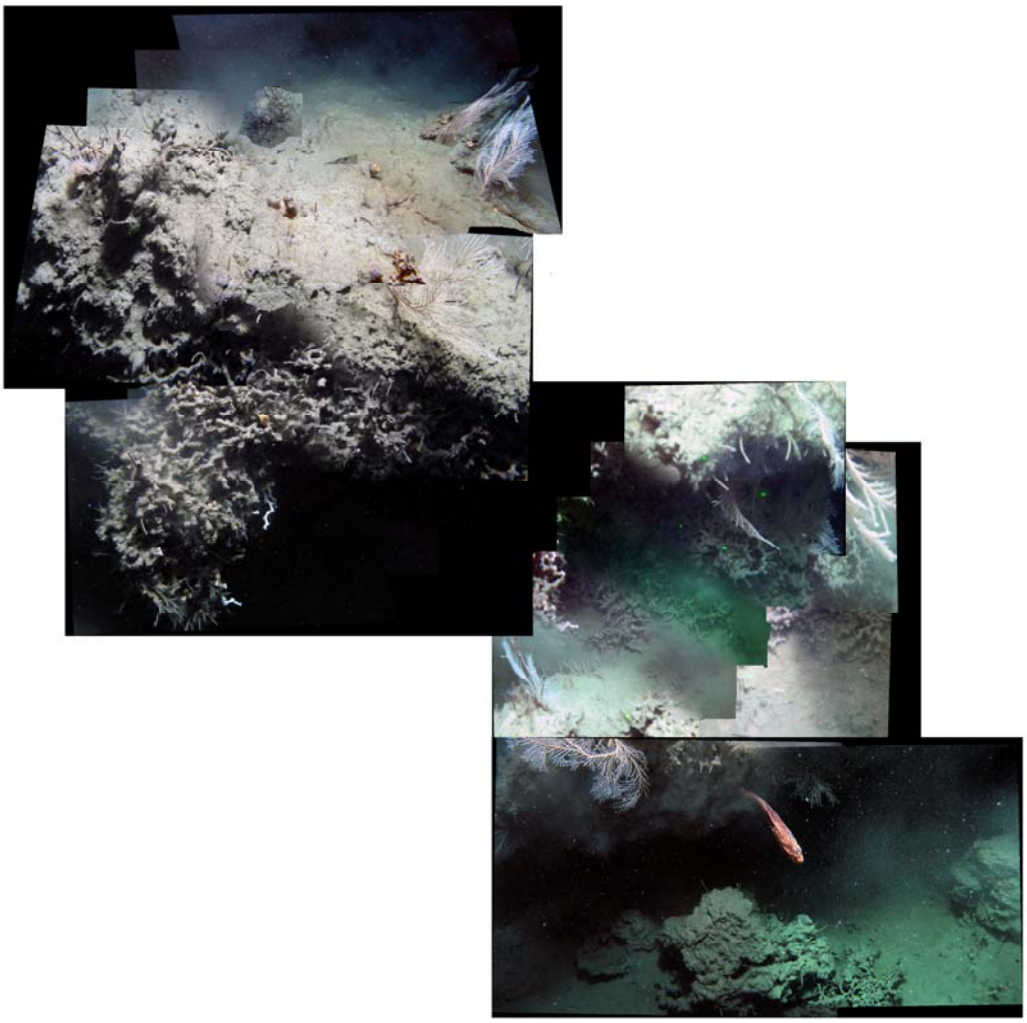

A.10. Green Canyon 184 – JSL Dive No. 4862.

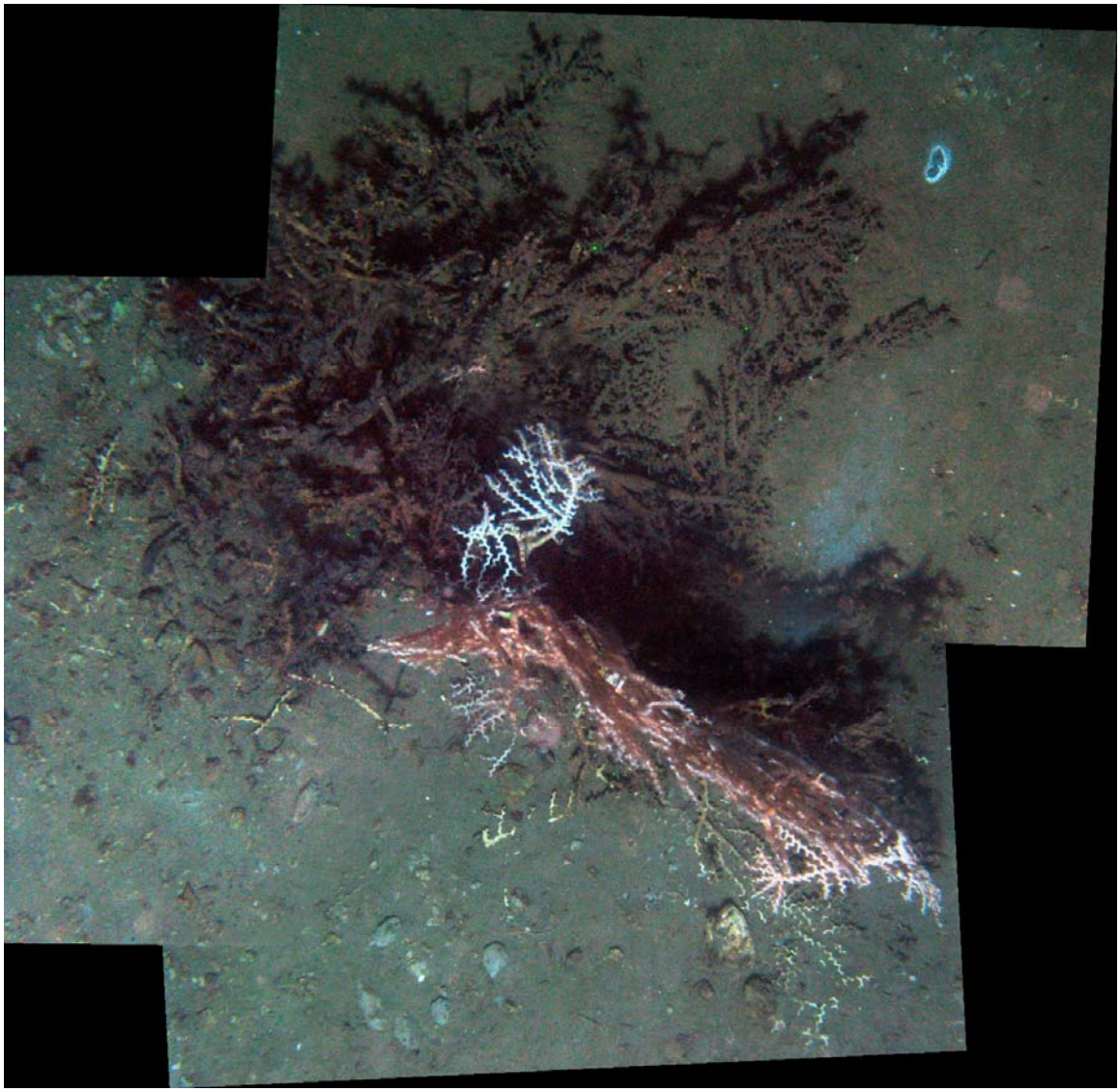

A.11. Mississippi Canyon 885 – JSL Dive No. 4863.

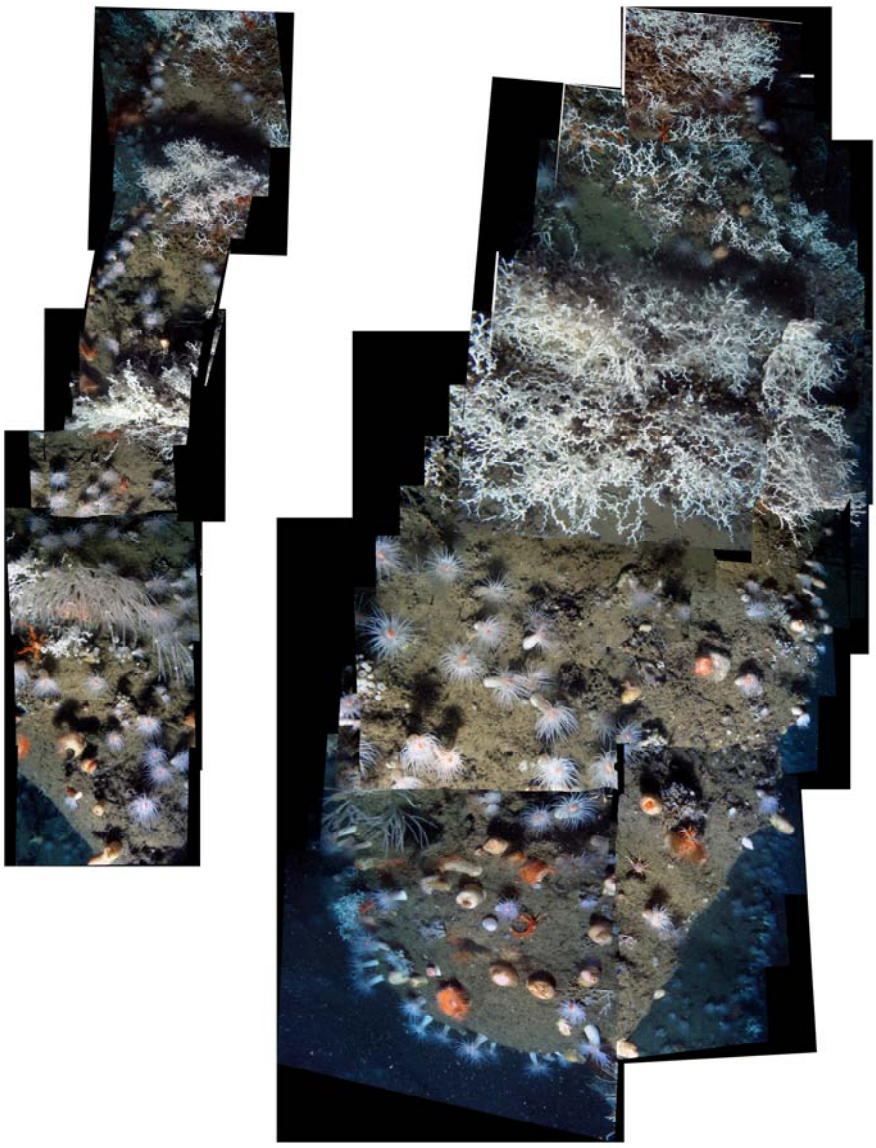

A.12. Viosca Knoll 862 – JSL Dive No. 4869.

Appendix B

Video Transect Graphs
Showing the Relative Positions of Transects
Taken at Study Sites During Cruises 1 and 2

Appendix B: Transect Analysis Graphs
B.1 Graphs showing latitude and longitude of transects taken at each of the study sites

B.1a VK 826. Transects 1-5 were taken in 2004; transects 6 and 7 were taken in 2005 but have no start and end coordinates.

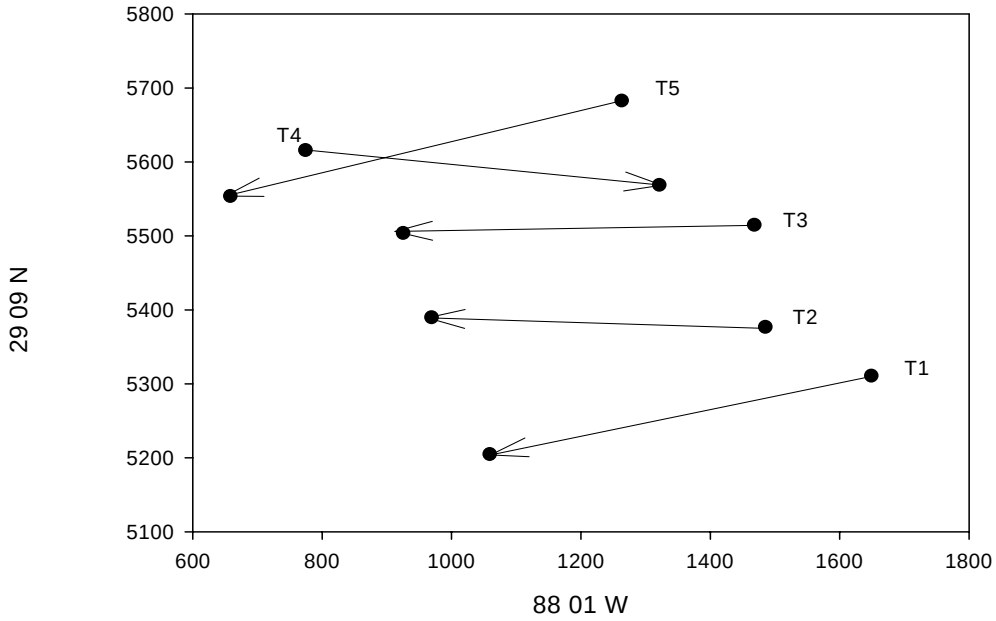

B.1b VK 826 NE

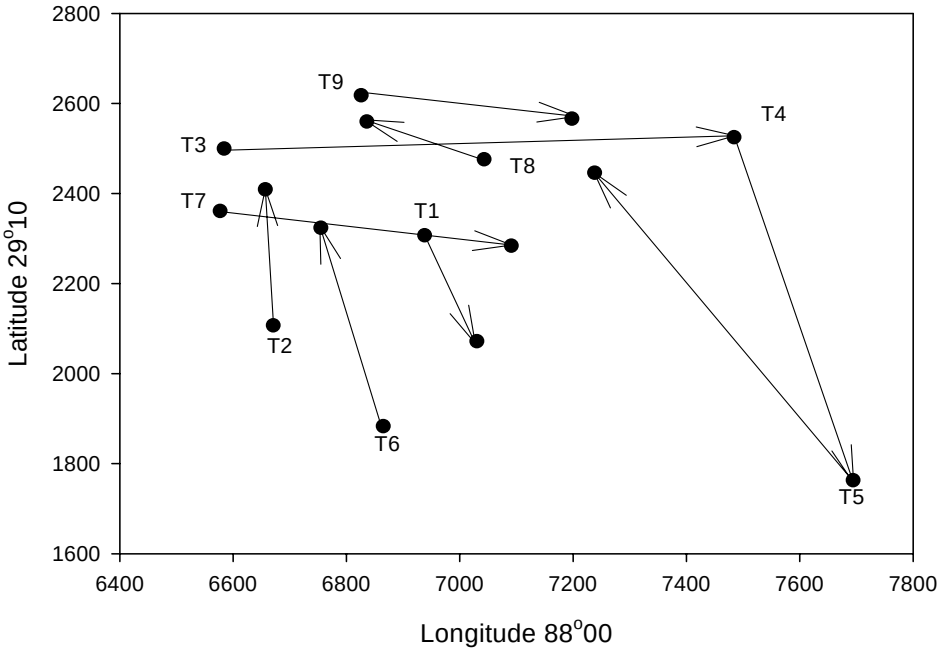

B.1c GC 234

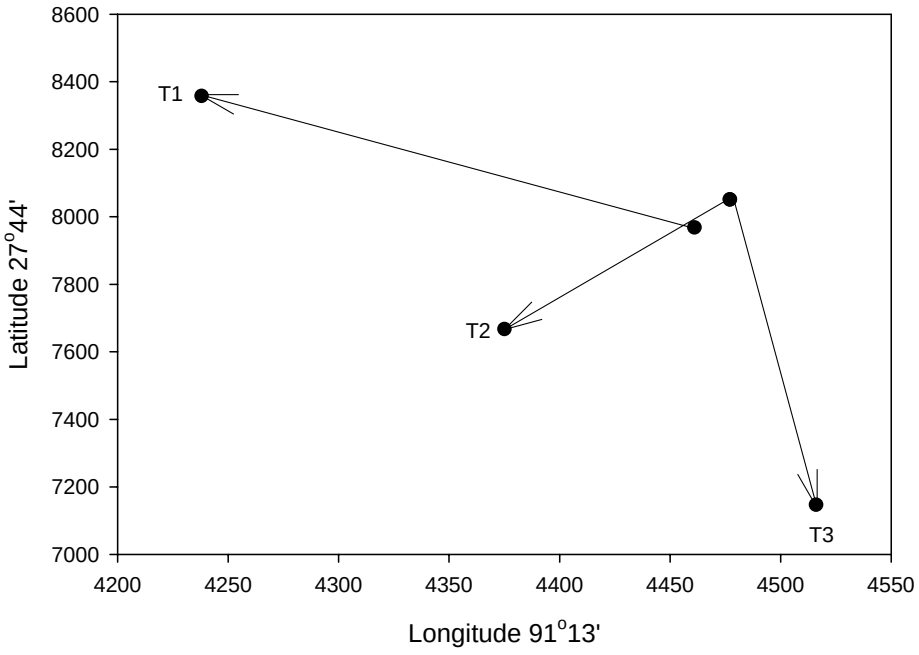

B.1d GC 354

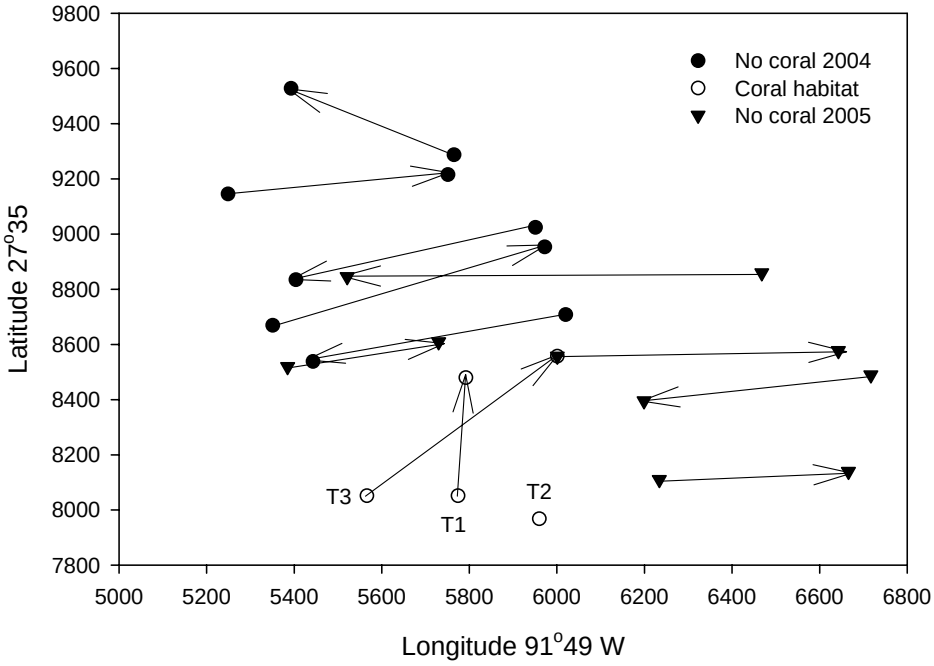

B.1e VK 862

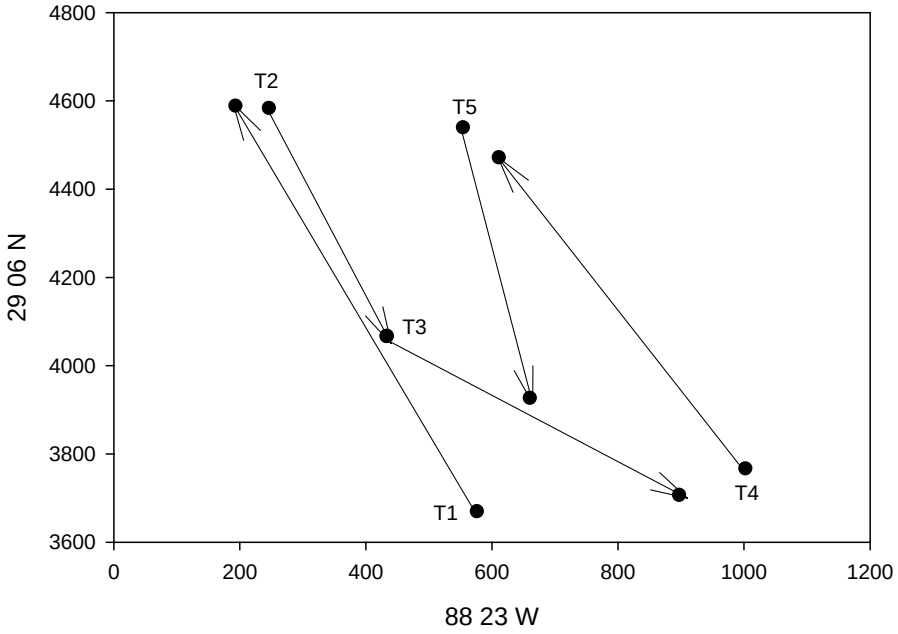

B.1f MC 885

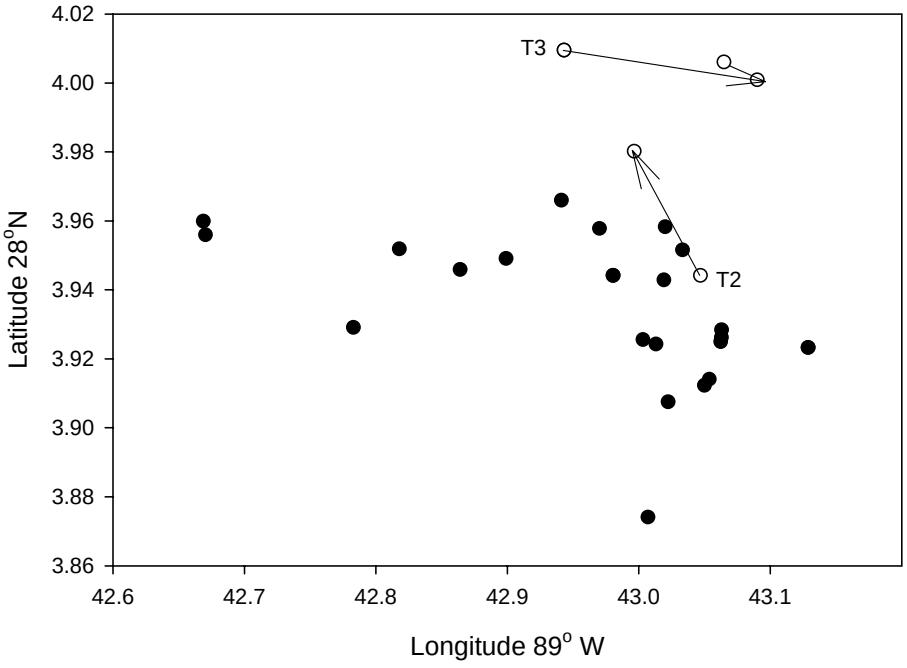

Appendix B.2 a-g: Graphs showing percentage cover of live (closed circles) and dead (open circles) of *L. pertusa* at VK826. Five transects were taken in 2004 (a-e) and two in 2005 (f-g).

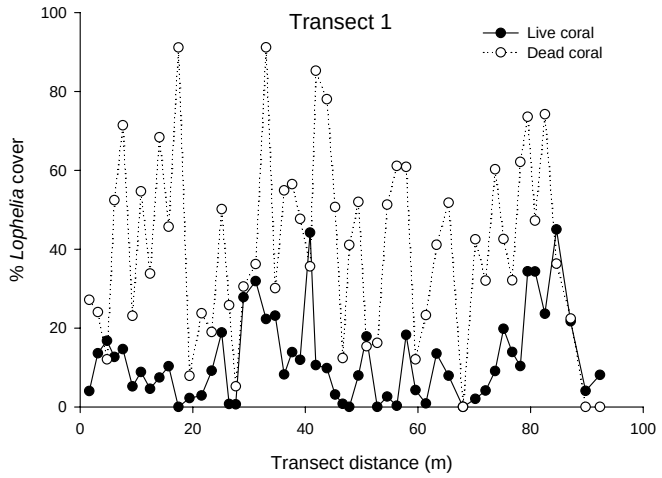

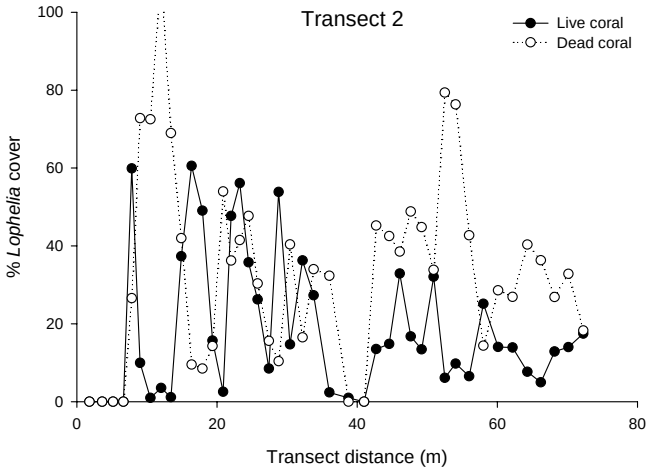

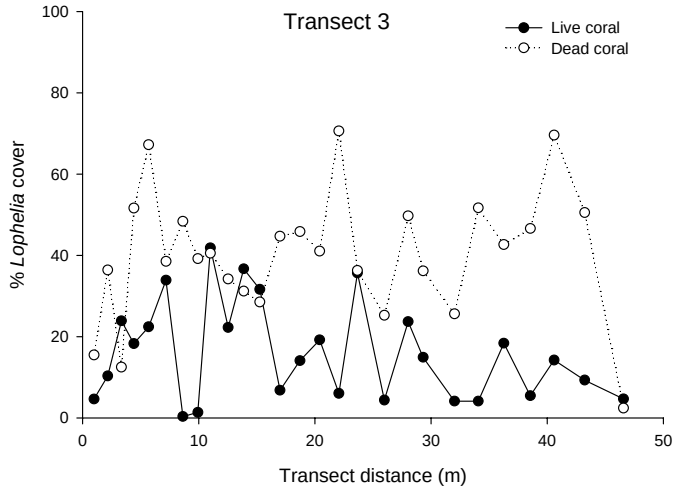

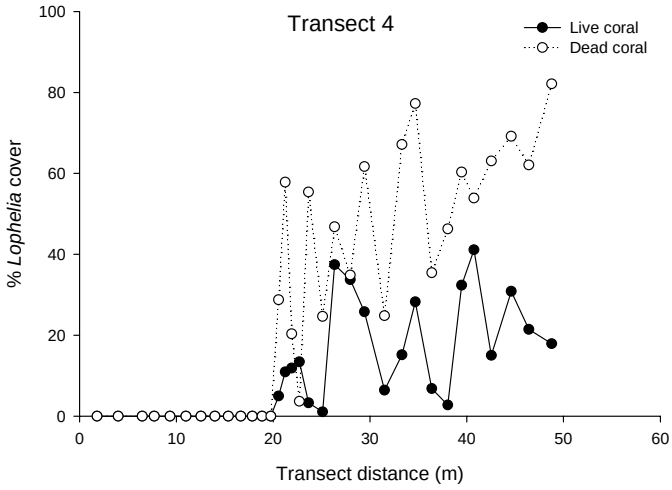

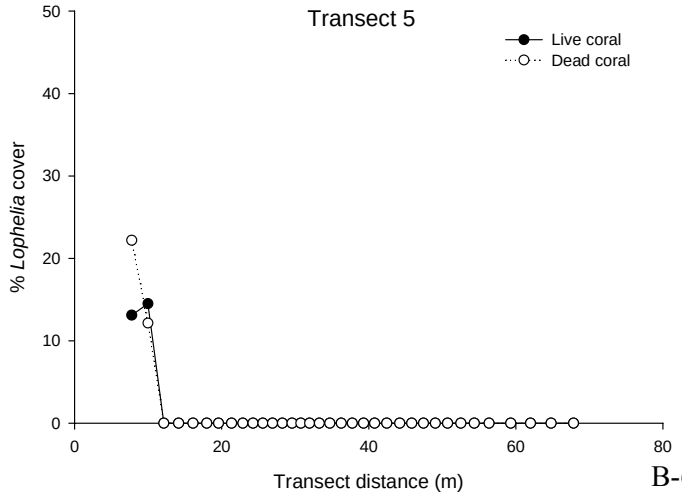

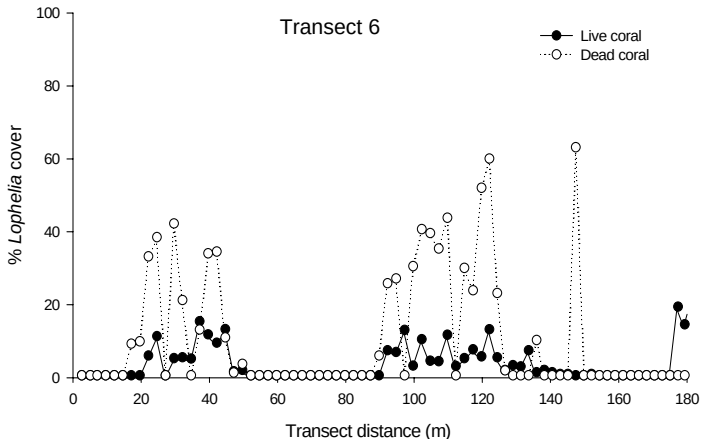
Transect 6
Live coral
Dead coral
% Lophelia cover
Transect distance (m)
0
20
40
60
80
100
120
140
160
180

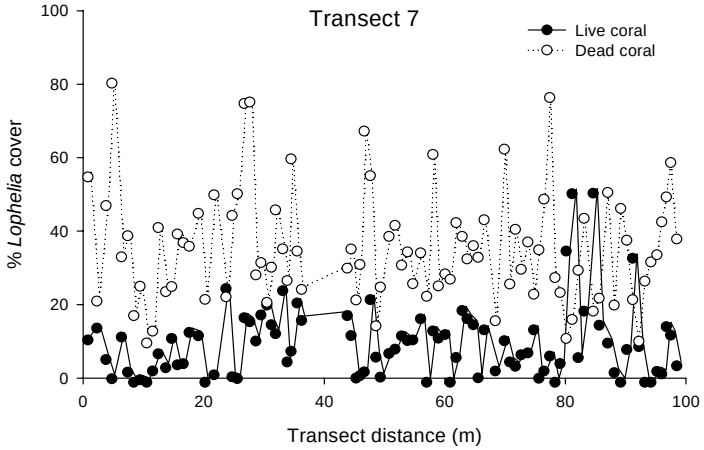
Transect 7
Live coral
Dead coral
% Lophelia cover
Transect distance (m)
0
20
40
60
80
100

Appendix B.3 a-i. Graphs showing percentage cover of live (closed circles) and dead (open circles) of *L. pertusa* at VK826 NE from nine transects taken in 2005.

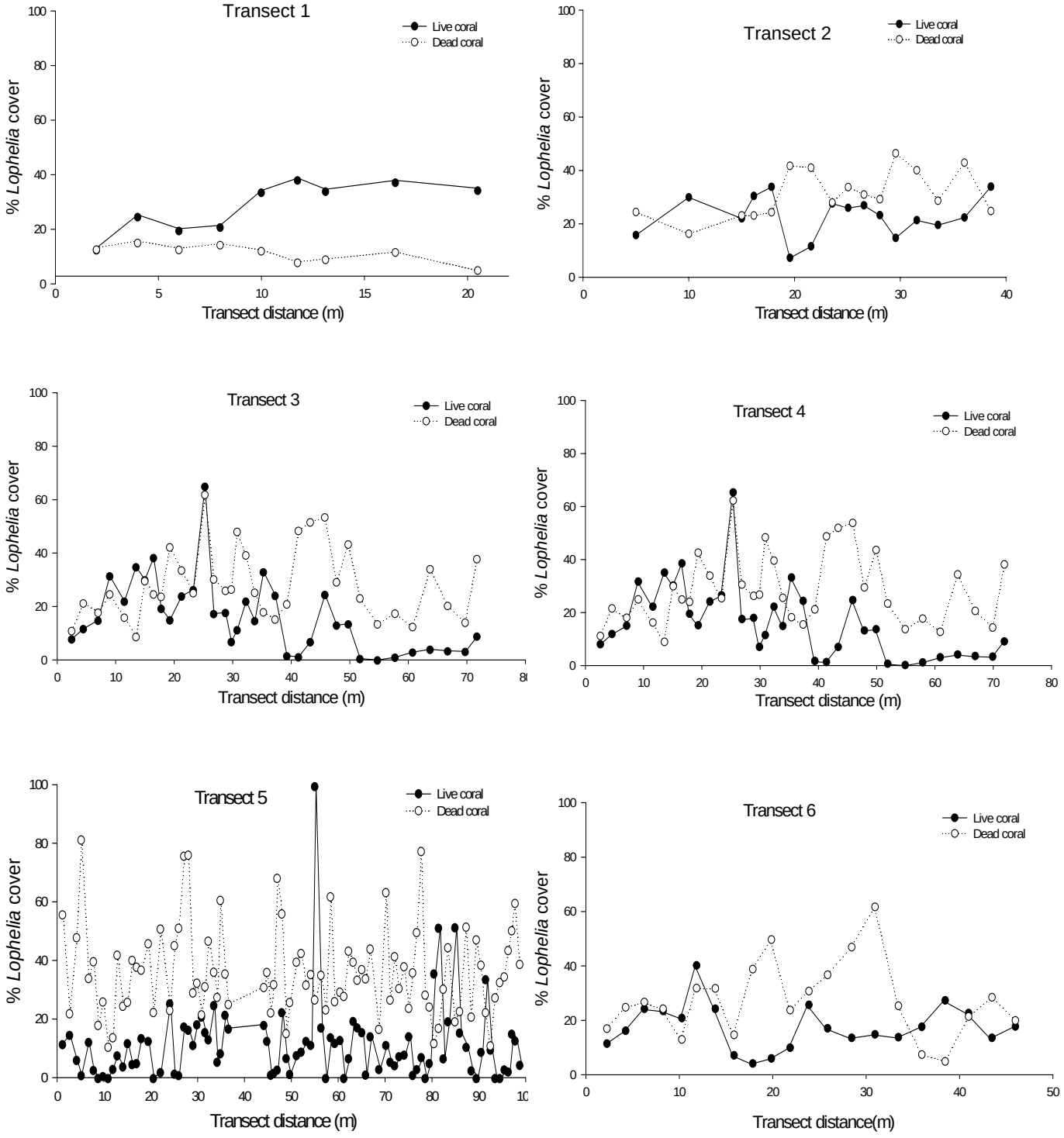

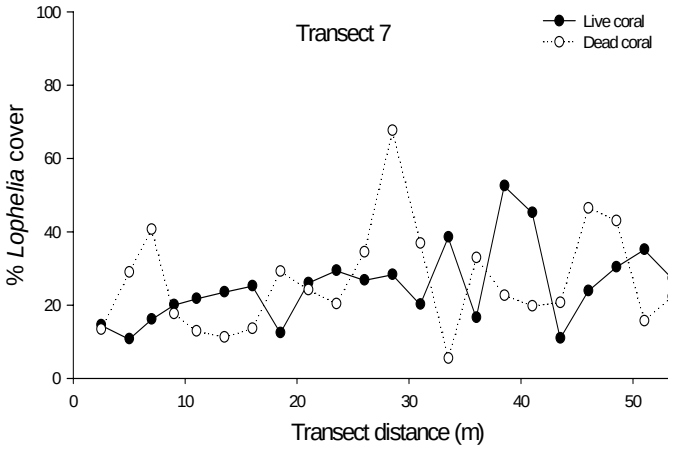
Transect 7
Live coral
Dead coral
% Lophelia cover
Transect distance (m)
0
10
20
30
40
50
60
80
100

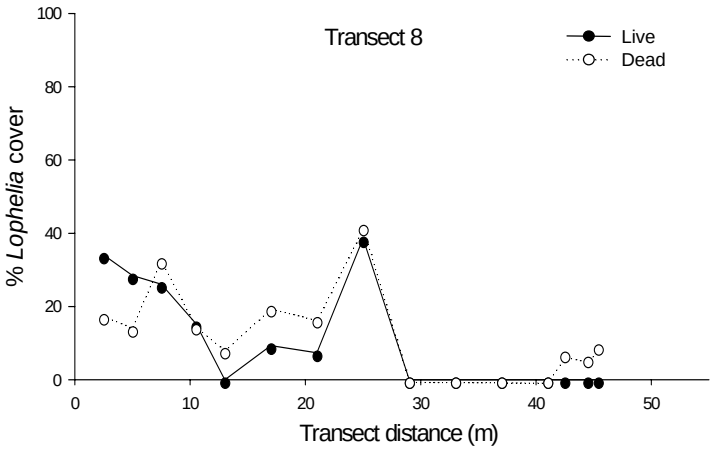
Transect 8
Live
Dead
% Lophelia cover
Transect distance (m)
0
10
20
30
40
50
60
80
100

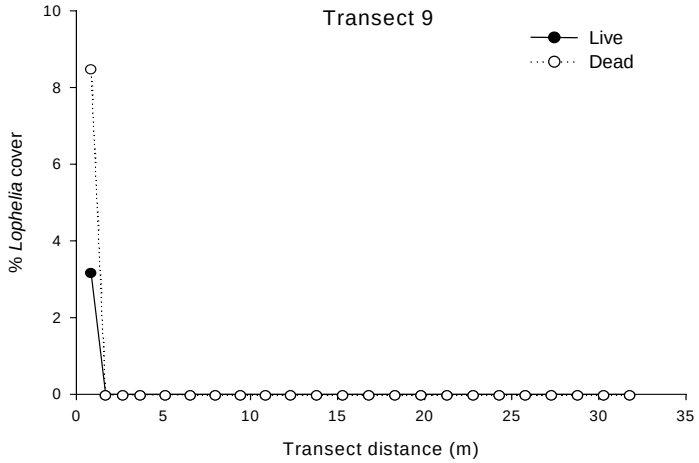
Transect 9
Live
Dead
% Lophelia cover
Transect distance (m)
0
2
4
6
8
10
0
5
10
15
20
25
30
35

Appendix B.4a-c Graphs showing percentage cover of live (closed circles) and dead (open circles) of *L. pertusa* at GC 234 and number of individuals from three transects taken in 2004

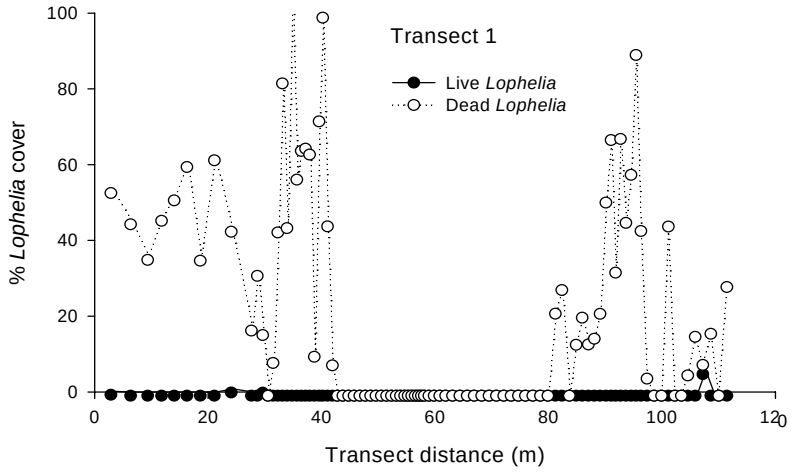

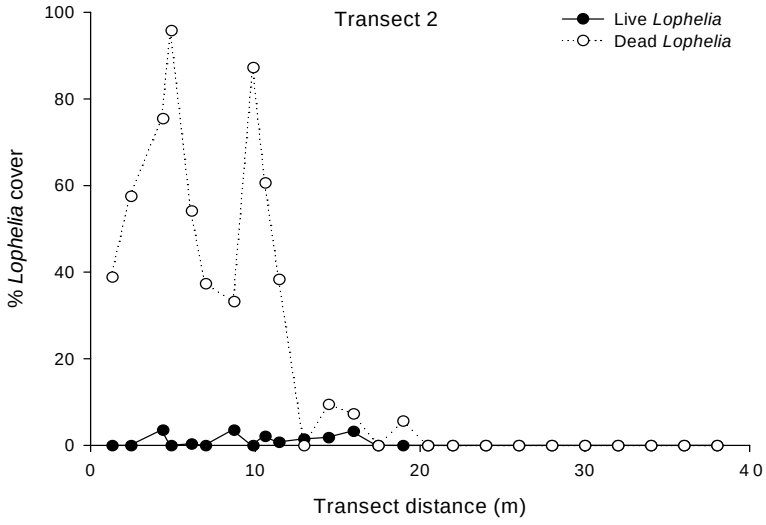

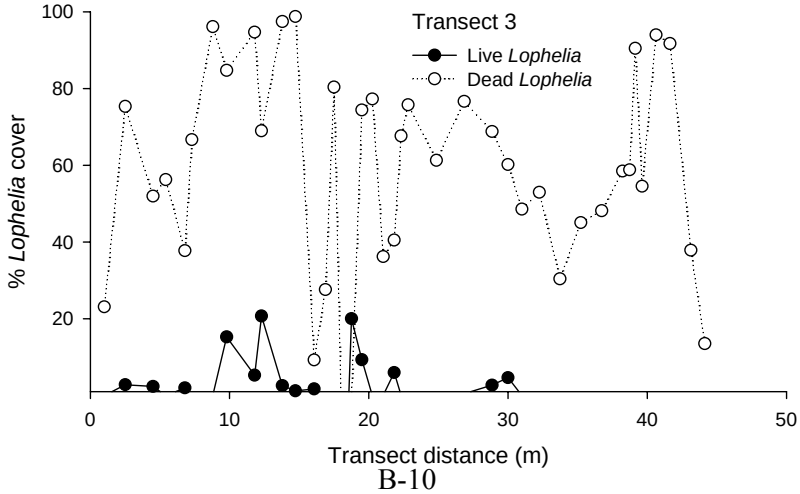

Appendix B.5a-c. Graphs showing percentage cover of live (closed circles) and dead (open circles) of *L. pertusa* at GC 354 from three transects were taken in 2004.

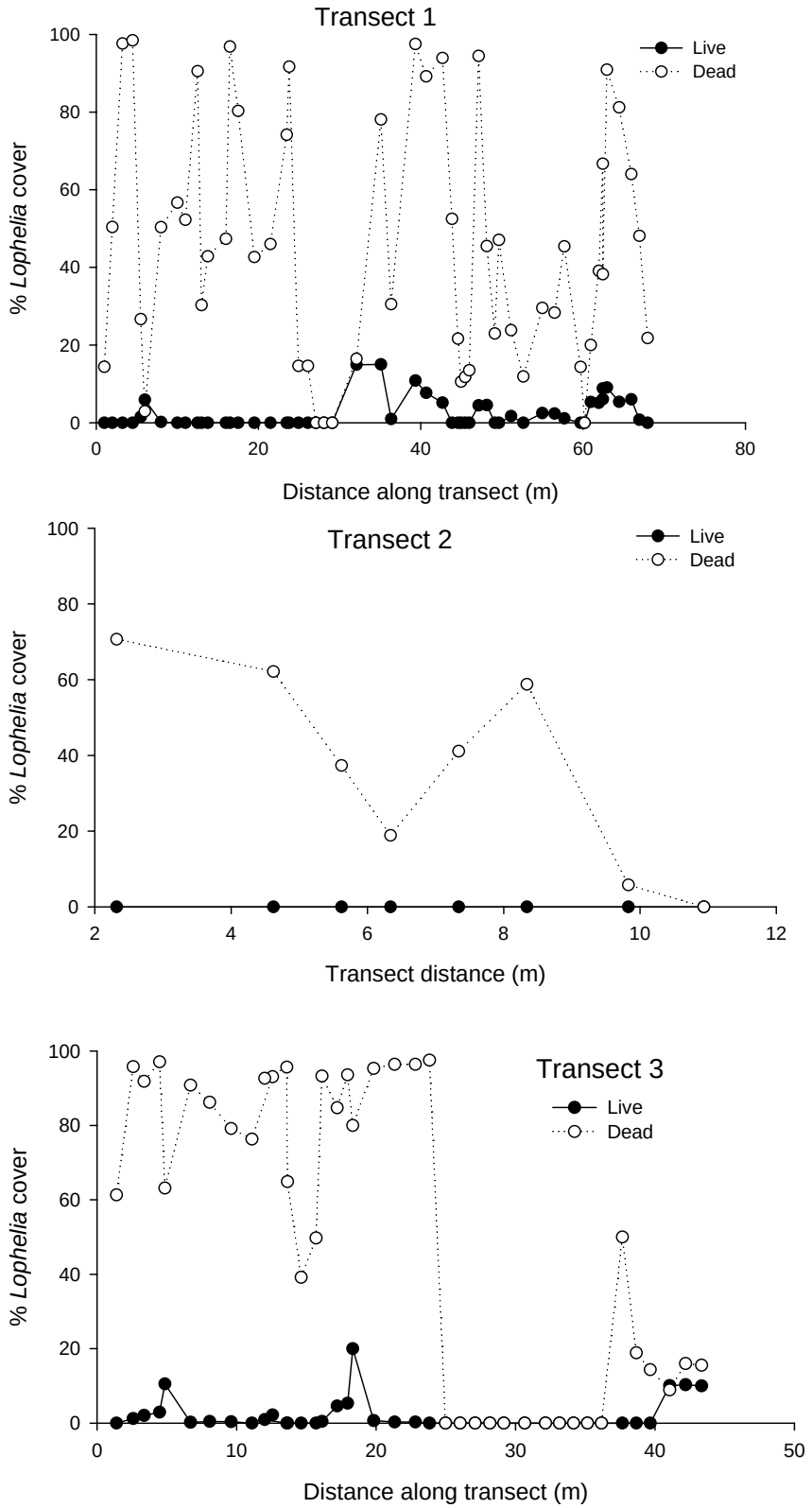

Appendix B.6 a-e. Graphs showing abundance of anemones along five transects at VK862, taken in 2004.

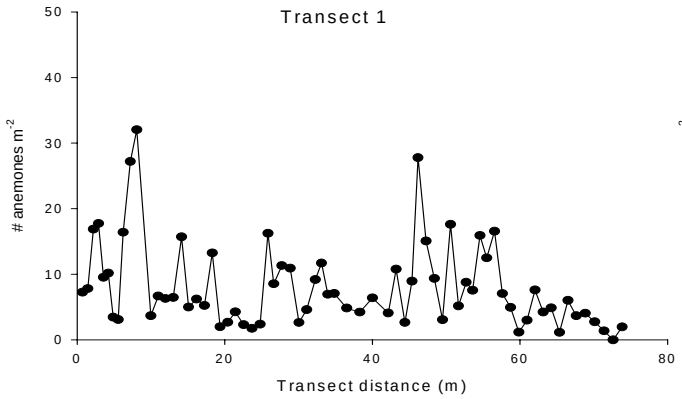

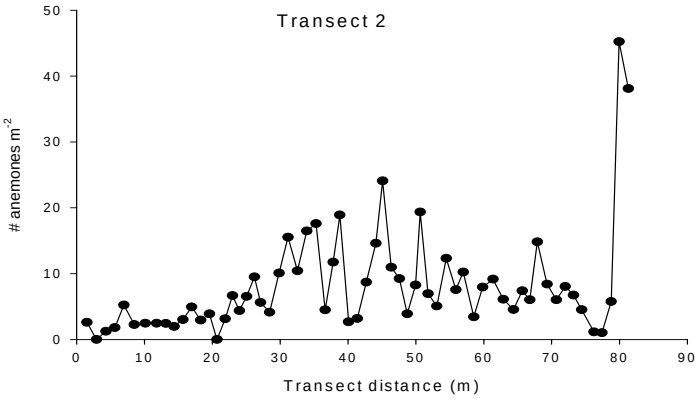

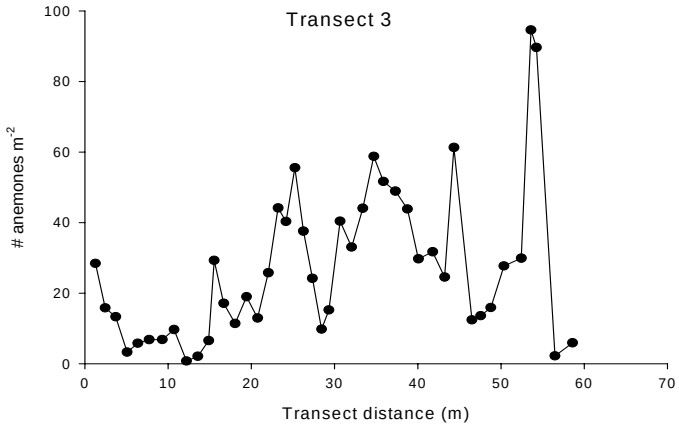

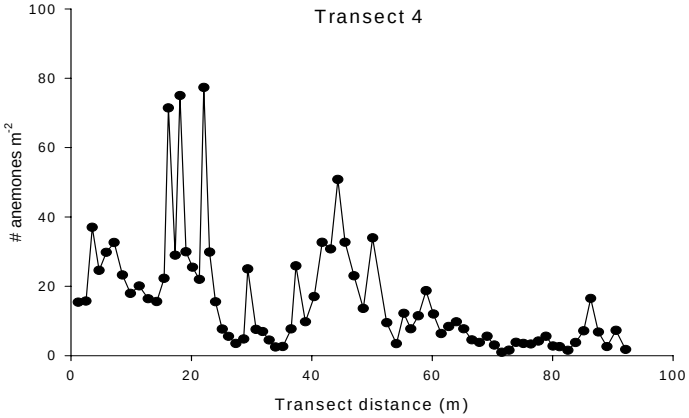

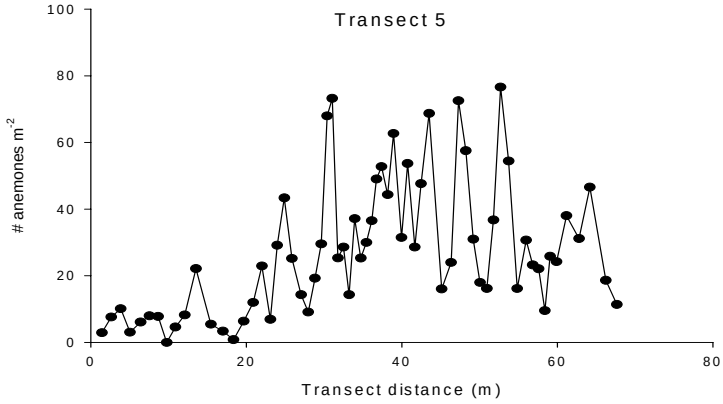

Appendix C

Common Cnidarians Observed and Collected at Sites During the Study Program

Leiopathes spp.

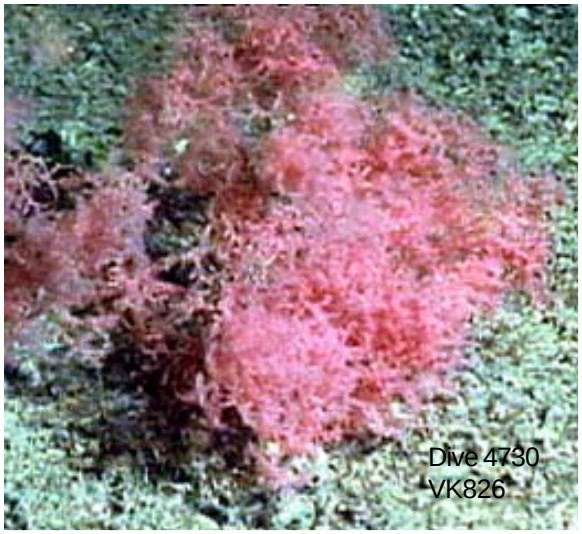

Keratoisis flexibilis

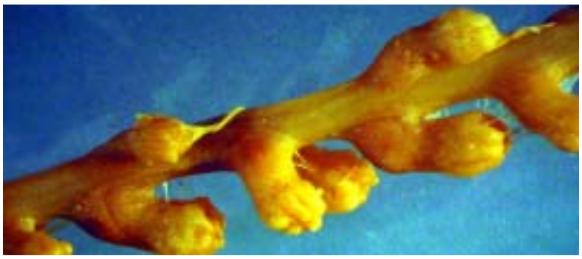

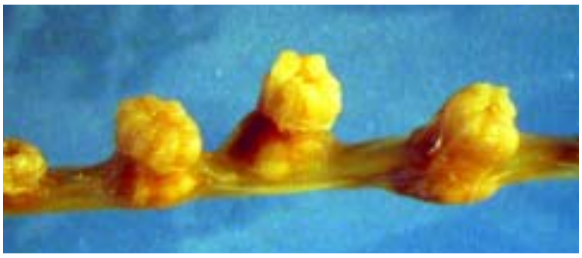

Muricides hirta

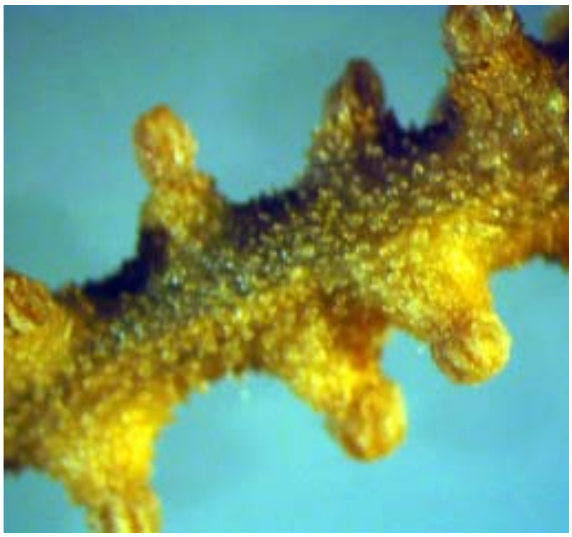

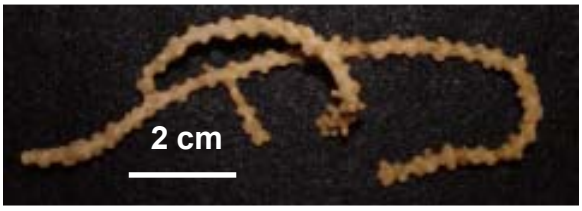

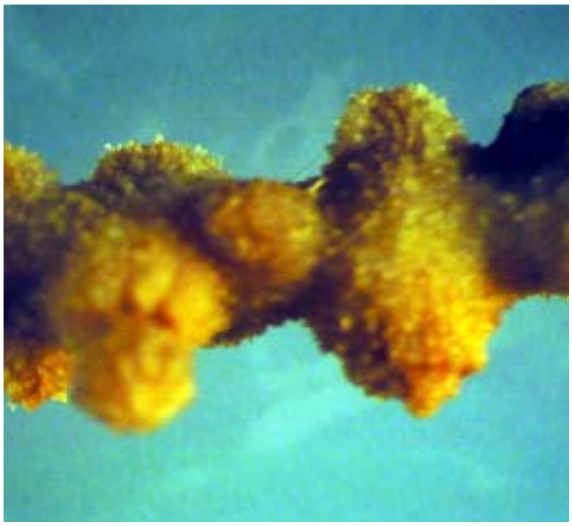

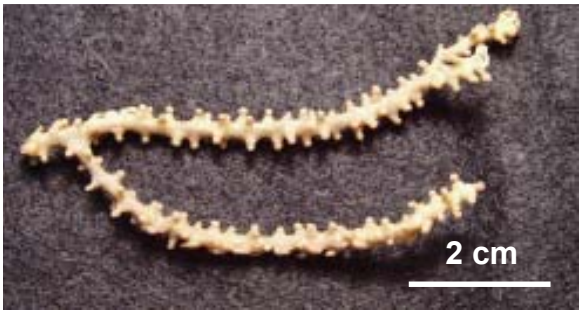

Callogorgia americana

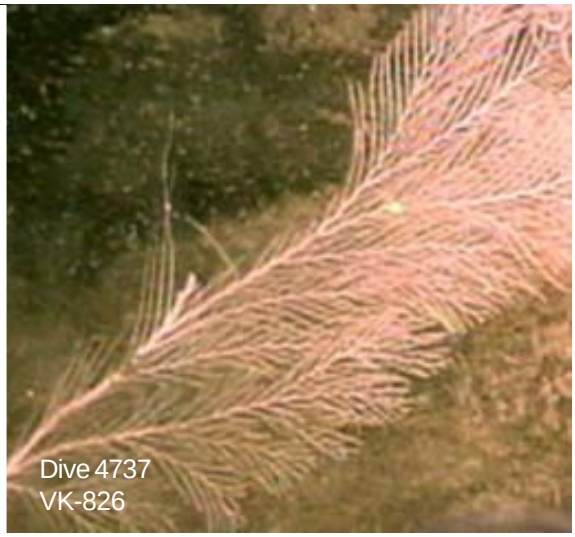

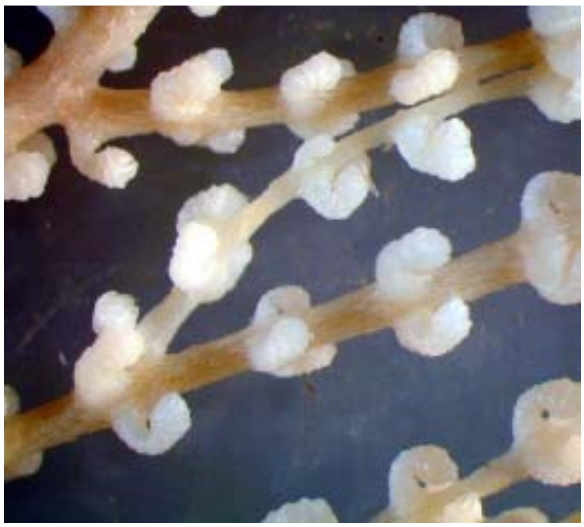

Anthothela tropicalis

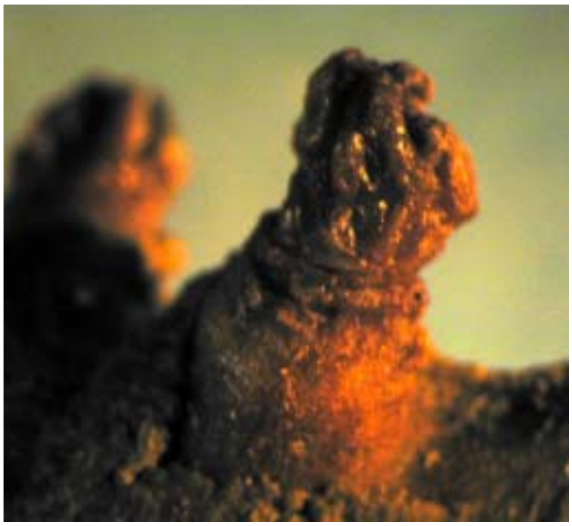

Placogorgia sp.

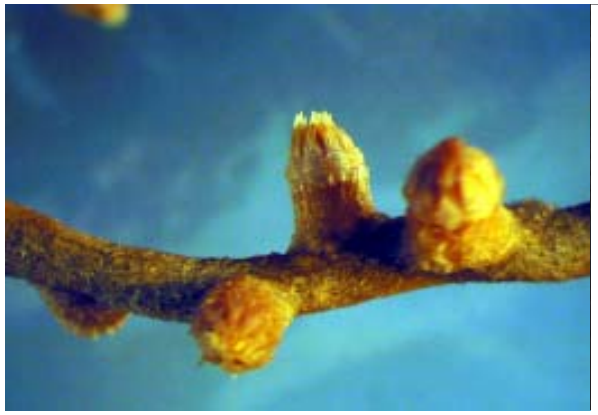

Ceriantheopsis americana

Javania cailleti (?)

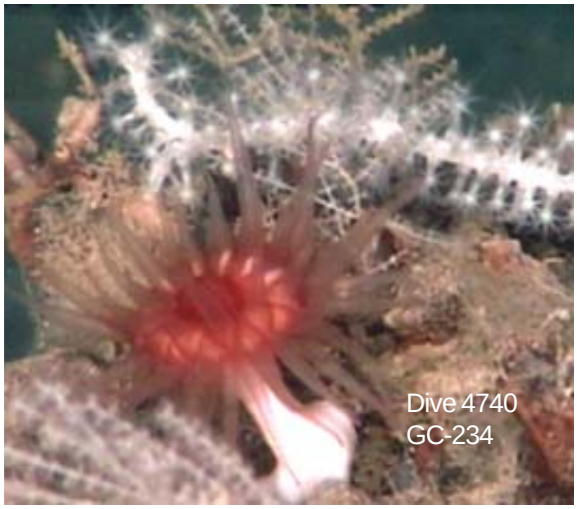

"Venus flytrap" anemone
(*Actino schyphiidae*)

Unidentified actinian

Echinomuricea sp.

Sibopathes macrospina

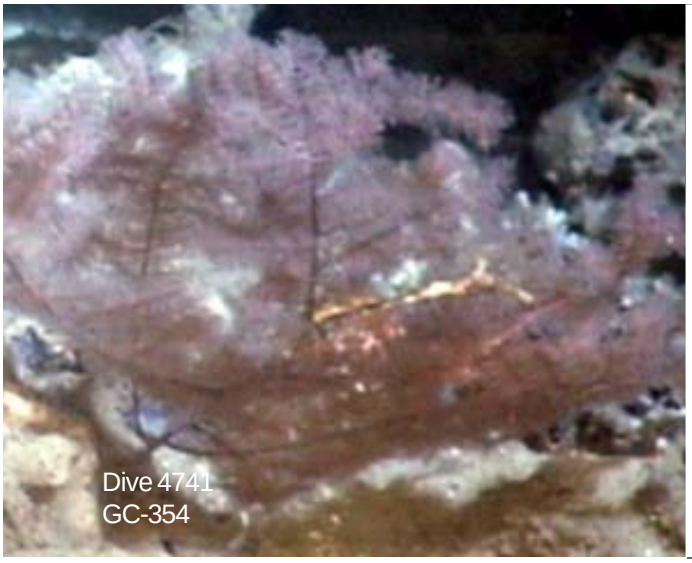

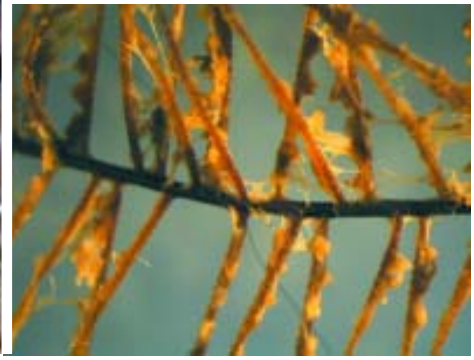

Paratcalyptrophora carinata

Anthopodium rubens

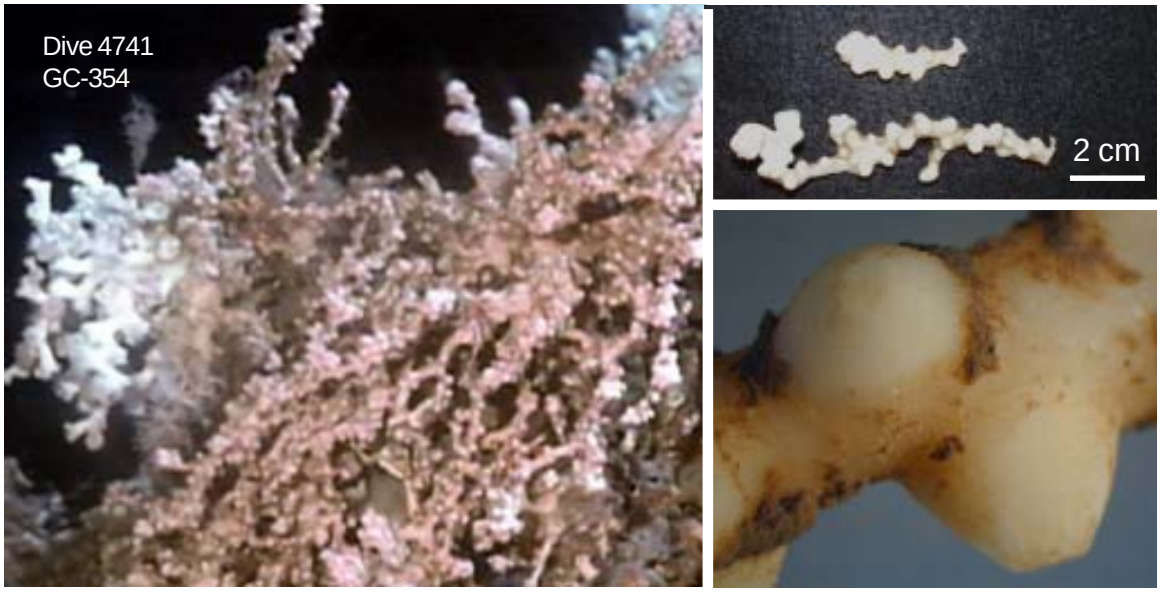

Paramuriceids

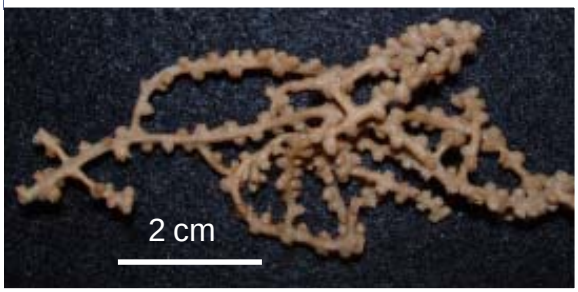

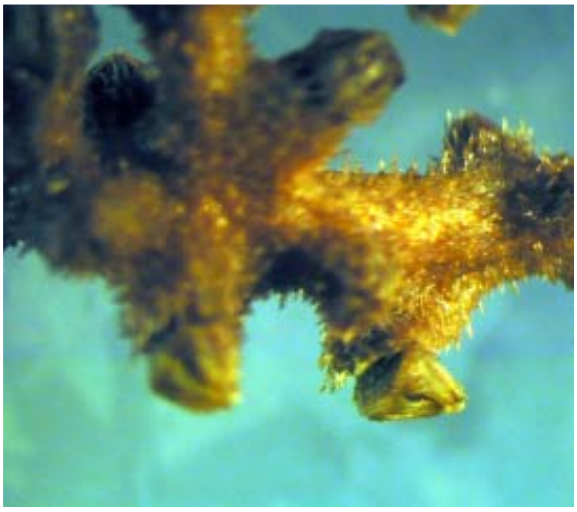

Anthomastus robustus delta

Lepidisis sp.

Appendix D

Lophelia Growth Study — Pre-Deployment and Post-Recovery Images of Colony Transplant Fragments

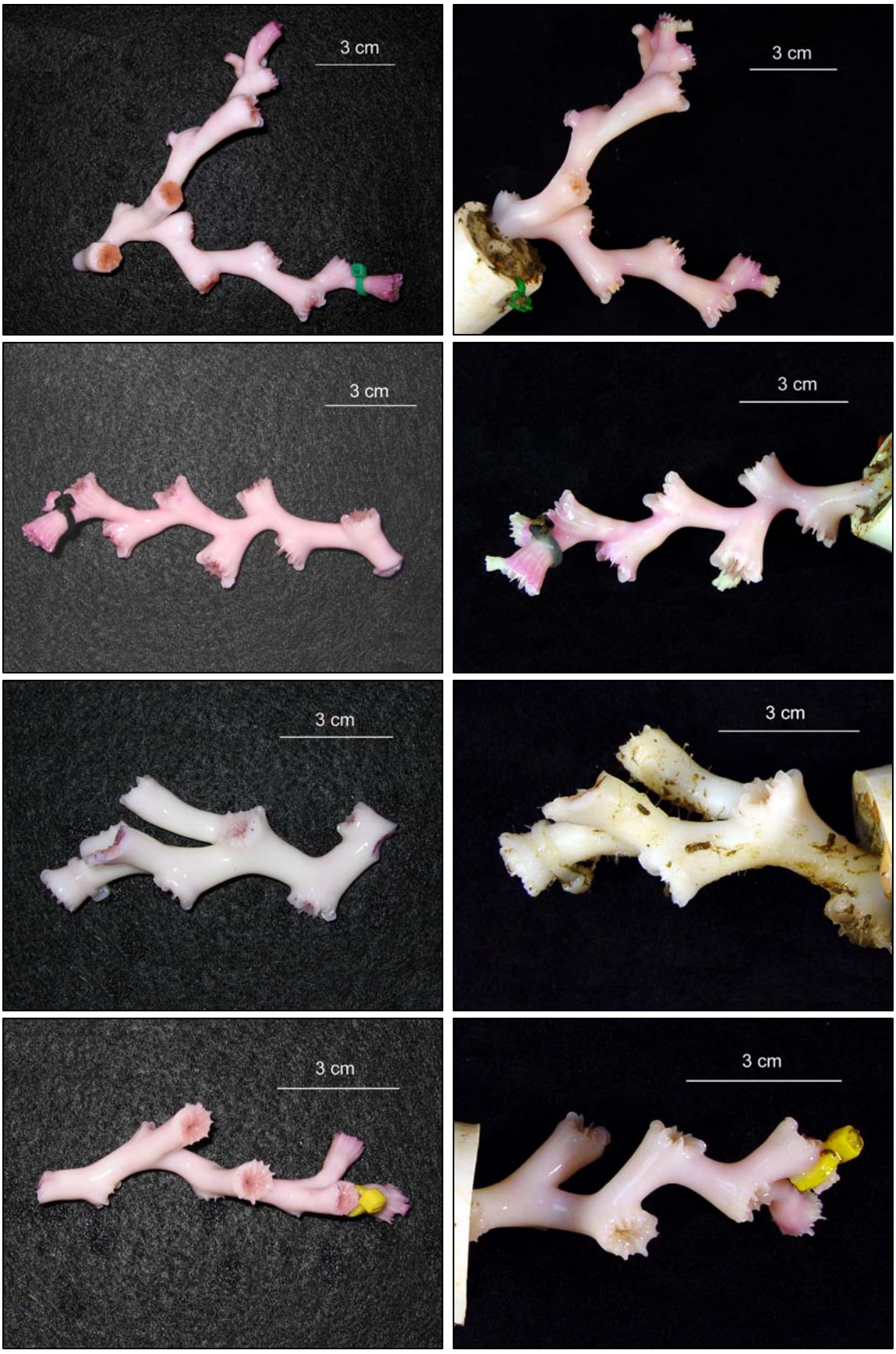
3 cm
3 cm
3 cm
3 cm
3 cm
3 cm
3 cm
3 cm

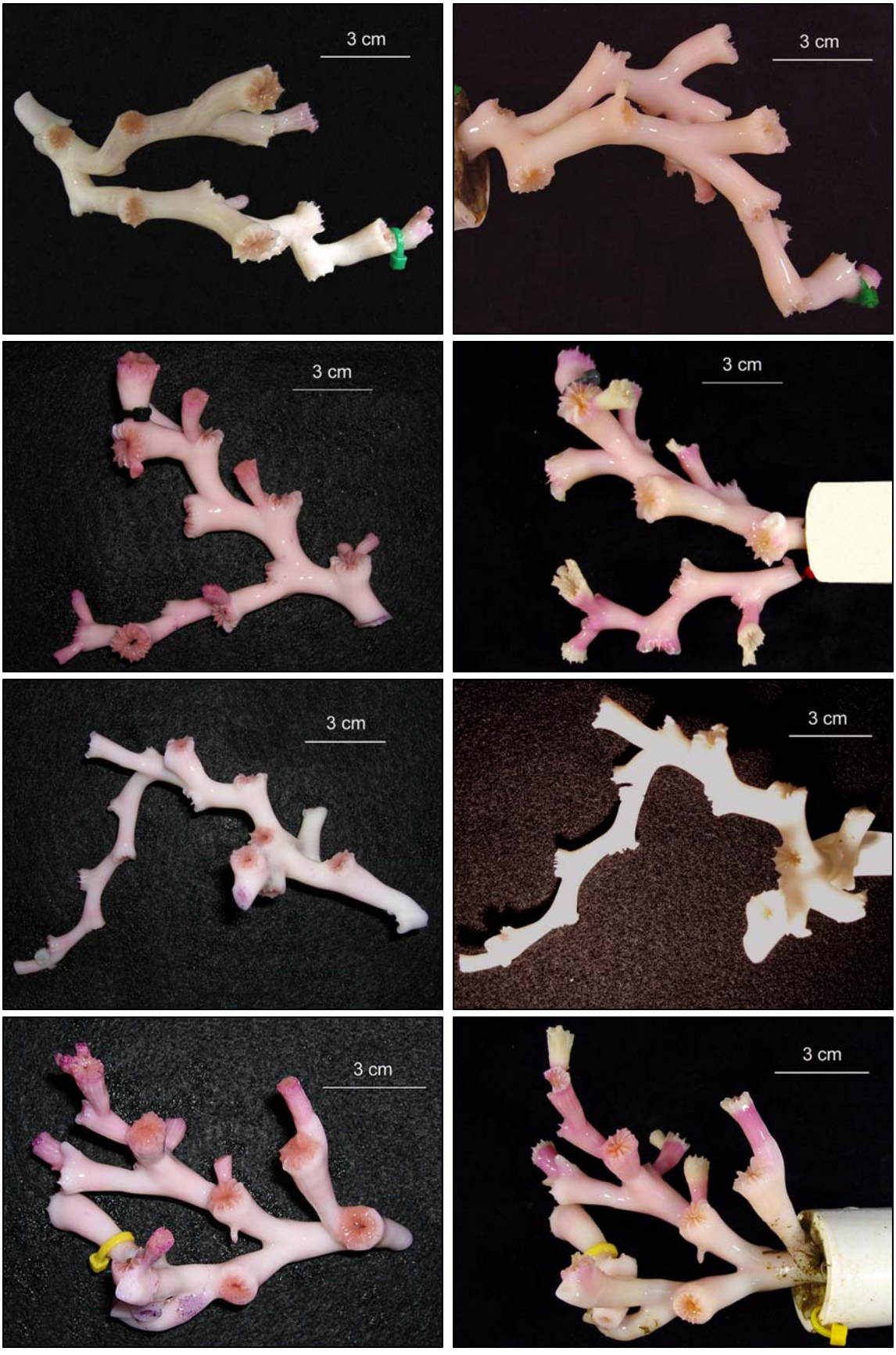
3 cm
3 cm
3 cm
3 cm
3 cm
3 cm
3 cm
3 cm

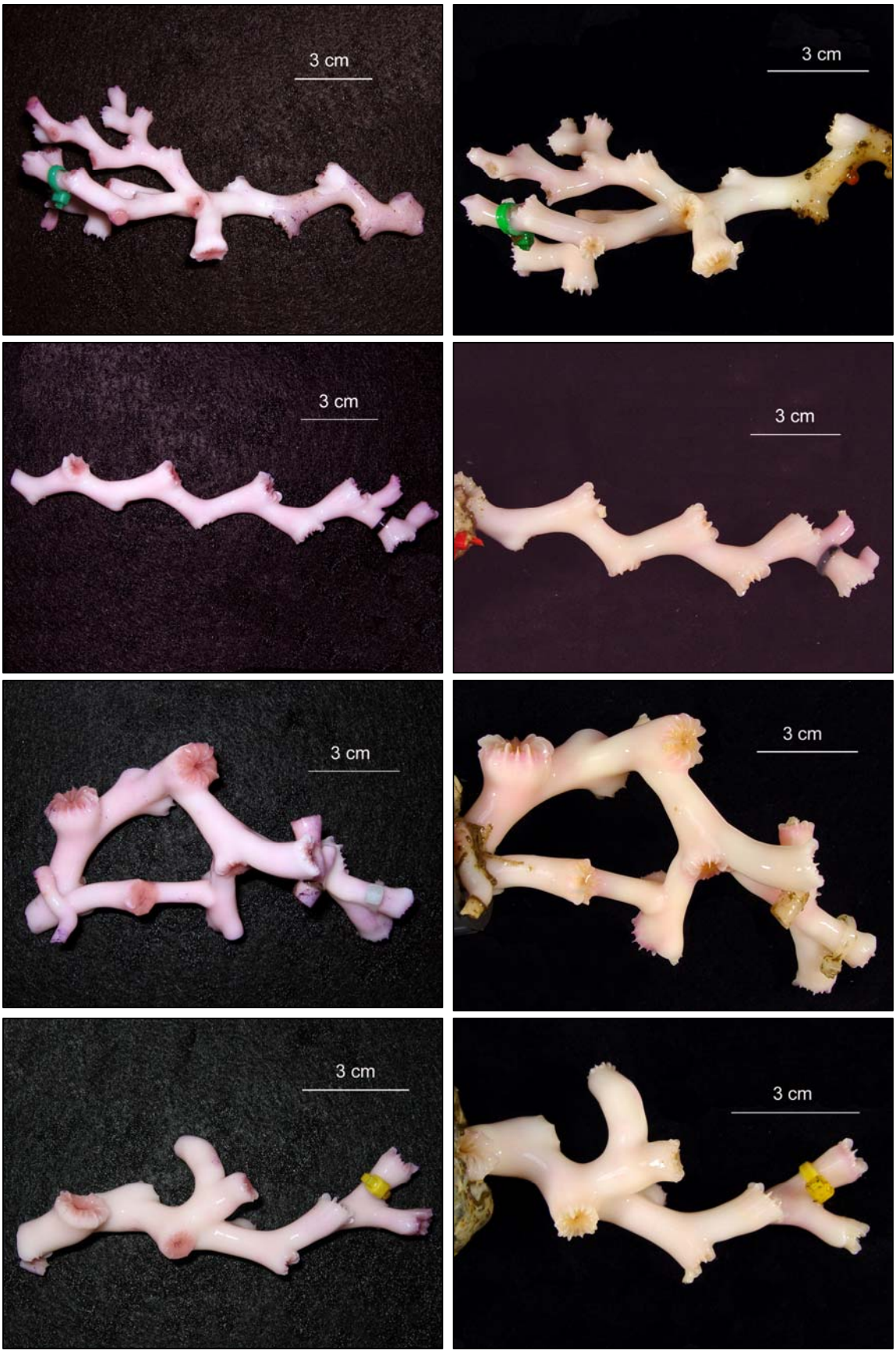
3 cm
3 cm
3 cm
3 cm
3 cm
3 cm
3 cm
3 cm

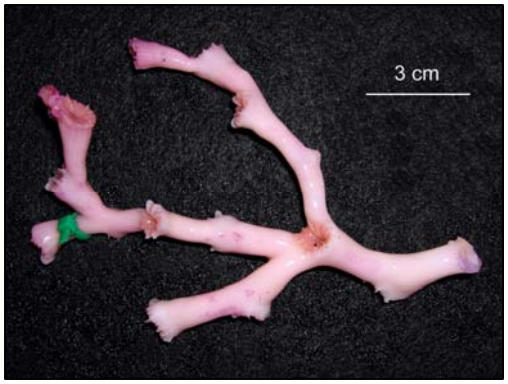
3 cm

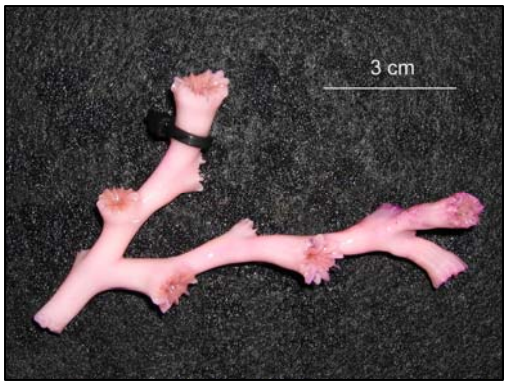
3 cm

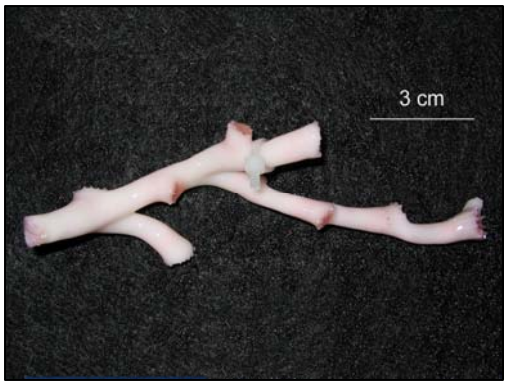
3 cm


3 cm

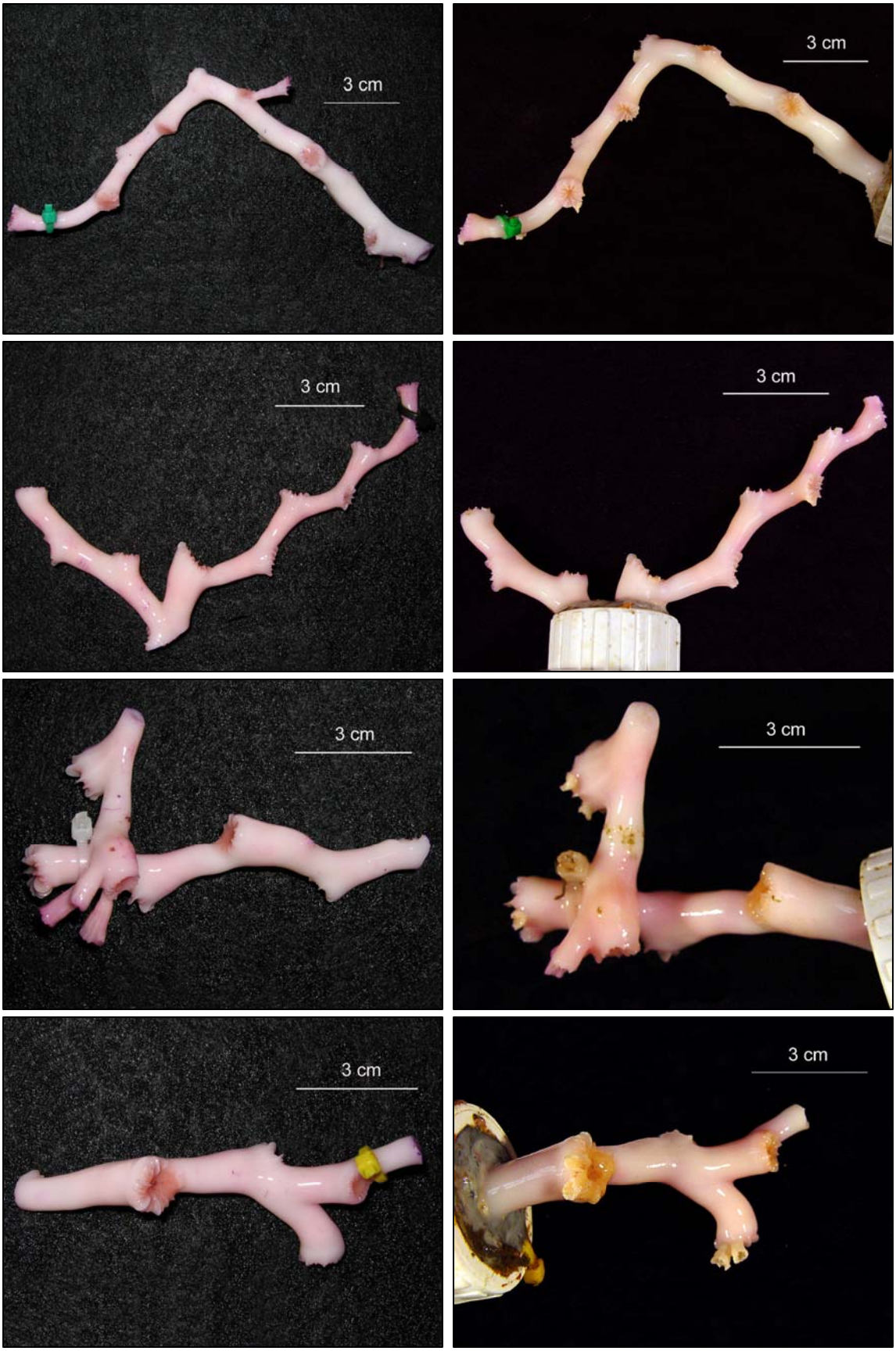
3 cm
3 cm
3 cm
3 cm
3 cm
3 cm
3 cm
3 cm

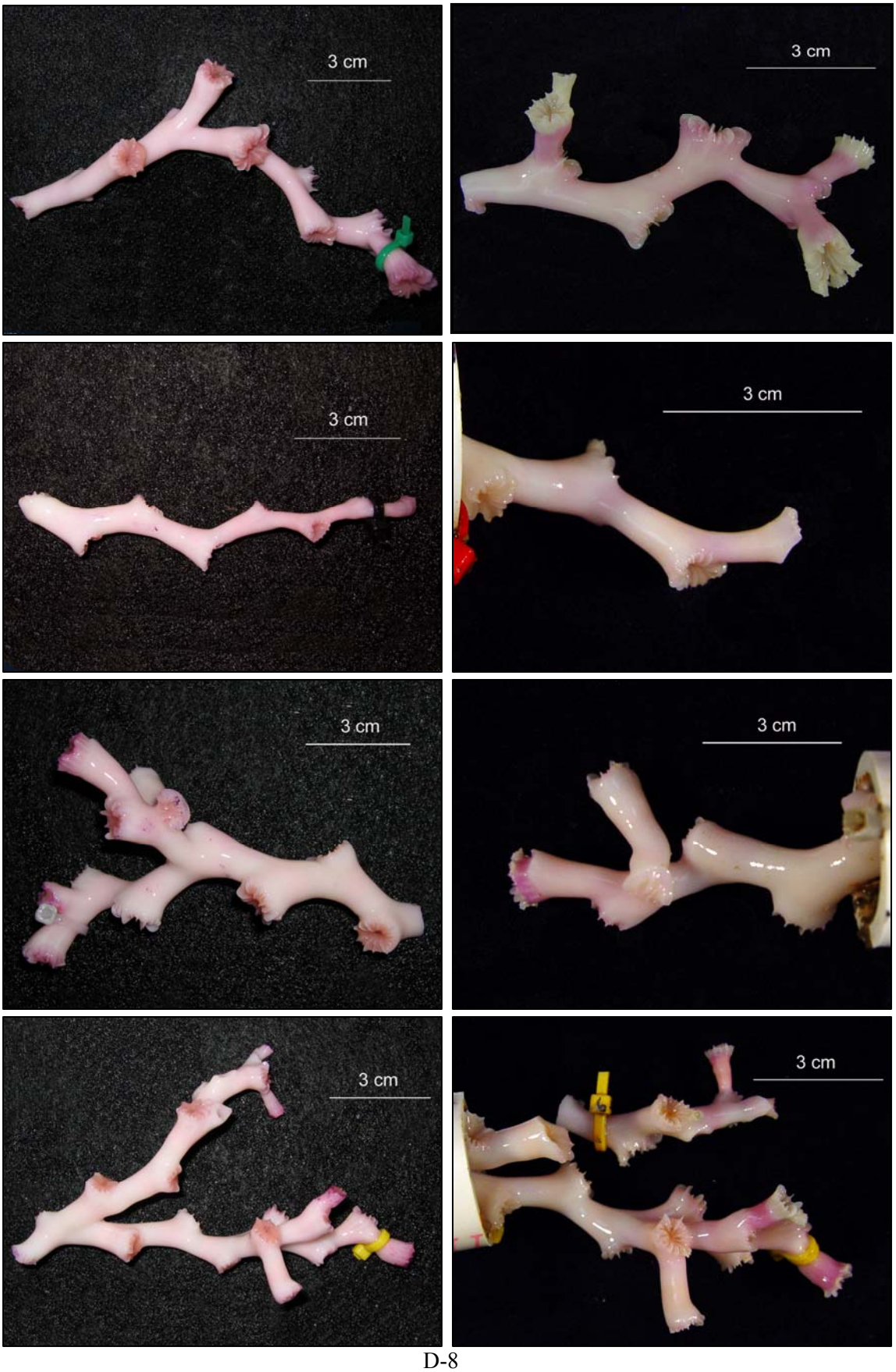
3 cm
3 cm
3 cm
3 cm
3 cm
3 cm
3 cm
3 cm

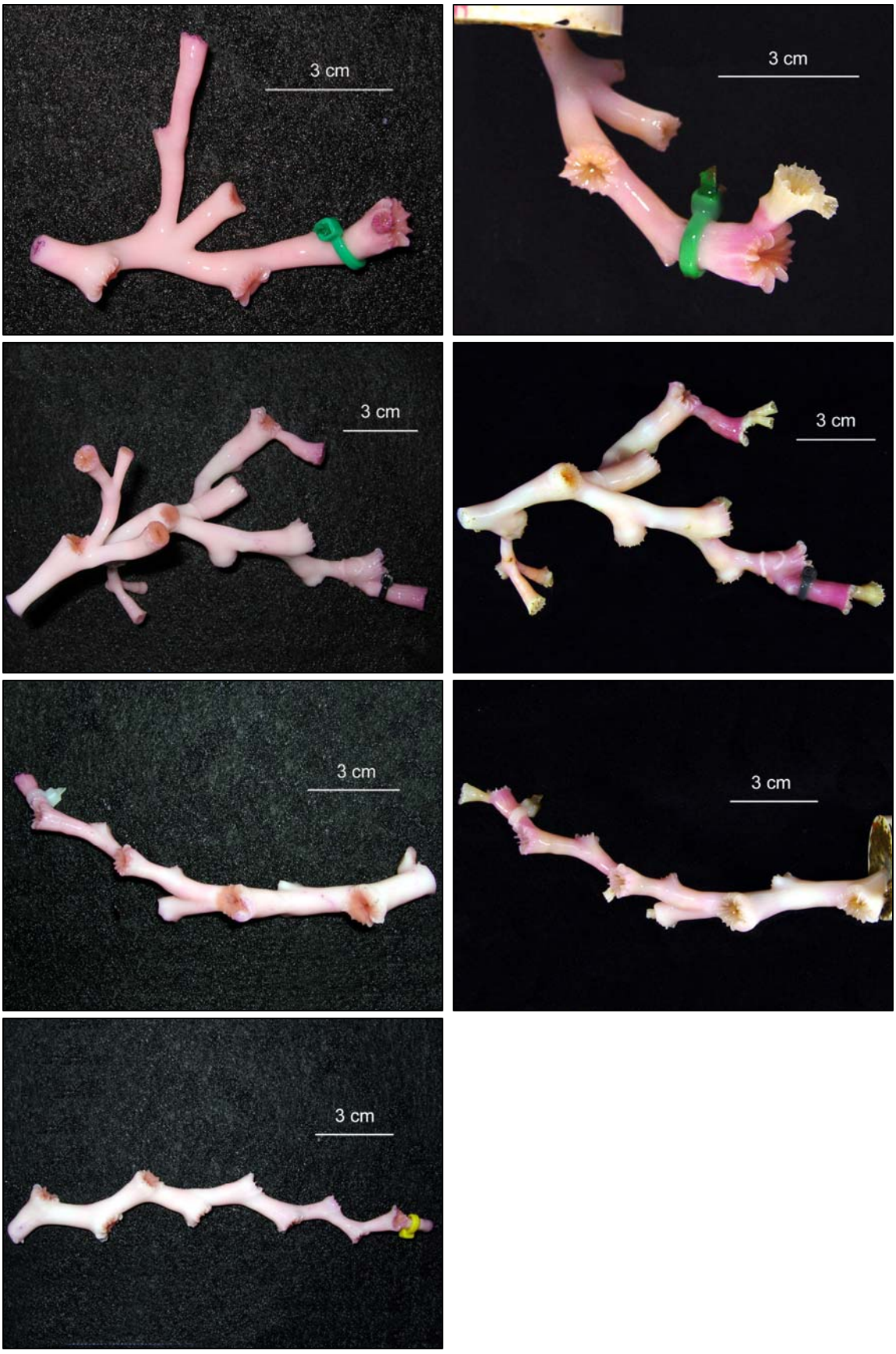
3 cm
3 cm
3 cm
3 cm
3 cm
3 cm
3 cm


3 cm


3 cm


3 cm


3 cm

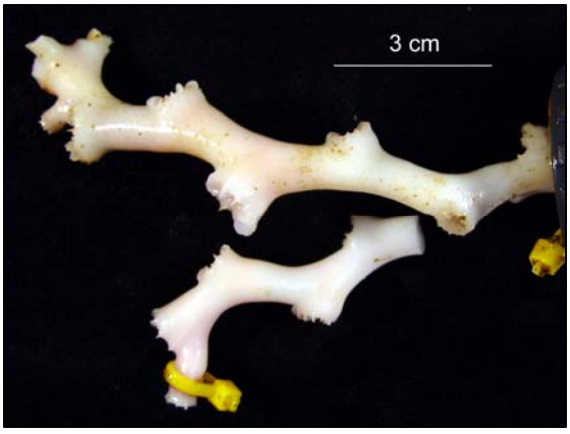
3 cm

The Department of the Interior Mission

As the Nation's principal conservation agency, the Department of the Interior has responsibility for most of our nationally owned public lands and natural resources. This includes fostering sound use of our land and water resources; protecting our fish, wildlife, and biological diversity; preserving the environmental and cultural values of our national parks and historical places; and providing for the enjoyment of life through outdoor recreation. The Department assesses our energy and mineral resources and works to ensure that their development is in the best interests of all our people by encouraging stewardship and citizen participation in their care. The Department also has a major responsibility for American Indian reservation communities and for people who live in island territories under U.S. administration.

The Minerals Management Service Mission

As a bureau of the Department of the Interior, the Minerals Management Service's (MMS) primary responsibilities are to manage the mineral resources located on the Nation's Outer Continental Shelf (OCS), collect revenue from the Federal OCS and onshore Federal and Indian lands, and distribute those revenues.

Moreover, in working to meet its responsibilities, the **Offshore Minerals Management Program** administers the OCS competitive leasing program and oversees the safe and environmentally sound exploration and production of our Nation's offshore natural gas, oil and other mineral resources. The MMS **Minerals Revenue Management** meets its responsibilities by ensuring the efficient, timely and accurate collection and disbursement of revenue from mineral leasing and production due to Indian tribes and allottees, States and the U.S. Treasury.

The MMS strives to fulfill its responsibilities through the general guiding principles of: (1) being responsive to the public's concerns and interests by maintaining a dialogue with all potentially affected parties and (2) carrying out its programs with an emphasis on working to enhance the quality of life for all Americans by lending MMS assistance and expertise to economic development and environmental protection.